PHOSPHORUS SPECIATION IN SOIL LEACHATE USING FIELD-FLOW FRACTIONATION AND FLOW INJECTION ANALYSIS

by

LAURA JANE GIMBERT

A thesis submitted to the University of Plymouth

in partial fulfilment for the degree of

DOCTOR OF PHILOSOPHY

School of Earth, Ocean and Environmental Sciences

In collaboration with

Institute of Grassland and Environmental Research,

North Wyke Research Station, Devon.

January 2005

ABSTRACT

PHOSPHORUS SPECIATION IN SOIL LEACHATE USING FIELD-FLOW FRACTIONATION AND FLOW INJECTION ANALYSIS

Laura Jane Gimbert

Colloidal material (0.001 – 1 μm) in soil leachate and agricultural drainage waters is an important route for the transport of contaminants such as phosphorus from land to catchments. Excessive phosphorus concentrations can result in eutrophication of natural waters. To be able to characterise the colloidal material, in terms of size distribution, a mild and relatively new separation technique field-flow fractionation (FFF) can be used to fractionate complex colloidal samples. By combining FFF and flow injection analysis (FIA) more detailed physico-chemical information on phosphorus species in soil leachates and agricultural runoff waters can be obtained.

Chapter 1 describes the methods used to determine phosphorus and also to characterise colloidal material, especially using FFF, and particularly focusing on the Flow FFF (FlFFF) sub-technique. Chapter 2 concentrates on the experimental considerations for FlFFF with recommended procedures for the setup and calibration of the system. In Chapter 3, SdFFF is used to compare the use of centrifugation and filtration for the fractionation of an Australian soil suspension, and demonstrates the uncertainties surrounding the use of conventional membrane filtration. FlFFF is used in Chapter 4 to optimise a sampling, treatment and preparation protocol for two contrasting soil types sampled in the UK. Centrifugation and filtration methods are also compared in a similar approach used in Chapter 3.

In Chapter 5 a portable FI monitor is optimised for the detection of reactive phosphorus. The linear range for the FI monitor is determined as 0.8 – 8.0 μM PO_4-P with a limit of detection of 0.6 μM PO_4-P. A digestion method is also optimised for the determination of total phosphorus using an acidic peroxydisulphate autoclaving method. In Chapter 6, FlFFF and FIA are combined in an experiment describing the fractionation of a soil suspension and the subsequent determination of phosphorus associated with different size fractions. The results from this combination show great potential and will help improve our understanding of the role of colloids in phosphorus transport from agricultural land to catchments.

TABLE OF CONTENTS

LIST OF TABLES

LIST OF FIGURES

LIST OF ABBREVIATIONS AND SYMBOLS

DAHP	Dissolved acid hydrolysable phosphorus
DOP	Dissolved organic phosphorus
DRI	Differential refractive index
DRP	Dissolved reactive phosphorus
ElFFF	Electrical field-flow fractionation
ESMS	Electrospray mass spectrometry
FIA	Flow injection analysis
FFF	Field-flow fractionation
FlFFF	Flow field-flow fractionation
FRP	Filterable reactive phosphorus
GrFFF	Gravitational field-flow fractionation
HPSEC	High performance size exclusion chromatography
ICP-AES	Inductively coupled plasma-atomic emission spectrometry
ICP-MS	Inductively coupled plasma-mass spectrometry
LIBS	Laser-induced breakdown spectroscopy
LLS	Laser light scattering
MALLS	Multi-angle laser light scattering
MRP	Molybdate reactive phosphorus
MWCO	Molecular weight cut off
MWD	Molecular weight distribution
PAHP	Particulate acid hydrolysable phosphorus
POP	Particulate organic phosphorus
PRP	Particulate reactive phosphorus
PSD	Particle size distribution
PS	Polystyrene beads
PSS	Poly(styrene sulfonate) sodium salt
RI	Refractive index
RMM	Relative molecular mass
RP	Reactive phosphorus
SEC	Size exclusion chromatography
SdFFF	Sedimentation field-flow fractionation
SF	SPLITT fractionation
SRP	Soluble reactive phosphorus
TAHP	Total acid hydrolysable phosphorus

TDP	Total dissolved phosphorus
ThFFF	Thermal field-flow fractionation
TOP	Total organic phosphorus
TP	Total phosphorus
TPP	Total particulate phosphorus
TRP	Total reactive phosphorus
UV	Ultraviolet detector

A	area of channel
A_p	projected area
d	hydrodynamic diameter
d_c	equivalent circular diameter
d_s	equivalent spherical diameter
D	diffusion coefficient
f	friction coefficient
F	driving force
g	gravitational acceleration constant (980 cm s^{-2})
h	peak height
K	Boltzmann's constant (1.38 x 10^{-16} g cm^2 s^{-2} K^{-1})
ℓ	mean layer thickness
M	relative molecular mass
R	retention ratio
r	centrifuge radius
t_b	breakthrough time
t^0	void time
t_r	retention time
T	absolute temperature
U	field induced transport velocity
$\langle v \rangle$	cross-sectional average velocity of carrier liquid
v_r	sample migration velocity
$\dot{V}$	volumetric channel flow rate
$\dot{V}_c$	volumetric crossflow rate
V^0	void volume
V_p	particle volume

V_r	retention volume
w	channel thickness
η	viscosity of carrier liquid (η=0.01 g cm^{-1} s^{-1} at 20°C)
λ	retention parameter
ρ	density (g cm^{-3})
$\Delta\rho$	density difference between the particles and the suspension medium (g cm^{-3})
ω	angular velocity of the centrifuge (rad s^{-1})

ACKNOWLEDGEMENTS

Firstly I would like to thank my supervisors Prof. Paul Worsfold from University of Plymouth and Dr. Phil Haygarth from IGER for their support, enthusiasm and guidance throughout the PhD. It was a FFF learning curve for us all. I also thank the EPSRC and the RSC for the funding of my studentship. It was a great opportunity.

I thank Dr. Ron Beckett for all his assistance with the FFF side of things and for his supervision during my 6 weeks visit to Monash University. I also thank Trisha Butler from IGER for her help with the soil preparation and for collecting runoff samples during storm events! I would like to thank the University of Plymouth, the technical staff including Andy, Andrew for concocting an azide waste disposal method, Sally and Ian, and the secretaries Elaine and Debbie.

I acknowledge the help and friendship of all the wonderful people I have met over the last 3 years and a bit, especially current BEACh group members: Utra, Alex, Angie, Simon, Omaka, Richard, Orif, Cathryn, Ying, Marta, Marie and Thierry. Also thanks to the past members of the Davy 106 group including Kate, Paula, Stephan, Grady, Paulo, German, Orawan, Yolanda, Yaqoob, Sonia, Luis, Dan, and my Spanish friend Rebeca.

Many thanks to Mum, Dad, Sarah, and my boyfriend Simon. You have given me encouragement, love and help throughout. Love to you all.

AUTHOR'S DECLARATION

At no time during the registration for the degree of Doctor of Philosophy has the author been registered for any other University award without prior agreement of the Graduate Committee.

This study was financed with the aid of a studentship from the Engineering and Physical Sciences Research Council and the Royal Society of Chemistry and carried out in collaboration with the Institute of Grassland and Environmental Research.

A programme of advanced study was undertaken, which included a 6 weeks visit to Monash University, Melbourne, Australia to learn more about the field-flow fractionation technique under the supervision of Dr. Ron Beckett.

Relevant scientific seminars and conferences were regularly attended at which work was often presented and several papers were prepared for publication.

Publications:

Comparison of Centrifugation and Filtration Techniques for the Size Fractionation of Colloidal Material in Soil Suspensions Using Sedimentation Field-Flow Fractionation, Laura J. Gimbert, Philip M. Haygarth, Ronald Beckett and Paul J. Worsfold, *Environmental Science & Technology*, **2005**, *39*, 1731-1735.

Sampling, Sample Treatment and Quality Assurance Issues for the Determination of Phosphorus Species in Natural Waters and Soils, Paul J. Worsfold, Laura J. Gimbert, Utra Mankasingh, Omaka Ndukaku Omaka, Grady Hanrahan, Paulo C.F.C. Gardolinski, Philip M. Haygarth, Benjamin L. Turner, Miranda J. Keith-Roach and Ian D. McKelvie, *Talanta*, (in press).

Environmental Applications of Flow Field-Flow Fractionation (FlFFF), Laura J. Gimbert, Kevin N. Andrew, Philip M. Haygarth, and Paul J. Worsfold, *Trends in Analytical Chemistry (TrAC)*, **2003**, *22*, 615-633.

Presentation and Conferences Attended:

1st BEACh Conference, University of Plymouth, UK, 17th December 2004, oral presentation: Comparison of centrifugation and filtration techniques for the size fractionation of colloidal material in soil suspensions using Sedimentation Field-Flow Fractionation.

Analytical Research Forum, University of Preston, UK, 19th-21st July 2004, oral presentation: Phosphorus speciation in soil leachate using field-flow fractionation and flow injection analysis.

WRAD50: Essential analytical chemistry for the next 50 years, 50th Anniversary of the Western Region Analytical Division, University of Plymouth, UK, 14th July 2004, poster presentation: Sedimentation and flow field-flow fractionation techniques combined with flow injection analysis for the characterisation of colloidal material in agricultural drainage waters.

Departmental research seminar, oral presentation: FFF techniques for the study of colloidal matter in soil leachate, February 2004.

The 4th Environmental Meeting on Environmental Chemistry (EMEC4), Plymouth, UK, 10th-13th December 2003, poster presentation: Sedimentation and flow field-flow fractionation techniques combined with flow injection analysis for the characterisation of colloidal material in agricultural drainage waters.

Analytical Research Forum incorporating Research and Development Topics, University of Sunderland, UK, 21st-23rd July 2003, poster presentation: Sedimentation and flow field-flow fractionation techniques combined with flow injection analysis for the characterisation of colloidal material in agricultural drainage waters.

Departmental research seminar, oral presentation: Characterisation of colloidal material in soil leachate using FFF and FIA, June 2003.

Flow Analysis IX, 9th International Conference on Flow Analysis, Geelong, Australia, 17th-21st February 2003, poster presentation: Determination of phosphorus in agricultural runoff waters using flow injection and spectrophotometric detection.

Analytical Research Forum incorporating Research and Development Topics, Kingston University, UK, 15th-17th July 2002, poster presentation: Determination of phosphorus in agricultural runoff waters using flow injection and flow field-flow fractionation.

FFF 2002 The Tenth International Symposium on Field-Flow Fractionation, University of Amsterdam, The Netherlands, 2nd-5th July 2002.

ISEAC 32 International Symposium on the Environmental & Analytical Chemistry, University of Plymouth, UK, 17th-21st June 2002.

Departmental research seminar, oral presentation: Determination of phosphorus in agricultural runoff waters using FIA and FFF, March 2002.

External Contacts:

Dr. Phil Haygarth, Soil Science and Environmental Quality Team, Institute of Grassland and Environmental Research, North Wyke Research Station, Okehampton, Devon, EX20 2SB, UK.

Dr. Ron Beckett, Water Studies Centre, Department of Chemistry, Monash University, Clayton, Victoria 3800, Australia.

Word count of main body of thesis: 29,689 words

Signed.....

Date....29/04/05.....

Chapter 1

Introduction

1. Introduction

1.1 Phosphorus

Phosphorus (P) is the eleventh most abundant element in the earth's crust [1,2], and 95 % of this phosphorus is present as the apatites: fluorapatite, hydroxyapatite and chlorapatite [2,3]. Phosphorus is an essential element for all life including plant growth and photosynthesis in algae [4,5,6], and is an important component in mononucleotides and nucleic acids which occur in all living matter, plants, soil and aquatic organisms [7]. The mononucleotides link together to form the nucleic acids, deoxyribonucleic acid (DNA) and ribonucleic acid (RNA), using phosphoric bond groups [2,7]. Phosphorus is also present in adenosine triphosphate (ATP), which is a mononucleotide that has been esterified to a triphosphoric acid, and which is essential for the transfer of chemical energy within a cell [2,7,8]. The chemical energy released by the phosphate bond reversibly moving between ATP and adenosine diphosphate (ADP) is used for the synthesis of complex molecules of life [2].

1.1.1 Sources of phosphorus

There are many different sources of phosphorus and excessive phosphorus concentrations can result in eutrophication of natural waters as discussed in section 1.1.2. The sources of phosphorus in natural waters arise from point and non-point (diffuse) sources [9], shown in Fig. 1.1. Point sources include sewage treatment works, industrial wastewater effluent, and runoff and leachate from waste disposal sites, whereas the main diffuse sources arise from surface runoff and sub-surface leaching from agricultural land [10-15]. Phosphorus can also enter the waterways by the weathering of igneous and sedimentary rocks, such as apatite, the decomposition of organic matter containing phosphorus compounds and soil erosion during storm events [16].

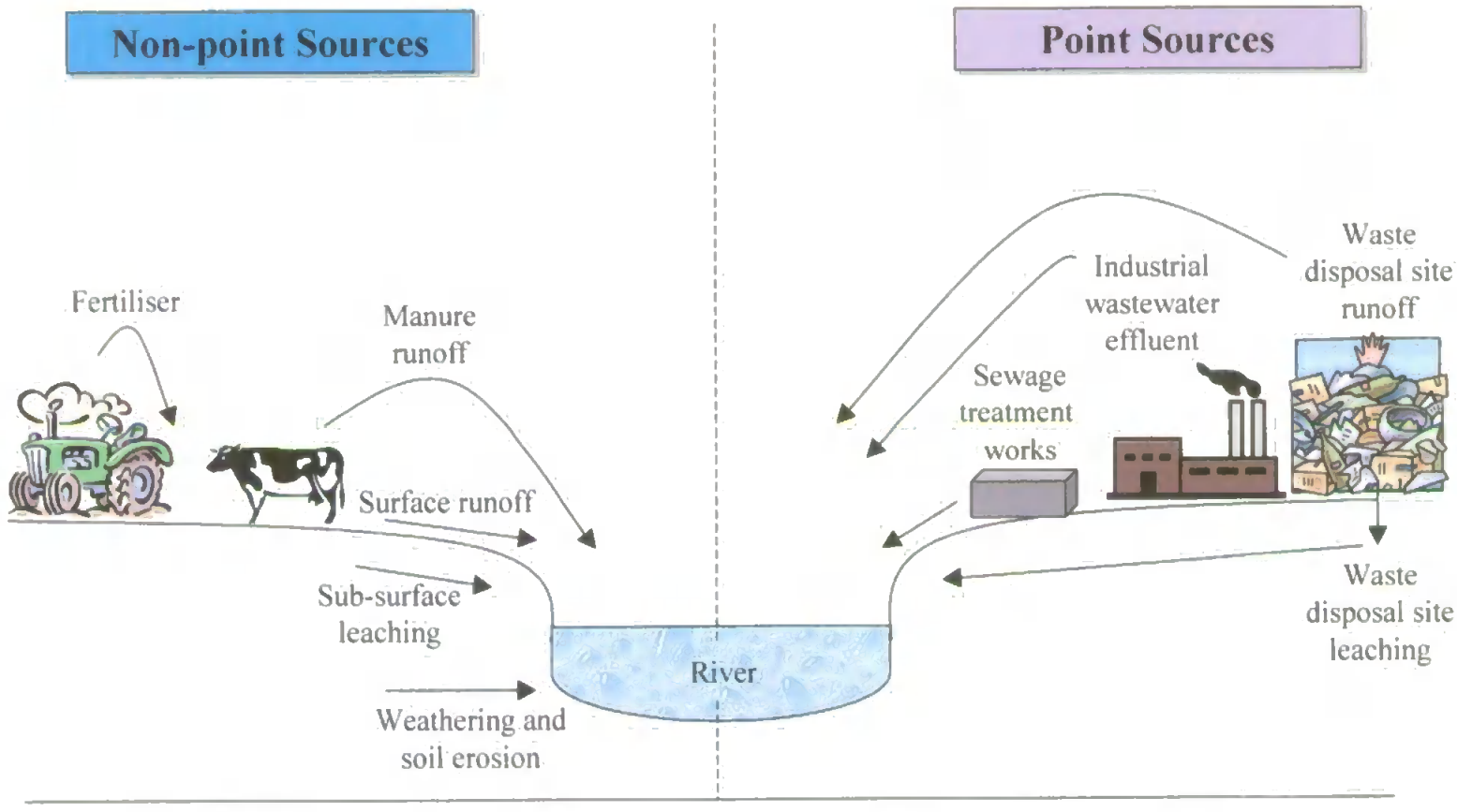

Figure 1.1. Different pathways of phosphorus transfer from point and non-point sources to natural waters.

Over the last twenty years the importance of point sources for the transport of phosphorus into the waterways has decreased because they have been easier to control than diffuse sources. This has been due to restrictions on the use of phosphorus containing detergents and improved wastewater treatment as P-stripping systems have been introduced to remove most of the phosphorus from the effluent. During this period there has also been an increase in agricultural production and fertiliser and manure applied to farmland in the UK and other European countries e.g. Germany, France, The Netherlands, Ireland, Denmark and Belgium [10,11,13-15,17-22]. In North America, non-point sources arising from intensive poultry and pig farming were reported as the dominant source of phosphorus in rivers, lakes and reservoirs, however it was also reported that point sources can contribute >50 % P in rivers in urban areas [10,12]. In the UK for three Welsh estuaries, it was estimated that phosphorus from sewage treatment works (STWs) can contribute typical values of 26-62 %, and 3-49 % from agricultural sources (livestock waste and inorganic fertiliser runoff), these values show that in some local areas STWs dominate [9]. Heathwaite *et al.* reported that trends in phosphorus concentration in rivers in lowland regions of the UK were considerably higher than in rivers in lowland regions of North America. This could possibly be due to the higher population density, increased number of livestock on grazing land and the greater intensity with which the land is cultivated for grass and arable crops in the UK than North America [18].

The use of fertilisers and manure have lead to an accumulation of phosphorus in the soil, as Higgs *et al.* reported that only about 10-25 % of the phosphorus applied is taken up by the crops [11], whereas Loehr reported that only 5-10 % is taken up [23]. Also animals retain only 30 % of phosphorus in their feed and the residual phosphorus ends up in manure, which is then applied on the land [15]. Phosphorus was historically thought to be immobile in soils and this has resulted in the overuse of fertilisers and manure because applications were based on the crop nitrogen (N) requirements [6,15]. The applied phosphorus can

either stay in the soil, thus adding to the phosphorus which occurs naturally within the soil, or be transported to natural waters by erosion, leaching or runoff [10,11,14,15,17,19,21,22]. Phosphorus can be transported from the soil in solution, or in particulate form, as phosphorus is relatively insoluble and strongly adheres to soil particles and organic matter [1,10,13-15,21,22,24]. In relatively acidic environments phosphorus is likely to be held strongly in soils through metal complex formation or adsorption onto clay particles and iron/manganese oxyhydroxides, and in strongly alkaline environments phosphorus will form insoluble calcium complexes [18]. During weathering phosphorus can be coprecipitated with aluminium and iron hydroxides and calcium compounds [1,25]. Phosphorus losses are increased during storm events due to surface runoff containing phosphorus adsorbed to soil particles, and to runoff from freshly applied fertilisers or manure containing dissolved phosphorus [1,10,15,19,21,22,24,26]. Sub-surface drainage and leaching may also be important pathways especially if the soil is overloaded with phosphorus [24], and hence the different forms of phosphorus from each pathway need to be determined [27]. This all leads to agricultural sources of phosphorus being an important factor in determining the eutrophic state of British waters [5,28].

1.1.2 Eutrophication

Eutrophication occurs when there is an enrichment of nutrients in natural waters, and is a worldwide problem [10,16,29-32]. Algae and higher plants require nutrients for growth and phosphorus is considered to be the growth-limiting nutrient for primary production in freshwaters. This is because phosphorus is not always readily available in sufficient amounts and the growth of algae and cyanobacteria is not limited by the availability of nitrogen in the water [4,16,24,29]. As phosphorus can be transferred from land to water in dissolved and particulate forms, the dissolved phosphorus as orthophosphate will be readily available for uptake by bacteria, algae and plants [8,18]. The particulate phosphorus may also release orthophosphate and organic phosphates which can then be

chemically or enzymatically hydrolysed to orthophosphate which is then also taken up by bacteria, algae and plants [8,18,29,33,34]. It was thought that algae utilised dissolved phosphorus while bacteria mineralised organic phosphorus, but it is now generally accepted that algae and bacteria compete for the available orthophosphate, however bacteria are known to utilise low concentrations of orthophosphate more efficiently than algae [16,35].

Vollenweider determined that eutrophication can occur when the springtime total phosphorus (TP) concentrations in a body of water exceeded 10 $\mu g\ L^{-1}$ [36], and the Organisation for Economic Co-operation and Development (OECD) set the limits for eutrophication between 35 and 100 $\mu g\ L^{-1}$ TP [37]. This shows that even low concentrations of phosphorus can affect algae, bacteria and plant growth in natural waters [5]. Therefore phosphorus in water is not considered to be directly toxic to humans and animals [10], but there may be indirect toxic effects e.g. from cyanobacteria. A small increase in algal and plant growth can affect drinking water supplies, as the water quality is reduced because of bad tastes and odours, which then require expensive treatment to remove the algae before consumption [2,10,31,32]. Algal and plant growth can also interfere with the use of water for fisheries, recreation, industry, and agriculture [4,8,10,32,38,39].

In freshwater, blue green algal blooms caused by excessive growth of phytoplankton, especially cyanobacteria, are the results of eutrophication [5,10,16,40]. These blooms can result in the formation of trihalomethanes during water chlorination in treatment plants [2,4,10,39]. They can also release water-soluble neuro- and hepatotoxins when the blooms die, which can kill livestock and pose a serious health hazard to humans [2,4,5,10,31,39], and decrease the concentration of dissolved oxygen in the water resulting in fish dying [2,4,8,10,24,31,32,39,40].

1.2 Phosphorus speciation

Phosphorus exists in different forms in soil leachates, agricultural runoff and natural waters. The dissolved fraction is operationally defined as the fraction that passes through a conventional 0.2 or 0.45 μm membrane, and the particulate fraction is retained on the membrane. The dissolved and particulate fractions can be further operationally defined as shown in Fig. 1.2 [41]. The most commonly measured fractions are dissolved reactive phosphorus (DRP), total dissolved phosphorus (TDP) and total particulate phosphorus (TPP) [16,42-44].

The dissolved fraction contains inorganic and organic compounds such as orthophosphate, inositol phosphates, nucleic acids, phospholipids, phosphoamides, phosphoproteins, sugar phosphates and condensed phosphates (polyphosphates, metaphosphates) [1,7,16,42]. The particulate fraction comprises material of biological origin (animal, plant, bacterial), weathering products (primary and secondary minerals), and authigenic mineral formation by direct precipitation of inorganic phosphorus or sorption to other precipitates [1,16,30,34,45]. Particulate phosphorus can also arise from formation of organic or inorganic coprecipitates or the inclusion of phosphorus by metal-P binding (Ca, Al, Fe, Mn) into organic aggregates [16,42]. However phosphorus associated with colloidal material (0.001-1 μm) will also be present in both the dissolved and particulate fractions [17,46,47]. The importance of colloids in the transport of phosphorus from land to water, and methods used to characterise colloidal material is discussed in section 1.5, and in Chapters 2, 3 and 4.

DRP is also termed as filterable reactive phosphorus (FRP), soluble reactive phosphorus (SRP), molybdate reactive phosphorus (MRP) or reactive phosphorus (RP). DRP is defined as the fraction of the dissolved phosphorus that can be determined spectrophotometrically after reacting with molybdate to form phosphomolybdenum blue (reaction described in

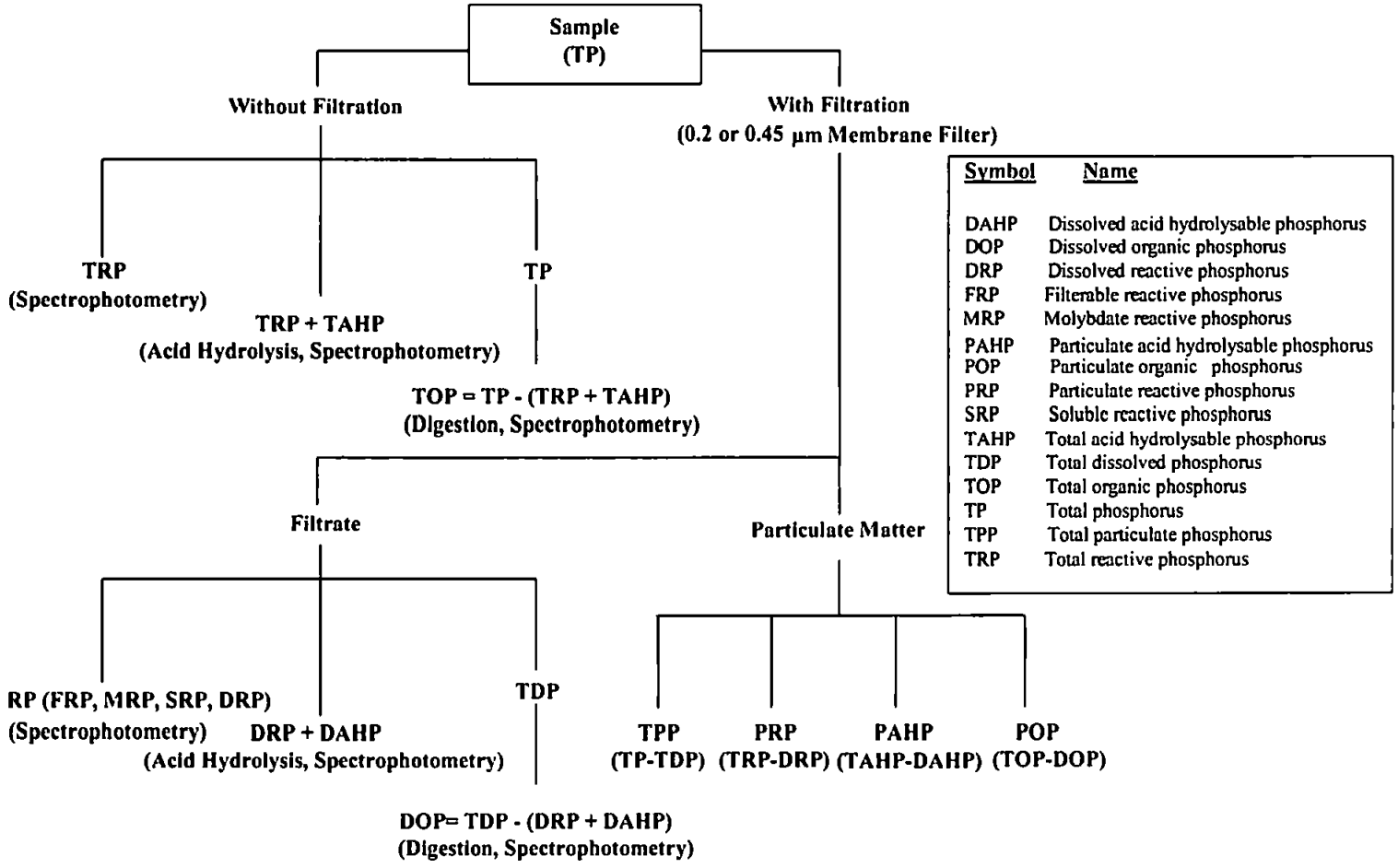

Figure 1.2. Operationally defined phosphorus fractions from Worsfold *et al.* [41].

section 1.3), and will consist of orthophosphate and labile condensed and organic phosphates. TDP consists of DRP and also unreactive forms of phosphorus that must undergo hydrolysis and oxidation before spectrophotometric detection [43]. The digestion methods used to determine TDP and TP are discussed in Chapter 5, whereas the methods used to determine the RP (or DRP) are described in section 1.3.

1.3 Analytical methods for phosphorus

Phosphorus can be transported from land to catchments in dissolved, particulate and colloidal forms therefore analytical methods are required to determine the different phosphorus species. There have been a number of different methods used for the determination of phosphorus which have been described in detail by McKelvie *et al.* [34], including ion chromatography [48-51] inductively coupled plasma atomic emission spectrometry (ICP-AES) [52,53], inductively coupled plasma mass spectrometry (ICP-MS) [54], and electrochemical techniques based on ion selective electrodes [55-58] and voltammetry [59-63].

The methods most widely used for the determination of RP are spectrophotometric methods and are usually based on the molybdenum blue method used by Murphy and Riley [34,64-66]. In this method [66] the RP reacts with molybdate to form 12-phosphomolybdic acid:

$$PO_4^{3-} + 12MoO_4^{2-} + 27H^+ \rightarrow H_3PO_4(MoO_3)_{12} + 12H_2O \qquad (1)$$

which is then reduced using ascorbic acid with an antimony potassium tartrate catalyst to phosphomolybdenum blue:

$$H_3PO_4(MoO_3)_{12} \xrightarrow{\text{Reduction}} \text{Phosphomolybdenum blue} \qquad (2)$$

This method does not strictly determine orthophosphate alone because of the presence of any acid hydrolysable phosphates leading to an overestimation of orthophosphate [64]. The intensity of the blue colour is proportional to the amount of RP ions incorporated into the

phosphomolybdenum blue complex and therefore the amount of RP in a sample can be determined spectrophotometrically [67], because the phosphomolybdenum blue complex has two absorbance maxima (λ_{max}) at 710 and 880 nm [66].

There have also been some studies where basic dye compounds were used to enhance the sensitivity of the molybdenum method such as the use of crystal violet [68,69], rhodamine B [70] and malachite green [71-74]. Malachite green however is not widely used, as the stability of the ion association complex is a problem unless stabilised by addition of a surfactant [16,34].

There are two types of molybdate methods and these are the "blue" method, reaction as described above [66,75-81] and the less commonly used "yellow" method [82-84]. The yellow spectrophotometric method involves ammonium molybdate reacting with ammonium metavanadate under acidic conditions to form the yellow coloured heteropoly acid, vanadomolybdophosphoric acid. This then reacts with the orthophosphate and absorbs below 400 nm of the visible spectrum [82,83]. The yellow method is faster, and more economical than the blue method because no reducing agent is involved [84] and has been preferred for relatively high phosphorus concentrations, whereas the blue method is more sensitive and therefore preferred for relatively low phosphorus concentrations [79,85].

The reaction described for the molybdenum blue method has been modified since 1962 with respect to reaction temperature, acid strength, and different reductants such as tin(II) chloride in attempts to improve the selectivity and stability of the blue chromophore produced [3,16,76]. Ascorbic acid has been preferred to tin(II) chloride because the reaction is less salt and temperature sensitive [34,64]. However tin(II) chloride has faster kinetics than ascorbic acid for the reduction of the yellow coloured Mo(VI) complex to the

blue Mo(V) complex [16,64,78] and hence is often preferred in flow systems. Janse *et al.* reported that the main problem with using tin(II) chloride was a drifting baseline but this was overcome by adding hydrazinium sulphate as a stabiliser [78]. van Staden and van der Merwe compared four different FIA and spectrophotometric analytical systems using tin(II) chloride, ascorbic acid, malachite green and rhodamine B. Of all these, the tin(II) chloride system gave the best overall results for the determination of phosphorus with a lower detection limit and relatively large linear working range compared to the other systems [79].

The molar ratio between $[H^+]$ and $[MoO_4^{2-}]$ is crucial for colour formation and optimal colour formation occurs for $[H^+]$:$[MoO_4^{2-}]$ molar ratios between 60 and 80. Interference effects may occur below a molar ratio of 60 because of the self-reduction of the MoO_4^{2-} ion, resulting in the formation of a molybdenum blue colour independent of the RP concentration, whereas if the molar ratio is above 80 the reaction becomes slow and incomplete [67].

The molybdenum blue method has been used in conjunction with flow injection and spectrophotometric detection for the determination of RP [3,34,45,77,80,81,86-89], and a method based on Hanrahan *et al.* [77] is described in Chapter 5. The molybdenum blue method can suffer from interferences which include silicate and this is also discussed in Chapter 5.

1.4 Flow injection analysis

Růžička and Hansen first reported flow injection analysis (FIA) in 1975 [90,91]. It is the injection of sample into an unsegmented continuously flowing carrier stream [91], and has been used to determine many different types of analytes [85]. Once injected, the sample undergoes physical dispersion by travelling through mixing coils, and chemical reactions

by introducing reagents during transport to the detector. The sample is transported through the manifold in narrow bore tubing (of about 0.5-0.8 mm i.d.) [90-92], and a simple FIA manifold is shown in Fig. 1.3 where the basic components consists of a pump to propel the sample, carrier and reagent streams, an injection valve for sample introduction, reaction manifold and flow-through detector (e.g. spectrophotometer).

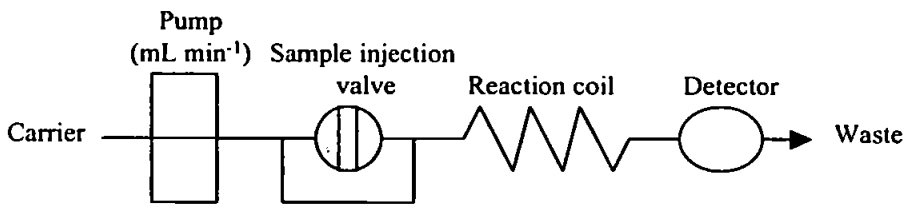

Figure 1.3. Simple single-line FIA manifold.

A typical detector response is in the form of a peak where the width, height and area are related to the concentration of the analyte being determined (Fig. 1.4). The time between sample injection and peak maximum (or peak height) is the residence time during which the chemical reaction takes place. Peak height is the most frequently measured parameter and is directly related to the detector response such as absorbance [93]. If a FIA system has been well designed the sampling cycle is fast with up to or greater than 120 samples being analysed in 1 h, and the sample injection volumes are usually small (125 μL of sample was used in the FIA system in Chapter 5). Therefore the advantages of FIA include low costs, low reagent consumption, high sample throughput, good reproducibility and small sample volumes [90].

FIA is based on the combination of three principles: sample injection, controlled dispersion of the injected sample zone and reproducible timing. When a sample is injected into the carrier stream it initially has a rectangular profile, as shown in Fig. 1.5A. As the sample is transported through the manifold the sample undergoes continuous dispersion and sudden dilution at points where confluent streams are added. Dispersion results from convection

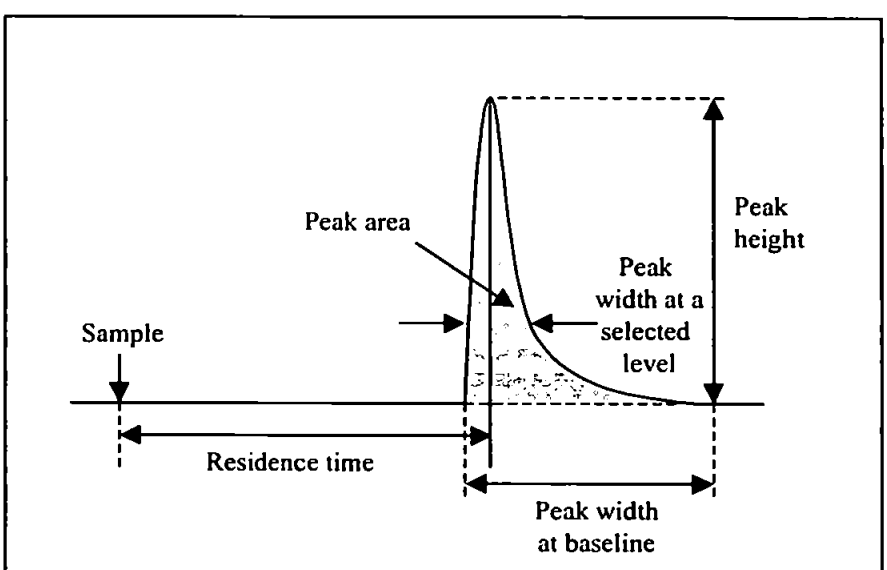

Figure 1.4. Typical FIA detector response.

and diffusion. The sample zone will adopt a parabolic flow profile where the velocity of the sample at the centre of the tube is twice that of the sample at the edge of the tube which tends to zero, this is caused by convection (Fig. 1.5B). Diffusion occurs perpendicular (radial) to the carrier stream and is dependent on the concentration differences between neighbouring fluid elements and the diffusion coefficient resulting in the flow profile approaching a Gaussian concentration profile as shown in Fig. 1.5C [80].

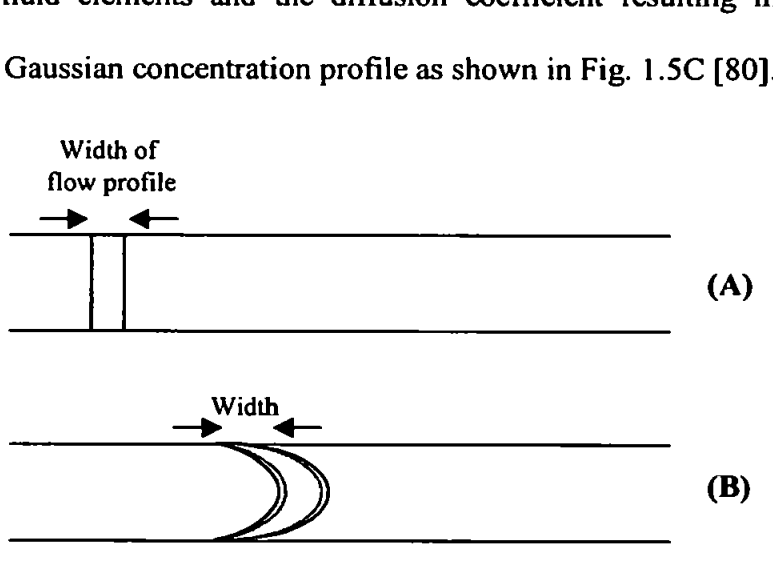

Figure 1.5. Effect of dispersion on the flow profile of the sample zone at different times during FIA: (A) Injection; (B) Convection; (C) Dispersion.

The peak observed at the detector reflects a continuum of concentrations forming a concentration gradient. It is important to know how the original sample has been diluted on transport to the detector and the time elapsed between injection and peak maximum. The dispersion coefficient (D) is used to quantify the degree of dispersion and is defined as:

$$D = \frac{C^0}{C} \tag{3}$$

where C^0 is the original concentration of the sample and C is the concentration at the detector. For measurements based on peak maximum this corresponds to the maximum of the recorded curve i.e. C^{max}. Sample dispersion has been defined as limited (D = 1-3), medium (D = 3-10) and large (D > 10) [93]. Limited dispersion is suitable when the injected sample is transported directly to the detector such as an ion-selective electrode or atomic absorption spectrometer. Medium dispersion is required when the injected sample must mix and react with the carrier reagent to form a product, which is subsequently detected. Large dispersion is used when the injected sample needs to be diluted to bring it into the measurement range [94].

Sample volume, channel length, flow rate and channel geometry can all affect dispersion and hence peak height. When the sample volume is increased the peak height will increase, and therefore C^{max}, until an upper limit has been reached. At this upper limit the concentration will be equal to C^0 i.e. there is no dispersion. When tubing of a small diameter is used the sample is less easily mixed and dispersed because the same sample volume will occupy a longer length of tubing resulting in an increase in peak height. As the flow rate decreases the peak height increases due to decreased dispersion of the sample zone. By using coiled tubes, the dispersion is decreased as the radial mixing is improved and axial dispersion limited resulting in a more symmetrical, narrower and higher peak than if a straight tube had been used. This is because in a coil the direction of the flow is changed causing the fluid at the edge of the tubing to flow into the centre of the tube

enhancing mixing [93]. The FIA peak is usually a result of two kinetic processes: the physical process and the chemical process. The physical parameters affecting peak height are described above, whereas the chemical processes result from reactions between the sample and reagents in the carrier stream [92-94].

1.5 Colloids

Colloids are found in natural waters, agricultural runoff and soil leachate in the size range 0.001-1 μm. The typical size ranges of organic and inorganic colloidal material found within the colloidal range is shown in Fig. 1.6. Inorganic colloids include amorphous iron and manganese oxides [95]. Organic colloids consist of natural organic matter (NOM) containing oligosaccharides, lipids, peptides and refractory organic matter termed as humic substances [95]. There may also be viruses and bacteria present [96].

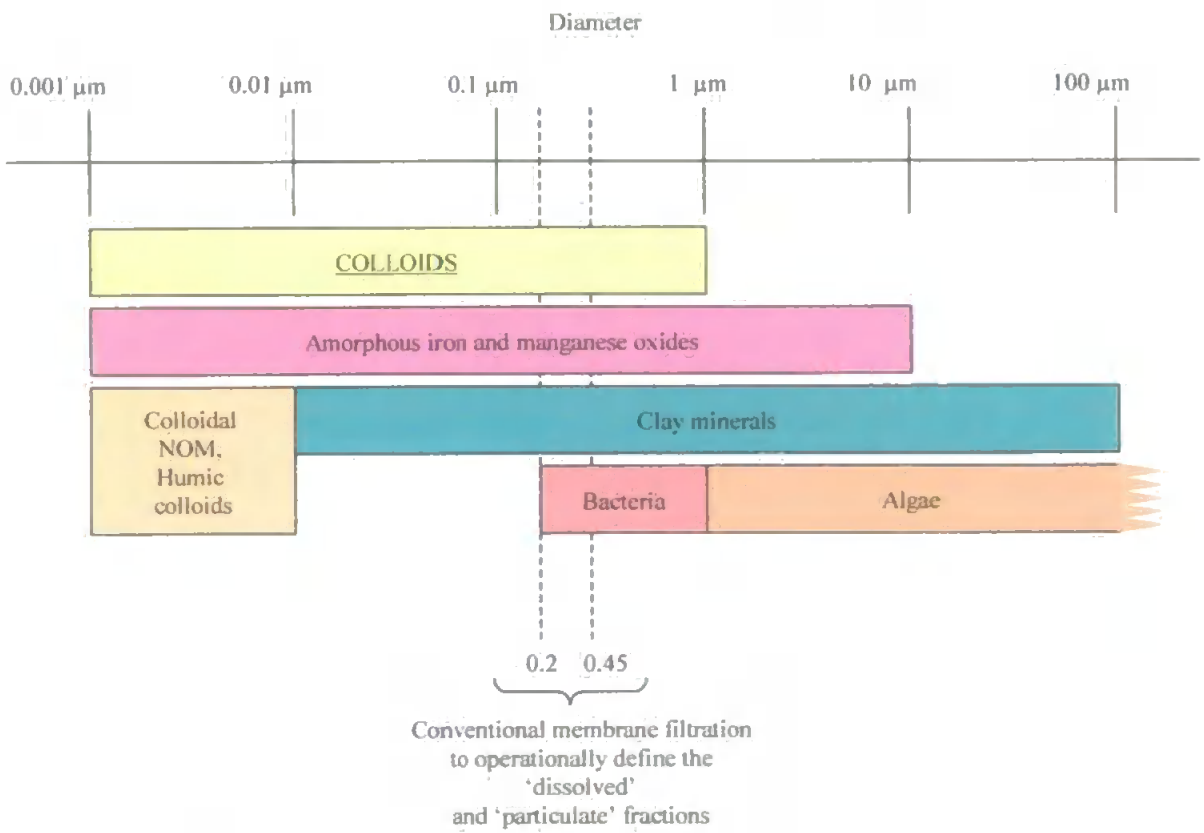

Figure 1.6. Approximate size ranges for organic and inorganic colloids, bacteria, algae and mineral particles. The colloidal material is found in both the 'dissolved' and 'particulate' fractions.

A water sample containing colloidal material is an unstable system where the colloids are continuously evolving through physical, chemical and microbial processes [97]. The association of inorganic and organic colloids with strongly sorbing contaminants is thought to enhance the mobility of the contaminants, and therefore colloids are important in the transport of contaminants from land to water [96,98,99]. Mobile colloids can considerably alter the transport of contaminants such as radionuclides and heavy metals in the subsurface environment, but it is unclear how colloids affect the mobility of phosphorus [100]. There have been some studies that have shown phosphorus to be associated with colloidal material [46,47], and also that colloidal phosphorus was present in the dissolved fraction of soil solutions and soil-water extracts [46,101,102]. The presence of colloidal material in the dissolved fraction is due to the dissolved fraction being operationally defined as the fraction that passes through a conventional 0.2 or 0.45 μm membrane. Therefore as colloids are <1 μm they will be present in both the dissolved and the particulate fractions. Experimental techniques are therefore required to fractionate and characterise the colloidal material in environmental samples.

1.5.1 Analytical techniques for colloidal material

There have been many different types of analytical methods used to fractionate and characterise colloidal material in terms of particle size distributions or molecular mass distributions. These include membrane and ultra-filtration [46,47,98,102-107], centrifugation [107,108], size exclusion chromatography [109-111] and gel chromatography [47,100,101,112]. Douglas *et al.* sequentially used sieving, centrifugation and tangential flow filtration for the separation of suspended particulate matter over the entire particulate and colloidal range with the tangential flow filtration technique used to separate the colloidal fraction further into coarse, fine and ultrafine fractions [113]. The determination of RP associated with colloidal material has been determined using

spectrophotometric methods after first fractionating the sample using one of the methods mentioned above [46,47,98,100,102,104-106,112].

All of these fractionation methods can be problematic, as membrane and ultrafiltration may suffer from artifacts including charge repulsion effect, solute adsorption, contamination of the membrane and membrane clogging [42,114-117]. Centrifugation can be time-consuming and costly, and there may be an increased collision rate causing aggregation or precipitation of colloids [42]. A comparison in filtration and centrifugation techniques for the size fractionation of colloidal material is discussed in Chapter 3. In size exclusion chromatography (SEC) there can be problems with adsorption due to van der Waals and electrostatic forces between the surface of the gel and the analyte molecules which will affect the retention time [110]. The SEC technique involves the injection of samples into a column containing a porous gel where the smaller molecules become included in the pores of the gel and the larger molecules excluded. This results in the larger molecules eluting first [109,110]. SEC is also referred to as high performance SEC (HPSEC) because of the use of tightly packed columns operating at high pressures of >500 psi to give fast, high-resolution chromatograms [110]. Gel chromatography, like ultra-filtration, can also have problems of charge repulsion effects and solute adsorption [114,115,118]. Gel chromatography is a technique similar to SEC except that there are other factors that make this separation different. Ion exclusion factors will result in a small charged molecule being excluded from the gel and eluting at about the same time as a large molecule that has not been able to penetrate the gel. Whereas adsorption factors will result in a large molecule absorbing onto the gel and eluting at about the same time as a small molecule that had penetrated the gel. Therefore a longer retention time does not necessarily indicate a lower size [7].

As the composition of colloidal material is constantly changing, samples need to be characterised as quickly as possible. Buffle and Leppard suggested that any method that results in energy changes e.g. heating, or chemical modifications of the system e.g. electrolyte or colloid concentration changes, should be avoided or at least minimised, in order for accurate determination of the colloidal material [97]. Therefore they suggested the use of a promising separation technique called field-flow fractionation (FFF) [115].

1.5.2 Field-flow fractionation

Giddings first proposed the theory of FFF in the 1960s [119]. It is a separation technique similar to liquid chromatography but, unlike chromatography, the separation channel does not require a stationary phase and contains no packing material [120]. In FFF, molecular degradation of samples is minimised [110] and there are fewer problems with adsorption or size exclusion [121] compared to the separation methods described in section 1.5.1. Particle size distributions, diffusion coefficient characterisation and relative molecular mass information can all be obtained using this relatively mild separation technique [122]. There are many sub-techniques of FFF, which include sedimentation (Sd), flow (Fl), thermal (Th), electrical (El) and gravitational (Gr) FFF, and the earliest commercial SdFFF, ThFFF and FlFFF instruments were available in the late 1980s and early 1990s from Du Pont and FFFractionation in the USA [120].

Of the different sub-techniques, FlFFF is the most versatile and widely used, because displacement of the sample components by a crossflow acting as the field is universal [120]. FlFFF is applicable to macromolecules, particles and colloids ranging from 0.001 μm (approximately 1,000 molecular mass) up to at least 50 μm in diameter [123]. FlFFF has great flexibility in terms of sample type, carrier liquid (solvent), pH and ionic strength [124]. It provides high selectivity and speed, simple coupling to detectors and ready collection of fractions [125]. A possible limitation of FlFFF can be molecular weight cut-

off of the membrane that determines the lowest molecular size that can be retained in the channel. Loss of sample through the membrane, or more likely by adsorptive interactions with the membrane, can also occur [110].

Variations of FlFFF incorporate the use of different channels [125], such as asymmetrical [126-128] and hollow-fibre channels [129,130]. The symmetrical FlFFF sub-technique was used in this work where the crossflow is achieved by pumping the carrier liquid directly across the channel through porous frits [131].

SPLITT fractionation (SF) is a technique similar to FFF except that it has the ability to separate relatively large quantities of sample (mg or g) in a reasonable amount of time. The channel is similar to a FFF channel and has at least one flow splitter at the outlet and sometimes at the inlet of the channel. It differs from FFF as it can only resolve the sample into two sharply defined fractions that are collected and analysed [120,132].

1.5.3 FlFFF instrumentation

Separation in FlFFF takes place in a thin, ribbon-like channel that has a rectangular cross-section and triangular end pieces. A schematic diagram of a FlFFF channel is shown in Fig. 1.7. The typical dimensions of a channel are 25-50 cm long, about 2-3 cm wide, and 50-250 μm thick [133]. The channel comprises two machined blocks with inset porous frits that clamp together a Mylar or Teflon spacer and a membrane. Plexiglas® (polymethylmethacrylate) blocks have been used when working with aqueous solutions [134-138], because the presence of any air pockets or bubbles can be easily observed through these blocks. Any bubbles will form regions of non-uniform crossflow, and will show up as broadened peaks, perhaps with spikes or a noisy baseline on the fractogram.

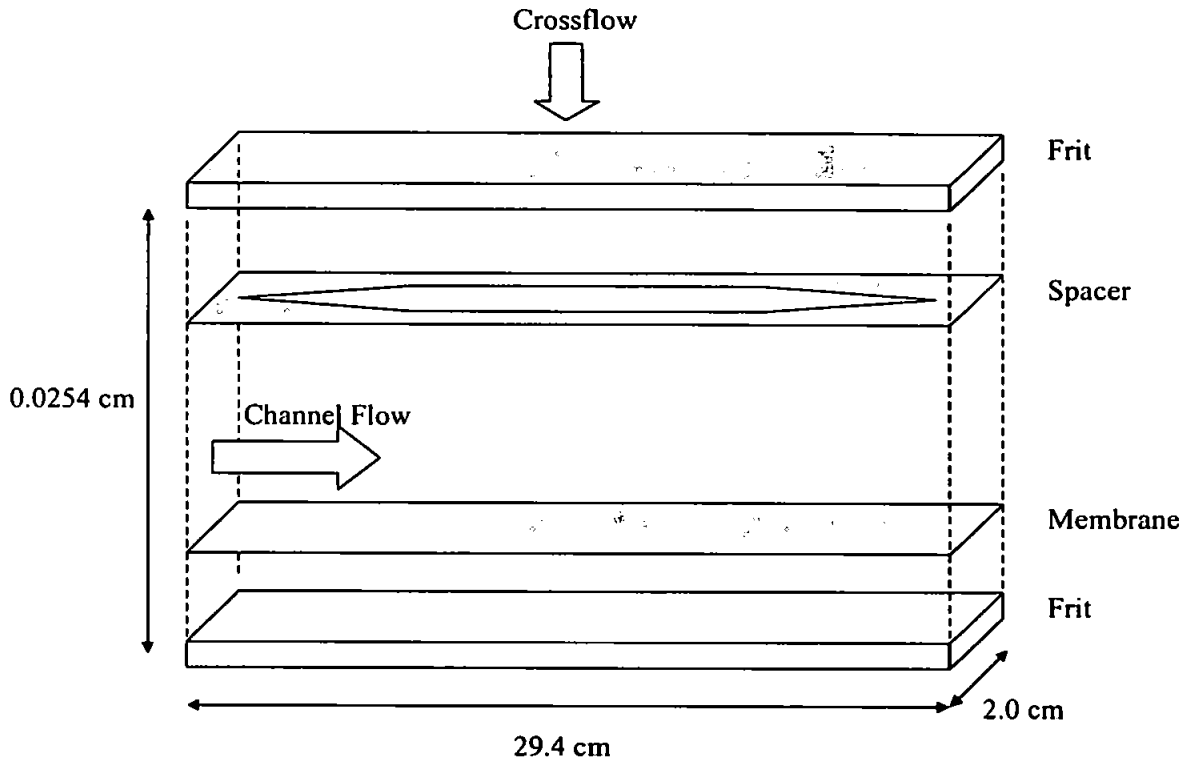

Figure 1.7. Schematic diagram of a FlFFF channel.

Ceramic frits with a pore size of 2-5 μm are used in commercial instruments [120]. The membrane acts as the accumulation wall and is stretched across the bottom frit. Selection of an appropriate membrane depends on the macromolecules or particles being separated and the pore size should be small enough to retain the analytes but large enough to allow the carrier solution to pass through it. There are many different types of membranes available with varying molecular weight cut-off points. However, it is essential that the membrane is flat and smooth because any flaws will affect the separation process.

Two pumps usually control the channel flow and crossflow in a FlFFF system; the most commonly used are high-performance liquid chromatography (HPLC) pumps because they supply accurately controlled flow rates in a convenient manner [120]. It is possible to use one pump and split the flow and, occasionally, an additional pump that pulls the liquid from the channel or crossflow outlet has been used [139-141]. This pump was used to achieve rapid flow equilibration and reduce or eliminate the need for flow measurement

and regulation. In general, flow rates in normal mode FlFFF range from 0.2–5 mL min^{-1}. In steric mode, faster flow rates lead to the formation of hyperlayers, which allow extremely fast, efficient separation of μm-sized particles [120].

Errors occur when the two incoming flow rates are not equal to the corresponding outgoing flow rates. When variations occur, retention times will be different to those predicted and may vary between runs, so the flow rates in FlFFF need to be accurately measured and regulated. This is achieved by either using a crossflow loop incorporating a HPLC or syringe pump (recirculating mode), or measuring the flow rates of the channel and crossflow outlets and placing a pressure restrictor on at least one outlet (non-recirculating mode). In recirculating mode, the rate of the crossflow entering the channel should be equal to the flow being drawn from the channel by the HPLC or syringe pump. In non-recirculating mode flow rates can be measured using a stopwatch and burette or, preferably, an electronic balance.

In the crossflow loop, the crossflow outlet is connected to the inlet of the pump, and the outlet is connected to the crossflow inlet. To avoid cavitation of the carrier liquid within the pump, the channel should be pressurised by placing a back-pressure regulator at the axial outlet of the channel. In FlFFF, the pore size of the membrane determines the pressure required to obtain the desired crossflow rate, but generally the pressures in the system are low, usually less than 100 psi.

1.5.4 Frit inlet and frit outlet

There are other variations of symmetrical FlFFF with channels that have a frit or split flow inlet. This configuration utilises either a frit element embedded in the wall opposite the accumulation wall of the channel near the inlet or a thin flow splitter that divides the inlet region into two flow spaces. Hydrodynamic relaxation achieved using this configuration is

an alternative to field driven relaxation, is rapid and does not require a stopflow procedure. The sample components are driven to the vicinity of their equilibrium positions by the channel flow, which does not need to be stopped or bypassed, thus avoiding disruption in the channel [142].

A frit outlet configuration has been used for concentration enhancement to increase the detection sensitivity. The sample free carrier liquid that flows above the sample layers is skimmed out so that only the concentrated sample flows through the detector [143]; this is especially useful when analysing environmental samples with low analyte concentrations [144]. Another method of on-line sample pre-concentration, called the opposed flow sample concentration (OFSC), has been used effectively to determine colloids in river water [137].

1.5.5 Carrier liquid

The carrier liquid used in FlFFF needs to be chosen carefully so that there is no appreciable swelling of the membrane, as this can lead to non-uniform flows in the channel. The carrier liquid should also be of low viscosity because the crossflow field required to produce a given crossflow is directly proportional to the viscosity of the medium. In FlFFF aqueous solutions are usually used as carrier liquids, although non-aqueous solvents have been used [139,145]. The aqueous carrier liquids are usually filtered through a 0.2 μm filter and sometimes degassed by heating or by bubbling helium gas through the carrier. Doubly distilled and deionised water is recommended for the preparation of aqueous carrier liquids and a surfactant or buffer is usually added. Several anionic and non-ionic surfactants have been used [120] and these are shown in Table 1.1. In choosing an appropriate surfactant, any interference with the detector response, potential interactions with channel materials, the resulting ionic strength, and the effective dispersion of the particles need to be considered. The use of buffers in aqueous carrier liquids is particularly useful when

analysing biological materials [124,143,146-148]. A bactericide such as sodium azide at a concentration of 0.01-0.02 % (m/v) is frequently added to prevent bacterial growth.

Table 1.1. Surfactants used in FlFFF

Surfactant Type	Name
Anionic	FL-70 (oleic acid, sodium carbonate, tergitol, tetrasodium EDTA, polyethylene glycol, and triethanolamine); SDS (sodium dodecyl sulphate)
Non-ionic	Brij-35 (polyoxyethylene ether: 23 lauryl ether); Pluronic F68®; Triton X-100 (octylphenoxy polyethoxy ethanol); Tween 20 (polyoxyethylene sorbitan: monolaurate); Tween 60 (polyoxyethylene sorbitan: monostearate)
Cationic	CTAB (cetyl trimethylammonium bromide)

1.5.6 Detectors

Many detectors have been used in FlFFF, but the most common detector is a UV/visible spectrophotometer. Photodiode arrays have been used to obtain the entire UV/visible spectra of eluting samples instead of monitoring a single wavelength [149,150]. By coupling detectors on-line, more detailed information can be obtained about the sample being analysed and UV/visible spectrophotometry has been coupled with e.g. multi-angle laser light scattering (MALLS), differential refractive index (DRI), fluorescence and, more recently, inductively coupled plasma-mass spectrometry (ICP-MS) [122,140,151-153]. Other detectors that have been occasionally used are electrospray mass spectrometry (ESMS) [154] and laser induced breakdown spectroscopy (LIBS) [155,156].

1.5.7 The separation process

In FlFFF there are two liquid flows acting on the sample components. One is the channel flow that runs through the channel, and the other is a crossflow that flows perpendicular to the channel and passes through the inlet frit into the channel and exits through the membrane and outlet frit. The channel flow is laminar with a parabolic flow profile [120] and hence the velocity is zero at the walls of the channel, because of frictional drag and increases to a maximum in the centre of the channel.

A common procedure for injecting a sample is called 'stopflow relaxation', in which a small volume sample (typically 3-10 μL) is injected into the channel flow. After a short delay period, that allows the sample to move into the channel from the injector, the channel flow is stopped for a certain amount of time (relaxation time or stopflow time), allowing only the crossflow to act on the sample [120]. A typical FlFFF manifold in both the load (stopflow) and inject (run) configurations is shown in Figs. 1.8A and 1.8B respectively. Stopflow time is determined to be sufficient by calculating the time for two channel volumes of crossflow to pass across the channel [157]. During this relaxation time the channel flow is diverted around the channel and flows directly to the detector to avoid a large baseline disturbance. The crossflow carrier liquid passes through the membrane during the relaxation time and the sample accumulates near the membrane surface.

A steady state distribution is reached when the crossflow driving force is balanced by the diffusion (Brownian motion) of macromolecules or particles back into the channel [149]. Exponential concentration distributions of different mean layer thicknesses are formed at the membrane for each different component [134]. The position of the macromolecules is determined by their diffusion coefficients; the smallest macromolecules, with the highest diffusion coefficients and largest mean layer thicknesses, will spread out farthest from the membrane. When the channel flow is reintroduced, the run commences and the smaller macromolecules that encounter the higher velocity of the laminar flow profile will be eluted from the channel first [158]. As a result, molecules of different sizes have different retention times and their diffusion coefficients can be calculated directly from theoretical equations, whereas their relative molecular masses are determined from a calibration graph. A separate calibration graph is needed for each type of polymer because of differences in molecular conformation. The theoretical aspects of this process are described in section 1.5.9.

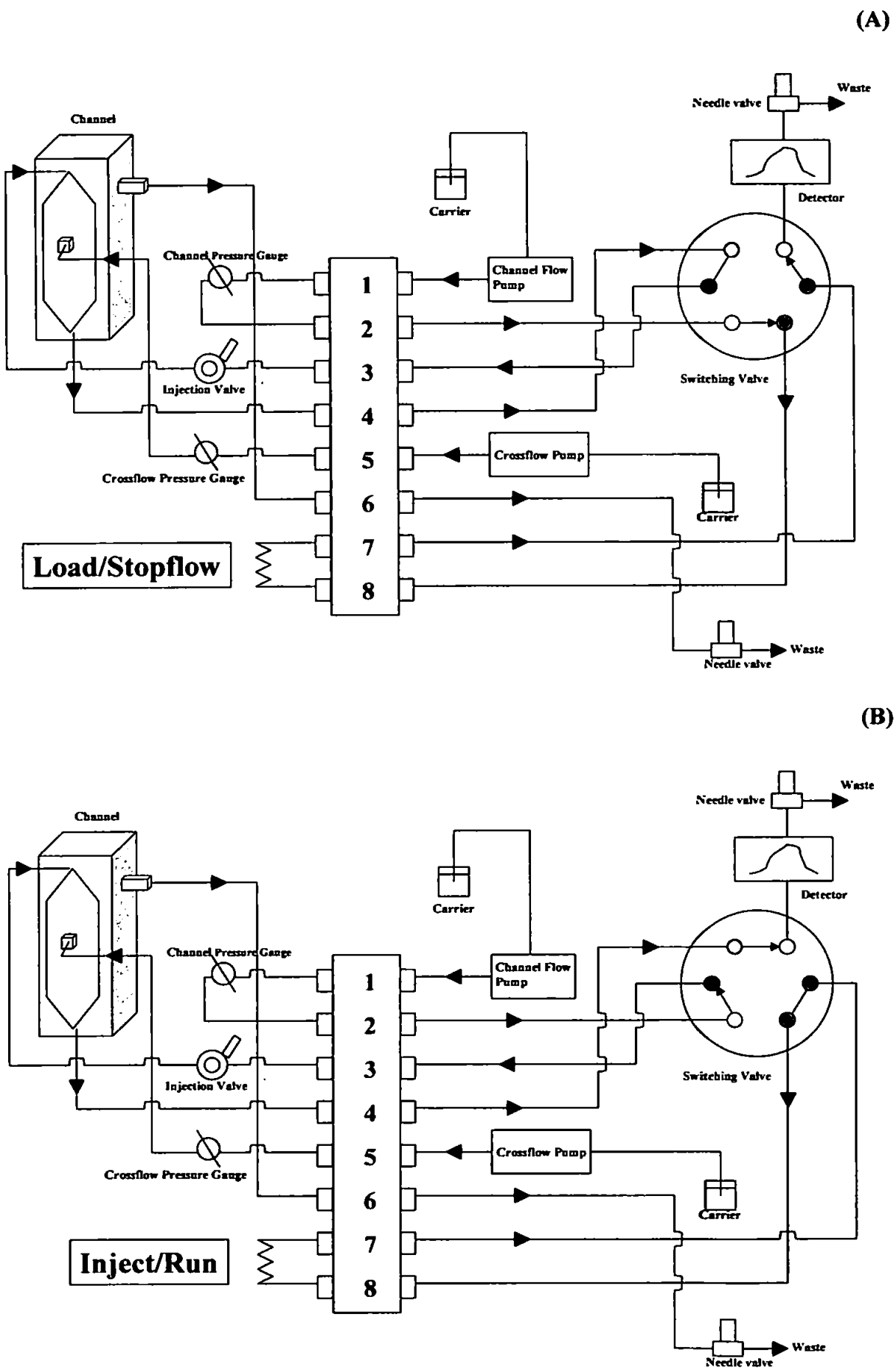

Figure 1.8. A typical FlFFF manifold in: (A) load (stopflow) position; (B) inject (run) position.

1.5.8 Operating modes in FlFFF

There are two operating modes in FlFFF. Normal or Brownian mode, as described above, is applicable to macromolecules and colloids less than about 1-2 μm in size. The alternative steric/hyperlayer mode can cover the range 0.5-100 μm [123]. A schematic diagram depicting how a sample is separated in normal mode is shown in Fig. 1.9A. The normal operating mode was so called because this was the only operating mode used in FFF until the steric mode was introduced in the late 1970s [135].

In the steric/hyperlayer operating mode, shown schematically in Fig. 1.9B, the larger particles elute first and this inversion in elution order is referred to as steric inversion [159]. It generally occurs around diameters of 1 μm when the Brownian motion of the molecules becomes too weak to oppose the field and all particles are initially forced onto the accumulation wall. The particles are also subjected to a lifting force from the channel flow along the membrane and reach an equilibrium position in the channel at which the lift forces balance the crossflow force. Larger particles experience greater lift and are therefore further away from the membrane and consequently elute before smaller particles [123].

Programmed FlFFF, in which the field strength or flow velocity is varied during the run in order to speed up the elution of slowly migrating components whilst maintaining the resolution of early eluting components, has also been used [120,135]. In flow programming, the incoming and outgoing flow rates need to be equalised at all times during the run. Again this can be achieved using a crossflow loop, with a flowmeter incorporated in the loop, as the outlet flow rate is forced to equal the incoming flow rate at all times. In this setup the channel needs to be pressurised by placing a back-pressure regulator at the axial outlet of the channel and this pressure should be higher than that needed to establish the desired crossflow rate. This method has been used successfully to analyse environmental [160] and biological [124] samples.

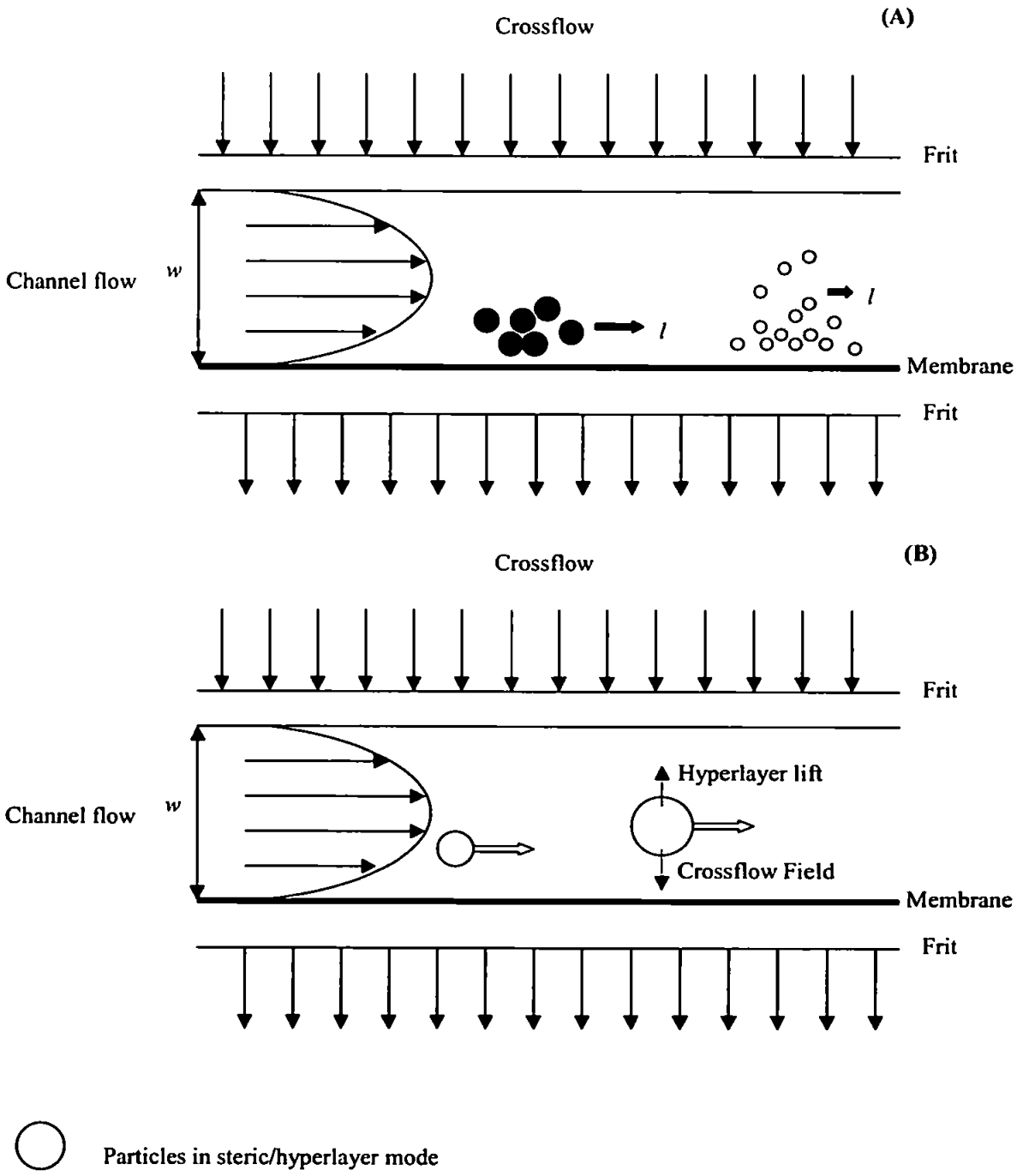

Figure 1.9. Separation of particles by: (A) Normal operating mode; (B) Steric/hyperlayer operating mode.

1.5.9 Theoretical aspects

The following is a summary of the important relationships between key instrumental parameters. They provide a sound basis for the experimental optimisation of the system.

A fractogram is obtained by plotting the detector response against the elution volume or time of the emerging sample. The relative elution behaviour of each sample component can be determined by calculating the retention ratio R, which is the ratio of the average velocities of the sample components and the carrier liquid [123]. From chromatographic theory the retention ratio is defined as:

$$R = \frac{v_r}{\langle v \rangle} = \frac{t^0}{t_r} = \frac{V^0}{V_r} \tag{4}$$

and from FFF theory as:

$$R = 6\lambda\left[\coth\left(\frac{1}{2\lambda}\right) - 2\lambda\right] \tag{5}$$

where v_r is the sample migration velocity, $\langle v \rangle$ is the cross-sectional average velocity of carrier liquid, t^0 is the void time, t_r is the retention time, V^0 is the void volume, V_r is the retention volume and λ is the retention parameter.

λ can be expressed as follows:

$$\lambda = \frac{\ell}{w} = \frac{D}{Uw} = \frac{kT}{Fw} \tag{6}$$

where ℓ is the mean layer thickness of each sample component, w is the channel width, D is the diffusion coefficient, U is the field-induced transport velocity, k is the Boltzmann's constant (1.38×10^{-16} g cm^2 s^{-2} K^{-1}), T is the absolute temperature, and F is the driving force. From equation (6) it can be seen that ℓ can be expressed in terms of the diffusion coefficient of the particle (D) and its field induced transport velocity (U) or the ratio of the thermal energy (kT) to the driving force (F) exerted on the particle.

When a crossflow is applied in FlFFF, the sample components will move with a field induced transport velocity (U) until they reach the accumulation wall. The field force is induced by the frictional drag on a particle held stationary by the membrane with carrier liquid flowing past [123]. This force (F) is expressed as:

$$F = fU \tag{7}$$

where f is the friction coefficient.

By substituting equation (7) into equation (6), an expression for λ is obtained:

$$\lambda = \frac{kT}{fUw} \tag{8}$$

U is obtained from the volumetric crossflow rate ($\dot{V}_c$) and the channel dimensions, therefore:

$$U = \frac{w\dot{V}_c}{V^0} \tag{9}$$

By substituting equation (9) into equation (8), λ can be expressed as:

$$\lambda = \frac{kTV^0}{w^2\dot{V}_c f} \tag{10}$$

The retention parameter can also be expressed using the Nernst-Einstein equation ($f = kT/D$) as:

$$\lambda = \frac{D}{wU} = \frac{V^0 D}{w^2\dot{V}_c} \tag{11}$$

and alternatively using the Stokes equation ($f = 3\pi\eta d$) as:

$$\lambda = \frac{kTV^0}{3\pi\eta w^2\dot{V}_c d} \tag{12}$$

where η is the viscosity of the carrier liquid (η=0.01 g cm^{-1} s^{-1} at 20 °C) and d is the hydrodynamic diameter.

For well-retained particles ($\lambda \ll 1$), equation (5) can be re-written as $R=6\lambda$. By substituting equation (12) into this reduced expression, the retention ratio is expressed as [95]:

$$R = \frac{2kTV^0}{\pi\eta w^2 \dot{V}_c d} \tag{13}$$

Rearranging equation (13) gives:

$$\dot{V}_c = \frac{2kTV^0}{\pi\eta w^2 dR} \tag{14}$$

As retention time can be approximated using $R = \frac{V^0}{t_r \dot{V}}$, then:

$$\dot{V}_c = \frac{2kTt_r\dot{V}}{\pi\eta w^2 d} \tag{15}$$

where $\dot{V}$ is the volumetric channel flow rate.

The retention time in FIFFF is expressed as:

$$t_r = \frac{\pi\eta w^2 d\dot{V}_c}{2kT\dot{V}} \tag{16}$$

These relationships were first derived by Giddings and further details can be found elsewhere [120]. The diffusion coefficient can therefore be calculated and related to relative molecular mass (M) (where A' and b are constants for a given polymer-solvent system) by:

$$D = A'M^{-b} \tag{17}$$

Using calibration standards, a calibration graph can be obtained by plotting log D against log M and relative molecular mass for sample components can be determined from equations (4), (5) and (11).

1.5.10 Applications

Tables 1.2-1.5 summarise the application of FlFFF to environmental (Table 1.2) and biological (Table 1.3) matrices and to the detection of polymers (Table 1.4) and inorganic colloids (Table 1.5). Each table is ordered alphabetically in terms of analytes and states the crossflow system, the membrane, the carrier liquid and the detector used in each application. There are also specific technical comments where appropriate. Environmental applications include assessments of colloids in freshwater and seawater, characterisation of dissolved organic material, including fulvic and humic acids, and colloidally associated trace elements in natural and effluent waters. The application of FFF to environmental matrices has to date used SdFFF as well as FlFFF.

In terms of the relative performance of FlFFF and SdFFF the following general statements can be made:

1. FlFFF extends the size range that can be separated below 50 nm, enabling the detection of dissolved macromolecules.
2. FlFFF separates on the basis of the size of the molecules/particles alone, and the process is independent of density whereas SdFFF separates on the basis of buoyant mass i.e. size density. Therefore the interpretation of the results from SdFFF is more difficult.

Both SdFFF and FlFFF techniques have been used for the analysis of soil suspensions and these are described in Chapters 3 and 4 respectively.

Table 1.2. Environmental applications

Analyte	Crossflow	Membrane*	Carrier Liquid	Detector	Comments	Ref.
Colloids (in coastal seawater)	Recirculating	Regenerated cellulose, 10,000 Da nominal MWCO	Seawater with addition of biological nonionic surfactant (Pluronic® F68) to final concentration of 0.1% (v/v)	UV (254 nm)	Used polystyrene latex beads (standards). Channel with frit outlet	[161]
Dissolved organic material (coloured, in river and coastal waters)	Recirculating	Regenerated cellulose, 3000 Da nominal MWCO for globular compounds (FFFractionation)	0.005% FL-70, 0.05 M Trisma and 0.029 M HCl prepared in organic-free distilled water, to give a pH of 8 and ionic strength of 0.08 M	UV (330 nm) and fluorescence	Frit inlet/frit outlet FIFFF (FIFO-FIFFF). Also used polystyrene sulphonate, sodium salt standards	[144]
Diesel soot particles	Not stated	Regenerated cellulose (YM-10, Amicon), 10,000 MWCO	Doubly distilled and deionised water containing 0.01% (w/v) Triton X-100, 0.02% (w/v) NaN_3	UV (254 nm)	Also used polystyrene latex standards	[162]
Dissolved organic carbon (in fresh and marine waters)	Non-recirculating	Modified polyether sulphone (Omega), 1000 MWCO - optimum membrane	(i) 25 mM Tris, 20 mM sodium chloride (ii) 10 mM borate, 20 mM sodium chloride - optimal carriers	UV (270 nm)	Various ultrafilter membranes and carrier solutions investigated. FIFFF system modified to allow on-channel preconcentration. Also used polystyrene sulphonate standards	[158]
Dissolved organic matter (pulp and paper mill effluents)	Non-recirculating	Cellulose acetate, (manufactured in laboratory), 20-50 µm thick	Distilled deionised water with 0.05 M tris buffer adjusted to pH 8.0 ± 0.1 by addition of HCl. Ionic strength about 0.03 M	UV (254 nm)	Used sodium polystyrene sulphonate standards and polystyrene latex beads. Membrane manufactured to overcome sample interaction problems in refs. [114,150]	[163,164]
Dissolved organic matter (in seawater)	Recirculating	Regenerated cellulose (YM-10, Amicon), 10,000 Da nominal MWCO	UV-oxidised seawater	UV and fluorescence	Flow-rate programmable FFF system. Dextrans used as model dissolved organic matter compounds. Also used polystyrene latex beads (standards) in same carrier with addition of 0.1% (v/v) FL-70	[160]
Fulvic acids	Not stated	Cellulose acetate membrane	Deionised water, with pH and ionic strength adjusted to that of samples with NaOH, HCl and NaCl	UV (254 nm)		[165]
Fulvic and humic acids	Not stated	Cellulose acetate membrane (Osmonics), 1000 g mol^{-1} nominal MWCO (determined with proteins)	Several carrier liquids studied (Tris and phosphate buffer), but DI water adjusted to pH 8.5 with NaOH - optimal carrier	UV (254 nm)	Two channel designs used: symmetric and asymmetric. Used polystyrene sulphonate standards	[131]
Fulvic and humic acids	Non-recirculating	Polypropylene-backed polysulphone, (PM10F, Amicon), 10,000 MWCO	Two carrier liquids used: (i) 0.05 M TRISMA, 0.0268 M HNO_3, 0.00308 M NaN_3 (ii) 0.05% FL-70 and 0.03% NaN_3, pH 7 - optimal carrier	UV (254 and 270 nm) with a reference at 450 nm	Also used polystyrene sulphonate standards	[149]
Fulvic and humic acids	Non-recirculating	Polysulphone (PTGC, Millipore), 10,000 nominal MWCO for globular proteins	0.05 M TRISMA, 0.0268 M HNO_3, 0.00308 M NaN_3, pH 7.9	UV (254 nm) or variable wavelength detector	Some sample wall interaction. Also used polystyrene sulphonate standards and some biological test samples	[114]
Fulvic and humic acids (adsorption with hematite	Recirculating	(A) Cellulose acetate, 1000 g mol^{-1} nominal MWCO (B) Regenerated cellulose, 10,000 g mol^{-1} nominal MWCO	Two carrier solutions used: (i) DI water used for adsorption products and hematite (ii) DI water containing 0.05 vol% FL-70, 0.02 wt% NaN_3 used for hematite	(A) UV (260 nm for hematite in FL-70, and 280 nm for adsorption products); (B) coupled with MALLS	Two instruments used: (A) and (B). Also used polystyrene latex particle standards	[166]
Humic substances	Recirculating	Different membranes: regenerated cellulose, 1 kDa (Wyatt Technology), 5 and 10kDa cutoff (Schleicher and Schuell); polyethersulphone, 2 and 4 kDa (Wyatt Technology). Regenerated cellulose with 5 kDa cutoff was optimum membrane	Different carriers: 0.01% Tween 20, 0.02 w/V% NaN_3; 10^{-4} M NaOH; 0.05 or 0.005 M Tris buffer. Ionic strength and pH adjusted by NaOH and $NaClO_4$ respectively. All solutions prepared in ultrapure water. Optimal carrier: 0.005 M Tris-buffer, pH 9.1	UV. Humic and fulvic acids (254 nm), polystyrene sulphonate reference colloids (225 nm)	Also used protein and polystyrene sulphonate reference colloids	[118]
Humic substances	Non-recirculating	Cellulose acetate	0.05 M TRISMA, 0.0268 M HNO_3, 0.00308 M NaN_3 at pH 7.8	UV (254 nm)	Used polystyrene sulphonate standards	[167]
Humic substances	Non-recirculating	(i) Polysulphone (PTGC, Millipore), 10,000 MWCO for globular proteins (ii) Cellulose (YC05, Amicon), with specified 500-Da pore size	0.05 M TRISMA, 0.0268 M HNO_3, 0.00308 M NaN_3, pH 7.9	UV (254 nm), several fractograms recorded with photodiode array detector	Same method as ref. [114]. Some sample interaction with membrane still occurs. Also used polystyrene sulphonate standards and some biological test samples	[150]
Humic substances	Recirculating	Not stated, but carrier solution in membrane filtrated (10,000 MWCO) water	0.05% SDS, 0.02% NaN_3 in ultrapurified, membrane filtrated water	UV, fluorescence and MALLS	Also used polystyrene latex beads. Crossflow field programming used	[168]
Humic substances (in drinking water sources)	Not stated	Cellulose acetate membrane, 100 MWCO	0.05M TRISMA, 0.0268 M HNO_3, 0.00308 M NaN_3, pH 7.9	UV (254 nm)	Used polystyrene sulphonate standards	[110]
Phytoliths (biosilicate plant microfossils)	Recirculating	Polypropylene membrane (Celgard, Hoechst-Celanese) having size cutoff of 50 nm	0.15% (v/v) FL-70, 0.02% (w/v) NaN_3 in deionised and degassed water	UV (260 nm)	Also used polystyrene latex standards. Flow field programming used	[133]
River sediment and water	Non-recirculating	0.03 µm Polycarbonate with hydrophilic poly(vinylpyrrolidone) (PVP) coating (Poretics) - optimal carrier	0.1% SDS, 0.1% NaN_3 in doubly distilled deionised water- optimal carrier	UV (254 nm)	Opposed flow sample concentration (OFSC) technique. Various ultrafiltration and microfiltration membranes and carrier solutions investigated. Also used proteins and polystyrene latex beads standards	[137]
Trace elements complexed to humic acids and colloidal organic material (in municipal wastewater)	Non-recirculating	Polyregenerated cellulose ultrafiltration membrane, 3000 Da MWCO	30 mM TRIS-HNO_3, pH 7.3 or doubly distilled water	UV (254 nm) and ICP-MS	Also used polystyrene sulphonate and protein standards (protein standards not suitable for calibrating humic acids)	[122]
Trace elements in colloidal material (in freshwaters)	Non-recirculating	1000 MWCO ultrafilter membrane (Omega)	Borate buffer solution in Milli-Q water - 5 mM borate, 10 mM sodium chloride, pH 8.1	UV (270 nm) and ICP-MS	Modified to allow injection of large sample volumes [140,158]	[153]
Trace elements in colloidal material (in natural waters)	Non-recirculating	1000 MWCO ultrafilter membrane (Omega)	pH 8.1 buffer containing 5 mM borate, 10 mM sodium chloride in Milli-Q water	UV (270 nm) and ICP-MS	Modified to allow injection of large sample volumes [158] (Preconcentration method). Also used polystyrene sulphonate standards	[140]

*Membrane type and manufacturer as written in the literature

Table 1.3. Biological applications

Analyte	Crossflow	Membrane*	Carrier Liquid	Detector	Comments	Ref.
DNA	Not stated	Regenerated cellulose (YM-30, Amicon)	Tris-HNO_3 at ionic strength of 0.1 M and pH 7.8	UV (260 nm)		[146]
DNA (cationic lipid complexes)	Non-recirculating	(i) Regenerated cellulose (Millipore), 30,000 MWCO (ii) 0.03 μm pore size polycarbonate (Osmonics) (iii) Polypropylene having 0.05 x 0.125 μm pore dimensions (Celgard 3402, Hoechst-Celanese)	(i) Distilled and deionised water containing 0.02% (w/v) NaN_3 (ii) 0.089 M Tris-borate buffer, pH 8.59	UV (260 nm), MALLS and RI	Two FlFFF channels used. Channel I with frit outlet. Three membranes and two carrier liquids investigated	[138]
DNA (linear and circular)	Non-recirculating	Diaflo ultrafiltration YM-30, Amicon	Tris-HNO_3 buffer of ionic strength 0.1 M and pH 8.0 with 1.0 mM EDTA. Used doubly distilled water	UV (260 nm)		[169]
Lipoproteins (in plasma)	Recirculating	Many ultrafiltration membranes studied. Most appropriate are YM-30 (30kDa MWCO), YM-100 (100kDa MWCO) and XM-300 (300kDa MWCO), Amicon	Phosphate-buffered saline (PBS) (138 mM sodium chloride, 2.7 mM potassium chloride, 10 mM phosphate buffer salts) at pH 7.4. Doubly distilled deionised water used	UV (280 nm)	Frit-inlet hydrodynamic relaxation FlFFF system. Used isocratic and programmed-field procedures. Also used proteins	[124]
Lipoproteins (in plasma)	Not stated	Regenerated cellulose (YM-30, Amicon)	Phosphate buffer at pH 7.4	UV (280 nm)	Frit inlet channel used, no stopflow procedure necessary	[146]
Lipoproteins and proteins	Recirculating	YM-1 or YM-10 ultrafiltration membranes, Amicon	Phosphate-buffered saline (PBS) (138 mM sodium chloride, 2.7 mM potassium chloride, 10 mM phosphate-buffered salts) at pH 7.4. Doubly distilled deionised water used	UV (280 nm)	Frit-inlet and frit-outlet FlFFF system	[143]
Liposomes	Not stated	Regenerated cellulose (YM-10, Amicon)	(i) TRIS-HCl buffer solution, pH 7.8 (ii) PBS buffer (iii) Lactose solution with NaCl (iv) 3.08 mM NaN_3	UV (254 nm)	Different carrier solutions used. Liposome samples (prepared in four different electrolyte solutions) are run using the corresponding solution as carrier. Also used polystyrene latex standards [carrier - 0.05% SDS and 0.02% NaN_3, in ultrapure water (purified by reverse osmosis and deionised)]	[170]
Mucin (biological surfactant)	Not stated	YM10, Amicon, 10,000 Da MWCO	PBS containing 0.1% FL-70	UV (254 nm)	Analysed bovine submaxillary gland mucin coating on polystyrene latex particles	[148]
Pollen grains	Not stated	Ultrafiltration membrane YM30, Amicon	Isoton II solution using doubly distilled deionised water	UV (254 nm)	Used frit inlet FlFFF channel	[171]
Protein conjugates	Not stated	Polypropylene (Celgard 2400, Hoechst-Celanese)	Water	UV (200 nm)		[146]
Proteins	Not stated	Regenerated cellulose, (YM-10, Amicon)	Tris-HNO_3 at ionic strength of 0.1 M and pH 7.8	UV (280 nm)		[146]
Proteins	Not stated	Polypropylene (Celgard 2400, Hoechst-Celanese)	Phosphate buffer at pH 7.5	UV (280 nm)		[146]
Proteins	Non-recirculating	Channel I: YM-10, Amicon, 10,000 MWCO Channel II: YC-5, Amicon, 5,000 MWCO Channel III: Cellulose, (YM5, Amicon), 5,000 MWCO	Channel I and III: Tris-HNO_3 (ionic strength 0.1 M) and 1mM EDTA (pH 7.9). Channel II: PBS (containing 120 mM sodium chloride, 2.7 mM potassium chloride, 10 mM phosphate buffer salts) at pH 7.4. Used doubly distilled water in all carriers	UV (280 nm)	Two frit inlet channels (hydrodynamic relaxation) and one conventional channel used for stopflow experiments	[147]
Proteins	Non-recirculating	Regenerated cellulose ultrafiltration membrane (FFFractionation), 3000 Da MWCO	0.1 M TRIS-HNO_3, pH 8	UV (280 nm) and ICP-MS		[172]
Proteins	Non-recirculating	Regenerated cellulose (YM10, Amicon), 10,000 MWCO	For PS: 0.1% FL-70 and 0.02% NaN_3; For protein standards: Tris buffer solution at various pH and ionic strengths; For real samples: potassium phosphate buffer	UV	Also used polystyrene latex standards	[173]
Proteins (wheat)	Recirculating to give optimum resolution	Cellulose (YM-10, Amicon), 10,000 Da MWCO	0.05 M acetic acid in deionised distilled water containing 0.002% FL-70, pH 3.1	UV (210 nm)	Different operating conditions using automated FIFO FlFFF. Optimum conditions was for frit inlet flow and crossflow to be recirculating. Also used protein standards	[174]
Proteins (wheat)	Not stated	Cellulose, (YM-10, Amicon)	0.05 M acetic acid with 0.002% FL-70	UV (210 nm)	Also used proteins	[175]
Proteins (wheat)	Not stated	YM-10 membrane	0.05 M acetic acid with different concentrations of surfactants: Brij 35, CTAB, FL-70, SDS, Tween 20, Tween 80, Triton X-100. Best choice was FL-70	UV (210 nm)	Also used proteins	[176]

* Membrane type and manufacturer as written in the literature

Table 1.4. Application to polymers

Analyte	Crossflow	Membrane*	Carrier Liquid	Detector	Comments	Ref.
Acrylate latex, polystyrene latex standards	Not stated	Regenerated cellulose (YM-30, Amicon)	Doubly distilled water with 0.05% (w/v) SDS, 0.02% (w/v) NaN_3	UV (254 nm)		[177]
Amphiphilic pullulan	Not stated	Not stated	0.1 M $LiNO_3$ for carboxymethylpullulan; 10 mM Tris-HCl, pH 7.4 in Milli-Q water for other amphiphilic pullulans	MALLS and DRI		[178]
Amphiphilic water-soluble copolymers	Recirculating	Ultrafiltration membrane of regenerated cellulose, 10,000 MWCO	0.1 M $LiNO_3$ and 0.02% NaN_3 in Milli-Q water	MALLS and RI		[179]
Gelatin/sodium polystyrene sulphonate, gelatin/sodium poly(2-acrylamido-2-methylpropanesulphonate) (NaPAMS)	Not stated	Not stated	10 mM sodium acetate buffered at pH 5.6 containing 0.1% Tween-20	UV (254 nm)	Also used polystyrene standards	[180]
Poly(ethylene oxide)	Non-recirculating	PLGC-regenerated cellulose ultrafiltration membrane (Millipore)	(i) Doubly distilled deionised water, (ii) 0.025 M sodium sulphate (iii) 0.025 M potassium sulphate	Interferometry		[136]
Poly(l-lactide) microspheres	Not stated	Regenerated cellulose (YM-30, Amicon)	Ultrapure water (reverse osmosis and deionised) containing 0.05% SDS and 0.02% NaN_3	UV (254 nm)	Also used polystyrene latex beads	[181]
Polyacrylamide standards, commercial flocculants	Recirculating	Regenerated cellulose, 10^6 nominal MWCO (FFFractionation)	Dilute nitric acid in Milli-Q water at pH 3.8 ± 0.1, vacuum filtered to 0.22 μm	MALLS and DRI	Channel with frit outlet. Crossflow field decay runs	[182]
Polyacrylamide, polystyrene-divinylbenzene latex standards	Recirculating	Regenerated cellulose, 10^6 nominal MWCO (FFFractionation)	Dilute nitric acid in Milli-Q water at pH 3.8 ± 0.1, bulk filtered to 0.2 μm - optimal carrier	UV (230 nm), MALLS and DRI	Also used commercial polyacrylamide. Channel with frit outlet. Crossflow field decay runs	[183]
Polysaccharide (gum arabic)	Not stated	Regenerated cellulose, 10,000 g mol^{-1} MWCO	0.1 M $LiNO_3$, using Milli-Q water	MALLS and DRI		[184]
Polysaccharide (pullulan)	Recirculating	Regenerated cellulose (YM-10)	Deionised and distilled water with 0.1 M $NaNO_3$, 0.02% (w/w) NaN_3	MALLS and DRI		[185]
Polystyrene	Non-recirculating	Cellulose nitrate membrane (El 41, Schleicher and Schuell)	Organic solvent ethylbenzene used	RI		[139]
Polystyrene core-shell latex particles	Not stated	Regenerated cellulose ultrafiltration membrane (YM30, Amicon)	Phosphate buffers at different pHs	UV (254 nm)	Also used polystyrene latex standards	[186]
Polystyrene latex and dextran	Recirculating	Not stated	0.1 M $NaNO_3$ containing 0.02% w/w NaN_3	MALLS and DRI	Also analysed cationic polyelectrolyte and a pectin solution. Also analysed bovine serum albumin (globular protein) and tobacco mosaic virus using SDS with NaN_3 as carrier	[121]
Polystyrene latex beads (standards)	Non-recirculating	Diaflo YM10 membrane, Amicon	Doubly distilled water with 0.1% FL-70, 0.02% NaN_3	UV (254 nm)	Two FlFFF systems: split inlet and frit inlet (hydrodynamic relaxation)	[142]
Polystyrene latex beads (standards)	Not stated	Celgard 2400 microfiltration membrane (Hoechst-Celanese) and YM30 ultrafiltration membrane (Amicon)	Doubly distilled deionised water containing 0.1% (w/v) FL-70 and 0.02% (w/v) NaN_3	UV (254 nm)	Also analysed latex beads (standards) and seeds using ultrafiltration YM10 membrane (Amicon)	[171]
Polystyrene latex microbeads, polyvinylchloride latex (standards)	Non-recirculating	YM10 membrane, Amicon	Doubly distilled water containing 0.1% (v/v) FL-70, 0.02% (w/w) NaN_3	UV (254 nm)	Thin FlFFF	[134]
Polystyrene latex spheres	Recirculating	Cellulose (YM10)	Deionised and double- distilled water containing 0.005% (w/w) SDS, 0.02% (w/w) NaN_3	MALLS and DRI	Used constant and programmable crossflow	[187]
Polystyrene latex standards	Non-recirculating	YM30, Amicon, 30,000 MWCO	Distilled deionised water containing 0.1% (w/w) FL-70, 0.02% (w/w) NaN_3	UV (254 nm)	Used isocratic (nonprogrammed) and programmed conditions	[188]
Polystyrene latex standards	Recirculating	YM30, Amicon, 30,000 MWCO	Distilled deionised water with 0.1% (w/w) FL-70, 0.02% (w/w) NaN_3	UV (254 nm)	Dual field and flow-programmed lift hyperlayer FFF	[135]
Polystyrene latex standards	Not stated	Regenerated cellulose (YM-30, Amicon), 30,000 MWCO	Surfactants were (i) SDS (ii) FL-70 (iii) Triton X-100. All with 0.02% NaN_3 and in reverse osmotically purified and deionised water	UV (254 nm)	Three surfactants and seven ionic strengths investigated	[189]
Polystyrene latex standards, polysaccharide dextran	Not stated	Not stated	For polystyrene: doubly distilled water containing 0.02% NaN_3, 0.05% (w/w) SDS; for dextran: 0.1M $NaNO_3$ solution, 0.02% (w/w) NaN_3	MALLS and RI	Results compared to FFFF-UV setup show good agreement	[190]
Polystyrene latices	Recirculating	Cellulose (YM10)	0.02% (w/w) SDS and 0.02% (w/w) NaN_3	MALLS and DRI		[191]
Polystyrene particles (aqueous mode), polystyrene polymers (nonaqueous mode)	Not stated	PA 30 PBT 100 ultrafiltration membrane (Hoechst Celanese), 30,000 MWCO	Variety of nonaqueous and aqueous carriers used: cyclohexane, heptane, isooctane, THF, toluene, water and xylene	UV	Development of a FlFFF instrument capable of operating at ambient and elevated temperatures	[145]
Polystyrene standards	Recirculating	Regenerated cellulose (Schleicher and Schuell), 5 kD MWCO	0.01% Tween 20 in ultrapure water at ionic strength of 10^{-3} M ($NaClO_4$)	LLS and LIBS	Sensitivity better in LIBS than LLS	[155]
Polystyrene sulphonate standards	Not stated	Polyether sulphone, 8K (Nadir, Hoechst-Celanese)	Sodium sulphate with ionic strength of 0.0195 M	UV (200 nm)		[146]
Polystyrene sulphonate standards	Non-recirculating	10,000 MWCO (Pellicon PTGC, Millipore)	Channel I used 67 mM sodium-potassium phosphate buffer solution at pH 7.4 with ionic strength of 0.17 M. Channel II used Tris-HNO_3 buffer at pH 7.3 with an ionic strength of 0.1 M	UV (254 nm)	Two FlFFF systems used. Channel II constructed with a split outlet and employed in high flow rate studies. Channel I used in field-programming experiments	[192]
Polystyrene sulphonate standards	Recirculating	Cellulose (YM10, FFFractionation)	Deionised and double- distilled water containing 0.1 M $NaNO_3$ and 0.02% (w/w) NaN_3	MALLS and DRI	Used constant and programmable crossflow	[193]
Polystyrene sulphonate standards, polysulphonated polysaccharide	Non-recirculating	Cellulose acetate	0.05 M Tris and 3.08 mM NaN_3, HNO_3 used to adjust pH to 8	UV (254 nm)		[141]
Polystyrene sulphonate, poly(2-vinylpyridine)	Non-recirculating	Isotactic polypropylene (Celgard 2400, Hoechst-Celanese), 50 nm nominal pore width but effective pore size 20 nm	For polystyrene sulphonate: 0.05 M TRIS-HNO_3 buffer at pH 8.6 containing 0.02% (w/w) NaN_3, ionic strength 0.0079 M; as 0.0065 M Na_2SO_4 with ionic strength 0.0195 M then used. For poly (2-vinylpyridine): 0.01 M HNO_3 at pH 2 containing 0.02% (w/w) NaN_3, ionic strength 0.013 M. Carrier solution prepared with distilled and deionised water	UV (254 nm)	Molecules smaller than membrane pores retained in channel	[194]
Polystyrene sulphonate standards, polyethylene glycol standards	Not stated	Modified polyethersulphone ultrafilter membrane (Omega), 1000 Da nominal MWCO	Various buffers of different pH (between 4.7 and 9.3) and ionic strength tested	Electrospray mass spectrometry	Polystyrene sulphonate standards and UV detector (254 nm) used for separation optimisation. Also analysed malto-oligosaccharides	[154]
Poly (styrenedivinylbenzene) latex beads	Non-recirculating	Diaflo ultrafiltration cellulose membrane type YM5 (Amicon), 5000 MWCO	Distilled water containing 0.1% FL-70, 0.02% NaN_3	UV (254 nm)	Flow/steric FFF	[195]
Polyvinyl pyrrolidone	Not stated	Regenerated cellulose and polysulphone membranes used, both with 10,000 MWCO	Distilled deionised water	MALLS and RI	Two channels used (i) frit inlet or frit outlet operating (ii) frit inlet and frit outlet (FIFO) operating	[196]
(i) Polyvinylpyridine standards (ii) Polystyrene sulphonate standards (iii) Polyacrylamide standards	Non-recirculating	For (i) and (ii): 25 μm thin isotactic polypropylene ultrafiltration membrane (Celgard 2400, Hoechst-Celanese). For (iii) and some (ii): polyethersulphone ultrafiltration membrane (Hoechst-Celanese), 8000 MWCO	For: (i) Aqueous solution of HNO_3; (ii) Tris-HNO_3 buffer; (iii) and some (ii) Aqueous solution of Na_2SO_4. All prepared in distilled and deionised water, and at different ionic strengths and pH	Variable wavelength UV, 254 nm for (i) and for some (ii); 200 nm for (iii) and low-load runs of (ii)		[197]
Poly (2-vinylpyridine) standards	Not stated	Polypropylene (Celgard 2400, Hoechst-Celanese)	0.015 M HNO_3, pH 1.8	UV (254 nm)		[146]
Starch polysaccharides	Not stated	Regenerated cellulose, 10,000 g mol^{-1} MWCO	Millipore water containing 0.02% NaN_3	MALLS and DRI	Channel with frit outlet	[198]

* Membrane type and manufacturer as written in the literature

Table 1.5. Application to inorganic colloids

Analyte	Crossflow	Membrane*	Carrier Liquid	Detector	Comments	Ref.
Bentonite colloids	Recirculating	Regenerated cellulose (Schleicher and Schuell), 5 kDa MWCO	0.01% Tween 20, at an ionic strength of 10^{-4} M ($NaClO_4$) buffered to pH ~9 using 5 mM Tris buffer solution	DAWN-DSP-F light scattering photometer and ICP-MS	Also used polystyrene standards	[156]
Silica (chromatographic)	Not stated	YM30 ultrafiltration membrane, Amicon	Doubly distilled deionised water containing 0.1% (w/v) FL-70 and 0.02% (w/v) NaN_3	UV (254 nm)		[171]
Silica (chromatographic)	Not stated	(i) Regenerated cellulose (YM10, Amicon) (ii) Regenerated cellulose (YM30, Amicon) (iii) Polypropylene (Celgard 2400, Hoechst-Celanese)	(i) 10^{-3} M NH_4OH used with Celgard 2400 membrane (ii) Doubly distilled water containing 0.1% FL-70, 0.02% NaN_3 used with YM10 and YM30 membranes	UV (254 nm)	Flow/hyperlayer FFF. Also used polystyrene latex standards	[199]
Silica (fumed)	Not stated	Celgard 2400 microfiltration membrane (Hoechst-Celanese)	Doubly distilled deionised water containing 0.001 M NH_4OH	UV (254 nm)		[171]
Silica spheres, polystyrene microsphere samples	Recirculating	Two channels used, one with membrane (regenerated cellulose, FFFractionation, 10,000 MWCO) and other without	For membrane and membraneless operation (i) 0.01% v/v Triton X-100, 0.02% w/v NaN_3 (ii) 0.01% w/v SDS in Milli-Q water respectively. 5 mM Tris added when effect of pH tested (pH set at 9.5)	UV (330 nm)	Hyperlayer/flow FFF. Comparison of membrane vs. no membrane	[200]

* Membrane type and manufacturer as written in the literature

1.6 Research aims and objectives

The overall aim of this project was to obtain unique information on the nature of colloidal species in natural and polluted waters e.g. runoff waters from agricultural land. This was achieved by combining the physical separation of these complex matrices using FFF with selective detection using FI with spectrophotometric detection for the determination of phosphorus species associated with the colloidal material.

The specific objectives of the project were to:

1. Systematically investigate and compare the generic potential of FlFFF and SdFFF for the physical separation of colloidal material in soil suspensions.
2. Compare centrifugation and filtration techniques for the separation of soil suspension samples into <0.2 and <0.45 μm fractions with subsequent FFF analysis.
3. Optimise a sampling, treatment and preparation method for soil suspension samples using soils with contrasting characteristics.
4. Optimise a portable FI monitor for the determination of RP, and to optimise a digestion method for the determination of TP.
5. Test the hypothesis that FlFFF can be combined with FI and spectrophotometric detection for the determination of RP and TP associated with different size fractions of the colloidal material in the soil suspension samples.
6. Investigate the potential of FlFFF to analyse real soil runoff samples using the optimised treatment and preparation protocol, and hence provide multi-dimensional information on the physico-chemical speciation of phosphorus in agricultural runoff waters.

1.7 References

[1] Holtan, H.; Kamp-Nielsen, L.; Stuanes, A. O. Phosphorus in soil, water and sediment: An overview. *Hydrobiologia* **1988**, *170*, 19-34.

[2] Smil, V. Phosphorus in the environment: Natural flows and human interferences. *Annual Review of Energy and the Environment* **2000**, *25*, 53-88.

[3] Zhang, J.-Z.; Chi, J. Automated analysis of nanomolar concentrations of phosphate in natural waters with liquid waveguide. *Environmental Science & Technology* **2002**, *36*, 1048-1053.

[4] Daniel, T. C.; Sharpley, A. N.; Lemunyon, J. L. Agricultural phosphorus and eutrophication: A symposium overview. *Journal of Environmental Quality* **1998**, *27*, 251-257.

[5] Haygarth, P. M.; Jarvis, S. C. Transfer of phosphorus from agricultural soils. *Advances in Agronomy*, **1999**, *66*, 195-249.

[6] McDowell, R. W.; Sharpley, A. N.; Condron, L. M.; Haygarth, P. M.; Brookes, P. C. Processes controlling soil phosphorus release to runoff and implications for agricultural management. *Nutrient Cycling in Agroecosystems* **2001**, *59*, 269-284.

[7] Thurman, E. M. *Organic Geochemistry of Natural Waters*, Martinus Nijhoff/Dr W. Junk Publishers, Dordrecht, The Netherlands, 1985.

[8] Correll, D. L. The role of phosphorus in the eutrophication of receiving waters: A review. *Journal of Environmental Quality* **1998**, *27*, 261-266.

[9] Site characterisation of the South West European Marine Sites, Plymouth Sound and Estuaries (candidate) Special Area of Conservation, Special Protection Area, Marine Biological Association Occasional Publication No. 9, Langston, W. J.; Chesman, B. S.; Burt, G. R.; Hawkins, S. J.; Readman, J.; Worsfold, P, April 2003.

[10] Carpenter, S. R.; Caraco, N. F.; Correll, D. L.; Howarth, R. W.; Sharpley, A. N.; Smith, V. H. Nonpoint pollution of surface waters with phosphorus and nitrogen. *Ecological Applications* **1998**, *8*, 559-568.

[11] Higgs, B.; Johnston,A. E.; Salter, J. L.; Dawson, C. J. Some aspects of achieving sustainable phosphorus use in agriculture. *Journal of Environmental Quality* **2000**, *29*, 80-87.

[12] Hooda, P. S.; Truesdale, V. W.; Edwards, A. C.; Withers, P. J. A.; Aitken, M. N.; Miller, A.; Rendell, A. R. Manuring and fertilization effects on phosphorus accumulation in soils and potential environmental implications. *Advances in Environmental Research* **2001**, *5*, 13-21.

[13] Hooda, P. S.; Edwards, A. C.; Anderson, H. A.; Miller. A. A review of water quality concerns in livestock farming areas. *The Science of the Total Environment* **2000**, *250*, 143-167.

[14] Quinton, J. N.; Catt, J. A.; Hess, T. M. The selective removal of phosphorus from soil: Is event size important? *Journal of Environmental Quality* **2001**, *30*, 538-545.

[15] Sharpley, A. N.; McDowell, R. W.; Kleinman, P. J. A. Phosphorus loss from land to water: integrating agricultural and environmental management. *Plant and Soil* **2001**, *237*, 287-307.

[16] Robards, K.; McKelvie, I. D.; Benson, R. L.; Worsfold, P. J.; Blundell, N. J.; Casey, H. Determination of carbon, phosphorus, nitrogen and silicon species in waters. *Analytica Chimica Acta* **1994**, *287*, 147-190.

[17] Haygarth, P. M.; Sharpley, A. N. Terminology for phosphorus transfer. *Journal of Environmental Quality* **2000**, *29*, 10-15.

[18] Heathwaite, A. L.; Johnes, P. J.; Peters, N. E. Trends in nutrients. *Hydrological Processes* **1996**, *10*, 263-293.

[19] Simard, R. R.; Beauchemin, S.; Haygarth, P. M. Potential for preferential pathways of phosphorus transport. *Journal of Environmental Quality* **2000**, *29*, 97-105.

[20] Withers, P. J. A.; Clay, S. D.; Breeze, V. G. Phosphorus transfer in runoff following application of fertilizer, manure, and sewage sludge. *Journal of Environmental Quality* **2001**, *30*, 180-188.

[21] Withers, P. J. A.; Lord, E. I. Agricultural nutrient inputs to rivers and groundwaters in the UK: policy, environmental management and research needs. *The Science of the Total Environment* **2002**, *282-283*, 9-24.

[22] Sharpley, A. N.; Kleinman, P.; McDowell, R. Innovative management of agricultural phosphorus to protect soil and water resources. *Communications in Soil Science and Plant Analysis* **2001**, *32*, 1071-1100.

[23] Loehr, R. C. Characteristics and comparative magnitude of non point sources. *WPFC* **1974**, *46*, 1849-1872.

[24] Mainstone, C. P.; Parr, W. Phosphorus in rivers - ecology and management. *The Science of the Total Environment* **2002**, *282-283*, 25-47.

[25] McDowell, R. W.; Sharpley, A. N. Uptake and release of phosphorus from overland flow in a stream environment. *Journal of Environmental Quality* **2003**, *32*, 937-948.

[26] Withers, P. J. A.; Davidson, I. A.; Foy, R. H. Prospects for controlling nonpoint phosphorus loss to water: A UK perspective. *Journal of Environmental Quality* **2000**, *29*, 167-175.

[27] Sharpley, A.; Tunney, H. Phosphorus research strategies to meet agricultural and environmental challenges of the 21st century. *Journal of Environmental Quality* **2000**, *29*, 176-181.

[28] Moss, B.; Johnes, P.; Phillips, G. The monitoring of ecological quality and the classification of standing waters in temperate regions: A review and proposal based on a worked scheme for British waters. *Biological Reviews* **1996**, *71*, 301-339.

[29] Delgado, A.; Torrent, J. Comparison of soil extraction procedures for estimating phosphorus release potential of agricultural soils. *Communications in Soil Science and Plant Analysis* **2001**, *32*, 87-105.

[30] Maher, W.; Woo, L. Procedures for the storage and digestion of natural waters for the determination of filterable reactive phosphorus, total filterable phosphorus and total phosphorus. *Analytica Chimica Acta* **1998**, *375*, 5-47.

[31] Moss, B. A land awash with nutrients - The problem of eutrophication. *Chemistry & Industry* **1996**, *11*, 407-411.

[32] Ferguson, A. J. D.; Pearson, M. J.; Reynolds, C. S. Eutrophication of natural waters and toxic algal blooms. In: Hester, R. E.; Harrison, R. M (Eds.), *Issues in Environmental Science and Technology, Agricultural Chemicals and the Environment, Issue 5*. Royal Society of Chemistry, Cambridge, 1996, pp. 27-41.

[33] Boström, B.; Persson, G.; Broberg, B. Bioavailability of different phosphorus forms in freshwater systems. *Hydrobiologia* **1988**, *170*, 133-155.

[34] McKelvie, I. D.; Peat, D. M. W.; Worsfold, P. J. Techniques for the quantification and speciation of phosphorus in natural waters. *Analytical Proceedings Including Analytical Communications* **1995**, *32*, 437-445.

[35] Jansson, M. Phosphate uptake and utilization by bacteria and algae. *Hydrobiologia* **1988**, *170*, 177-189.

[36] Vollenweider, R. A. Scientific fundamentals of the eutrophication of lakes and flowing waters, with particular reference to nitrogen and phosphorus as factors of eutrophication. Rep. No. GP OE/515. Organisation for Economic Co-operation and Development, Paris, 1968.

[37] OECD. Eutrophication of waters, monitoring, assessment and control. Organisation for Economic Co-operation and Development, Paris, 1982.

[38] Biggs, B. J. F. Eutrophication of streams and rivers: dissolved nutrient- chlorophyll relationships for benthic algae. *Journal of the North American Benthological Society* **2000**, *19*, 17-31.

[39] Sharpley, A.; Foy, B.; Withers, P. Practical and innovative measures for the control of agricultural phosphorus losses to water: An overview. *Journal of Environmental Quality* **2000**, *29*, 1-9.

[40] Dodds, W. K.; Jones, J. R.; Welch, E. B. Suggested classification of stream trophic state: Distributions of temperate stream types by chlorophyll, total nitrogen, and phosphorus. *Water Research* **1998**, *32*, 1455-1462.

[41] Worsfold, P. J.; Gimbert, L. J.; Mankasingh, U.; Omaka, O. N., Hanrahan, G.; Gardolinski, P. C. F. C.; Haygarth, P. M.; Turner, B. L.; Keith-Roach, M. J.; McKelvie, I. D. Sampling, sample treatment and quality assurance issues for the determination of phosphorus species in natural waters and soils. *Talanta* (in press).

[42] Broberg, O.; Persson, G. Particulate and dissolved phosphorus forms in freshwater – composition and analysis. *Hydrobiologia* **1988**, *170*, 61-90.

[43] McKelvie, I. D.; Hart, B. T.; Caldwell, T. J.; Cattrall, R. W. Spectrophotometric determination of dissolved organic phosphorus in natural waters using in-line photo-oxidation and flow injection. *Analyst*, **1989**, *114*, 1459-1463.

[44] Vaz, M. D. R.; Edwards, A. C.; Shand, C. A.; Cresser, M. Determination of dissolved organic phosphorus in soil solutions by an improved automated photo-oxidation procedure. *Talanta* **1992**, *39*, 1479-1487.

[45] Denison, F. H.; Haygarth, P. M.; House, W. A.; Bristow, A. W. The measurement of dissolved phosphorus compounds: Evidence for hydrolysis during storage and implications for analytical definitions in environmental analysis. *International Journal of Environmental Analytical Chemistry* **1998**, *69*, 111-123.

[46] Haygarth, P. M.; Warwick, M. S.; House, W. A. Size distribution of colloidal molybdate reactive phosphorus in river waters and soil solution. *Water Research* **1997**, *31*, 439-448.

[47] Hens, M.; Merckx, R. The role of colloidal particles in the speciation and analysis of "dissolved" phosphorus. *Water Research* **2002**, *36*, 1483-1492.

[48] Grudpan, K.; Jakmunee, J.; Sooksamiti, P. Flow injection dialysis for the determination of anions using ion chromatography. *Talanta* **1999**, *49*, 215-223.

[49] Halliwell, D. J.; McKelvie, I. D.; Hart, B. T.; Dunhill, R. H. Separation and detection of condensed phosphates in waste waters by ion chromatography coupled with flow injection. *Analyst* **1996**, *121*, 1089-1093.

[50] Heckenberg, A. L; Haddad, P. R. Determination of inorganic anions at parts per billion levels using single-column ion chromatography without sample preconcentration. *Journal of Chromatography* **1984**, *299*, 301-305.

[51] Wetzel, R. A.; Anderson, C. L.; Schleicher, H.; Crook, G. D. Determination of trace level ions by ion chromatography with concentrator columns. *Analytical Chemistry* **1979**, *51*, 1532-1535.

[52] Manzoori, J. L.; Miyazaki, A.; Tao, H. Rapid differential flow injection of phosphorus compounds in wastewater by sequential spectrophotometry and inductively coupled plasma atomic emission spectrometry using a vacuum ultraviolet emission line. *Analyst* **1990**, *115*, 1055-1058.

[53] Varma, A. *Handbook of Inductively Coupled Atomic Emission Spectrometry*, CRC Press, Boca Ranton, Florida, USA, 1991.

[54] Jiang, S.-J.; Houk, R. S. Inductively coupled plasma mass spectrometric detection for phosphorus and sulfur compounds separated by liquid chromatography. *Spectrochimica Acta* **1988**, *43B*, 405-411.

[55] Chen, Z. L.; Grierson, P.; Adams, M. A. Direct determination of phosphate in soil extracts by potentiometric flow injection using a cobalt wire electrode. *Analytica Chimica Acta* **1998**, *363*, 191-197.

[56] Coetzee, J. F.; Gardner, C. W. Determination of sulfate, orthophosphate, and triphosphate ions by flow injection analysis with the lead ion selective electrode as detector. *Analytical Chemistry* **1986**, *58*, 608-611.

[57] Davey, D. E.; Mulcahy, D. E.; O'Connell, G. R. Flow-injection determination of phosphate with a cadmium ion-selective electrode. *Talanta* **1990**, *37*, 683-687.

[58] De Marco, R.; Pejcic, B.; Chen, Z. L. Flow injection potentiometric determination of phosphate in waste waters and fertilisers using a cobalt wire ion-selective electrode. *Analyst* **1998**, *123*, 1635-1640.

[59] Carpenter, N. G.; Hodgson, A. W. E.; Pletcher, D. Microelectrode procedures for the determination of silicate and phosphate in waters - Fundamental studies. *Electroanalysis* **1997**, *9*, 1311-1317.

[60] Fogg, A. G.; Bsebsu, N. K. Flow injection voltammetric determination of phosphate: direct injection of phosphate into molybdate reagent. *Analyst* **1982**, *107*, 566-570.

[61] Harden, S. M.; Nonidez, W. K. Determination of orthophosphate by flow injection analysis with amperometric detection. *Analytical Chemistry* **1984**, *56*, 2218-2223.

[62] Hight, S. C.; Bet-Pera, F.; Jaselskis, B. Differential pulse polarographic determination of orthophosphate in aqueous media. *Talanta* **1982**, *29*, 721-724.

[63] Matsunaga, K.; Kudo, I.; Yanada, M.; Hasebe, K. Differential-pulse anodic voltammetric determination of dissolved and adsorbed phosphate in turbid natural waters. *Analytica Chimica Acta* **1986**, *185*, 355-358.

[64] Broberg, O.; Pettersson, K. Analytical determination of orthophosphate in water. *Hydrobiologia* **1988**, *170*, 45-59.

[65] Ciavatta, C.; Antisari, L. V.; Sequi, P. Interference of soluble silica in the determination of orthophosphate-phosphorus. *Journal of Environmental Quality* **1990**, *19*, 761-764.

[66] Murphy, J.; Riley, J. P. A modified single solution method for the determination of phosphate in natural waters. *Analytica Chimica Acta* **1962**, *27*, 31-36.

[67] Jarvie, H. P.; Withers, P. J. A.; Neal, C. Review of robust measurement of phosphorus in river water: sampling, storage, fractionation and sensitivity. *Hydrology and Earth System Sciences* **2002**, *6*, 113-132.

[68] Burns, D. T.; Chimpalee, N.; Harriott, M. Spectrophotometric determination of phosphorus as phosphate in organic compounds and materials of biological origin using a flow-injection manifold with a mixing chamber. *Fresenius Journal of Analytical Chemistry* **1992**, *342*, 734-736.

[69] Burns, D. T.; Chimpalee, D.; Chimpalee N.; Ittipornkul, S. Flow-injection spectrophotometric determination of phosphate using Crystal Violet. *Analytica Chimica Acta* **1991**, *254*, 197-200.

[70] Más, F.; Estela, J. M.; Cerdá, V. Simultaneous spectrophotometric determination of silicate and phosphate by flow injection analysis. *International Journal of Environmental Analytical Chemistry* **1991**, *43*, 71-78.

[71] D'Angelo, E.; Crutchfield, J.; Vandiviere, M. Rapid, sensitive, microscale determination of phosphate in water and soil. *Journal of Environmental Quality* **2001**, *30*, 2206-2209.

[72] Motomizu, S.; Oshima, M.; Ma, L. On-site analysis for phosphorus and nitrogen in environmental water samples by flow-injection spectrophotometric method. *Analytical Sciences* **1997**, *13*, 401-404.

[73] Motomizu, S.; Oshima, M. Spectrophotometric determination of phosphorus as orthophosphate based on solvent extraction of the ion associate of molybdophosphate with malachite green using flow injection. *Analyst* **1987**, *112*, 295-300.

[74] Susanto, J. P.; Oshima, M.; Motomizu, S.; Mikasa, H.; Hori, Y. Determination of micro amounts of phosphorus with malachite green using a filtration-dissolution preconcentration method and flow injection-spectrophotometric detection. *Analyst* **1995**, *120*, 187-191.

[75] Crouch, S. R.; Malmstadt, H. V. A mechanistic investigation of molybdenum blue method for determination of phosphate. *Analytical Chemistry* **1967**, *39*, 1084-1089.

[76] Drummond, L.; Maher, W. Determination of phosphorus in aqueous solution via formation of the phosphoantimonylmolybdenum blue complex - Re-examination of optimum conditions for the analysis of phosphate. *Analytica Chimica Acta* **1995**, *302*, 69-74.

[77] Hanrahan, G.; Gledhill, M.; Fletcher, P. J.; Worsfold, P. J. High temporal resolution field monitoring of phosphate in the River Frome using flow injection with diode array detection. *Analytica Chimica Acta* **2001**, *440*, 55-62.

[78] Janse, T. A. H. M.; Van Der Wiel, P. F. A.; Kateman, G. Experimental optimization procedures in the determination of phosphate by flow-injection analysis. *Analytica Chimica Acta* **1983**, *155*, 89-102.

[79] van Staden, J. F.; van der Merwe, J. Evaluation of a number of methods for the determination of trace amounts of phosphates with flow injection analysis (FIA). *Water Sa* **1997**, *23*, 169-174.

[80] Wiryawan, A. Use of flow injection analysis for continuous monitoring of river water quality. *Laboratory Robotics and Automation* **2000**, *12*, 142-148.

[81] Worsfold, P. J.; Clinch, J. R.; Casey, H. Spectrophotometric field monitor for water quality parameters: The determination of phosphate. *Analytica Chimica Acta* **1987**, *197*, 43-50.

[82] Bowden, M.; Sequiera, M.; Krog, J. P.; Gravesen, P.; Diamond, D. Analysis of river water samples utilising a prototype industrial sensing system for phosphorus based on micro-system technology. *Journal of Environmental Monitoring* **2002**, *4*, 767-771.

[83] Bowden, M.; Sequeira, M.; Krog, J. P.; Gravesen, P.; Diamond, D. A prototype industrial sensing system for phosphorus based on micro system technology. *Analyst* **2002**, *127*, 1-4.

[84] Li, Y-S.; Muo, Y.; Xie, H-M. Simultaneous determination of silicate and phosphate in boiler water at power plants based on series flow cells by using flow injection spectrophotometry. *Analytica Chimica Acta* **2002**, *455*, 315-325.

[85] Chen, D.; Luque de Castro, M. D.; Valcárcel, M. Determination of anions by flow injection – A review. *Analyst* **1991**, *116*, 1095-1111.

[86] Auflitsch, S.; Peat, D. M. W; McKelvie, I. D.; Worsfold, P. J. Determination of dissolved reactive phosphorus in estuarine waters using a reversed flow injection manifold. *Analyst* **1997**, *122*, 1477-1480.

[87] Hirai, Y.; Yoza, N.; Ohashi, S. Flow injection analysis of inorganic polyphosphates. *Analytica Chimica Acta* **1980**, *115*, 269-277.

[88] Narusawa, Y. Flow-injection spectrophotometric determination of silicate, phosphate and arsenate with on-line column separation. *Analytica Chimica Acta* **1988**, *204*, 53-62.

[89] Narusawa, Y.; Hashimoto, T. Simultaneous determination of phosphate, silicate and arsenate by on-line column flow injection analysis. *Chemistry Letters* **1987**, *7*, 1367-1370.

[90] Blundell, N. J.; Worsfold, P. J.; Casey, H.; Smith, S. The design and performance of a portable, automated flow injection monitor for the in-situ analysis of nutrients in natural waters. *Environment International* **1995**, *21*, 205-209.

[91] Růžička, J.; Hansen, E. H. Flow injection analyses Part I. A new concept of fast continuous flow analysis. *Analytica Chimica Acta* **1975**, *78*, 145-157.

[92] Harvey, D. *Modern Analytical Chemistry*, 1st Edition, Mc-Graw-Hill: Dubuque, IA, 2000.

[93] Růžička, J.; Hansen, E. H. *Flow Injection Analysis*, 2nd Edition, John Wiley & Sons, Chichester, 1988.

[94] Christian, G. D. *Analytical Chemistry*, 5th Edition, John Wiley & Sons Ltd., New York, USA, 1994.

[95] Hassellöv, M. Thesis, Göteborg University, Sweden, 1999.

[96] Chen, Y.-W.; Buffle, J. Physicochemical and microbial preservation of colloid characteristics of natural water samples. I: Experimental conditions *Water Research* **1996**, *30*, 2178-2184.

[97] Buffle, J.; Leppard, G. G. Characterization of aquatic colloids and macromolecules. 1. Structure and behavior of colloidal material. *Environmental Science & Technology* **1995**, *29*, 2169-2175.

[98] Heathwaite, L.; Haygarth, P.; Matthews, R.; Preedy, N.; Butler, P. Evaluating colloidal phosphorus delivery to surface waters from diffuse agricultural sources. *Journal of Environmental Quality* **2005**, *34*, 287-298.

[99] Kretzschmar, R.; Borkovec, M.; Grolimund, D.; Elimelech, M. Mobile subsurface colloids and their role in contaminant transport. *Advances in Agronomy* **1999**, *66*, 121-193.

[100] Hens, M.; Merckx, R. Functional characterization of colloidal phosphorus species in the soil solution of sandy soils. *Environmental Science & Technology* **2001**, *35*, 493-500.

[101] Pant, H. K.; Edwards, A. C.; Vaughan, D. Extraction, molecular fractionation and enzyme degradation of organically associated phosphorus in soil solutions. *Biology and Fertility of Soils* **1994**, *17*, 196-200.

[102] Sinaj, S.; Mächler, F.; Frossard, E.; Faïsse, C.; Oberson, A.; Morel, C. Interference of colloidal particles in the determination of orthophosphate concentrations in soil water extracts. *Communications in Soil Science and Plant Analysis* **1998**, *29*, 1091-1105.

[103] Assemi, S.; Newcombe, G.; Hepplewhite, C.; Beckett, R. Characterization of natural organic matter fractions separated by ultrafiltration using flow field-flow fractionation. *Water Research* **2004**, *38*, 1467-1476.

[104] Mayer, T. D.; Jarrell, W. M. Assessing colloidal forms of phosphorus and iron in the Tualatin River Basin. *Journal of Environmental Quality* **1995**, *24*, 1117-1124.

[105] McDowell, R. W.; Sharpley, A. N. Soil phosphorus fractions in solution: influence of fertiliser and manure, filtration and method of determination. *Chemosphere* **2001**, *45*, 737-748.

[106] Shand, C. A.; Smith, S.; Edwards, A. C.; Fraser, A. R. Distribution of phosphorus in particulate, colloidal and molecular-sized fractions of soil solution. *Water Research* **2000**, *34*, 1278-1284.

[107] Villholth, K. G. Colloid characterization and colloidal phase partitioning of polycyclic aromatic hydrocarbons in two creosote-contaminated aquifers in Denmark. *Environmental Science & Technology* **1999**, *33*, 691-699.

[108] Hilger, S.; Sigg, L.; Barbieri, A. Size fractionation of phosphorus (dissolved, colloidal and particulate) in two tributaries to Lake Lugano. *Aquatic Sciences* **1999**, *61*, 337-353.

[109] Geckeis, H.; Rabung, Th.; Manh, T. N.; Kim, J. I.; Beck, H. P. Humic colloid-borne natural polyvalent metal ions: Dissociation experiment. *Environmental Science & Technology* **2002**, *36*, 2946-2952.

[110] Pelekani, C.; Newcombe, G.; Snoeyink, V. L.; Hepplewhite, C.; Assemi, S.; Beckett, R. Characterization of natural organic matter using high performance size exclusion chromatography. *Environmental Science & Technology* **1999**, *33*, 2807-2813.

[111] Wrobel, K.; Sadi, B. B. M.; Wrobel, K.; Castillo, J. R.; Caruso, J. A. Effect of metal ions on the molecular weight distribution of humic substances derived from municipal compost: Ultrafiltration and size exclusion chromatography with spectrophotometric and inductively coupled plasma-MS detection. *Analytical Chemistry* **2003**, *75*, 761-767.

[112] McKelvie, I. D.; Hart, B. T.; Cardwell, T. J.; Cattrall, R. W. Speciation of dissolved phosphorus in environmental samples by gel filtration and flow-injection analysis. *Talanta* **1993**, *40*, 1981-1993.

[113] Douglas, G. B.; Beckett, R.; Hart, B. T. Fractionation and concentration of suspended particulate matter in natural waters. *Hydrological Processes* **1993**, *7*, 177-191.

[114] Beckett, R.; Jue, Z.; Giddings, J. C. Determination of molecular weight distributions of fulvic and humic acids using flow field-flow fractionation. *Environmental Science & Technology* **1987**, *21*, 289-295.

[115] Buffle, J.; Leppard, G. G. Characterization of aquatic colloids and macromolecules. 2. Key role of physical structures on analytical results. *Environmental Science & Technology* **1995**, *29*, 2176-2184.

[116] Burba, P.; Aster, B.; Nifant'eva, T.; Shkinev, V.; Spivakov, B. Ya. Membrane filtration studies of aquatic humic substances and their metal species: a concise overview - Part 1. Analytical fractionation by means of sequential-stage ultrafiltration. *Talanta* **1998**, *45*, 977-988.

[117] Morrison, M. A.; Benoit, G. Filtration artifacts caused by overloading membrane filters. *Environmental Science & Technology* **2001**, *35*, 3774-3779.

[118] Thang, N. M.; Geckeis, H.; Kim, J. I.; Beck, H. P. Application of the flow field flow fractionation (FFFF) to the characterization of aquatic humic colloids: evaluation and optimization of the method. *Colloids and Surfaces A: Physicochemical and Engineering Aspects* **2001**, *181*, 289-301.

[119] Giddings, J. C. A new separation concept based on a coupling of concentration and flow nonuniformities, *Separation Science* **1966**, *1*, 123-125.

[120] Schimpf, M.; Caldwell, K. D.; Giddings, J. C. (Eds.), *Field-Flow Fractionation Handbook*, Wiley, New York, 2000.

[121] Thielking, H.; Kulicke, W.-M. Determination of the structural parameters of aqueous polymer solutions in the molecular, partially aggregated, and particulate states by means of FFFF/MALLS. *Journal of Microcolumn Separations* **1998**, *10*, 51-56.

[122] Amarasiriwardena, D.; Siripinyanond, A.; Barnes, R. M. Trace elemental distribution in soil and compost-derived humic acid molecular fractions and colloidal organic matter in municipal wastewater by flow field-flow fractionation-inductively coupled plasma mass spectrometry (flow FFF-ICP-MS). *Journal of Analytical Atomic Spectrometry* **2001**, *16*, 978-986.

[123] Beckett, R.; Hart, B. T., Use of Field-Flow Fractionation Techniques to Characterize Aquatic Particles, Colloids, and Macromolecules, in Buffle, J. and van Leeuwen, H. P. (Eds.), *Environmental Particles*, Volume 2, Lewis Publishers Boca Raton, Florida, 1993, pp. 165-205.

[124] Li, P.; Hansen, M.; Giddings, J. C. Separation of lipoproteins from human plasma by flow field-flow fractionation. *Journal of Liquid Chromatography & Related Technologies* **1997**, *20*, 2777-2802.

[125] Giddings, J. C. Field-flow fractionation: Analysis of macromolecular, colloidal, and particulate materials. *Science* **1993**, *260*, 1456-1465.

[126] Kirkland, J. J.; Dilks, Jr., C. H.; Rementer, S. W. Molecular weight distributions of water-soluble polymers by flow field-flow fractionation. *Analytical Chemistry* **1992**, *64*, 1295-1303.

[127] van Bruijnsvoort, M.; Wahlund, K.-G.; Nilsson, G.; Kok, W.Th. Retention behaviour of amylopectins in asymmetrical flow field-flow fractionation studied by multi-angle light scattering detection. *Journal of Chromatography A* **2001**, *925*, 171-182.

[128] Wittgren, B.; Wahlund, K.-G. Fast molecular mass and size characterization of polysaccharides using asymmetrical flow field-flow fractionation-multiangle light scattering. *Journal of Chromatography A* **1997**, *760*, 205-218.

[129] Jönsson, J. Å.; Carlshaf, A. Flow field flow fractionation in hollow cylindrical fibers. *Analytical Chemistry* **1989**, *61*, 11-18.

[130] Wijnhoven, J. E. G. J.; Koorn, J. P.; Poppe, H.; Kok, W.Th. Hollow-fibre flow field-flow fractionation of polystyrene sulphonates. *Journal of Chromatography A* **1995**, *699*, 119-129.

[131] Schimpf, M. E.; Petteys, M. P. Characterization of humic materials by flow field-flow fractionation. *Colloids and Surfaces A: Physicochemical and Engineering Aspects* **1997**, *120*, 87-100.

[132] Fuh, C. B.; Myers, M. N.; Giddings, J. C. Analytical SPLITT fractionation: Rapid particle size analysis and measurement of oversized particles. *Analytical Chemistry* **1992**, *64*, 3125-3132.

[133] Hansen, B. T.; Plew, M. G.; Schimpf, M. Elucidation of size patterning in phytolith assemblages by field-flow fractionation. *Journal of Archaeological Science* **1998**, *25*, 349-357.

[134] Jensen, K. D.; Williams, S. K. R.; Giddings, J. C. High-speed particle separation and steric inversion in thin flow field-flow fractionation channels. *Journal of Chromatography A* **1996**, *746*, 137-145.

[135] Ratanathanawongs, S. K.; Giddings, J. C. Dual-field and flow-programmed lift hyperlayer field-flow fractionation. *Analytical Chemistry* **1992**, *64*, 6-15.

[136] Benincasa, M.-A.; Caldwell, K. D. Flow field-flow fractionation of poly(ethylene oxide): effect of carrier ionic strength and composition. *Journal of Chromatography A* **2001**, *925*, 159-169.

[137] Lee, H.; Williams, S. K. R.; Giddings, J. C. Particle size analysis of dilute environmental colloids by flow field-flow fractionation using an opposed flow sample concentration technique. *Analytical Chemistry* **1998**, *70*, 2495-2503.

[138] Lee, H.; Williams, S. K. R.; Allison, S. D.; Anchordoquy, T. J. Analysis of self-assembled cationic lipid-DNA gene carrier complexes using flow field-flow fractionation and light scattering. *Analytical Chemistry* **2001**, *73*, 837-843.

[139] Brimhall, S. L.; Myers, M. N.; Caldwell, K. D.; Giddings, J. C. Separation of polymers by flow field-flow fractionation. *Journal of Polymer Science Part C: Polymer Letters* **1984**, *22*, 339-345.

[140] Hassellöv, M.; Lyvén, B.; Haraldsson, C.; Sirinawin, W. Determination of continuous size and trace element distribution of colloidal material in natural water by on-line coupling of flow field-flow fractionation with ICPMS. *Analytical Chemistry* **1999**, *71*, 3497-3502.

[141] Nguyen, M.; Beckett, R. Calibration methods for field-flow fractionation using broad standards. II. Flow field-flow fractionation. *Separation Science and Technology* **1996**, *31*, 453-470.

[142] Liu, M.-K.; Williams, P. S.; Myers, M. N.; Giddings, J. C. Hydrodynamic relaxation in flow field-flow fractionation using both split and frit inlets. *Analytical Chemistry* **1991**, *63*, 2115-2122.

[143] Li, P.; Hansen, M.; Giddings, J. C. Advances in frit-inlet and frit-outlet flow field-flow fractionation. *Journal of Microcolumn Separations* **1998**, *10*, 7-18.

[144] Zanardi-Lamardo, E.; Clark, C. D.; Zika, R. G. Frit inlet/frit outlet flow field-flow fractionation: methodology for colored dissolved organic material in natural waters. *Analytica Chimica Acta* **2001**, *443*, 171-181.

[145] Miller, M. E.; Giddings, J. C. Development of a universal separator: Characterization of macromolecular and particulate material by aqueous and nonaqueous flow FFF at ambient and elevated operating temperatures. *Journal of Microcolumn Separations* **1998**, *10*, 75-78.

[146] Giddings, J. C.; Benincasa, M. A.; Liu, M.-K.; Li, P. Separation of water soluble synthetic and biological macromolecules by flow field-flow fractionation. *Journal of Liquid Chromatography* **1992**, *15*, 1729-1747.

[147] Liu, M.-K.; Li, P.; Giddings, J. C. Rapid protein separation and diffusion coefficient measurement by frit inlet flow field-flow fractionation. *Protein Science* **1993**, *2*, 1520-1531.

[148] Shi, L.; Caldwell, K. D. Mucin adsorption to hydrophobic surfaces. *Journal of Colloid and Interface Science* **2000**, *224*, 372-381.

[149] Dycus, P. J. M.; Healy, K. D.; Stearman, G. K., Wells, M. J. M. Diffusion coefficients and molecular weight distributions of humic and fulvic acids determined by flow field-flow fractionation. *Separation Science and Technology* **1995**, *30*, 1435-1453.

[150] Beckett, R.; Bigelow, J. C.; Jue, Z.; Giddings, J. C. Analysis of humic substances using flow field-flow fractionation in *Influence of Aquatic Humic Substances on Fate and Treatment of Pollutants*, MacCarthy, P.; Suffet, I. H., Eds., Acs Advances in Chemistry Series No. 219, American Chemical Society, Washington D. C., 1989, pp.65-80.

[151] Taylor, H. E.; Garbarino, J. R.; Murphy, D. M.; Beckett, R. Inductively coupled plasma mass-spectrometry as an element-specific detector for field-flow fractionation particle separation. *Analytical Chemistry* **1992**, *64*, 2036-2041.

[152] Murphy, D. M.; Garbarino, J. R.; Taylor, H. E.; Hart, B. T.; Beckett, R. Determination of size and element composition distributions of complex colloids

by sedimentation field-flow fractionation inductively-coupled plasma-mass spectrometry *Journal of Chromatography* **1993**, *642*, 459-467.

[153] Andersson, K.; Hassellöv, M.; Lyvén, B. Colloidal trace element size distributions in freshwaters determined by flow field-flow fractionation coupled to ICPMS – a comparison of 12 Scandinavian rivers in: Hassellöv, M. Thesis, Göteberg University, Sweden, 1999.

[154] Hassellöv, M.; Hulthe, G.; Lyvén, B.; Stenhagen, G. Electrospray mass spectrometry as online detector for low molecular weight polymer separations with flow field-flow fractionation. *Journal of Liquid Chromatography & Related Technologies* **1997**, *20*, 2843-2856.

[155] Thang, N. M.; Knopp, R.; Geckeis, H.; Kim, J. I.; Beck, H. P. Detection of nanocolloids with flow field-flow fractionation and laser-induced breakdown detection. *Analytical Chemistry* **2000**, *72*, 1-5.

[156] Plaschke, M.; Schäfer, T.; Bundschuh, T.; Manh, T. N.; Knopp, R.; Geckeis, H.; Kim, J. I. Size characterization of bentonite colloids by different methods. *Analytical Chemistry* **2001**, *73*, 4338-4347.

[157] F-1000 Manual from FFFractionation, LLC, Salt Lake City, Utah.

[158] Lyvén, B.; Hassellöv, M.; Haraldsson, C.; Turner, D. R. Optimisation of on-channel preconcentration in flow field-flow fractionation for the determination of size distributions of low molecular weight colloidal material in natural waters. *Analytica Chimica Acta* **1997**, *357*, 187-196.

[159] Giddings, J. C. Retention (steric) inversion in field-flow fractionation: Practical implications in particle size, density and shape analysis. *Analyst* **1993**, *118*, 1487-1494.

[160] Williams, S. K. R.; Keil, R. G. Monitoring the biological and physical reactivity of dextran carbohydrates in seawater incubations using flow field-flow fractionation. *Journal of Liquid Chromatography & Related Technologies* **1997**, *20*, 2815-2833.

[161] Vaillancourt, R. D.; Balch, W. M. Size distribution of marine submicron particles determined by flow field-flow fractionation. *Limnology and Oceanography* **2000**, *45*, 485-492.

[162] Kim, W.-S.; Park, Y. H.; Shin, J. Y.; Lee, D. W.; Lee, S. Size determination of diesel soot particles using flow and sedimentation field-flow fractionation. *Analytical Chemistry* **1999**, *71*, 3265-3272.

[163] Beckett, R.; Wood, F. J.; Dixon, D. R. Size and chemical characterization of pulp and paper mill effluents by flow field-flow fractionation and resin adsorption techniques. *Environmental Technology* **1992**, *13*, 1129-1140

[164] Dixon, D. R.; Wood, F. J.; Beckett, R. Characterization of organics in pulp and paper mill effluents before and after physicochemical treatment. *Environmental Technology* **1992**, *13*, 1117-1127.

[165] Lead, J. R.; Wilkinson, K. J.; Balnois, E.; Cutak, B. J.; Larive, C. K.; Assemi, S.; Beckett, R. Diffusion coefficients and polydispersities of the suwannee river fulvic

acid: Comparison of fluorescence correlation spectroscopy, pulsed-field gradient nuclear magnetic resonance, and flow field-flow fractionation. *Environmental Science & Technology* **2000**, *34*, 3508-3513.

[166] Petteys, M. P.; Schimpf, M. E. Characterization of hematite and its interaction with humic material using flow field-flow fractionation. *Journal of Chromatography A* **1998**, *816*, 145-158.

[167] van den Hoop, M. A. G. T.; van Leeuwen, H. P. Influence of molar mass distribution on the complexation of heavy metals by humic material. *Colloids and Surfaces A: Physicochemical and Engineering Aspects* **1997**, *120*, 235-242.

[168] Kammer, F. v. d.; Förstner, U. Natural colloid characterization using flow-field-flow-fractionation followed by multi-detector analysis. *Water Science and Technology* **1998**, *37*, 173-180.

[169] Liu, M.-K. Giddings, J. C. Separation and measurement of diffusion coefficients of linear and circular DNAs by flow field-flow fractionation. *Macromolecules* **1993**, *26*, 3576-3588.

[170] Moon, M. H.; Park, I.; Kim, Y. Size characterization of liposomes by flow field-flow fractionation and photon correlation spectroscopy: Effect of ionic strength and pH of carrier solutions. *Journal of Chromatography A* **1998**, *813*, 91-100.

[171] Ratanathanawongs, S. K.; Giddings, J. C. Particle-size analysis using flow field-flow fractionation. *Acs Symposium Series* **1993**, *521*, 13-29.

[172] Siripinyanond, A.; Barnes, R. M. Flow field-flow fractionation-inductively coupled plasma mass spectrometry and metal speciation in proteins: A feasibility study. *Journal of Analytical Atomic Spectrometry* **1999**, *14*, 1527-1531.

[173] Song, J. H.; Kim, W.-S.; Park, Y. H.; Yu, E. K.; Lee, D. W. Retention characteristics of various proteins in flow field-flow fractionation: Effects of pH, ionic strength, and denaturation. *Bulletin of the Korean Chemical Society* **1999**, *20*, 1159-1164.

[174] Stevenson, S. G.; Ueno, T.; Preston, K. R. Automated frit inlet/frit outlet flow field-flow fractionation for protein characterization with emphasis on polymeric wheat proteins. *Analytical Chemistry* **1999**, *71*, 8-14.

[175] Stevenson, S. G.; Preston, K. R. Flow field-flow fractionation of wheat proteins. *Journal of Cereal Science* **1996**, *23*, 121-131.

[176] Stevenson, S. G.; Preston, K. R. Effects of surfactants on wheat protein fractionation by flow field-flow fractionation. *Journal of Liquid Chromatography & Related Technologies* **1997**, *20*, 2835-2842.

[177] Lee, S.; Rao, S. P.; Moon, M. H.; Giddings, J. C. Determination of mean diameter and particle size distribution of acrylate latex using flow field-flow fractionation, photon correlation spectroscopy, and electron microscopy. *Analytical Chemistry* **1996**, *68*, 1545-1549.

[178] Duval, C.; Le Cerf, D.; Picton, L.; Muller, G. Aggregation of amphiphilic pullulan derivatives evidenced by on-line flow field flow fractionation/multi-angle laser light scattering. *Journal of Chromatography B* **2001**, *753*, 115-122.

[179] Glinel, K.; Vaugelade, C.; Muller, G.; Bunel, C. Analysis of new biodegradable amphiphilic water-soluble copolymers with various hydrophobe content by multi-angle light scattering on line with flow field flow fractionation. *International Journal of Polymer Analysis and Characterization* **2000**, *6*, 89-107.

[180] Tan, J. S.; Harrison, C. A.; Li, J. T.; Caldwell, K. D. Characterization of soluble polyelectrolyte-gelatin complexes by differential size-exclusion chromatography and flow field-flow fractionation. *Journal of Polymer Science: Part B: Polymer Physics* **1998**, *36*, 537-542.

[181] Moon, M. H.; Kim, K.; Byun, Y.; Pyo, D. Size characterization of core-shell poly(l-lactide) microspheres by flow/hyperlayer field-flow fractionation. *Journal of Liquid Chromatography & Related Technologies* **1999**, *22*, 2729-2740.

[182] Hecker, R.; Fawell, P. D.; Jefferson, A.; Farrow, J. B. Flow field-flow fractionation of polyacrylamides: Commercial flocculants. *Separation Science and Technology* **2000**, *35*, 593-612.

[183] Hecker, R.; Fawell, P. D.; Jefferson, A.; Farrow, J. B. Flow field-flow fractionation of high-molecular-mass polyacrylamide. *Journal of Chromatography A* **1999**, *837*, 139-151.

[184] Picton, L.; Bataille, I.; Muller, G. Analysis of a complex polysaccharide (gum arabic) by multi-angle laser light scattering coupled on-line to size exclusion chromatography and flow field flow fractionation. *Carbohydrate Polymers* **2000**, *42*, 23-31.

[185] Adolphi, U.; Kulicke, W.-M. Coil dimensions and conformation of macromolecules in aqueous media from flow field-flow fractionation/multi-angle laser light scattering illustrated by studies on pullulan. *Polymer* **1997**, *38*, 1513-1519.

[186] Ratanathanawongs, S. K.; Shiundu, P. M.; Giddings, J. C. Size and compositional studies of core-shell latexes using flow and thermal field-flow fractionation. *Colloids and Surfaces A: Physicochemical and Engineering Aspects* **1995**, *105*, 243-250.

[187] Thielking, H.; Roessner, D.; Kulicke, W.-M. On-line coupling of flow field-flow fractionation and multiangle laser light scattering for the characterization of polystyrene particles. *Analytical Chemistry* **1995**, *67*, 3229-3233.

[188] Botana, A. M.; Ratanathanawongs, S. K.; Giddings, J. C. Field-programmed flow field-flow fractionation. *Journal of Microcolumn Separations* **1995**, *7*, 395-402.

[189] Moon, M. H. Effect of carrier solutions on particle retention in flow field-flow fractionation. *Bulletin of the Korean Chemical Society* **1995**, *16*, 613-619.

[190] Roessner, D.; Kulicke, W.-M. On-line coupling of flow field-flow fractionation and multi-angle laser light scattering. *Journal of Chromatography A* **1994**, *687*, 249-258.

[191] Bartsch, S.; Kulicke, W.-M.; Fresen, I.; Moritz, H.-U. Seeded emulsion polymerization of styrene: Determination of particle size by flow field-flow fractionation coupled with multi-angle laser light scattering. *Acta Polymerica* **1999**, *50*, 373-380.

[192] Wahlund, K.-G.; Winegarner, H. S.; Caldwell, K. D.; Giddings, J. C. Improved flow field-flow fractionation system applied to water-soluble polymers: Programming, outlet stream splitting, and flow optimization. *Analytical Chemistry* **1986**, *58*, 573-578.

[193] Thielking, H.; Kulicke, W.-M. On-line coupling of flow field-flow fractionation and multiangle laser light scattering for the characterization of macromolecules in aqueous solution as illustrated by sulfonated polystyrene samples. *Analytical Chemistry* **1996**, *68*, 1169-1173.

[194] Benincasa, M. A.; Giddings, J. C. Separation and molecular weight distribution of anionic and cationic water-soluble polymers by flow field-flow fractionation. *Analytical Chemistry* **1992**, *64*, 790-798.

[195] Giddings, J. C.; Chen, X.; Wahlund, K.-G.; Myers, M. N. Fast particle separation by flow/steric field-flow fractionation. *Analytical Chemistry* **1987**, *59*, 1957-1962.

[196] Jiang, Y.; Miller, M. E.; Li, P.; Hansen, M. E. Characterization of water-soluble polymers by flow FFF-MALS. *American Laboratory* **2000**, *32*, 98-108.

[197] Benincasa, M. A.; Giddings, J. C. Separation and characterization of cationic, anionic, and nonionic water-soluble polymers by flow FFF: Sample recovery, overloading, and ionic strength effects. *Journal of Microcolumn Separations* **1997**, *9*, 479-495.

[198] Roger, P.; Baud, B.; Colonna, P. Characterization of starch polysaccharides by flow field-flow fractionation-multi-angle laser light scattering-differential refractometer index. *Journal of Chromatography A* **2001**, *917*, 179-185.

[199] Ratanathanawongs, S. K.; Giddings, J. C. Rapid size characterization of chromatographic silicas by flow field-flow fractionation. *Chromatographia* **1994**, *38*, 545-554.

[200] Reschiglian, P.; Melucci, D.; Zattoni, A.; Malló, L.; Hansen, M.; Kummerow, A.; Miller, M. Working without accumulation membrane in flow field-flow fractionation. *Analytical Chemistry* **2000**, *72*, 5945-5954.

Chapter 2

Practical Considerations for Flow Field-Flow Fractionation

2.1 Introduction

The theoretical aspects of Flow Field-Flow Fractionation (FlFFF) have been discussed in Chapter 1. Here the practical aspects of FlFFF are considered. Methods discussed in this chapter relate to the FlFFF instrument used throughout this work with channel dimensions of: length 29.6 cm, breadth 2.0 cm, thickness 0.0254 cm, and geometric void volume 1.41 mL.

There are several steps that need to be carried out before real samples can be analysed using FlFFF. Firstly the FlFFF system needs to be correctly set-up. This can be more challenging than Sedimentation Field-Flow Fractionation (SdFFF) because of the need to balance the channel flow and crossflow rates [1]. The membrane needs to be installed correctly and replaced whenever necessary, i.e. if sample is accumulating on the surface of the membrane. Whenever the membrane is replaced the channel or void volume (V^0) and channel thickness (w) need to be determined as these will affect the retention times of eluting particles, and the determination of particle size and molecular weight distributions [2]. An example of how to calculate the void volume and channel thickness is shown in section 2.6 using polystyrene bead standards of known diameter.

The experimental procedure and calculation of void volume and channel thickness for SdFFF are not discussed in this chapter, as the methods used are very similar to those for FlFFF. For SdFFF only one pump is required, and there is no membrane in the channel, therefore there is no need to balance flow rates or replace membranes.

The aim of this chapter therefore is to describe the FlFFF system set-up and the experimental procedure for a FlFFF run, the installation and replacement of the channel membrane, and the methods used to calibrate the channel dimensions.

2.2 FlFFF instrumental set-up

The FlFFF system is shown in Fig. 2.1. There are two pumps, one for the channel flow and one for the crossflow. The pump that controls the channel flow is a Waters 515 HPLC pump (Waters, Milford, MA, USA), and the pump that controls the crossflow is a Varian Inert 9012 HPLC pump (Varian Chromatography Systems, California, USA). A Waters 2487 dual wavelength absorbance detector (Waters, Milford, MA, USA) records the absorbance at 254 nm. The FlFFF channel (F-1000, formerly FFFractionation, now PostNova Analytics, Salt Lake City, Utah, USA) and the computer that runs the FLOW160 and FFF Analysis software is also shown.

The FLOW160 software switches the valve between the two operating modes (load and inject) and also acquires data from the dual wavelength absorbance detector. The parameters for the void volume, the channel thickness, and dead volumes are required to be entered into the system utilities section of the FLOW160 program. These values are used to calculate the injector to channel dead volume, the channel to detector dead volume and the relaxation time. The injector to channel dead volume is then used to calculate the injection delay to allow sufficient time for the sample to be flushed from the 20 μL sample loop of the Rheodyne injector valve into the top of the channel. This is calculated by multiplying the injector to channel dead volume by 120 and dividing by the channel flow rate. The channel to detector dead volume is used to calculate the outlet dead time in order to correct the elution time, and the relaxation time is calculated as the time taken for two channel or void volumes of crossflow to pass across the channel.

The data acquired by the FLOW160 software is opened up as a .dat file in the FFF Analysis software. The FFF Analysis program is used to correct the fractograms by adjusting the baseline and removing the outlet dead time. The run can then be saved as an .out file which is then opened as an Excel file and converted into particle size distributions.

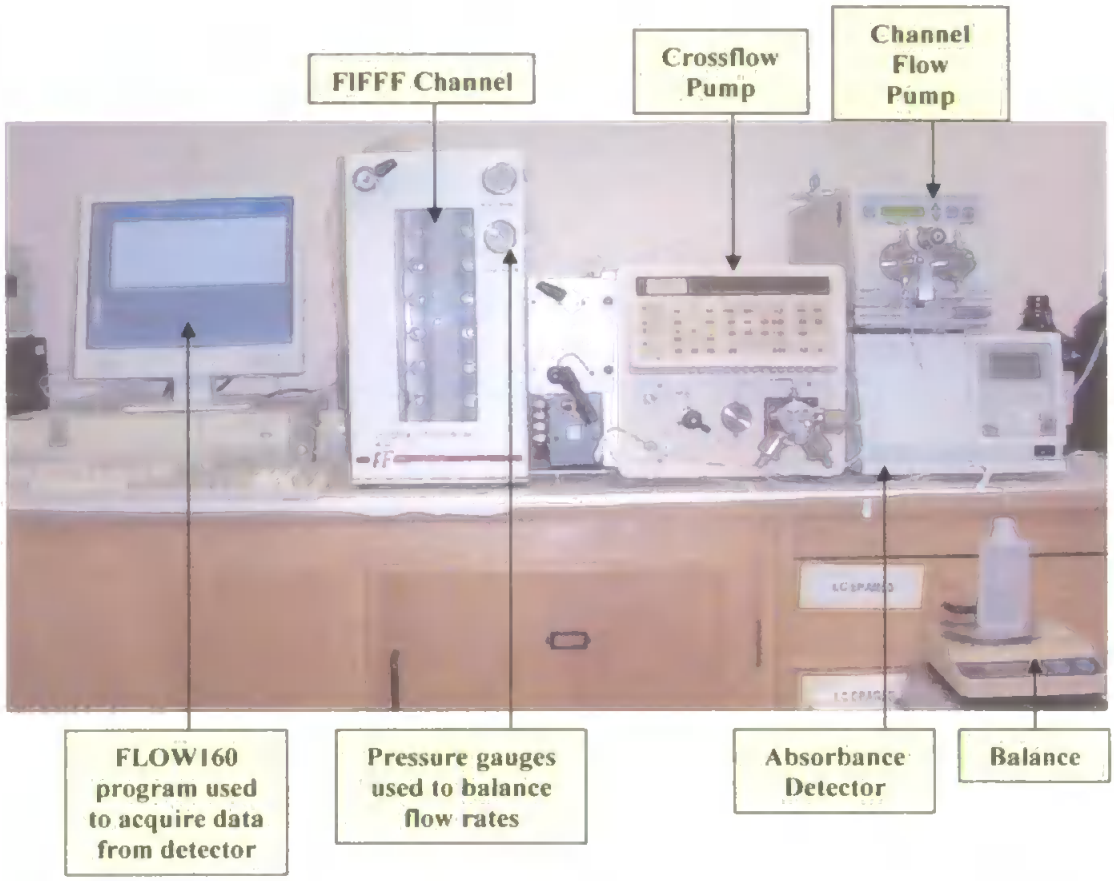

Figure 2.1. FIFFF system set-up in the laboratory: a balance to collect the eluent from the detector is used to measure the flow rates and two pumps are used to provide the channel flow and crossflow (field applied to sample).

2.3 Balancing flow rates

Before a run can start it is important that the channel flow and crossflow rates are balanced in the load (stopflow) and inject (run) modes otherwise retention times may differ between runs. This was achieved in this system using pressure gauges and a balance. The pressure in the channel should not exceed 150 psi as stated in the F-1000 manual [3], and pressures used throughout this work were usually below 100 psi. The FLOW160 program has a facility to measure the flow rates. Firstly the system was switched to load (stopflow) mode, and the pressures were adjusted using a needle valve on the end of the crossflow line. The flow rates were measured using a balance. Once the required flow rates were obtained, the system was then switched to inject (run) mode. The flow rates were again checked using the balance. If the flow rates were the same in both modes then the system was ready, if

not, then the pressures were adjusted and the process repeated until the flow rates in both modes were balanced.

2.4 Operation of FlFFF system during a run

Once the flow rates were balanced and a stable baseline obtained, the system was ready to run samples. The Rheodyne injector valve was injected with sample, which was then flushed into the channel. After the short injection delay the switching valve was changed automatically to load (stopflow) mode and the carrier bypassed the channel and flowed directly to the detector. During this time, the crossflow was flowing continuously through the channel and acting on the sample. At the end of the relaxation time, the switching valve then automatically changed back to inject (run) mode allowing the channel flow to flow through the channel and the run commenced.

2.5 Installation and replacement of the membrane

This section describes how to install or replace a membrane in the FlFFF channel. Membranes need replacing when there is a build-up of material on the membrane, and on average were replaced every six months. Each time the channel is opened and the membrane either cleaned or replaced the void volume and channel thickness need to be re-calculated, and the determination of these parameters is described in section 2.6.

The membrane used in this work was a 10,000 molecular weight cut-off (MWCO) regenerated cellulose membrane (PostNova Analytics Europe, Landsberg, Germany). The membrane is sandwiched between two perspex blocks with porous frits and a spacer that defines the shape of the channel. The blocks are clamped together with eighteen nuts and bolts. The procedure of installing or replacing a membrane takes about two hours to complete. This is because of the numerous nuts and bolts that need to be tightened to a

pressure of 40 psi pressure using a torque wrench. The following is a step-by-step guide used to replace the membrane in this FlFFF system.

2.5.1 Step-by-step guide to replacing membrane

Tools needed: 3/16 inch hex wrench

1/2 inch socket

Torque wrench

1. All external fittings to the channel were disconnected and the carrier solution was then drained from the channel.
2. The channel was removed from its standing position in the system using the hex wrench to remove the four screws holding the channel in place (Fig. 2.2A).
3. The eighteen nuts and bolts were loosened using the 1/2 inch socket in the anticlockwise direction, and removed. To avoid cracking and damaging the perspex blocks, the nuts and bolts are loosened beginning at the ends and working inwards in a criss-cross pattern or as shown in Fig. 2.2B.
4. The perspex blocks were carefully pulled apart to reveal the spacer and the membrane. The spacer was then carefully removed off the membrane, before the membrane was gently peeled off the frit (Fig. 2.2C).
5. The frits should then be rinsed carefully with ultra-pure water to remove any dirt in the channel.
6. The new membrane was then wetted with ultra-pure water and placed on the frit (smooth side facing up for the regenerated cellulose membranes). The spacer was placed over the alignment pins and onto the membrane (Fig. 2.2D).
7. The perspex blocks were then joined together and the nuts and bolts replaced. These were then tightened in a criss-cross pattern, this time working inwards out as shown in Fig. 2.2E. The nuts and bolts were tightened initially at 25 psi using the torque wrench

in a clockwise direction. The nuts and bolts were then tightened to 30 psi, and then to the final maximum pressure of 40 psi (Fig. 2.2F). Any tighter then this may cause the perpsex blocks to crack, or the channel to leak once re-connected into the system [4].

8. The channel was replaced in the mount in its original position by replacing the four screws, and the inlet fittings were re-attached (Fig. 2.2A).
9. Carrier was then pumped using the crossflow pump into the channel to allow the crossflow reservoir to fill up with carrier (visible from the front). Once the reservoir was full and any air present bled out, the crossflow outlet tubing was re-attached, and carrier from the channel pump was allowed to flow through the channel.
10. The new channel was then purged with carrier for at least one hour, and then left for twelve hours before any measurements to determine void volume and channel thickness. This was to allow for any swelling of the membrane.

2.6 Determination of void volume and channel thickness

Every time a membrane is changed or the channel is opened the void volume and channel thickness need to be re-calculated. This is because the spacer used compresses the membrane, resulting in the uncompressed section of the membrane (i.e. the section where the spacer defines the shape of the channel) protruding into the channel, giving a different observed void volume to the calculated geometric void volume [2].

There are two methods for the determination of the void volume and the channel thickness, the breakthrough method and the retention times method. Both methods presented here used polystyrene (PS) beads (Bangs Laboratories Inc., IN, USA) of 50 and 110 nm diameter. The stock solutions containing 10 % solids and sodium azide (0.1 % m/v) were diluted to 1 % m/v concentrations with ultra-pure water and stored at 4 °C in the dark.

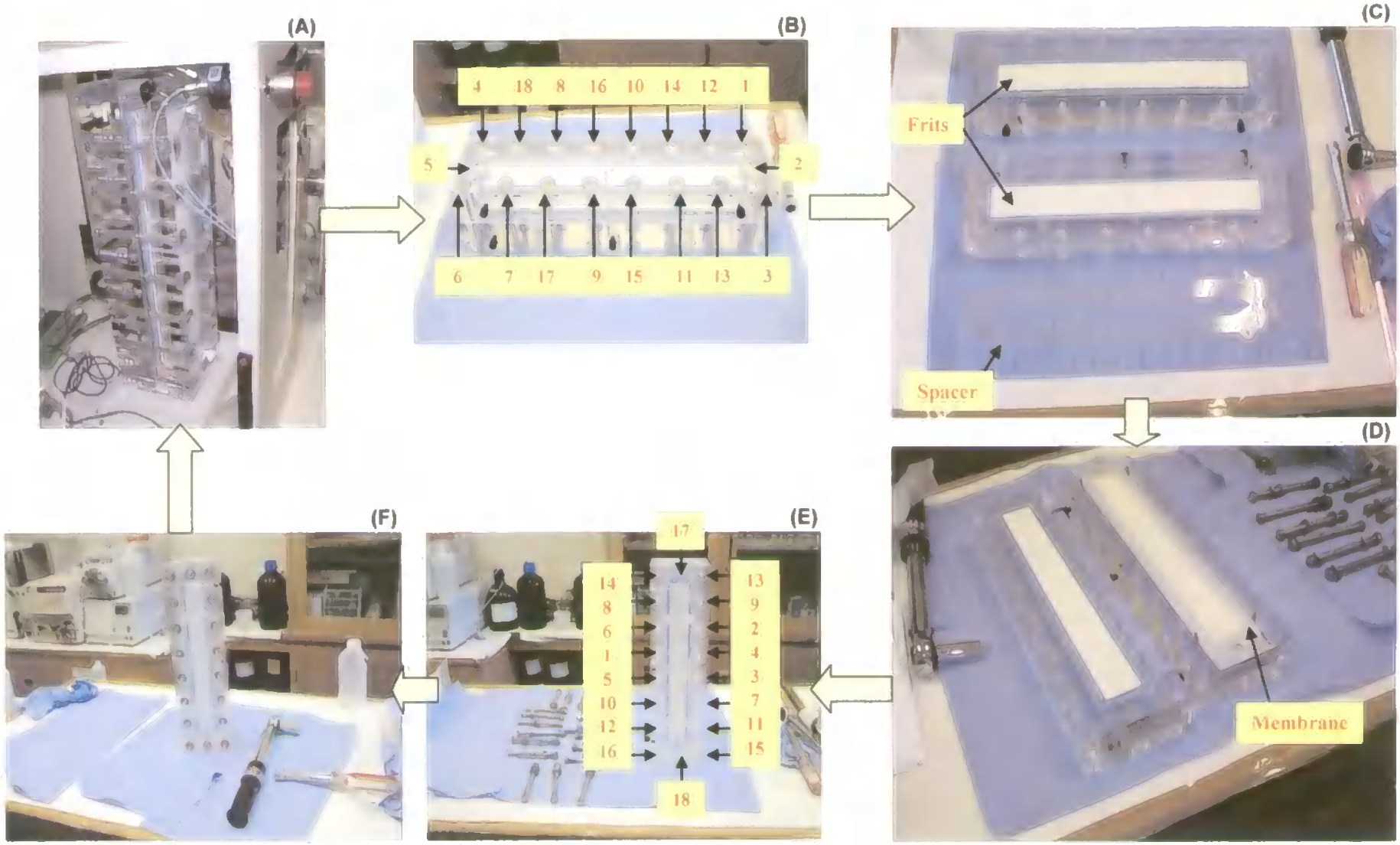

Figure 2.2. Step-by-step guide to replacing the membrane in the FIFFF channel

2.6.1 Breakthrough method

The breakthrough method is described in detail elsewhere [2]. The 1 % m/v stock PS solutions required diluting to 0.2 % m/v for the 50 nm beads and 0.05 % m/v for the 110 nm beads. The PS beads were injected into the FlFFF with a sample load of 2 μL and 3 μL for the 50 and 110 nm beads respectively. The channel flow rate was 1.2 mL min^{-1}, and the crossflow rate was 0.1 mL min^{-1}. No relaxation time was applied on the sample, which meant that the sample flowed directly to the UV detector, resulting in a very narrow peak. The breakthrough time (t_b) was determined to be the time measured at 0.86 of the peak maximum height (0.86 h_{max}), and this is used to determine the void time (t^0) using equation (1):

$$t^0 = \frac{3}{2} t_b \tag{1}$$

The void volume (V^0) can then be determined using equation (2) where $\dot{V}$ is the volumetric channel flow rate:

$$V^0 = \dot{V} t^0 \tag{2}$$

Once the void volume is known the channel thickness (w) can be calculated using equation (3), where A is the area of the channel as defined by the spacer which for this system was 55.6 cm^2:

$$w = \frac{V^0}{A} \tag{3}$$

It was noticed that the values for the response axis from the FFF Analysis program were different to those obtained by the dual wavelength absorbance detector. Therefore the relationship between the two was obtained by recording the values at different absorbance measurements and plotting them as shown in Fig. 2.3. Therefore the absorbance values shown in the fractograms have been calculated from the raw data given in the FFF Analysis software using the equation of the best-fit line.

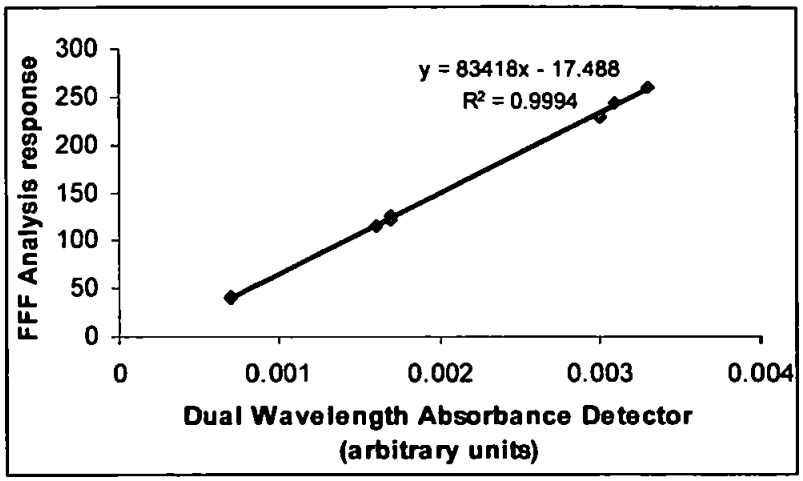

Figure 2.3. Calibration graph to demonstrate the linear relationship between the FFF Analysis program output and the dual wavelength absorbance detector reading.

The fractograms obtained for three runs of the 50 and 110 nm PS beads (Fig. 2.4) were baseline adjusted and the outlet dead time was removed (which was calculated as the channel to detector dead volume multiplied by 60 and divided by the channel flow rate).

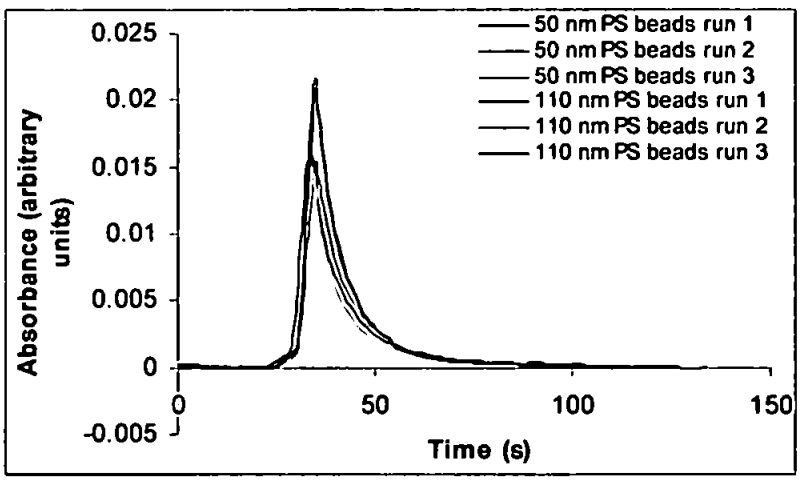

Figure 2.4. Fractograms showing the breakthrough curves for 3 runs of 50 and 110 nm PS beads.

The results obtained from these fractograms were averaged to obtain the void volume and channel thickness, which was calculated as 0.9984 mL (standard deviation = 0.0209 mL, n = 6) and 0.0180 cm (standard deviation = 0.0004 cm, n =6) respectively and the results are presented in Table 2.1.

Table 2.1. Calculation of void volume and channel thickness from breakthrough time determined from the fractograms shown in Fig. 2.4.

Sample	Diameter (cm)	h_{max} (arbitrary units)	$0.86^{*}h_{max}$	t_b (min)	t^0 (min)	V^0 (mL)	w (cm)
50 nm PS beads run 1	5×10^{-6}	0.0158	0.0136	0.538	0.807	0.968	0.0174
50 nm PS beads run 2	5×10^{-6}	0.0152	0.0131	0.563	0.845	1.013	0.0182
50 nm PS beads run 3	5×10^{-6}	0.0139	0.0119	0.542	0.813	0.976	0.0175
110 nm PS beads run 1	1.1×10^{-5}	0.0217	0.0187	0.559	0.839	1.006	0.0181
110 nm PS beads run 2	1.1×10^{-5}	0.0205	0.0177	0.565	0.848	1.017	0.0183
110 nm PS beads run 3	1.1×10^{-5}	0.0208	0.0179	0.561	0.842	1.010	0.0182

2.6.2 Retention times method

The 1 % m/v stock solutions were diluted to 0.2 % m/v concentrations for both the 50 and 110 nm PS beads. The crossflow rate was 0.6 mL min^{-1} and the channel flow rate was 1.2 mL min^{-1}. These flow rates were chosen to give a retention ratio (R) greater than 0.03 for the largest particle analysed in the sample. R decreases with increasing diameter and retention time in the normal mode of operation as shown by equation (4):

$$R = \frac{V^0}{t_r \dot{V}} = \frac{2kTV^0}{\pi\eta w^2 d\dot{V}_c} \tag{4}$$

where t_r is the retention time (min), k is Boltzmann's constant (1.38×10^{-16} g cm^2 s^{-2} K^{-1}), T is the absolute temperature (K), η is viscosity of carrier liquid (η = 0.01 g cm^{-1} s^{-1} at 20 °C), d is the hydrodynamic diameter (cm), and $\dot{V}_c$ is the volumetric crossflow rate (mL min^{-1}). For the 50 and 110 nm PS beads at a crossflow rate of 0.6 mL min^{-1} the retention ratio was 0.18 and 0.08 respectively.

The diluted PS solutions were injected in triplicate into the FlFFF, and the sample load was 20 µL and 10 µL for the 50 and 110 nm PS beads respectively. After the relaxation time, the samples were eluted from the channel giving the fractograms shown in Fig. 2.5. The fractograms have again been baseline adjusted and the outlet dead time subtracted.

The retention time at peak maximum was recorded and used to determine the channel thickness using equation (5):

$$t_r = \frac{\pi\eta w^2 d\dot{V}_c}{2kT\dot{V}} \tag{5}$$

The channel void volume can then be calculated once the channel thickness is determined using equation (3). The results from using the retention times method are given in Table 2.2. These values were again averaged to give a void volume of 0.9763 mL (standard deviation =0.0165 mL, n = 6) and a channel thickness of 0.0176 cm (standard deviation = 0.0003 cm, n = 6).

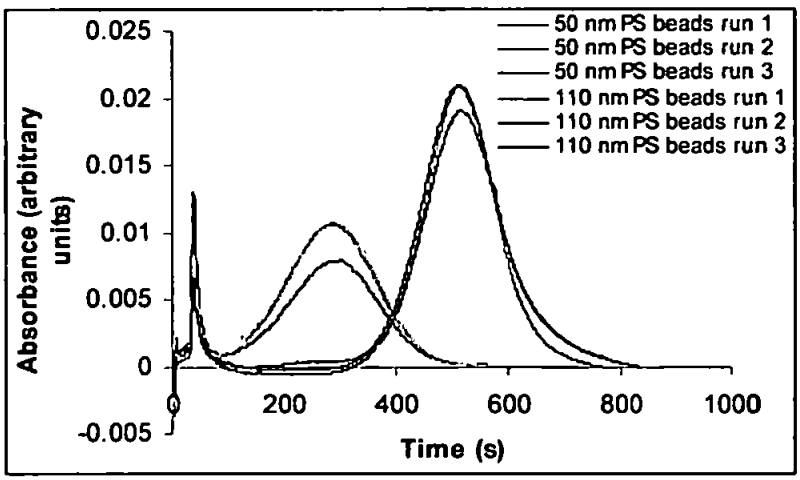

Figure 2.5. Fractograms for 3 runs of 50 and 110 nm PS beads, where the retention time at peak maximum is calculated.

Table 2.2. Calculation of void volume and channel thickness from retention time determined from fractograms shown in Fig. 2.5.

Sample	Diameter (cm)	t_r (s)	π	w^2 (cm)	w (cm)	V^0 (mL)
50 nm PS beads run 1	5×10^{-6}	303.2	3.142	3.57×10^{-4}	0.0189	1.050
50 nm PS beads run 2	5×10^{-6}	290.6	3.142	3.42×10^{-4}	0.0185	1.028
50 nm PS beads run 3	5×10^{-6}	284.9	3.142	3.35×10^{-4}	0.0183	1.018
110 nm PS beads run 1	1.1×10^{-5}	516.0	3.142	2.76×10^{-4}	0.0166	0.924
110 nm PS beads run 2	1.1×10^{-5}	511.5	3.142	2.74×10^{-4}	0.0165	0.920
110 nm PS beads run 3	1.1×10^{-5}	510.0	3.142	2.73×10^{-4}	0.0165	0.918

All results for the void volume and channel thickness of both methods were averaged to give a final void volume of 1.0010 mL (standard deviation = 0.0360 mL) and a channel thickness of 0.0180 cm (standard deviation = 0.0006 cm) which were used in all further calculations.

2.7 Conversion of fractograms into particle size distributions

Once the void volume and channel thickness were known, the raw fractograms could be converted into particle size distributions (PSDs) to give more detailed information about the particle diameters. The following demonstrates how to convert a fractogram into a PSD using a 50 nm PS bead standard.

A typical Excel file with all the raw data is shown in Fig. 2.6. The equations shown demonstrate how the parameters are calculated in each column for the first row of cells only and are discussed in more detail below. In Column G the diameter is calculated using equation (5) for each of the retention time data points in Column B. This is the diameter in cm and needs to be converted to μm by multiplying by 10,000 (Column H). The elution volume at each point also needs to be calculated and this is achieved by multiplying the retention time by the channel flow rate and dividing by 60 (Column F).

Once the diameter and volume is calculated, the values can be used to calculate the relative mass, as:

$$\frac{dm}{dd} = \frac{dV}{dd} \cdot \frac{dm}{dV} \qquad (6)$$

where $\frac{dm}{dd}$ is the relative mass, and $\frac{dm}{dV}$ is the dual wavelength absorbance detector response, and $\frac{dV}{dd}$ is the difference in volume divided by the difference in diameter for consecutive points which is shown in column I. As previously discussed the absorbance needs to be converted from the FFF Analysis program values to the detector values using

%STRS 4
sample = Retention Times method 0.2% m/v 50 nm PS, 20 uL
solvent = MQ + 0.02% NaN3
file Name = LG10FRG.out
type = normal_flow
%ENDSTRS
%VARS 5
T = 298
V0 = 1.02
w = 0.018
ETA = 0.008904
ETA298 = 0.008904
%ENDVARS
%COLS 4
t
r
Vdot
Vc
%ENDCOLS
%DATA 399

D22 = (C22+17.488)/83418

E22 = D22-0.00021

F22 = (B22*1.2)/60

x 10,000

I22 = (F23-F22)/(H23-H22)

J22 = E22*I22

	B	C	D	E	F	G	H	I	J
21	Time (s)	FFF Analysis response	$\frac{dm}{dV}$	Corrected $\frac{dm}{dV}$	Volume (mL)	Diameter (cm)	Diameter (μm)	$\frac{dV}{dd}$	$\frac{dm}{dd}$
22	0.0	-257.6	-0.0029	-0.0031	0	0	0	110.14	-0.3402
23	1.5	-257.6	-0.0029	-0.0031	0.03	2.72E-08	0.0003	110.14	-0.3402
24	3.0	-257.6	-0.0029	-0.0031	0.06	5.45E-08	0.0005	110.14	-0.3402
25	4.5	-256.6	-0.0029	-0.0031	0.09	8.17E-08	0.0008	110.14	-0.3388
26	6.0	-126.6	-0.0013	-0.0015	0.12	1.09E-07	0.0011	110.14	-0.1672
27	7.5	-50.6	-0.0004	-0.0006	0.15	1.36E-07	0.0014	110.14	-0.0668
28	9.0	-1.6	0.0002	0.0000	0.18	1.63E-07	0.0016	110.14	-0.0021
29	10.5	32.4	0.0006	0.0004	0.21	1.91E-07	0.0019	110.14	0.0427
30	12.0	54.4	0.0009	0.0007	0.24	2.18E-07	0.0022	110.14	0.0718
31	13.5	71.4	0.0011	0.0009	0.27	2.45E-07	0.0025	110.14	0.0942
32	15.0	83.4	0.0012	0.0010	0.3	2.72E-07	0.0027	110.14	0.1101
33	16.5	92.4	0.0013	0.0011	0.33	3.00E-07	0.0030	110.14	0.1220
34	18.0	99.4	0.0014	0.0012	0.36	3.27E-07	0.0033	110.14	0.1312
35	19.5	102.4	0.0014	0.0012	0.39	3.54E-07	0.0035	110.14	0.1352
36	21.0	106.4	0.0015	0.0013	0.42	3.81E-07	0.0038	110.14	0.1405
37	22.5	111.4	0.0015	0.0013	0.45	4.09E-07	0.0041	110.14	0.1471
38	24.0	117.4	0.0016	0.0014	0.48	4.36E-07	0.0044	110.14	0.1550
39	25.5	118.4	0.0016	0.0014	0.51	4.63E-07	0.0046	110.14	0.1563
40	27.0	119.4	0.0016	0.0014	0.54	4.90E-07	0.0049	110.14	0.1576
41	28.5	121.4	0.0017	0.0015	0.57	5.18E-07	0.0052	110.14	0.1603
42	30.0	124.4	0.0017	0.0015	0.6	5.45E-07	0.0054	110.14	0.1642
43	31.5	132.4	0.0018	0.0016	0.63	5.72E-07	0.0057	110.14	0.1748
44	33.0	162.4	0.0022	0.0019	0.66	5.99E-07	0.0060	110.14	0.2144
45	34.5	277.4	0.0035	0.0033	0.69	6.26E-07	0.0063	110.14	0.3662

Figure 2.6. Excel program showing how the raw data is converted into particle size information, only the first page of the file is shown as an example using 50 nm PS beads.

the equation $y = 83418x - 17.488$, and these are shown in Column D. The absorbance values then need to be corrected as at y = 0, x = 0.00021, and therefore this value is subtracted from all the values in column D, to give the corrected $\frac{dm}{dV}$ in column E. Once $\frac{dV}{dd}$ has been calculated and the values for $\frac{dm}{dV}$ corrected, they can be multiplied together for each point to give the relative mass at each point (Column J). When columns H and J are plotted, the particle size distribution is obtained for the sample (Fig. 2.7).

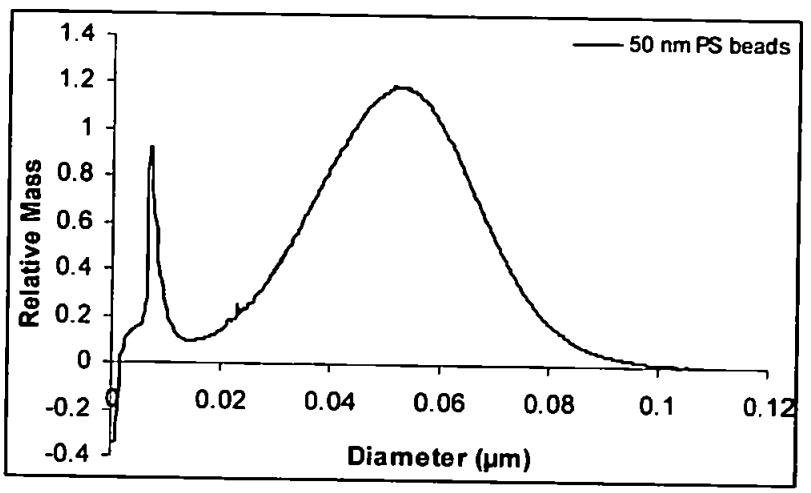

Figure 2.7. PSD for 50 nm PS bead standard as calculated from raw fractogram.

2.8 Selection of appropriate crossflow rates for particles <1 µm

As mentioned in section 2.6.2, the flow rates need to be chosen to ensure a retention ratio greater than 0.03 for the largest particles. When unsuitable flow rates are chosen this can result in samples being forced onto the membrane, in the case of soil suspension samples an extreme example is shown in Fig. 2.8 where the components of the soil have clearly stuck on the membrane. Before replacing the membrane shown in Fig. 2.8 it was observed that replicate injections of Milli-Q blanks resulted in fractograms with large void peaks (peak at the start of the fractogram due to the elution of non-retained particles) as shown in Fig. 2.9A. At this point it was considered that the membrane needed replacing to obtain blank runs with smaller void peaks, also shown in Fig. 2.9A. To prevent soil becoming stuck on the membrane the crucial experimental parameter was therefore identified as the

crossflow rate and this was remedied using equation (4). Therefore for samples with upper particle size thresholds of 0.2, 0.45 and 1 µm at crossflow rates of 0.4, 0.2 and 0.1 mL min^{-1} respectively a retention ratio between 0.05 and 0.07 was achieved and these crossflow rates were used in Chapter 4 to ensure that the largest particle size in each fraction had a retention ratio >0.03. Once the membrane had been replaced and calibrated using the methods described in section 2.6, the reliability of the system was investigated. This was achieved by injecting a 50 nm PS bead standard to determine whether the same particle size distribution was obtained over time, and this is shown in Fig. 2.9B. The stability of the membrane was also examined by routinely injecting 20 µL of a Milli-Q blank at a crossflow rate of 0.1 mL min^{-1} and a channel flow rate of 1.2 mL min^{-1} i.e. the same conditions used for <1 µm soil suspension samples. Blank runs carried out between March and August 2004 are shown in Fig. 2.9C and it can be seen that the particle size distribution of the runs were very similar eve n though >320 soil suspension samples had been analysed using the same membrane over many months.

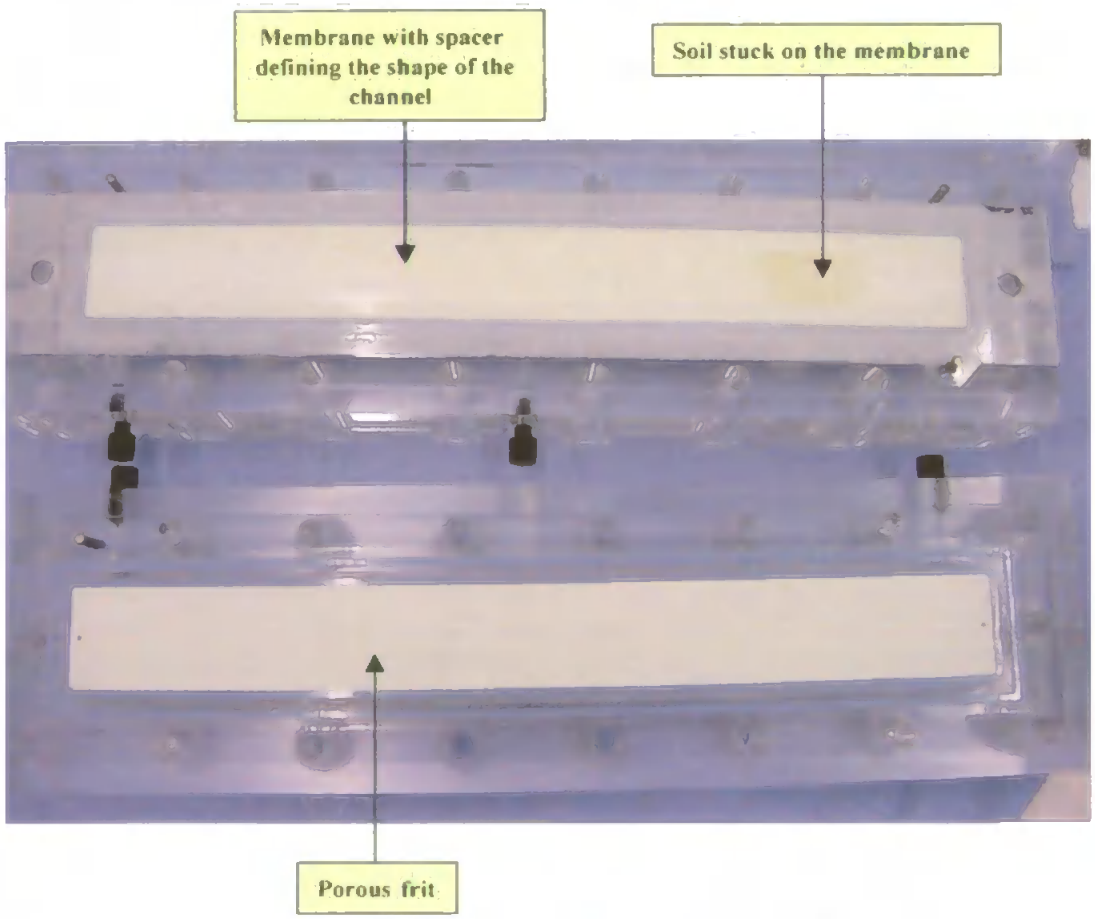

Figure 2.8. FlFFF membrane on opening the channel after using non-ideal flow rates.

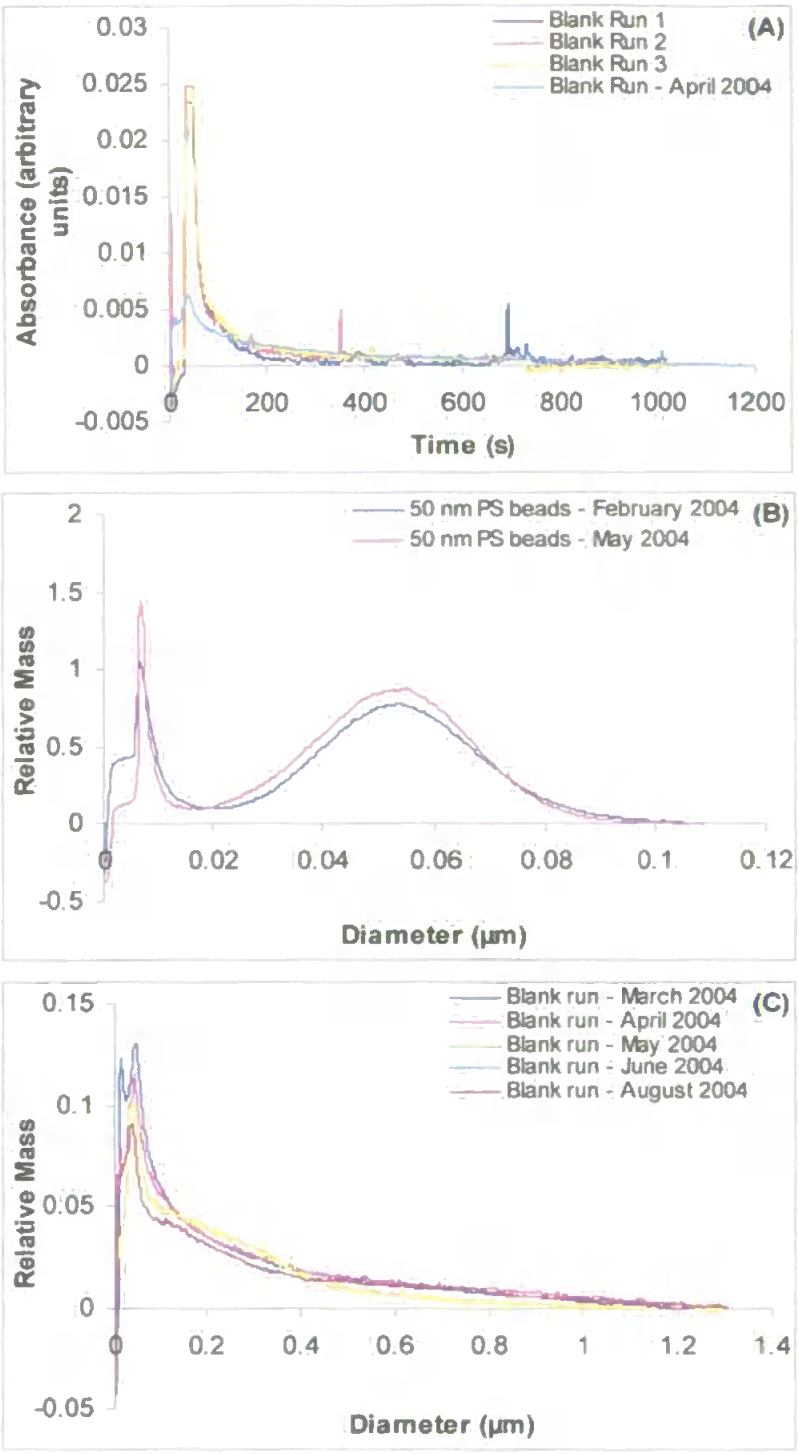

Figure 2.9. Effect of crossflow rates on membrane reliability: (A) Fractograms of Milli-Q blanks with large void peaks prior to membrane replacement and a Milli-Q blank (April 2004) run after membrane replacement; (B) PSDs of 50 nm PS bead standards to test the reliability of the membrane over several months; (C) PSDs of Milli-Q blanks to test the stability of the membrane over several months.

2.9 Application to lower (5190, 15200 and 43300 Dalton) molecular weights

The void peak is the sharp narrow peak at the start of the fractogram (Fig. 2.5) or the particle size distribution (Fig. 2.7). As previously mentioned, this peak is due to the elution of non-retained particles. These particles are smaller than the lower size limit of the FlFFF, which depends on the experimental conditions used. The use of higher crossflow rates increases the fractionating power so that smaller sample components are better resolved from the void peak and this will be demonstrated in section 2.9.1.

Molecular weight distributions rather than particle size distributions are required when analysing samples of low molecular weight. The procedure of converting fractograms into molecular weight distributions is similar to the conversion of fractograms into PSDs. This method is usually used when working with humic substances [5-10]. Instead of using polystyrene beads to calibrate the channel, a different set of standards is required. Two sets of standards have been tested by Beckett *et al.*; these were poly(styrene sulfonate) standards which are linear random-coil molecules subject to charge repulsion effects and some protein molecular weight standards which are more rigid than the poly(styrene sulfonate) standards [7]. The poly(styrene sulfonate) standards were observed to be better suited for the determination of molecular weights of humic substances.

In this work poly(styrene sulfonate) sodium salt (PSS) standards of 5190, 15200 and 43300 daltons were used (Polymer Standards Service, Mainz, Germany) to calibrate the FlFFF system. The PSS standards (0.1 g) were diluted in ultra-pure water (100 mL) to give 0.1 % m/v concentration.

2.9.1 Optimisation of channel flow and crossflow rates

Before a calibration could be carried out with the PSS standards, the channel flow and crossflow rates were optimised. The sample used to determine the optimum flow rates was a mix of the three PSS standards (500 µL of the 5190 and 15200 dalton standards, and 800 µL of the 43300 dalton standard). The sample load injected was 10 µL. Fig. 2.10A shows that when the channel flow rate was kept constant at 1.2 mL min^{-1}, and the crossflow rate was increased, the sample was separated more from the void peak, increasing resolution and retention time. Fig. 2.10B shows that when the crossflow rate was kept constant at 2.8 mL min^{-1}, and the channel flow rate was increased, the resolution of the sample components and retention time decreased. It can also be seen that as the channel flow rate decreases the retention time increases resulting in some band broadening for the larger MW standard i.e. the 43300 MW standard because the peak profile was asymmetrical. It should be noted that light scattering is dependent on many inter-related factors including the concentration of scattering particles suspended in the medium; size distribution, shape, orientation and surface condition of the scattering particles; refractive index of the scattering particles, and of the suspension medium; and the wavelength of the light source employed. Therefore particle size will have an influence on the detector sensitivity across the size range analysed. The optimum flow rates were chosen as a crossflow rate of 2.5 mL min^{-1}, and a channel flow rate of 0.6 mL min^{-1}, so that a compromise between resolution in the separation process and analysis time was obtained to minimise band broadening.

One unusual observation from the fractogram was that although the membrane has a 10,000 MWCO, the 5190 MW standard was retained in the channel and eluted. This is due to charge repulsion effects between the PSS standards and the membrane and therefore the 5190 MW standard does not pass through the membrane. Dycus *et al.* were also able to determine PSS standards lower than the MWCO of the membrane, as standards of 1800,

5400 and 8000 MW were eluted when a 10,000 dalton polypropylene-backed polysulfone membrane was used [11].

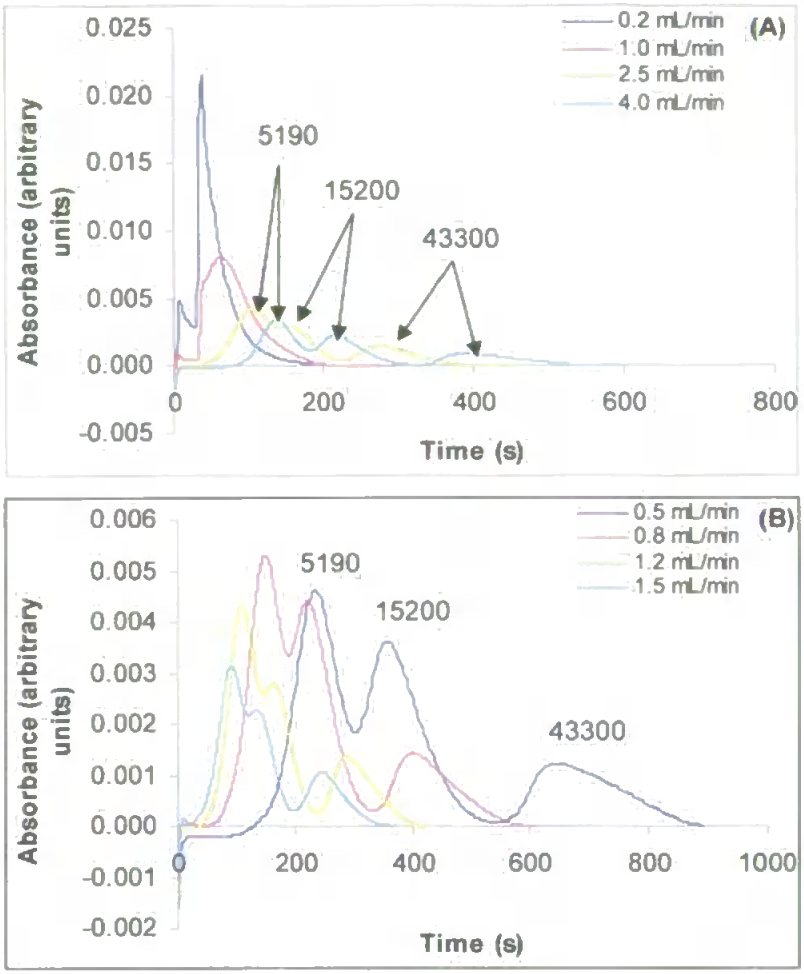

Figure 2.10. Fractograms for PSS standards (mix of 5190, 15200 and 43300 daltons): (A) Channel flow rate kept constant at 1.2 mL min^{-1}, and crossflow rate increased from 0.2 to 4 mL min^{-1}; (B) Crossflow rate kept constant at 2.8 mL min^{-1}, and channel flow rate increased from 0.5 to 1.5 mL min^{-1}.

2.9.2 Calibration of FIFFF channel using PSS

The optimum conditions were used to calibrate the FIFFF system. The PSS standards of 5190, 15200 and 43300 daltons (0.1 % m/v) were injected in triplicate into the FIFFF with a sample load of 2 µL. The fractograms for the PSS standards are shown in Fig. 2.11, and it can be seen that the peaks obtained were of a Gaussian profile.

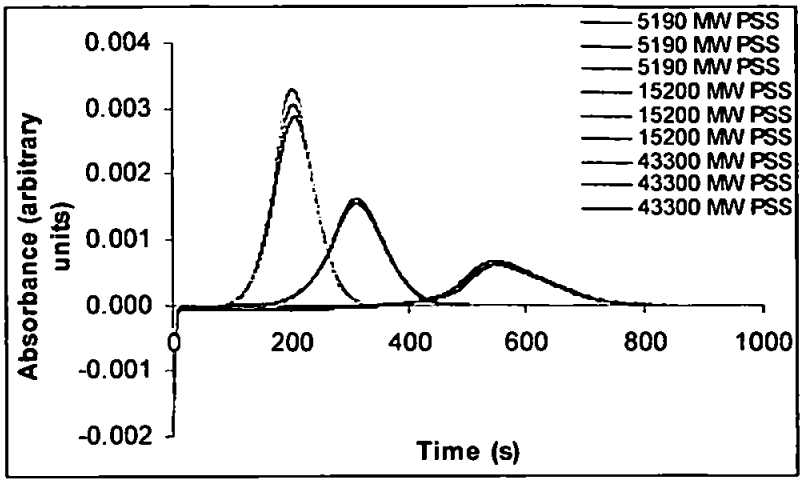

Figure 2.11. Fractograms showing replicate runs of 5190, 15200 and 43300 dalton PSS standards at a channel flow rate of 0.6 mL min^{-1} and a crossflow rate of 2.5 mL min^{-1}.

The retention time at peak maximum is calculated from the fractograms, and used to determine the diffusion coefficients (D), shown in Table 2.3, at peak maximum using equation (7):

$$t_r = \frac{\dot{V}_c w^2}{6D\dot{V}} \tag{7}$$

The diffusion coefficient is related to molecular weight by:

$$D = \frac{A'}{M^b} \tag{8}$$

When a calibration graph of log D against log M is plotted (Fig. 2.12), the equation of the best-fit line is:

$$\log D = \log A' - b \log M \tag{9}$$

The constants A' and b can be obtained from the equation of the best-fit line, $y = -0.4639x - 4.1773$, giving values of 6.65×10^{-5} and 0.464 for A' and b respectively. Similar values ($A' = 7.05 \times 10^{-5}$ and $b = 0.422$) were obtained by Beckett *et al.* using a Millipore 10,000 dalton polysulfone membrane [7]. When A' and b are known, the elution volume or retention time can be converted into molecular weight using equations (7) and (8).

Table 2.3. Calculation of diffusion coefficients from retention time calculated from the fractograms shown in Fig. 2.11.

M (daltons)	log M	t_r (s)			D_{max} (cm^2 s^{-1})			log D_{max}			Mean log D_{max}	Standard Deviation
		1	2	3	1	2	3	1	2	3		
5190	3.715	206.52	204.54	203.22	1.21E-06	1.23E-06	1.23E-06	-5.916	-5.912	-5.909	-5.912	0.0035
15200	4.182	311.34	312.12	311.34	8.05E-07	8.03E-07	8.05E-07	-6.094	-6.095	-6.094	-6.094	0.0006
43300	4.636	549.96	549.96	544.74	4.56E-07	4.56E-07	4.60E-07	-6.341	-6.341	-6.337	-6.340	0.0024

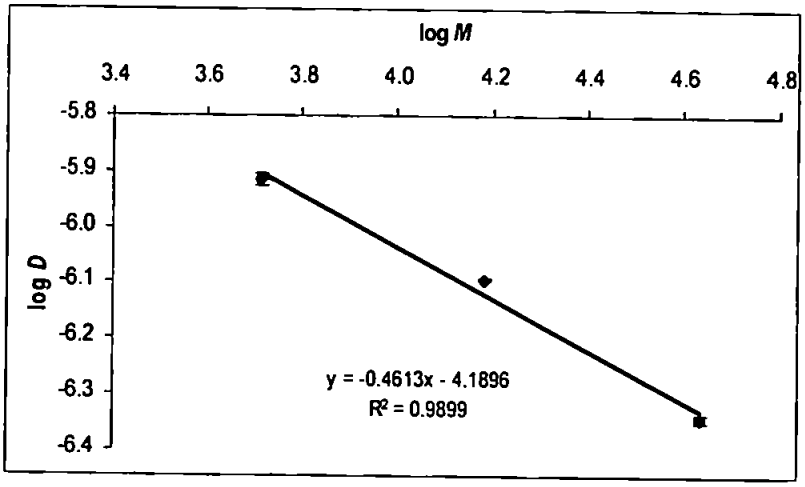

Figure 2.12. Calibration graph obtained from the fractograms for 5190, 15200 and 43300 dalton PSS standards shown in Fig. 2.11. Error bars ± 3 standard deviations, n = 3.

The transformation from fractogram into molecular weight distribution then follows a similar method to that described in section 2.7, but in this case the following is used:

$$\frac{dm}{dM} = \frac{dm}{dV} \cdot \frac{dV}{dM} \qquad (10)$$

where $\frac{dm}{dM}$ is the relative mass, $\frac{dm}{dV}$ is the dual wavelength absorbance detector response and $\frac{dV}{dM}$ is the difference in volume divided by the difference in molecular weight for consecutive points.

3. Conclusions and recommendations

There are several conclusions and recommendations regarding the experimental practicalities of FlFFF:

- Firstly the FlFFF system needs to be set-up correctly, ensuring that the flow rates are balanced, to avoid differing retention times between runs.
- The flow rates need to be chosen so that the crossflow is not too strong to avoid sample components being forced against the membrane, thereby causing irreversible retention and, ultimately, clogging of the membrane.
- Whenever the membrane does need changing (on average every 6 months) a replacement protocol should be followed similar to the one recommended in section 2.5.
- Every time the channel is opened or the membrane replaced the void volume and channel thickness must be re-calculated before any analysis takes place. This can be done with PS beads of known diameter using two methods, the breakthrough method and the retention times method.
- FlFFF is applicable for the determination of particle size distributions (PSDs) and molecular weight distributions (MWDs). PSDs are obtained when working with samples that contain <1 μm particles e.g. colloidal soil suspension samples, and MWDs are more suited for samples that contain 'particles' of lower molecular weight e.g humic and fulvic acids. An added advantage when determining MWDs is that diffusion coefficients can also be calculated.
- When determining MWDs of samples, the channel needs to be calibrated using suitable standards. When humic substances are analysed, poly(styrene sulfonate) sodium salt standards of known molecular weight are recommended.

4. References

[1] Gimbert, L. J.; Andrew, K. N.; Haygarth, P. M.; Worsfold, P. J. Environmental applications of flow field-flow fractionation (FlFFF). *Trends in Analytical Chemistry (TrAC)* **2003**, *22*, 615-633.

[2] Giddings, J. C.; Williams, P. S.; Benincasa, M. A. Rapid breakthrough measurement of void volume for field-flow fractionation channels. *Journal of Chromatography* **1992**, *627*, 23-35.

[3] F-1000 Manual, FFFractionation, LLC, Salt Lake City, Utah, USA.

[4] Schimpf, M.; Caldwell, K. D.; Giddings, J. C. (Eds.), *Field-Flow Fractionation Handbook*, Wiley, New York, USA, 2000.

[5] Amarasiriwardena, D.; Siripinyanond, A.; Barnes, R. M. Trace elemental distribution in soil and compost-derived humic acid molecular fractions and colloidal organic matter in municipal wastewater by flow field-flow fractionation-inductively coupled plasma mass spectrometry (flow FFF-ICP-MS). *Journal of Analytical Atomic Spectrometry* **2001**, *16*, 978-986.

[6] Beckett, R.; Hart, B. T. Use of Field-Flow Fractionation Techniques to Characterize Aquatic Particles, Colloids, and Macromolecules, in Buffle, J. and van Leeuwen, H. P. (Eds.), *Environmental Particles*, Volume 2, Lewis Publishers, Boca Raton, Florida, 1993, pp. 165-205.

[7] Beckett, R.; Bigelow, J. C.; Jue, Z.; Giddings, J. C. Analysis of humic substances using flow field-flow fractionation in *Influence of Aquatic Substances on Fate and Treatment of Pollutants*, MacCarthy, P. and Suffet, I., Eds., Acs Advances in Chemistry Series No. 219, American Chemical Society, Washington D. C., 1989, pp. 65-80.

[8] Beckett, R.; Jue, Z.; Giddings, J. C. Determination of molecular weight distributions of fulvic and humic acids using flow field-flow fractionation. *Environmental Science & Technology* **1987**, *21*, 289-295.

[9] Lyvén, B.; Hassellöv, M.; Haraldsson, C.; Turner, D. R. Optimisation of on-channel preconcentration in flow field-flow fractionation for the determination of size distributions of low molecular weight colloidal material in natural waters. *Analytica Chimica Acta* **1997**, *357*, 187-196.

[10] Thang, N. M.; Geckeis, H.; Kim, J. I.; Beck, H. P. Application of the flow field flow fractionation (FFFF) to the characterization of aquatic humic colloids: evaluation and optimization of the method. *Colloids and Surfaces A: Physicochemical and Engineering Aspects* **2001**, *181*, 289-301.

[11] Dycus, P. J. M.; Healy, K. D.; Stearman, G. K., Wells, M. J. M. Diffusion coefficients and molecular weight distributions of humic and fulvic acids determined by flow field-flow fractionation. *Separation Science and Technology* **1995**, *30*, 1435-1453.

Chapter 3

Comparison of Centrifugation and Filtration Techniques for the Size Fractionation of Colloidal Material in Soil Suspensions Using Sedimentation Field-Flow Fractionation

3.1 Introduction

Colloidal material (0.001 – 1 μm) in soil leachate and drainage waters is an important vehicle for the transport of contaminants [1,2] such as phosphorus species [3,4], pathogens [5-7], persistent organic pollutants [8] and nitrogen species [9,10]. Therefore accurate and sensitive methods for the separation of particulate and colloidal material from soil suspension samples are essential [11-13].

Conventional filtration methods have traditionally been used for the separation of dissolved and particulate fractions in environmental samples, using an operationally defined filter pore size of 0.2 or 0.45 μm as the 'threshold' [14]. The colloidal fraction, which spans a wider range than these nominal pore sizes, has therefore been difficult to study. Haygarth *et al.* [15] and Heathwaite *et al.* [16] used membrane and ultrafiltration methods to separate different colloidal size ranges in river water and soil leachates, but found that colloids aggregated at the membrane surface. Colloids also interact directly with the membrane, resulting in material being retained [17], and there can also be memory effects, contamination from the filter and variable pressure across the membrane.

Many studies have used centrifugation and filtration methods sequentially to prepare soil samples [18-21]. Del Castilho *et al.* [22] studied the difference between centrifuged and membrane-filtered soil suspensions in order to remove suspended material at a threshold of <0.45 μm and then analysed the resulting fractions for a range of elements. They found that colloid-associated properties differed between membrane filtration and centrifugation, with membrane filtration producing higher values, and therefore suggested that membrane filtration, being the simpler method, was the preferred technique for the removal of colloidal material. Douglas *et al.* [23] sequentially used three separation techniques: sieving, continuous flow centrifugation and tangential flow filtration (TFF) to fractionate suspended material in river waters over the particulate and colloidal ranges. The above

studies focused on how the elemental content of environmental samples differed using different separation techniques, but did not quantitatively investigate the colloidal size distribution.

To overcome the uncertainties encountered with membrane filtration, and also to be able to characterise the colloidal material, Buffle and Leppard suggested the use of "a promising new technique", field-flow fractionation (FFF), for colloidal fractionation [17]. This emerging separation technique can be used to obtain information on particle size or relative molecular mass (RMM) distributions in complex environmental matrices over the entire colloidal size range. There are many sub-techniques of FFF of which sedimentation (Sd) and flow (Fl) are the most commonly used. FlFFF separates molecules or particles using a crossflow field, and the process is independent of density, whereas SdFFF separates on the basis of buoyant mass (i.e. size and density) using a centrifugal field.

SdFFF has been used successfully to determine the size distribution of colloids in environmental samples such as soil and sediment solutions [24,25]. Results have been verified by collecting different size fractions and analysing them using electron microscopy [25-27]. Previous studies of soil, sediment and river water samples have usually used SdFFF coupled with detectors such as ICP-MS to determine elemental composition with respect to different size fractions [24,25,27-32]. Most of these studies pretreated the samples using gravity sedimentation [27] or centrifugation [24,25,28,31,32] to obtain a <1 μm cut-off to avoid steric interferences [29]. For a sample containing particles of <1 μm in diameter, the normal operating mode is applicable, in which the smaller particles elute first. When a sample contains particles with diameters >1 μm in diameter, the steric/hyperlayer operating mode is applicable and larger particles will elute first. Hence if a sample contains particles that span the 1 μm threshold, steric interference will occur resulting in larger particles eluting at the same time as smaller particles [33,34].

Therefore normal mode SdFFF can be used to determine the particle size distributions of colloidal samples with upper thresholds of <1 μm.

The aim of this work was to use SdFFF with UV detection to systematically investigate the effect of traditional membrane filtration and centrifugation procedures on the isolation of specific size fractions from soil suspensions. Particle size thresholds of <0.2 μm and <0.45 μm were selected to represent the two most common operational fractions isolated by traditional membrane filtration [17].

3.2 Experimental section

3.2.1 Laboratory ware

All glassware and plastic bottles were pre-washed overnight in 5 % nutrient P-free detergent (Extran®), rinsed with ultra-pure water (Milli-Q, Modulab® Analytical, Continental® Water Systems Corporation, 18.2 MΩ) three times and then left overnight in 5 % Extran®, again rinsed with ultra-pure water three times and dried at room temperature. All solutions were prepared with ultra-pure water and all reagents were of AnalaR grade (VWR International, UK) or equivalent, unless otherwise stated.

The SdFFF carrier solution consisted of 0.05 % (m/v) sodium dodecyl sulphate (SDS; VWR, Poole, England) and 0.02 % (m/v) sodium azide (NaN_3; VWR, Poole, England) in ultra-pure water. The carrier was de-gassed before use by evacuation for at least 30 min, and used as the channel flow.

3.2.2 Sedimentation field-flow fractionation

Details of the SdFFF instrumentation used in this work have been reported elsewhere [31]. The channel dimensions were: radius 15.1 cm, length 86.1 cm, breadth 2.0 cm and width 0.0144 cm. The observed channel thickness and void volume were determined to be 0.0144

cm and 2.45 mL respectively, using the breakthrough method [35]. The channel is different to the channel used in FlFFF as it is circular and is placed in a centrifuge, and contains no membrane (Fig. 3.1). Therefore the accumulation wall is the wall of the channel and not the membrane for this FFF technique. The carrier was pumped through the channel by a ConstaMetric®3000 solvent delivery system (LDC Analytical, USA) at a flow rate of 1 mL min^{-1}. The flow rate was monitored using an Ohaus® Precision Plus balance and a flowmeter. All runs were carried out at 25 °C. A schematic diagram of the SdFFF instrumental set-up is shown in Fig. 3.2.

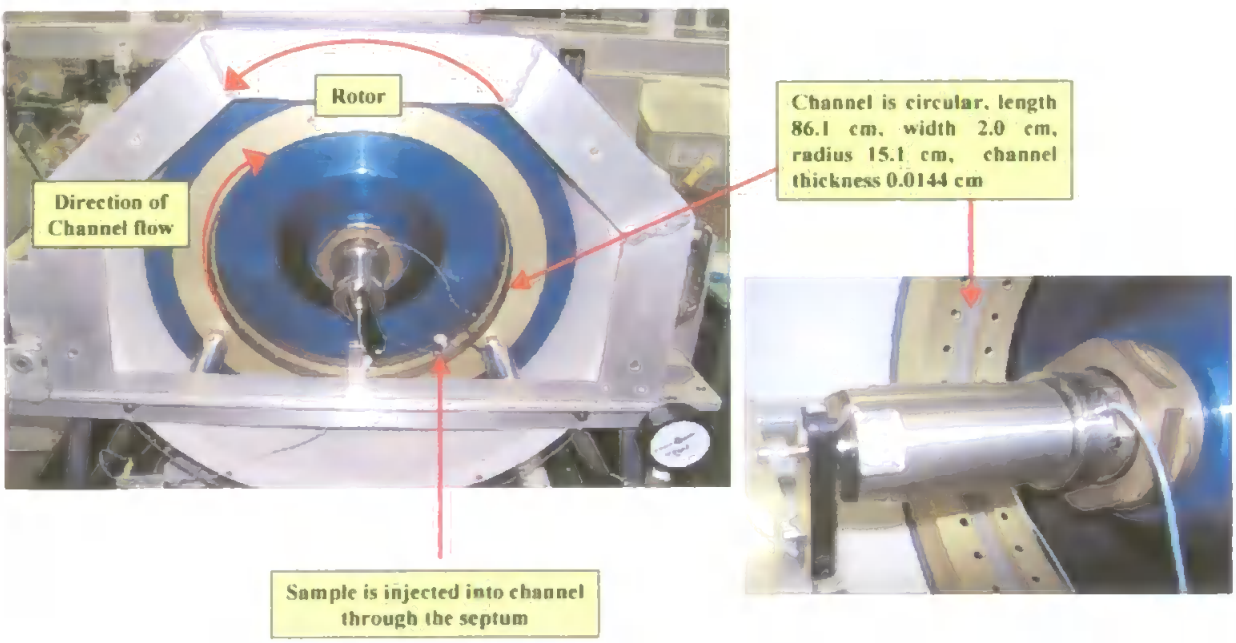

Figure 3.1. SdFFF channel with a close-up of the circular channel placed in a centrifuge.

The SdFFF instrument was run using a laptop and a power program in which, after the relaxation time, the initial field was held for time t_i and then decayed to a holding field where the time constant t_a determined how rapidly the field decayed [36]. This software also acquired data from the UV detector. The constants t_i and t_a were determined using a computer programme written by P. S. Williams (University of Utah, Salt Lake City, UT, USA).

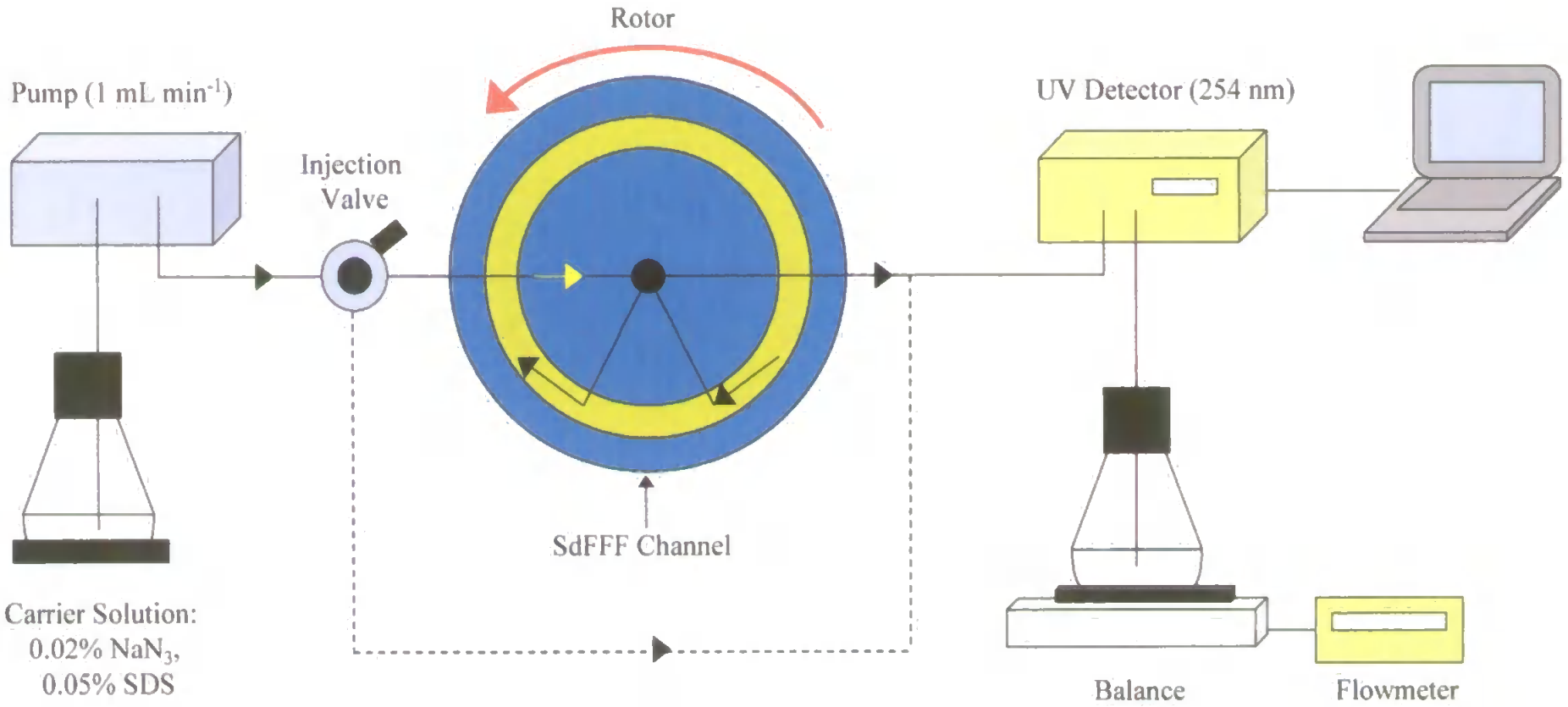

Figure 3.2. Schematic diagram of the SdFFF instrumentation, bold lines indicate direction of carrier in inject (run) mode; dashed lines indicate direction of carrier in load (stopflow) mode.

The samples were injected through a rubber septum into the channel. The sample was flushed from the loop with carrier solution into the top of the channel, and after a few seconds the system was switched to load (stopflow) mode and the carrier bypassed the channel and flowed directly to the detector. During this time the channel was constantly rotating at 1000 rpm (169 *g*) allowing the centrifugal field to act on the sample. At the end of the 10 min relaxation time, the system was changed back to inject (run) mode, restoring the channel flow and the run commenced. The initial field of 1000 rpm was held for a time lag, t_l, of 5.3 min once the relaxation time had finished. The decay parameter t_a of – 42.0 min then reduced the field to a holding rotation of 20 rpm (0.067 *g*). This field programming allowed the elution of larger particles in a reasonable time. A DC motor and speed controller (Bodine Electric Company) powered the rotor.

The absorbance of the eluent was recorded using a Spectra 100 variable wavelength detector (Spectra-Physics, USA) at 254 nm with a sensitivity of 0.02 AUFS. Two runs were carried out for each sample, and the sample load was 80 μL.

3.2.3 Sample preparation

A clay soil sample was previously collected from the B-horizon at Lilydale in Melbourne, Australia [28]. This is a reddish brown (5YR4/3), light clay Krasnozem soil with a moderate polyhedral structure, 10 – 20 mm peds, rough fabric and a firm consistence. The content was 55 % clay (<2 μm), 22 % silt (2-20 μm), 23 % sand (20 μm-2 mm) with a pH of 5.2 (in water) and 4.4 (in calcium chloride). The particle size classification used here was the International Soil Science Society (ISSS) system as the cut-off between silt and sand was at 20 μm instead of the British system where 60 μm is used as the limit between fine sand and silt.

The sample was suspended in ultra-pure water and screened through a 25 μm mesh nylon sieve. The <1 μm diameter fraction was isolated by repeated centrifugation and stored at 4 °C. The concentration of the <1 μm fraction was determined by drying 10 mL of sample in an oven overnight at 100 °C. The weight of the dried soil sample was 5 g, giving a concentration of 50 % m/v in the suspension.

3.2.4 Fractionation of soil sample

The 50 % m/v soil sample was diluted in ultra-pure water to give a 1 % m/v suspension which was used to prepare the filtered and centrifuged <0.2 and <0.45 μm soil fractions as outlined below.

Filtration: Two different size fractions (<0.2 and <0.45 μm) were obtained by sequential filtration. The 1 % m/v soil suspension (25 mL) was sequentially filtered under suction through a 0.45 μm Activon cellulose nitrate membrane filter (47 mm dia) and a 0.2 μm Whatman cellulose nitrate membrane filter (47 mm dia) using a conventional glass filtration unit.

Centrifugation: The 1 % m/v soil suspension was pipetted into polypropylene tubes (1.7 mL volume) and placed into an Avanti® 30 High-Performance bench-top centrifuge with the F2402 fixed-angle rotor. The settling time for each fraction (<0.2 and <0.45 μm) was determined using the following equations:

$$\omega = \left(\frac{2\pi}{60}.rpm\right) \tag{1}$$

$$t = \frac{18\eta \ln\left(\frac{R}{S}\right)}{\omega^2 d^2 \Delta\rho} \tag{2}$$

where ω is the angular velocity of the centrifuge (rad s^{-1}), d is the particle diameter (cm), $\Delta\rho$ is the density difference between the particles and the suspension medium (g cm^{-3}), η

is the viscosity of the suspension medium (g cm^{-1} s^{-1}) where the viscosity of water at 20 °C is 0.010 g cm^{-1} s^{-1}, t is the settling time (s), R is the distance (cm) from the axis of rotation to the level from where the supernatant is decanted from the tube), and S is the distance from the axis of rotation to the surface of the suspension in the tube (cm).

From the above equations, it was determined that the 1 % m/v soil suspension (containing <1 μm particles) required a centrifugation time of 10 min at 2000 rpm (357 *g*) at 20 °C to obtain the <0.45 μm fraction. The supernatant was decanted and the pellet was re-suspended in ultra-pure water and re-centrifuged to ensure that any remaining <0.45 μm particles retained in the pellet were recovered. This was repeated a third time and the decanted supernatants from the three centrifuge runs were pooled. This process was repeated to obtain the <0.2 μm fraction by centrifuging the 1 % m/v soil suspension at 4500 rpm (1810 *g*) for 10 min (at 20 °C).

Soil particle density. SdFFF separates particles on the basis of buoyant mass (i.e. size and density, therefore the density of the particles being analysed is required. There is broad agreement on reported values for the density of soil mineral particles. Sainz Rozas *et al.* [37] assumed that the density was 2.65 g cm^{-3}, Adriano and Weber [38,39] reported that the typical density range for agricultural soils was 2.6 to 2.75 g cm^{-3}, and arable surface soils with a high mineral content had a particle density of 2.65 g cm^{-3}, and Wienhold and Tanaka reported the same value [40]. Other literature sources have assumed a particle density of 2.5 g cm^{-3} for mineral rich sediments [29-32]. A density of 2.6 g cm^{-3} (hence a density difference of 1.6 g cm^{-3}) represents a typical literature value for agricultural soils of the type used in this study and was therefore used in this work for all centrifugation and SdFFF calculations [41].

3.3 Results and Discussion

3.3.1 Data analysis

Fractograms were obtained by plotting detector response against elution time (or volume) of the emerging sample. The fractograms were converted to particle size distributions using an analysis program (Field-Flow Fractionation Research Centre Software, University of Utah, 1990). The fractograms were not corrected for light scattering [30,32,42]. The negative peak at 2.7 min after the start of each fractogram, resulting from the sample matrix being different to the carrier solution, has been removed from the figures for clarity. The conversion from fractograms into PSDs is similar to the FlFFF conversions described in Chapter 2, section 2.7, and although these conversions were made using an analysis program, the calculations used in this program to determine the PSDs will be briefly outlined below.

The diameter at each retention time is calculated differently to those used in FlFFF because SdFFF separates particles using a centrifugal field and not a crossflow field. Therefore the diameter is calculated using equation (3):

$$d = \sqrt[3]{\frac{36kTV_r}{\pi\omega^2 rw\Delta\rho V^0}} \qquad (3)$$

where d is the hydrodynamic diameter (cm), k is Boltzmann's constant (1.38×10^{-16} g cm^2 s^{-2} K^{-1}), T is the absolute temperature (K), V_r is the retention volume (mL), ω is the angular velocity of the centrifuge (rad s^{-1}), r is the centrifuge radius (cm), w is the channel thickness (cm), $\Delta\rho$ is the density difference between the particles and the suspension medium (g cm^{-3}), and V^0 is the void volume (mL).

From equation (3) it can be seen that the angular velocity of the centrifuge (ω) is required for each data point and this is calculated using equation (4). The velocity changes because of the field decay program used where an initial constant speed ω_0 is applied for a period t_1 after which time the speed decays according to equation (4):

$$\omega = \omega_0 \left(\frac{t_1 - t_a}{t - t_a} \right)^4 \tag{4}$$

where t is the run time and t_a is the constant that controls the decay rate.

Once the diameter at each data point of the fractogram is calculated, the fractogram can be converted into a PSD using equation (5):

$$\frac{dm}{dd} = \frac{dV}{dd} \cdot \frac{dm}{dV} \tag{5}$$

where $\frac{dm}{dd}$ is the relative mass, and $\frac{dm}{dV}$ is the detector response, and $\frac{dV}{dd}$ is the difference in volume divided by the difference in diameter for consecutive points.

3.3.2 Fractograms of Lilydale soil suspensions

The differences in fractograms for the centrifuged and filtered fractions with the <1 μm starting material are shown in Figs. 3.3A and 3.3B, respectively. All data are the means of duplicate injections. The UV response for the filtered fractions for both size cut-offs was significantly lower than for the corresponding centrifuged fractions. Typical reproducibility for duplicate injections of the centrifuged and filtered fractions is shown in Figs. 3.4A and 3.4B for the <0.45 and <0.2 μm runs respectively.

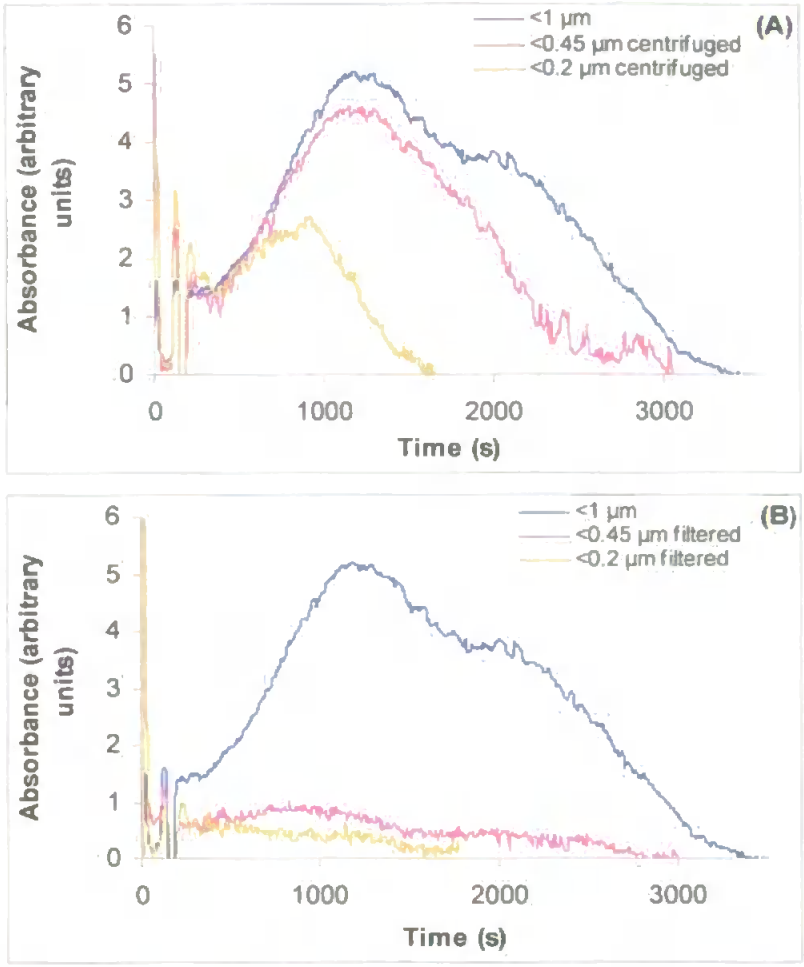

Figure 3.3. SdFFF fractograms for the soil samples comparing filtered and centrifuged fractions with <1 µm starting material: (A) Fractogram for <0.2 and <0.45 µm centrifuged fractions with data averaged for the two runs; (B) Fractogram for <0.2 and <0.45 µm filtered fractions with data averaged for the two runs.

3.3.3 Particle size distributions of Lilydale soil suspensions

The fractograms were converted into particle size distributions (PSDs) and the data for duplicate injections of the starting material, the <0.45 and the <0.2 µm centrifuged fractions were averaged. These data (Fig. 3.5A) showed that the <1 µm soil sample had a log normal distribution of particle sizes with a maximum at 0.13 µm and an upper threshold at 0.6 µm. Chen *et al.* also reported a 0.6 µm threshold value for the same Lilydale sample [28].

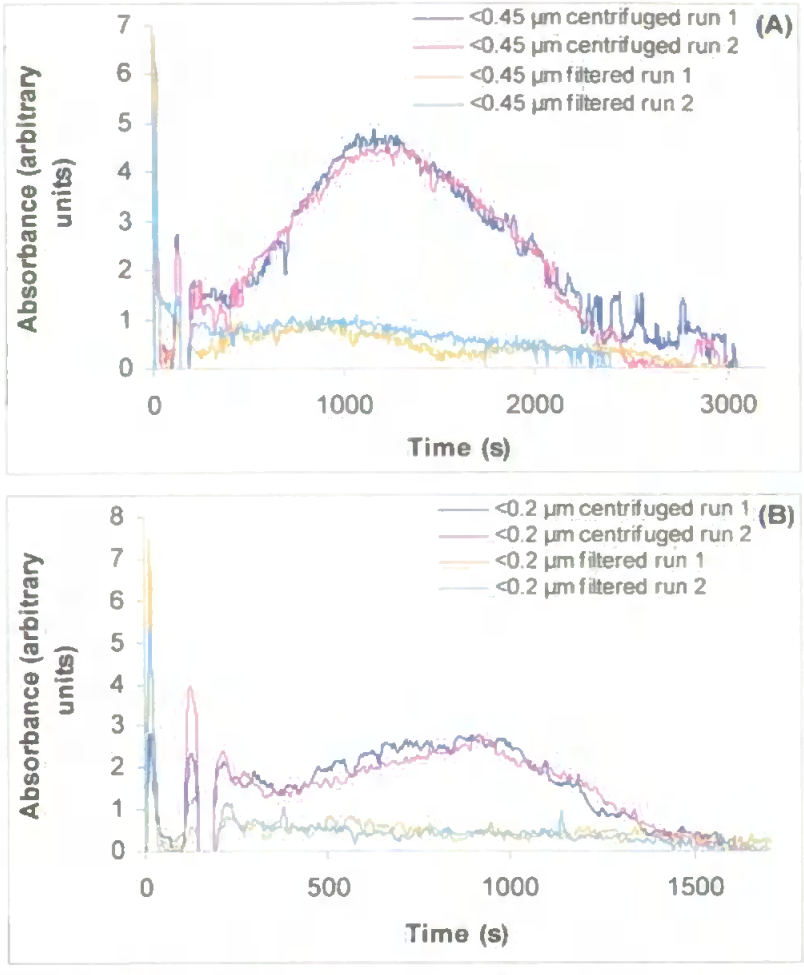

Figure 3.4. SdFFF fractograms for the soil samples showing the good reproducibility observed between two runs: (A) Fractograms for <0.45 µm filtered and centrifuged runs; (B) Fractograms for <0.2 µm filtered and centrifuged runs.

This size threshold was lower than the expected 1 µm based on the sample preparation method used but similar findings have been reported for other environmental samples [24,25,27,31,32,42]. Chittleborough *et al.* [27] reported a threshold value of 0.4 µm for loamy sand samples and van Berkel *et al.* [25] reported a threshold of 0.6 µm for both soil and suspended river colloids.

The PSDs for the centrifuged <0.45 and <0.2 µm fractions had upper size thresholds of about 0.40 and 0.18 µm which are close to the expected cut-offs (Figs. 3.5B and 3.5C). However, some material less than these cut-off diameters was also removed by centrifugation. This may be due to the heterogeneity of the particle shapes and the

assumption made about soil particle density in the calculations applied to the raw fractograms.

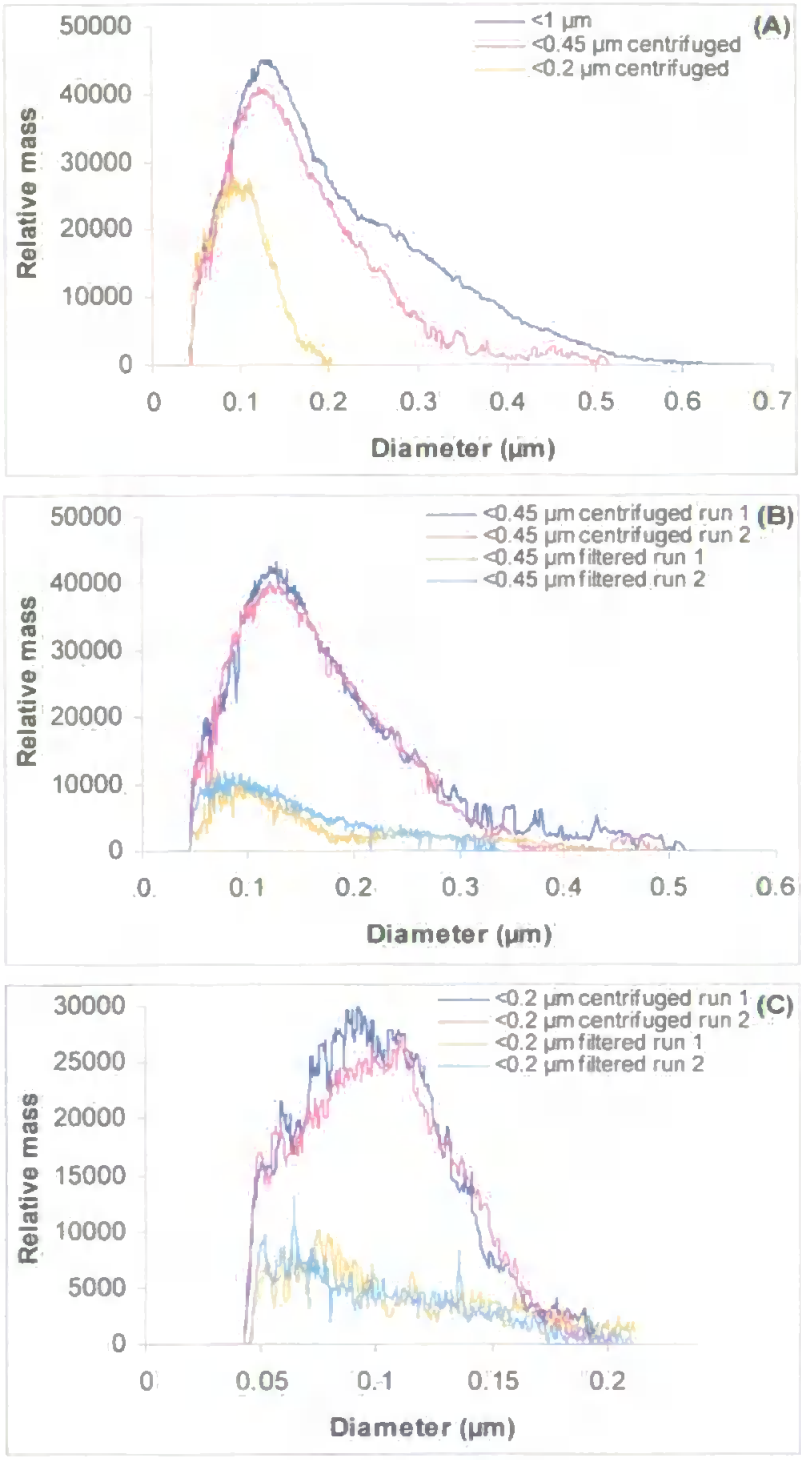

Figure 3.5. SdFFF particle size distributions for the soil samples: (A) Particle size distribution for <0.2 and <0.45 µm centrifuged fractions and <1 µm starting material with data averaged for two runs; (B) Particle size distribution for two runs of <0.45 µm filtered and centrifuged fractions; (C) Particle size distribution for two runs of <0.2 µm filtered and centrifuged fractions.

The particle size distributions for the filtered <0.45 and <0.2 μm fractions show the same particle size thresholds, of about 0.40 and 0.18 μm respectively, as the centrifuged fractions (Figs. 3.5B and 3.5C). Most important, however, is the observation that the relative mass of the filtered fractions is much lower than the centrifuged fractions. By determining the peak area it was observed that membrane filtration recovered 79 % and 73 % less than the centrifugation for the <0.45 and <0.2 μm fractions respectively.

The filtration process would have been more affected by particle shape than the centrifugation process because 'platey' particles of smaller equivalent spherical diameter (d_s) would be more effectively removed than spherical or cubic particles for any given nominal filter pore size. However, the effect observed in these results is unlikely to be explained by shape. As an example, if all the particles in the soil suspension were plates (unlikely) with an aspect ratio of 10:1 then the volume of a plate would be one tenth the volume of a cube with the same edge length as the plate dimension. This would result in a decrease in the d_s by a factor of about 2.1. The calculations for this example are described below.

This example is for a cube and a clay plate particle both of 0.45 μm in length, but with different volumes (Fig. 3.6). Firstly the equivalent spherical diameter (d_s) and the equivalent circular diameter (d_c) for a cube need to be calculated using equations (6) and (7) [26]:

$$V_p = \frac{\pi d_s^3}{6} \tag{6}$$

where V_p is the particle volume.

$$A_p = \frac{\pi d_c^2}{4} \tag{7}$$

where A_p is the projected area.

For a cube with 0.45 μm (or 4.5×10^{-5} cm) edge length, then $A_p = (4.5 \times 10^{-5})^2 = 2.025 \times 10^{-9}$ cm^2, and $V_p = (2.025 \times 10^{-9}) \times (4.5 \times 10^{-5}) = 9.11 \times 10^{-14}$ cm^3. By substituting these values into equations (6) and (7), $d_s = 5.58 \times 10^{-5}$ cm and $d_c = 5.08 \times 10^{-5}$ cm for the cube.

The circular diameter is related to the area of the particle and will therefore be the same between a plate and a cube with the same edge length of 0.45 μm, whereas the spherical diameter will be different as this relates to the volume of the particle where the volume of the plate is one tenth that of the cube volume.

If a clay plate particle has an aspect ratio of 10:1, and has the same d_c (5.08×10^{-5} cm) as the cube, the spherical diameter can be calculated using equation (8) giving $d_s = 2.70 \times 10^{-5}$:

$$\text{Aspect ratio} = \frac{3}{2}\left(\frac{d_c}{d_s}\right)^3 \qquad (8)$$

Once both equivalent spherical diameters are known for the cube and the plate the ratio between the two $= \frac{d_s cube}{d_s plate} = \frac{5.58 \times 10^{-5}}{2.70 \times 10^{-5}} = 2.1$

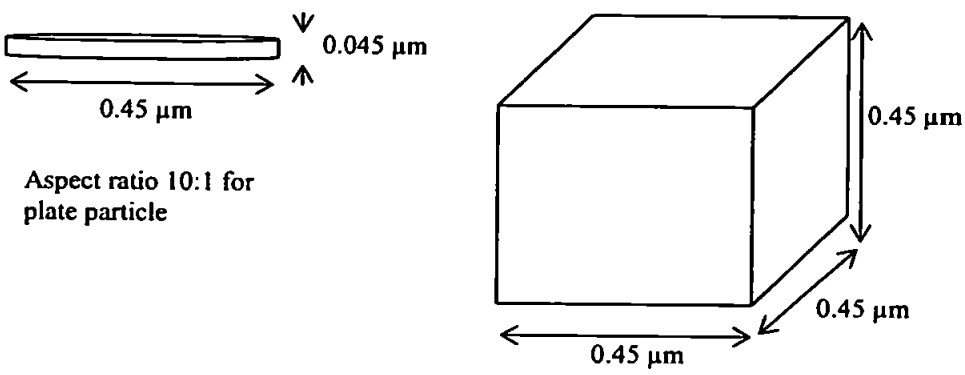

Figure 3.6. Representation of a plate and cube particle of edge length 0.45 μm.

Our results show removal by filtration much lower than the d_s of 0.27 μm for a given filter. Furthermore, SdFFF gives the d_s irrespective of the shape of the particles. The results therefore suggest that conventional <0.45 and <0.2 μm membrane filtration techniques for the separation of soil suspensions, and by implication other aquatic matrices, remove much more of the particulate material than the corresponding centrifugation procedure. An added advantage of centrifugation is that it is a less aggressive approach than membrane filtration for the size fractionation of colloids from environmental matrices.

3.4 Conclusions

This study has demonstrated the uncertainties of using conventional membrane filtration for soil suspension samples, because colloidal material can interact with the membrane and the increased concentrations of the retained particles at the membrane surface appears to result in the aggregation of smaller colloids [17]. Del Castilho *et al.* [22] suggested that membrane filtration was preferable to centrifugation as it was the easiest method to use. However, in the present study, the centrifugation method was found to be quick, efficient and yielded fractions with upper size cut-offs much closer to the required values than membrane filtration. Therefore it is recommended that centrifugation be used to fractionate soil suspension samples instead of filtration. This finding has serious implications for the many size based contaminant speciation studies that have relied on filtration for accurate size fractionation of the particles e.g. the operationally defined filterable reactive phosphorus fraction.

This study has also emphasised the need for a separation technique where a sample can be analysed for the entire colloidal size range, and also be analysed further for pollutants that are transported from land to water by colloidal material. It has been demonstrated that SdFFF can determine the particle size distribution of colloidal material (<1 μm fraction) in

soil suspensions, and therefore has great potential as a robust but mild technology for the physical investigation of the colloidal fraction in aquatic environmental matrices.

3.5. References

[1] Buffle, J.; Leppard, G. G. Characterization of aquatic colloids and macromolecules. 1. Structure and behavior of colloidal material. *Environmental Science & Technology* **1995**, *29*, 2169-2175.

[2] Haygarth, P. M.; Jarvis, S. C., Eds.; *Agriculture, Hydrology and Water Quality*; CABI Publishing, Oxford, New York, 2002, pp. 1-502.

[3] Haygarth, P. M.; Hepworth, L.; Jarvis, S. C. Forms of phosphorus transfer in hydrological pathways from soil under grazed grassland. *European Journal of Soil Science* **1998**, *49*, 65-72.

[4] Haygarth, P. M.; Jarvis, S. C. Transfer of phosphorus from agricultural soils. *Advances in Agronomy* **1999**, *66*, 195-249.

[5] Abuashour, J.; Joy, D, M.; Lee, H.; Whiteley, H. R.; Zelin, S. Transport of microorganisms through soil. *Water, Air, and Soil Pollution*, **1994**, *75*, 141-158.

[6] Jones, D. L.; Campbell, G.; Kaspar, C. W. Human enteric pathogens. In *Agriculture, Hydrology and Water Quality*; Haygarth, P. M.; Jarvis, S.C., Eds.; CAB International, Wallingford, 2002.

[7] Oliver, D. M.; Clegg, C. D.; Haygarth, P. M.; Heathwaite, A. L. Assessing the potential for pathogen transfer from grassland soils to surface waters. *Advances in Agronomy* (in press).

[8] Gevao, B.; Jones, K. C. Pesticides and persistent organic pollutants. In *Agriculture, Hydrology and Water Quality*; Haygarth, P. M.; Jarvis, S.C., Eds.; CAB International, Wallingford, 2002.

[9] Goulding, K. Nitrate leaching from arable and horticultural land. *Soil Use and Management* **2000**, *16*, 145-151.

[10] Scholefield, D.; Tyson, K. C.; Garwood, E. A.; Armstrong, A. C.; Hawkins, J.; Stone, A. C. Nitrate leaching from grazed grassland lysimeters – effects of fertilizer input, field drainage, age of sward and patterns of weather. *Journal of Soil Science* **1993**, *44*, 601-613.

[11] Buffle, J.; Deladoey, P.; Haerdi, W. The use of ultrafiltration for the separation and fractionation of organic ligands in fresh waters. *Analytica Chimica Acta* **1978**, *101*, 339-357.

[12] Kretzschmar, R.; Borkovec, M.; Grolimund, D.; Elimelech, M. Mobile subsurface colloids and their role in contaminant transport. *Advances in Agronomy* **1999**, *66*, 121-193.

[13] Rowland, A. P.; Haygarth, P. M. Determination of total dissolved phosphorus in soil solutions. *Journal of Environmental Quality* **1997**, *26*, 410-415.

[14] Haygarth, P. M.; Sharpley, A. N. Terminology for phosphorus transfer. *Journal of Environmental Quality* **2000**, *29*, 10-15.

[15] Haygarth, P. M.; Warwick, M. S.; House, W. A. Size distribution of colloidal molybdate reactive phosphorus in river waters and soil solution. *Water Research*, **1997**, *31*, 439-448.

[16] Heathwaite, L.; Haygarth, P.; Matthews, R.; Preedy, N.; Butler, P. Evaluating colloidal phosphorus delivery to surface waters from diffuse agricultural sources. *Journal of Environmental Quality* **2005**, *34*, 287-298.

[17] Buffle, J.; Leppard, G. G. Characterization of aquatic colloids and macromolecules. 2. Key role of physical structures on analytical results. *Environmental Science & Technology* **1995**, *29*, 2176-2184.

[18] Martínez, C. E.; Jacobson, A. R.; McBride, M. B. Aging and temperature effects on DOC and elemental release from a metal contaminated soil. *Environmental Pollution* **2003**, *122*, 135-143.

[19] Hilger, S.; Sigg, L.; Barbieri, A. Size fractionation of phosphorus (dissolved, colloidal and particulate) in two tributaries to Lake Lugano. *Aquatic Sciences* **1999**, *61*, 337-353.

[20] McDowell, R. W.; Sharpley, A. N. Soil phosphorus fractions in solution: influence of fertiliser and manure, filtration and method of determination. *Chemosphere* **2001**, *45*, 737-748.

[21] Tyler, G. Effects of sample pretreatment and sequential fractionation by centrifuge drainage on concentrations of minerals in a calcareous soil solution. *Geoderma* **2000**, *94*, 59-70.

[22] del Castilho, P.; van Faassen, R.; Moerman, R. Differences between super-centrifuged and membrane-filtrated soil solutions obtained from bulked and non-bulked topsoils by soil centrifugation. *Fresenius Journal of Analytical Chemistry* **1996**, *354*, 756-759.

[23] Douglas, G. B.; Beckett, R.; Hart, B. T. Fractionation and concentration of suspended particulate matter in natural-waters. *Hydrological Processes* **1993**, *7*, 177-191.

[24] Chen, B.; Beckett, R. Development of SdFFF-ETAAS for characterising soil and sediment colloids. *Analyst* **2001**, *126*, 1588-1593.

[25] van Berkel, J.; Beckett, R. Determination of adsorption characteristics of the nutrient orthophosphate to natural colloids by sedimentation field-flow fractionation. *Journal of Chromatography A* **1996**, *733*, 105-117.

[26] Beckett, R.; Murphy, D.; Tadjiki, S.; Chittleborough, D. J.; Giddings, J. C. Determination of thickness, aspect ratio and size distributions for platey particles using sedimentation field-flow fractionation and electron microscopy. *Colloids and Surfaces A: Physicochemical and Engineering Aspects* **1997**, *120*, 17-26.

[27] Chittleborough, D. J.; Hotchin, D. M.; Beckett, R. Sedimentation field-flow fractionation - a new technique for the fractionation of soil colloids. *Soil Science* **1992**, *153*, 341-348.

[28] Chen, B.; Hulston, J.; Beckett, R. The effect of surface coatings on the association of orthophosphate with natural colloids. *The Science of the Total Environment* **2000**, *263*, 23-35.

[29] Hassellöv, M.; Lyvén, B.; Beckett, R. Sedimentation field-flow fractionation coupled online to inductively coupled plasma mass spectrometry - New possibilities for studies of trace metal adsorption onto natural colloids. *Environmental Science & Technology* **1999**, *33*, 4528-4531.

[30] Murphy, D. M.; Garbarino, J. R.; Taylor, H. E.; Hart, B. T.; Beckett, R. Determination of size and element composition distributions of complex colloids by sedimentation field-flow fractionation inductively-coupled plasma-mass spectrometry *Journal of Chromatography* **1993**, *642*, 459-467.

[31] Ranville, J. F.; Chittleborough, D. J.; Shanks, F.; Morrison, R. J. S.; Harris, T.; Doss, F.; Beckett, R. Development of sedimentation field-flow fractionation-inductively coupled plasma mass-spectrometry for the characterization of environmental colloids. *Analytica Chimica Acta* **1999**, *381*, 315-329.

[32] Taylor, H. E.; Garbarino, J. R.; Murphy, D. M.; Beckett, R. Inductively coupled plasma mass-spectrometry as an element-specific detector for field-flow fractionation particle separation. *Analytical Chemistry* **1992**, *64*, 2036-2041.

[33] Beckett, R.; Hart, B. T., Use of Field-Flow Fractionation Techniques to Characterize Aquatic Particles, Colloids, and Macromolecules, in Buffle, J. and van Leeuwen, H. P. (Eds.), *Environmental Particles*, Volume 2, Lewis Publishers Boca Raton, Florida, 1993, pp. 165-205.

[34] Giddings, J. C. Retention (steric) inversion in field-flow fractionation: Practical implications in particle size, density and shape analysis. *Analyst* **1993**, *118*, 1487-1494.

[35] Giddings, J. C.; Williams, P. S.; Benincasa, M. A. Rapid breakthrough measurement of void volume for field-flow fractionation channels. *Journal of Chromatography* **1992**, *627*, 23-35.

[36] Williams, P. S.; Giddings, J. C. Power programmed field-flow fractionation – a new program form for improved uniformity of fractionating power. *Analytical Chemistry* **1987**, *59*, 2038-2044.

[37] Sainz Rozas, H. R.; Echeverría, H. E.; Picone, L. I. Denitrification in maize under no-tillage: Effect of nitrogen rate and application time. *Soil Science Society of America Journal* **2001**, *65*, 1314-1323.

[38] Adriano, D. C.; Weber, J. T. Influence of fly ash on soil physical properties and turfgrass establishment. *Journal of Environmental Quality* **2001**, *30*, 596-601.

[39] Brady, N. C. *The nature and properties of soils*, MacMillan: New York, 1984.

[40] Wienhold, B. J.; Tanaka, D. L. Soil property changes during conversion from perennial vegetation to annual cropping. *Soil Science Society of America Journal* **2001**, *65*, 1795-1803.

[41] Rowell, D. L. *Soil Science: Methods and Applications*, Longman Scientific & Technical: Essex, England, 1994.

[42] Beckett, R.; Nicholson, G.; Hart, B. T.; Hansen, M.; Giddings, J. C. Separation and size characterization of colloidal particles in river water by sedimentation field-flow fractionation. *Water Research* **1988**, *22*, 1535-1545.

Chapter 4

Effects of Sample Preparation on the Performance of Flow Field-Flow Fractionation Using Two Contrasting Soils

4.1 Introduction

Flow Field-Flow Fractionation (FlFFF) is an emerging separation technique that has been used for a range of environmental applications; these include assessments of colloids in seawater [1], characterisation of dissolved organic material [2-5], including fulvic and humic acids [6-15], and colloidally associated trace elements in natural and effluent waters [16-18]. This separation technique can be used to obtain information on particle size or relative molecular mass (RMM) distributions in complex environmental matrices over the entire colloidal size range (0.001 μm - 1μm), and separates molecules or particles using a crossflow field. For many of the environmental samples studied, such as fulvic and humic acids [6,7,8,11,13-15], colloidally associated trace elements in natural waters [17,18], dissolved organic material [2,3,5], and dissolved organic carbon in natural waters [19] molecular weight distributions have been determined rather than particle size distributions. This is due to the greater resolution FlFFF has at the lower size end than other FFF techniques such as Sedimentation Field Flow-Fractionation (SdFFF), as FlFFF can resolve down to 0.001 μm (or 1000 daltons), whereas the lower size end for SdFFF is about 0.03 μm [20].

Colloidal material (0.001 μm - 1μm) in soil leachate and drainage waters is an important vehicle for the transport of contaminants [21,22] such as phosphorus species [23,24], pathogens [25-27], persistent organic pollutants [28] and nitrogen species [29,30]. For a sample containing particles of <1 μm in diameter, the normal operating mode is applicable, in which the smaller particles elute first. When a sample contains particles with diameters >1 μm in diameter, the steric/hyperlayer operating mode is applicable and larger particles will elute first. Hence if a sample contains particles that span the 1 μm threshold, steric interference will occur resulting in larger particles eluting at the same time as smaller particles [20,31]. Therefore normal mode FlFFF can be used to determine the particle size distributions of colloidal samples with upper thresholds of <1 μm.

Most of the environmental applications using FlFFF have initially filtered samples through 0.45 μm membranes but by filtering at this threshold only part of the colloidal material is analysed. Therefore samples need to be fractionated to <1 μm rather than <0.45 μm before FlFFF analysis for the particle size distribution of the entire colloidal range to be determined. This has commonly been achieved through gravitational settling or centrifugation [32-37] for samples analysed using SdFFF and therefore gravitational settling was adopted in this work to obtain the <1 μm fraction.

There have been few FlFFF studies where sediments [38,39] or soil suspensions [9] have been analysed. Two of these studies were concerned with extracting humic substances for subsequent FlFFF analysis [9,39], whereas the third used a river sediment standard to determine the optimum carrier before an opposed flow sample concentration technique was used to analyse dilute river water samples [38]. SdFFF has been used more extensively to determine the size distribution of colloids in soil and sediment solutions [32-35,37,40].

In the previous chapter centrifugation and filtration methods were compared for the size fractionation of colloidal material in a clay rich Lilydale soil suspension using SdFFF. In this chapter a different FFF sub-technique, FlFFF, is used and two different soil types. The two soils chosen here were a Rowden soil (non-calcareous clayey soil of the Hallsworth series), and a Dartmoor Peat (Crowdy 2 series).

The aim of this work was to determine how the preparation of soil suspension samples using different gravitational settling methods, centrifugation and filtration affected the results obtained using FlFFF. There are two parts to the study; the first focuses on the preparation of soil suspension samples to determine the optimum gravitational settling conditions. The second describes experiments using the optimised settling conditions on two different soil types to see how effective the FlFFF separation technique is for these

environmental samples. As with the SdFFF work, particle size thresholds of <0.2 μm and <0.45 μm were selected to represent the two most common operational fractions isolated by traditional membrane filtration [41].

4.2 Experimental

4.2.1 Laboratory ware

All glassware and bottles were first cleaned overnight in nutrient free detergent (Neutracon®, Decon Laboratories, UK), rinsed three times with ultra-pure water (Elga Maxima®, 18.2 MΩ), soaked in 10 % (v/v) HCl for 24 h, again rinsed three times with ultra-pure water and dried at room temperature. All solutions were prepared with ultra-pure water and all reagents were of AnalaR grade (VWR International, UK) or equivalent, unless otherwise stated.

The FlFFF carrier solution consisted of 0.02 % m/v sodium azide (NaN_3; VWR, Poole, England) in ultra-pure water. The carrier was de-gassed before use by filtering through a 0.2 μm polycarbonate membrane under suction. This carrier was used for both the channel flow and crossflow.

4.2.2 Flow field-flow fractionation

The channel used was an F-1000 (formerly FFFractionation, now PostNova Analytics, Salt Lake City, UT, USA) with channel dimensions of length 29.6 cm, width 2.0 cm, and geometric channel thickness 0.0254 cm. The observed channel thickness and void volume were determined to be 0.018 cm and 1.0 mL respectively, using the breakthrough method [42] and the retention time method with polystyrene beads of 50 and 110 nm diameter. The membrane used was regenerated cellulose of 10,000 molecular weight cut-off (MWCO) (PostNova Analytics Europe, Landsberg, Germany). The carrier was pumped through the channel by a Waters 515 HPLC pump (Waters, Milford, MA, USA) at a flow rate of 1.2

mL min^{-1}, and the flow rate was monitored using an Ohaus balance (Ohaus Corporation, NJ, USA). All runs were carried out at 25 °C. The crossflow was provided by a Varian Inert 9012 HPLC pump (Varian Chromatography Systems, California, USA), and applied perpendicular to the channel. The crossflow was non-recirculating to avoid contamination.

The samples were injected into a Rheodyne injector valve with 20 µL sample loop overfilling five times with 100 µL sample to ensure complete loop filling, and greater precision. The sample was flushed from the loop with carrier solution into the top of the channel. After an injection delay of 2.7 s, the switching valve was changed automatically to load (stopflow) mode and the carrier bypassed the channel and flowed directly to the detector. During this time the crossflow was flowing continuously through the channel and acting on the sample. At the end of the relaxation time (which was calculated as the time taken for two channel volumes of crossflow to pass across the channel) the switching valve then automatically changed back to inject (run) mode, allowing the channel flow to flow through the channel to the detector and the run commenced (i.e. time zero).

The absorbance of the eluent was recorded using a Waters 2487 dual wavelength absorbance detector (Waters, Milford, MA, USA) at 254 nm with a sensitivity of 0.02 AUFS. All samples were injected in triplicate runs and results shown are means of three runs, unless otherwise stated.

Conditions were optimised by adjusting the crossflow rate for different particle size sample ranges, whilst keeping the channel flow rate constant at 1.2 mL min^{-1}. Therefore the crossflow rate for <1 µm, <0.45 µm and <0.2 µm particle size ranges were V_c = 0.1, 0.2 and 0.4 mL min^{-1} respectively. The field increases for smaller size fractions so that smaller species can be resolved from the void peak (which is the sharp narrow peak that appears at the start of the fractogram due to the elution of non-retained particles smaller than the

lower size limit of the FlFFF, which depends on the experimental conditions used) for increased resolution and reasonable analysis time.

4.2.3 Sample preparation

Rowden soil: The Rowden soil, which is a non-calcareous clayey soil of the Hallsworth series (USDA typic haplaquepts, FAO dystric gleysols) was sampled at the Rowden plot at the Institute of Grassland and Environmental Research (IGER), North Wyke, Devon 7 km north of Dartmoor (NGR SX 650 995) (Fig. 4.1). The soil is a typic haplaquept overlaying shales of the Crackington Formation and the grass is dominated by perennial ryegrass (*Lolium perenne* L.). The content was 38 % clay (<2 μm), 50 % silt (2-60 μm), 12 % sand (60μm–2mm) as determined by the hydrometer method with a pH of 5.3 (in water) and 4.9 (in calcium chloride) [43].

Figure 4.1. Rowden plot at IGER, North Wyke where soil was sampled.

The cut-off points between the sand and silt for this soil were different to the Lilydale soil analysed in Chapter 3. This was because the Rowden soil was separated using standard

British sieves and therefore the cut-off between sand and silt occurs at 60 μm instead of 20 μm in the International Soil Science Society (ISSS) definition. The chemical constituent of the soil contained 37 g kg^{-1} organic carbon, 7.5 mg kg^{-1} Olsen phosphorus and 540 mg kg^{-1} total phosphorus. A stainless steel foot-driven soil corer was used to sample to 7.5 cm depth of soil, and the top grassy layer was discarded. This was then oven dried at 30 °C for 5 days, and sieved through a 2 mm and then a 63 μm mesh. Finally, the sieved soil was allowed to dry at room temperature for 3 days.

Dartmoor peat: The peat of the Crowdy 2 association (Crowdy series) was sampled from Dartmoor near Merrivale and Princetown (NGR SX 559 746) (Fig. 4.2). The soil is defined as a raw oligo-amorphous peat soil with rough vegetation of dominant rushes and purple moor grass. The 0-10 cm horizon is black (10 YR 2/1) very slightly stony humified peat; moderately developed fine granular; wet; very weak soil strength; with abundant fine fibrous roots [44].

Figure 4.2. Dartmoor site where peat was sampled near Merrivale and Princetown.

The top 10 cm was sampled using a trowel and the grassy layer was discarded. This was then oven dried at 40 °C for 5 days, and sieved through a 2 mm mesh and then a 63 μm mesh. This was then allowed to dry at room temperature for 3 days.

4.2.4 Optimisation of settling conditions for soil suspensions

A series of settling experiments were carried out to determine the optimum sample preparation protocol for the soil suspension samples:

1. Different settling times from 1 h to 25.6 h were used to investigate the effect of settling time on the observed particle size distribution of the Rowden soil.
2. The repeatability of settling for five Rowden and five Dartmoor Peat samples was examined.
3. Re-settling of the same Rowden sample six times to investigate the effect on the particle size distribution.

1. Effect of settling time. Rowden soil suspension samples of 1 % m/v were prepared by dissolving 1 g of the <63 μm sieved Rowden soil in 100 mL of ultra-pure water. These were shaken gently for 16 h on a mechanical shaker so that the suspension was constantly moving during this shaking period. The soil suspensions were then settled in six 100 mL measuring cylinders in a water bath at 20 °C at different settling times of 1, 2, 3, 6, 12 and 25.6 h to obtain the <1 μm fraction.

The settling depths were determined using the following calculation:

$$x = \frac{t\Delta\rho g d^2}{18\eta} \qquad (1)$$

where x is the settling depth (cm), t is the settling time (s), $\Delta\rho$ is the density difference between the particles and the suspension medium (g cm^{-3}), g is the gravitational acceleration constant (980 cm s^{-2}), d is the particle diameter (cm), and η is the viscosity of

the suspension medium (g cm^{-1} s^{-1}) where the viscosity of water at 20 °C is 0.010 g cm^{-1} s^{-1}. From this calculation the settling depths were determined as 0.3, 0.6, 0.9, 1.9, 3.8 and 8 cm for settling times of 1, 2, 3, 6, 12 and 25.6 h respectively (Fig. 4.3) to obtain the <1 μm particles. The top layer was dominated with <1 μm particles and this was extracted from the soil suspension using a pipette at the end of each settling period as there needs to be a sample cut-off at 1 μm to avoid steric interference. It can also be seen that as the settling time increases so does the settling depth and volume of the top layer. All of the settled samples were injected once into the FlFFF channel, as soon as each of the settling times had finished, with a sample load of 20 μL.

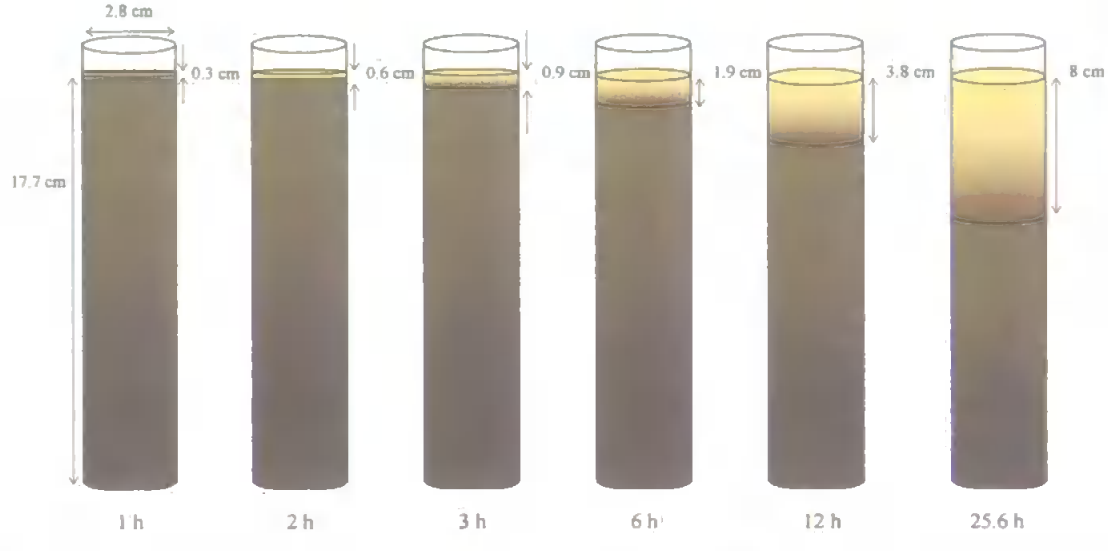

Figure 4.3. Laboratory set-up showing the settling depths at different settling times using measuring cylinders containing 100 mL soil suspension. The lighter top layer is pipetted out and is dominated by the <1 μm fraction.

2. Settling of replicate samples. Five Rowden and five Dartmoor Peat soil suspensions, all of 1 % m/v concentration, were shaken gently for 16 h and settled in 100 mL measuring cylinders. These were settled for 1 h, after which time the <1 μm fraction was extracted from each sample using a pipette, and injected once into the FlFFF channel with a sample load of 20 μL.

3. Re-settling of the same sample. In this experiment, only the Rowden soil was used and a 1 % m/v soil suspension was prepared and shaken gently for 16 h. This was then settled for 1 h in a 600 mL beaker. A small aliquot (100 μL) was pipetted from the beaker, and injected once (20 μL sample loop) into the FlFFF channel. The Rowden soil suspension was then shaken for 10 min and re-settled in the beaker for 1 h. After this time another small aliquot (100 μL) was pipetted out, and injected into the FlFFF channel. This was repeated a total of six times.

4.2.5 Comparison of centrifugation and filtration for two contrasting soils

The optimised settling procedure for the extraction of the <1 μm fraction was used as the starting point for further experiments using centrifugation and filtration to give smaller particle size thresholds of <0.2 and <0.45 μm in a similar manner to the SdFFF work on the Lilydale soil in Chapter 3. However before these fractions were prepared an experiment was carried out to determine how stable the soil suspension samples were. This was done using the 1 % m/v Rowden soil suspension and the optimised settling conditions.

Stability experiment. A Rowden soil suspension of 1 % m/v concentration was shaken gently for 16 h and settled in a 600 mL beaker for 1 h. The top 20 mL layer was pipetted out to give the <1 μm fraction. This fraction was injected in triplicate into the FlFFF channel each day for 3 days. During these 3 days the sample was kept at room temperature. The data from the three runs from each day were averaged for clarity. Once the stability of the soil suspensions was investigated, the <0.2 and <0.45 μm fractions for the Rowden and Dartmoor Peat were prepared as follows and assessed using FlFFF.

Optimised settling protocol. Rowden and Dartmoor Peat soil suspensions of 1 % m/v concentration were prepared by suspending 1 g soil in 100 mL ultra-pure water. These were shaken gently for 16 h and settled in a 600 mL beaker. The top 20 mL layer containing the <1 μm fraction was pipetted out and used to prepare the filtered and centrifuged fractions (<0.2 and <0.45 μm).

Filtration: Two different size fractions (<0.2 and <0.45 μm) were obtained by sequential filtration. The 1 % m/v soil suspension (5 mL) was sequentially filtered under suction through a 0.45 μm Whatman cellulose nitrate membrane filter (47 mm dia) and a 0.2 μm Whatman cellulose nitrate membrane filter (47 mm dia) using a conventional plastic (Nalgene) filtration unit.

Centrifugation: The 1 % m/v soil suspension was pipetted into polypropylene tubes (1.5 mL volume) and placed into an MSE MicroCentaur microcentrifuge (Sanyo, UK). The settling time for each fraction (<0.2 and <0.45 μm) was determined using the following equations:

$$\omega = \left(\frac{2\pi}{60}.rpm\right) \tag{1}$$

$$t = \frac{18\eta \ln\left(\frac{R}{S}\right)}{\omega^2 d^2 \Delta\rho} \tag{2}$$

where ω is the angular velocity of the centrifuge (rad s^{-1}), d is the particle diameter (cm), $\Delta\rho$ is the density difference between the particles and the suspension medium (g cm^{-3}), η is the viscosity of the suspension medium (g cm^{-1} s^{-1}) where the viscosity of water at 20 °C is 0.010 g cm^{-1} s^{-1}, t is the settling time (s), R is the distance (cm) from the axis of rotation to the level from where the supernatant is decanted from the tube), and S is the distance from the axis of rotation to the surface of the suspension in the tube (cm).

From the above equations, it was determined that the 1 % m/v soil suspension (containing <1 μm particles) required a centrifugation time of 4 min at 3000 rpm (at 25 °C) to obtain the <0.45 μm fraction. The centrifugation process needs to be repeated by re-suspending the sample pellet in ultra-pure water and re-centrifuging until the supernatant is clear. It was observed, however, that the supernatant was clear on centrifuging the sample a second time, indicating that the entire <0.45 μm fraction had been obtained. Therefore the soil suspension was only centrifuged once to obtain the different sized fractions. This process was repeated to obtain the <0.2 μm fraction by centrifuging the 1 % m/v soil suspension at 8000 rpm for 3 min (at 25 °C).

4.2.6 Effect of sample dilution

Rowden soil suspensions of lower concentrations (0.5 and 0.25 % m/v) were prepared by dissolving 0.5 and 0.25 g soil in 100 mL ultra-pure water respectively. The soil suspensions were shaken gently for 16 h and settled in 600 mL beakers. The <1 μm fraction was extracted and used to prepare the centrifuged and filtered fractions in the same way as for the 1 % m/v soil suspensions. This was to determine how centrifugation and filtration compared when diluted soil suspensions were used. In Chapter 3 there was an observed significant difference between the centrifuged and filtered fractions at 1 % m/v concentration using SdFFF, so these experiments were carried out to see if the same trend was observed at this concentration and with more dilute soil suspensions (0.5 and 0.25 % m/v).

4.2.7 Real soil runoff samples

Throughout this chapter soil suspensions have been used to optimise the FlFFF system. These were chosen as models for soil runoff or leachate samples. Once the system was optimised, real runoff samples were analysed to determine the performance of FlFFF. The runoff samples (five in total) were collected during a storm event from a lysimeter (plot 7)

at IGER. The plot is part of a long-term field scale experiment called the Rowden Experiment (NGR SX 650 995), and each lysimeter is 1 ha in size [45]. The runoff was sampled from a V-notch weir (Fig. 4.4) on plot 7 every 2 h from 9 am on 6th May 2004. The flow rates of the runoff from the lysimeter were also recorded at the same time as each sample was collected. The samples were stored overnight in the dark at 4 °C and collected the next day. The samples were gently shaken for 10 min and then settled in 600 mL beakers for 1 h. The top 20 mL was extracted (<1 μm fraction) and 20 μL of each sample was injected once into the FlFFF.

Figure 4.4. V-notch weir on the Rowden plot at IGER, North Wyke where the runoff samples were collected.

4.3 Results and Discussion

4.3.1 Data analysis

Fractograms were obtained by plotting detector response against elution time (or volume) of the emerging sample. The dead volume (which is the volume from the end of the channel to the UV detector) was removed from each of the fractograms to give corrected elution time (or volume). Blank runs were carried out for each experiment where 20 μL of ultra-pure water was injected into the FlFFF channel. All sample runs were then blank-subtracted as some response was seen with blank injections. All results shown are therefore corrected for this effect. The fractograms were then converted to particle size distributions

(PSDs) using an Excel program but were not corrected for light scattering effects [36,46,47].

4.3.2 Optimisation of settling conditions

1. Effect of settling time. The difference in UV absorbance for each of the different settling times is shown in Fig. 4.5A. The UV response was greater at shorter settling times and therefore when converted to particle size distributions, the relative mass was also greater for shorter settling times. The peak areas were calculated in Microcal™ ORIGIN® 6.0 software by integrating the peaks giving peak areas of 0.09526 and 0.03497 for 1h and 25.6 h settling times respectively (Fig. 4.5B). There was also a shift in peak maximum from 0.1 μm after 1 h settling to 0.29 μm after 25.6 h settling.

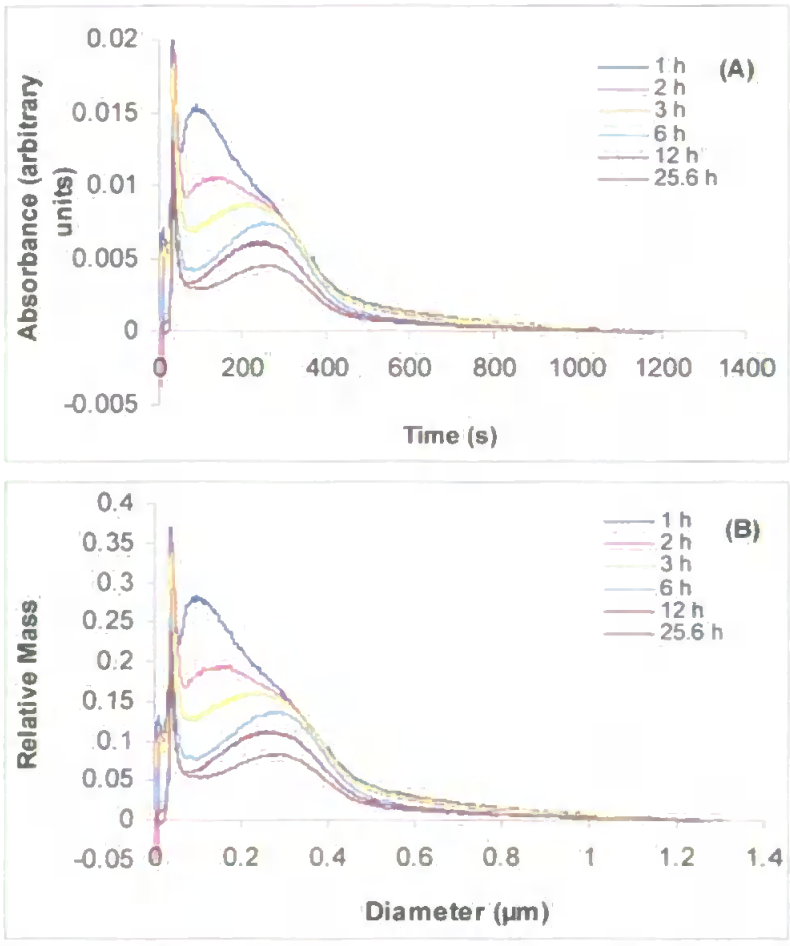

Figure 4.5. Effect of settling time: (A) Fractograms for Rowden soil suspensions at different settling times; (B) PSDs for Rowden soil suspensions at different settling times.

Williams and Keil monitored, with model dextran carbohydrates, how the molecular weight distributions of seawater incubations changed over a 23 h period [4]. The seawater samples were incubated with the dextrans either as whole seawater samples or filtered seawater samples (<0.02 μm). The filtered samples contained natural dissolved organic matter (DOM), whereas the whole seawater samples contained DOM and microorganisms. They observed that for the filtered (<0.02 μm) seawater sample, the molecular weight at peak maximum shifted to higher molecular weights for incubations longer than 12 h, with peak height decreasing but peak area remaining the same. It was suggested that this was due to aggregation of the dextrans with DOM present in the seawater. The molecular weight distributions for the whole seawater samples showed a decrease in response over the 23 h period, and also a shift in peak maxima towards higher molecular weights with a decrease in peak area. Aggregation of the dextrans with DOM and degradation of the dextrans by microorganisms were suggested as the causes of this change in response.

Although the samples studied here were a different matrix, the processes were probably similar because microbes present in the soil suspension samples were not destroyed by pre-treatment prior to FlFFF analysis. Therefore the shift in the fractograms towards longer retention times at peak maximum, and hence the shift in particle size distributions towards larger diameters and decrease in peak area, could be due to aggregation processes as the settling time increased, and degradation due to microbial utilisation. Temperature is also an important parameter in the settling process; Chen and Buffle reported that during the settling process for non-thermostated samples the particles did not follow the expected settling behaviour because of flotation effects [48]. Therefore it was important that samples undergoing gravitational settling were kept at the same temperature throughout the settling process. Soil suspension samples settled in this work were therefore kept at a constant temperature of 20 °C in a water bath during the settling process, and settled in as short a time as possible, i.e. 1 h, to minimise the effect of any aggregation processes.

2. Settling of replicate samples. The fractograms for the five replicate samples of the Rowden and the Dartmoor Peat soil suspensions were very similar (Fig. 4.6A). The fractograms were converted to PSDs and the means of the five samples for each soil sample are shown for clarity (Fig. 4.6B). The peak area for each sample was then determined from the PSDs giving peak areas of 0.0667 and 0.3990 for the Rowden and Dartmoor Peat respectively. The RSDs for peak area for the Rowden and Dartmoor Peat samples were 3.4 and 3.2 % respectively. This shows good repeatability between samples using the 1 h settling method.

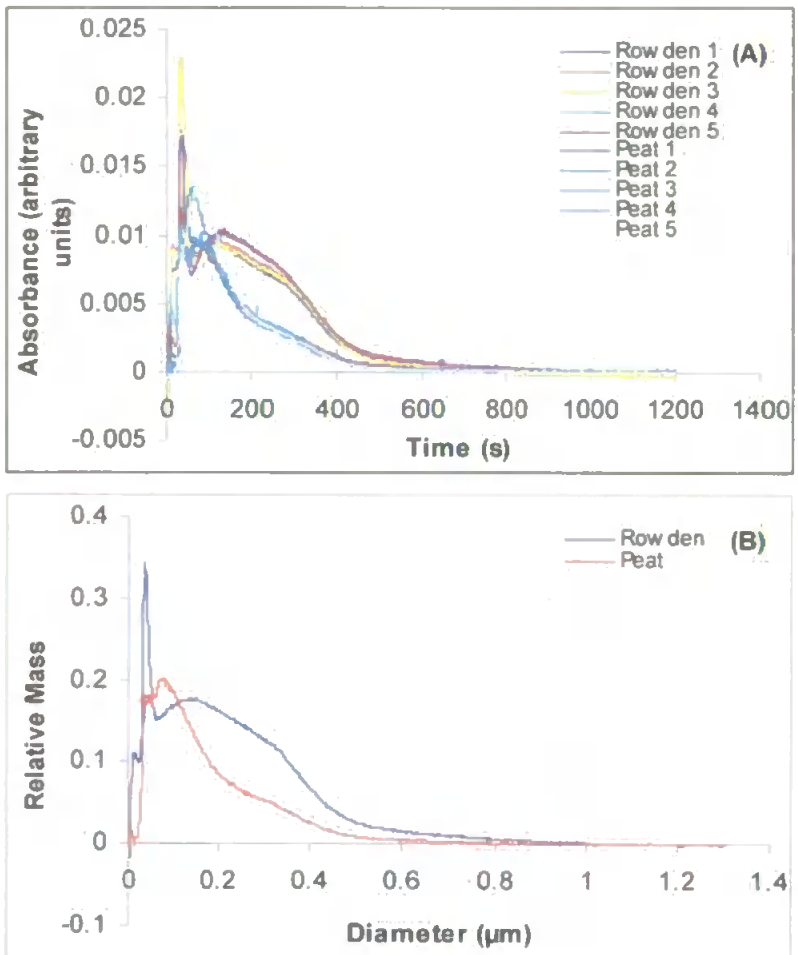

Figure 4.6. Settling of replicate samples: (A) Fractograms for Rowden and Dartmoor Peat soil suspensions after 1 h settling; (B) PSDs for Rowden and Dartmoor Peat soil suspensions after 1 h settling showing the mean for the five replicate samples.

3. Re-settling of the same sample. The fractograms for repeated re-settling of the same Rowden soil suspension were very similar (Fig. 4.7A). The peak area for the PSDs (Fig. 4.7B) for the six times re-settled Rowden soil suspension sample were 0.0435, 0.0369, 0.0446, 0.0379, 0.0374, and 0.0381 in order of repeated re-settling, giving a mean peak area of 0.0397 and an RSD of 8.5 %. This result shows that as long as the sample is shaken before re-settling, then the PSD for the <1 μm soil sample does not change significantly during 12 h of analysing the same sample.

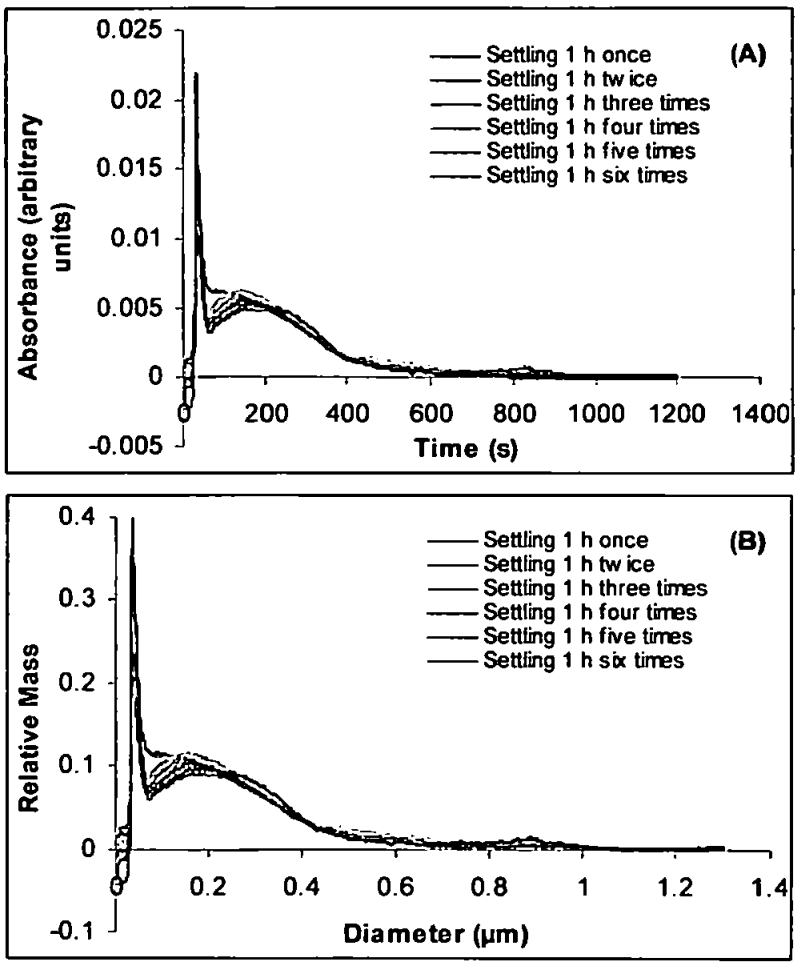

Figure 4.7. Re-settling of same sample: (A) Fractograms for Rowden soil suspensions after repeated 1 h settling; (B) PSDs for Rowden soil suspensions after repeated 1 h settling.

4.3.3 Comparison of centrifugation and filtration for two contrasting soils

Stability experiment. The fractograms for the averaged data over three days showed a decrease in absorbance (Fig. 4.8A). The peak area for the PSDs also decreased over the three days by 31 % (Fig. 4.8B). The decrease in area suggests that something is happening to the sample during this time when it is kept at room temperature. This change in response is similar to that observed with the seawater incubations [4] where after 23 h the peak height for the whole seawater incubations had decreased. Therefore there could be degradation processes occurring in the soil suspension sample over the three days, probably due to microbial utilisation. However unlike the seawater samples or the response seen for the first settling experiments here, aggregation does not seem to have occurred, as there is no shift in peak maximum for larger particle diameters. Therefore an alternative or complementary explanation is that sample is being lost by sticking to the walls of the container, and therefore not available for analysis.

Optimised settling protocol. The optimum conditions for preparing and analysing the samples were to settle 1 % m/v soil suspensions (total volume 100 mL) in 600 mL beakers for 1 h. The top 20 mL layer containing the <1 μm particles was extracted using a pipette. This <1 μm fraction was then analysed within 12 h to minimise any changes in the soil suspension samples.

Chen and Buffle suggested that colloidal natural water samples should be pre-fractionated as quickly as possible to remove particles >1 μm by gravitational settling, and stored for no more than 2-3 days in the dark at 4 °C [48,49]. In this work it has been shown that soil suspension samples that were fractionated to <1 μm by gravitational settling were stable for at least 12 h when stored at room temperature. The samples were kept at room temperature to be compatible with the temperature conditions used for the FIFFF

experiments. Also storage of samples for longer than 12 h was not necessary as all experiments were completed within this time.

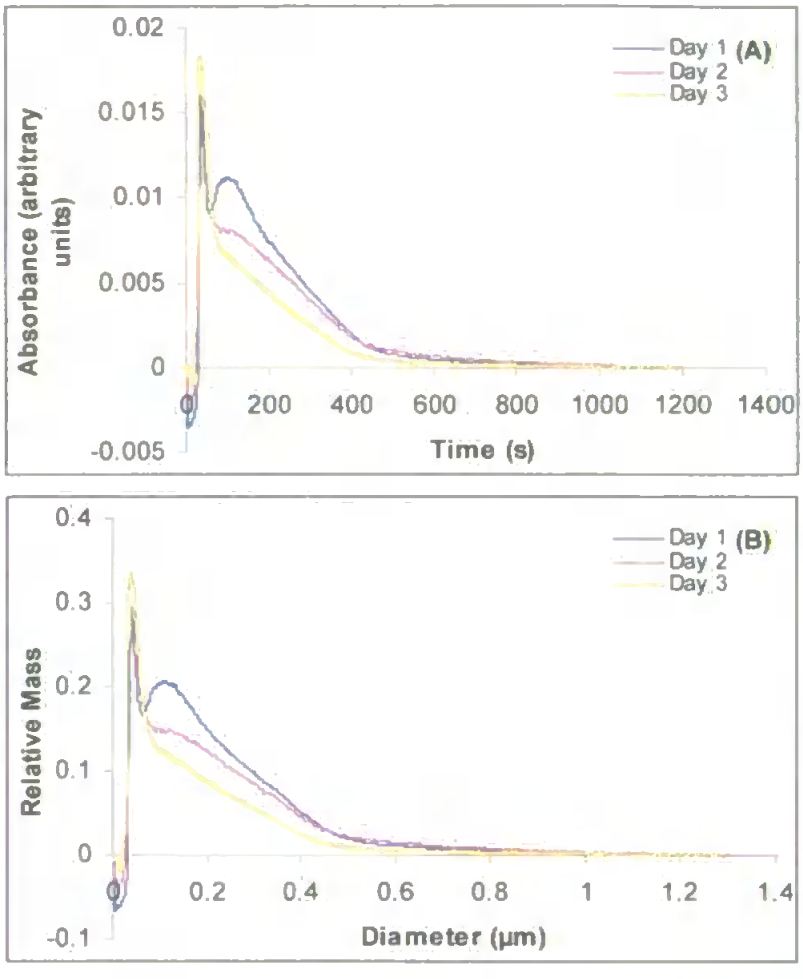

Figure 4.8. Stability experiment: (A) Fractograms for Rowden soil suspensions with data averaged for three runs of <1 µm sample each day for a period of three days; (B) PSDs for Rowden soil suspensions with data averaged for three runs each day for a period of three days.

Fractograms for Rowden soil suspensions (1 % m/v). The fractograms for the <1 µm Rowden soil suspensions and the centrifuged and filtered fractions (<0.2 and <0.45 µm) are shown in Figs. 4.9A and 4.9B respectively. A decrease in response can be seen for the filtered fractions in comparison with the centrifuged fractions. The fractograms have been baseline subtracted by subtracting the response observed when blank runs were carried out. It was observed that the responses for the filtered fractions were similar to the response for

the blank runs, thus when the fractograms were baseline subtracted, the fractograms lie close to the *x* axis as seen in Fig. 4.9B.

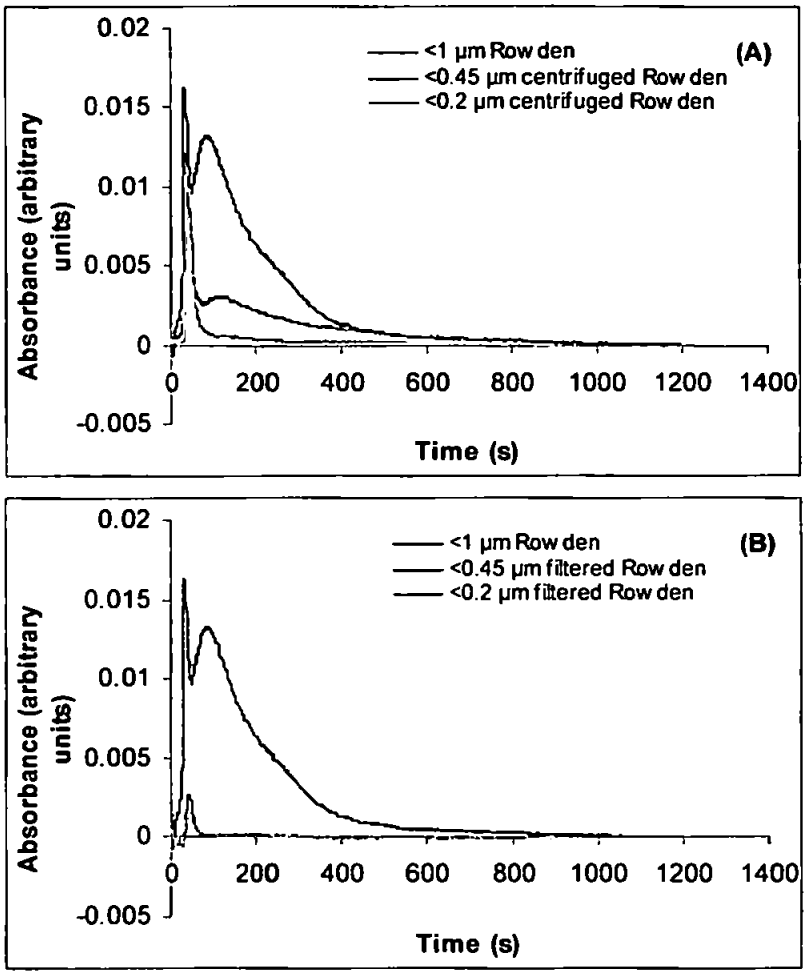

Figure 4.9. FlFFF fractograms for the Rowden soil suspensions (1 % m/v) comparing filtered and centrifuged fractions with <1 µm starting material: (A) Fractogram for <0.2 and <0.45 µm centrifuged fractions with data averaged for the three runs; (B) Fractogram for <0.2 and <0.45 µm filtered fractions with data averaged for the three runs.

Particle size distributions for Rowden soil suspensions (1 % m/v). The PSDs for the <1 µm and centrifuged fractions are compared in Fig. 4.10A. The particle size threshold for each fraction was close to the expected thresholds of 0.2, 0.45 and 1 µm. Some material was removed using centrifugation, as the peak areas were 14 % and 40 % of the <1 µm fraction for the <0.2 and <0.45 µm centrifuged fractions respectively. However it can be seen that more material was removed using filtration for each of the lower size fractions

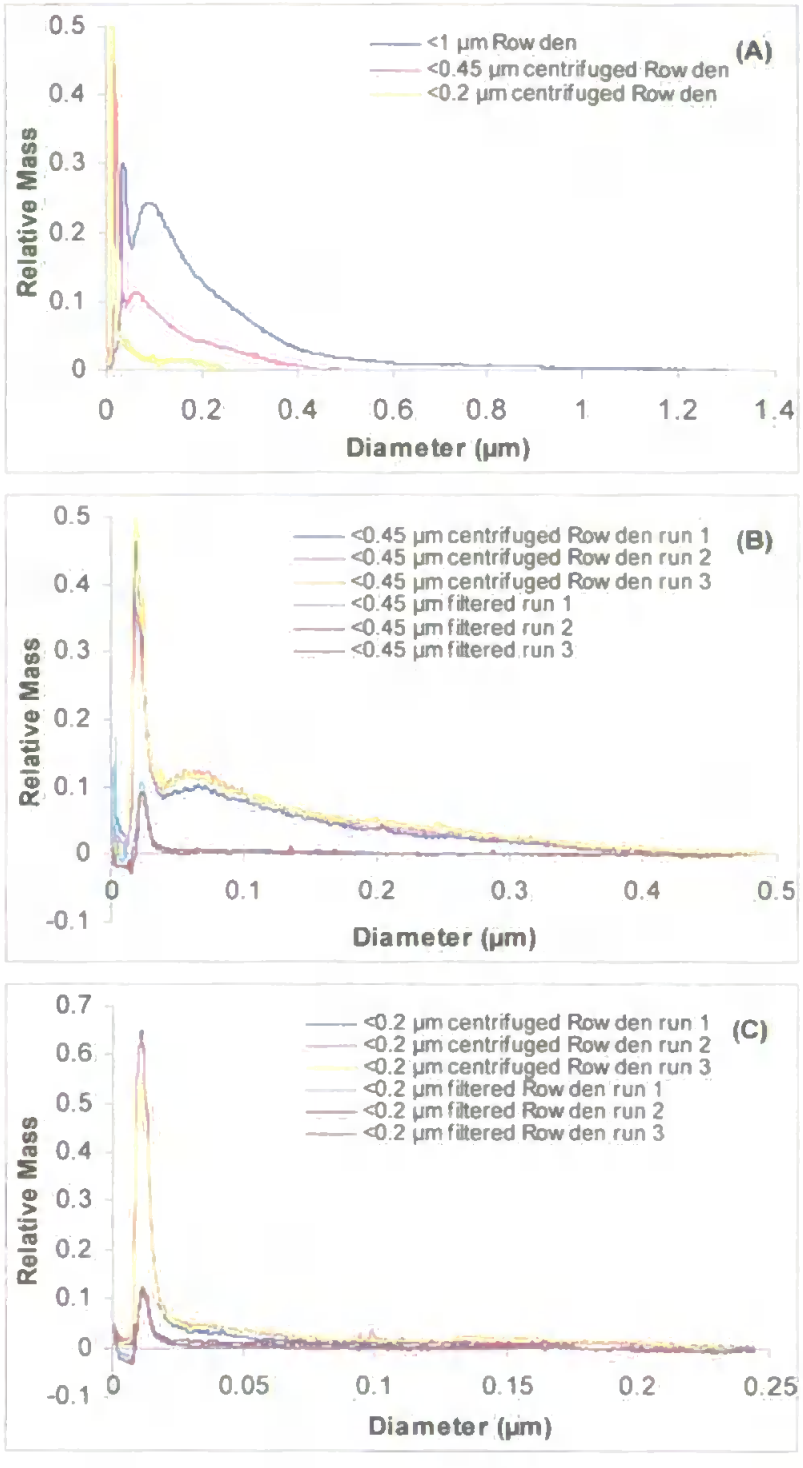

Figure 4.10. FlFFF particle size distributions for Rowden soil suspensions (1 % m/v): (A) PSDs for <0.2 and <0.45 µm centrifuged fractions and <1 µm starting material with data averaged for three runs; (B) PSDs for three runs of <0.45 µm filtered and centrifuged fractions; (C) PSDs for three runs of <0.2 µm filtered and centrifuged fractions.

(<0.2 and <0.45 µm fractions), as the peak areas were 1 % and 3 % of the <1 µm fraction for the <0.2 and <0.45 µm fractions respectively. Figs. 4.10B and 4.10C showed good

reproducibility for three runs of each sample and for the difference between the amount of material recovered from centrifugation and filtration methods. The decrease in peak area for the filtered fractions as compared with the centrifuged fractions was 89 % and 93 % for the <0.2 and <0.45 μm fractions respectively. Assemi *et al.* characterised natural organic matter (NOM) fractions separated by ultrafiltration membranes using FlFFF [50]. They found that the ultrafiltration membranes did not separate the NOM from natural water samples into fractions with the expected molecular weight and size. This supports the finding of this work that membrane filtration is not a reliable preparation method for fractionating environmental samples.

Centrifugation has been shown to fractionate Rowden soil suspensions yielding larger recoveries for the <0.2 and <0.45 μm fractions than conventional filtration methods. However FlFFF is capable of analysing the whole colloidal range of soil suspensions providing that the samples have been pre-fractionated to <1 μm to avoid steric inversion. Therefore there is no need to prepare the soil suspensions by centrifugation or filtration prior to FlFFF analysis, as more information can be obtained about the particle size distribution by injecting the entire <1 μm sample.

Fractograms for Dartmoor peat suspensions (1 % m/v). The fractograms for the <1 μm Dartmoor Peat soil suspensions and the centrifuged and filtered fractions (<0.2 and <0.45 μm) are shown in Figs. 4.11A and 4.11B respectively. There was a decrease in response for the filtered fractions compared to the centrifuged fractions, as was observed for the Rowden soil suspensions.

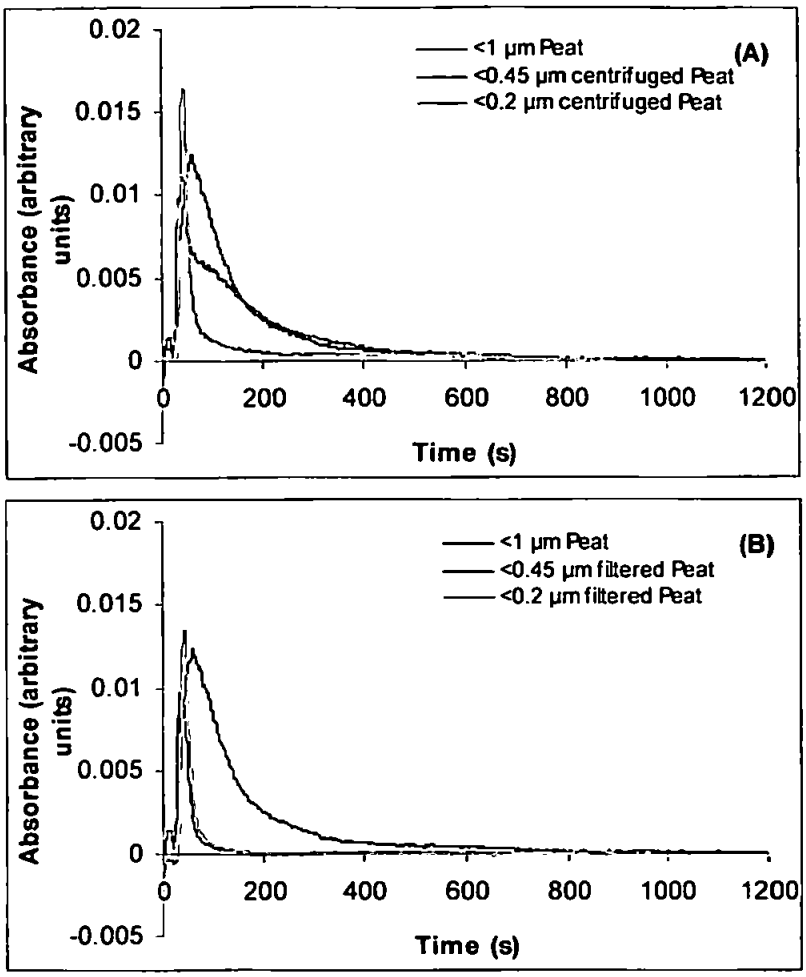

Figure 4.11. FlFFF fractograms for the Dartmoor Peat soil suspensions (1 % m/v) comparing filtered and centrifuged fractions with <1 µm starting material: (A) Fractogram for <0.2 and <0.45 µm centrifuged fractions with data averaged for the three runs; (B) Fractogram for <0.2 and <0.45 µm filtered fractions with data averaged for the three runs.

Particle size distributions for Dartmoor peat soil suspensions (1 % m/v). The PSDs for the <1 µm and centrifuged fractions (<0.2 and <0.45 µm) are compared in Fig. 4.12A. The particle diameter at peak maximum for the Dartmoor Peat was at 0.06 µm for the <1 µm fraction.

Figs. 4.12B and 4.12C show good reproducibility for three runs of each sample and the difference between the amount of material recovered from centrifugation and filtration

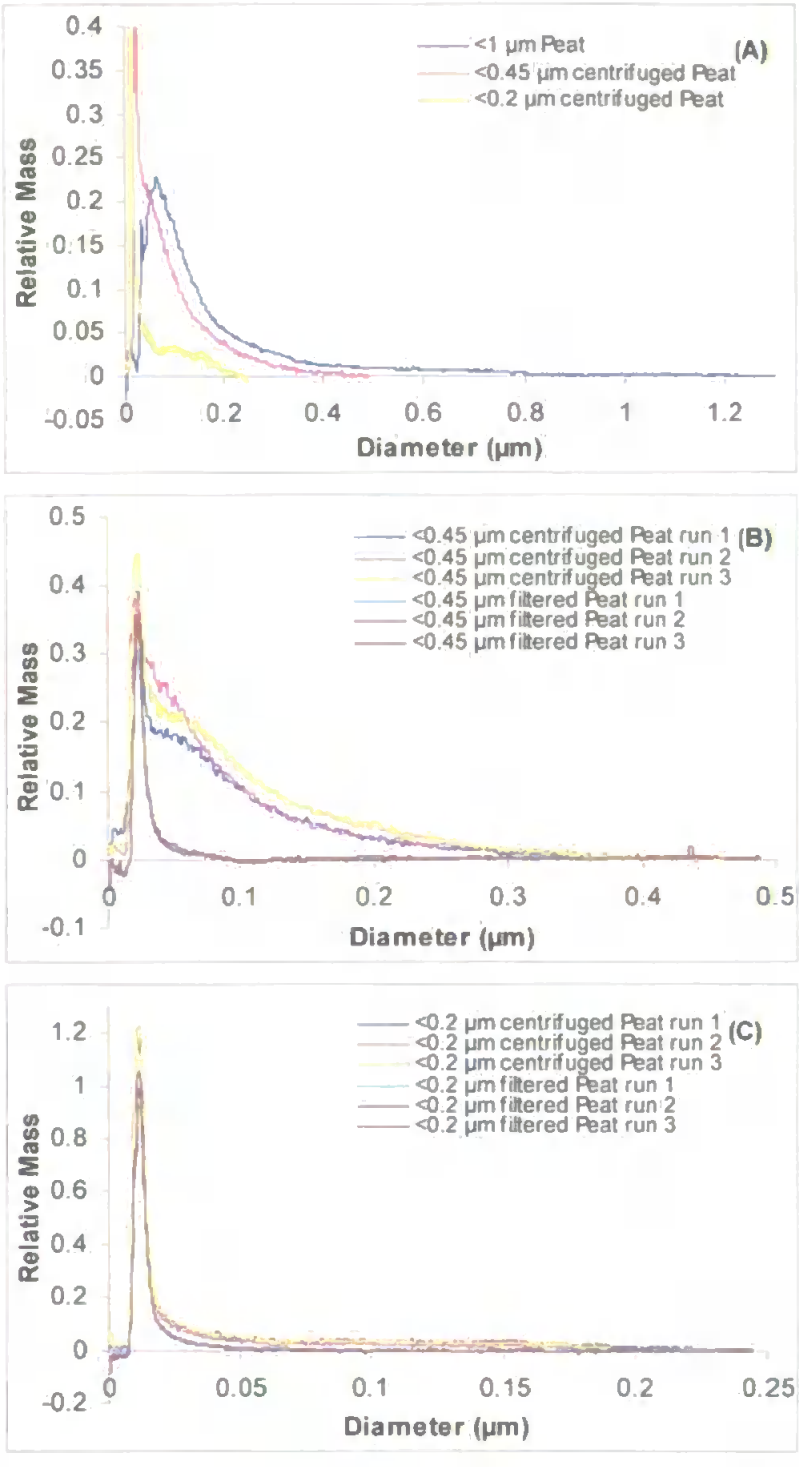

Figure 4.12. FlFFF particle size distributions for Dartmoor Peat soil suspensions (1 % m/v): (A) PSDs for <0.2 and <0.45 µm centrifuged fractions and <1 µm starting material with data averaged for three runs; (B) PSDs for three runs of <0.45 µm filtered and centrifuged fractions; (C) PSDs for three runs of <0.2 µm filtered and centrifuged fractions.

methods. There was a decrease in peak area for the filtered fractions from the centrifuged fractions of 53 % and 84 % for the <0.2 and <0.45 μm fractions respectively.

The PSD for the Dartmoor Peat was compared with the Rowden soil for the <1 μm fraction (Fig. 4.13). A difference can be seen between the soil samples in terms of diameter at peak height, which was 0.06 and 0.1 μm for the Peat and Rowden soil suspensions respectively. However it should be stressed that this work was not intended to give a catalogue of soil profiles, as only two were chosen, but instead to test the performance of FlFFF with two contrasting soils as examples.

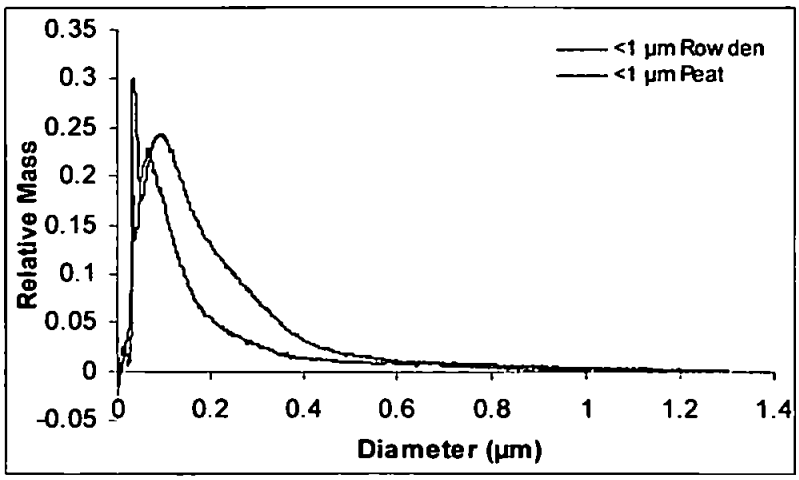

Figure 4.13. FlFFF PSDs to compare the <1 μm fraction for the Dartmoor Peat and the Rowden soil suspensions of 1 % m/v concentration.

4.3.4 Effect of sample dilution

The results presented here follow a similar pattern to that seen for 1 % m/v Rowden soil suspensions. Therefore only the PSDs are shown with the data for three runs of each sample averaged for clarity, as it has already been shown (section 4.3.3) that the reproducibility between soil suspension samples is good.

Particle size distributions for Rowden soil suspensions (0.5 % m/v). The PSDs for the 0.5 % m/v Rowden soil suspensions (Fig. 4.14) again show a decrease in mass for the filtered fractions compared with the centrifuged fractions. Therefore the results for the <0.2 and <0.45 μm centrifuged and filtered fractions show that at half the soil suspension concentration (0.5 % m/v), there is still material being lost by filtration. The peak areas for the filtered samples compared with the centrifuged samples decrease by 85 % and 94 % for the <0.2 and <0.45 μm fractions respectively, which is very similar to the decrease in areas for the filtered fractions using 1 % m/v Rowden soil suspension.

Particle size distributions for Rowden soil suspensions (0.25 % m/v). The final experiment to determine the effect of diluted soil suspensions used a 0.25 % m/v Rowden soil suspension. This was chosen as the lowest concentration that could be examined successfully to observe the difference between the filtered and centrifuged fractions. Any lower concentration than this would give fractograms close to the detection limit of the system. The PSDs (Fig. 4.15) show that, although the relative masses for the 0.25 % m/v samples are smaller than for the PSDs where the starting concentration was 1 % m/v (Fig. 4.10), a difference between the filtered and centrifuged fractions can still be observed. Again there is a difference in peak areas between the filtered and centrifuged fractions, where the peak area for the filtered runs was 63 % and 92 % less than the centrifuged runs for <0.2 and <0.45 μm fractions respectively. The results summarised in Table 4.1 show that for each of the concentrations used (1, 0.5 and 0.25 % m/v) the filtered fractions gave lower responses than the centrifuged fractions. This difference could be due to colloids interacting directly with the membrane during filtration, resulting in material being retained. There could also be memory effects, contamination from the filter and variable pressure across the membrane. The results therefore suggest that conventional <0.45 and <0.2 μm membrane filtration techniques for the separation of soil suspensions remove much more of the particulate material than the corresponding centrifugation procedure.

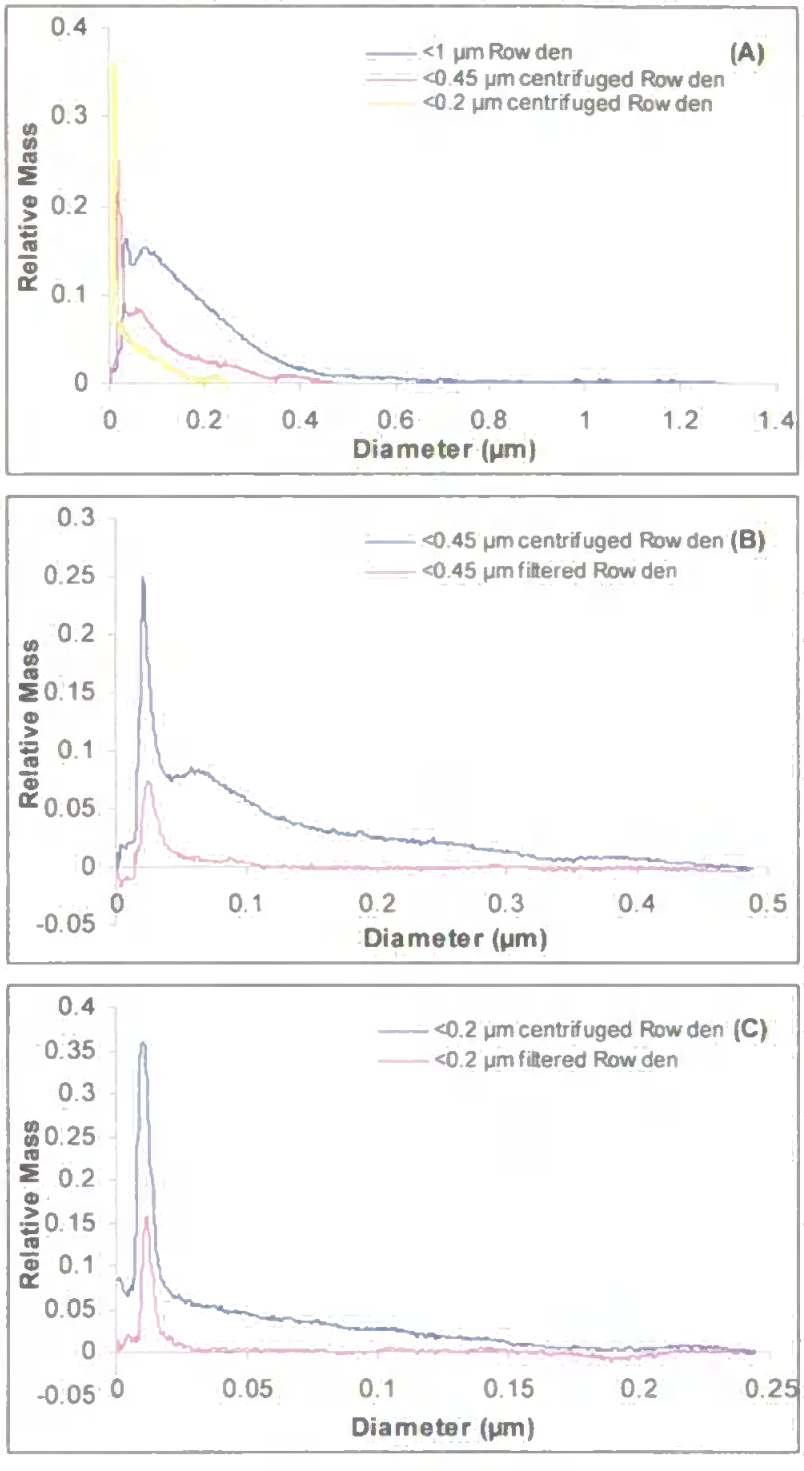

Figure 4.14. FlFFF particle size distributions for Rowden soil suspensions (0.5 % m/v): (A) PSDs for <0.2 and <0.45 µm centrifuged fractions and <1 µm starting material with data averaged for three runs; (B) PSDs for <0.45 µm filtered and centrifuged fractions with data averaged for three runs; (C) PSDs for <0.2 µm filtered and centrifuged fractions with data averaged for three runs.

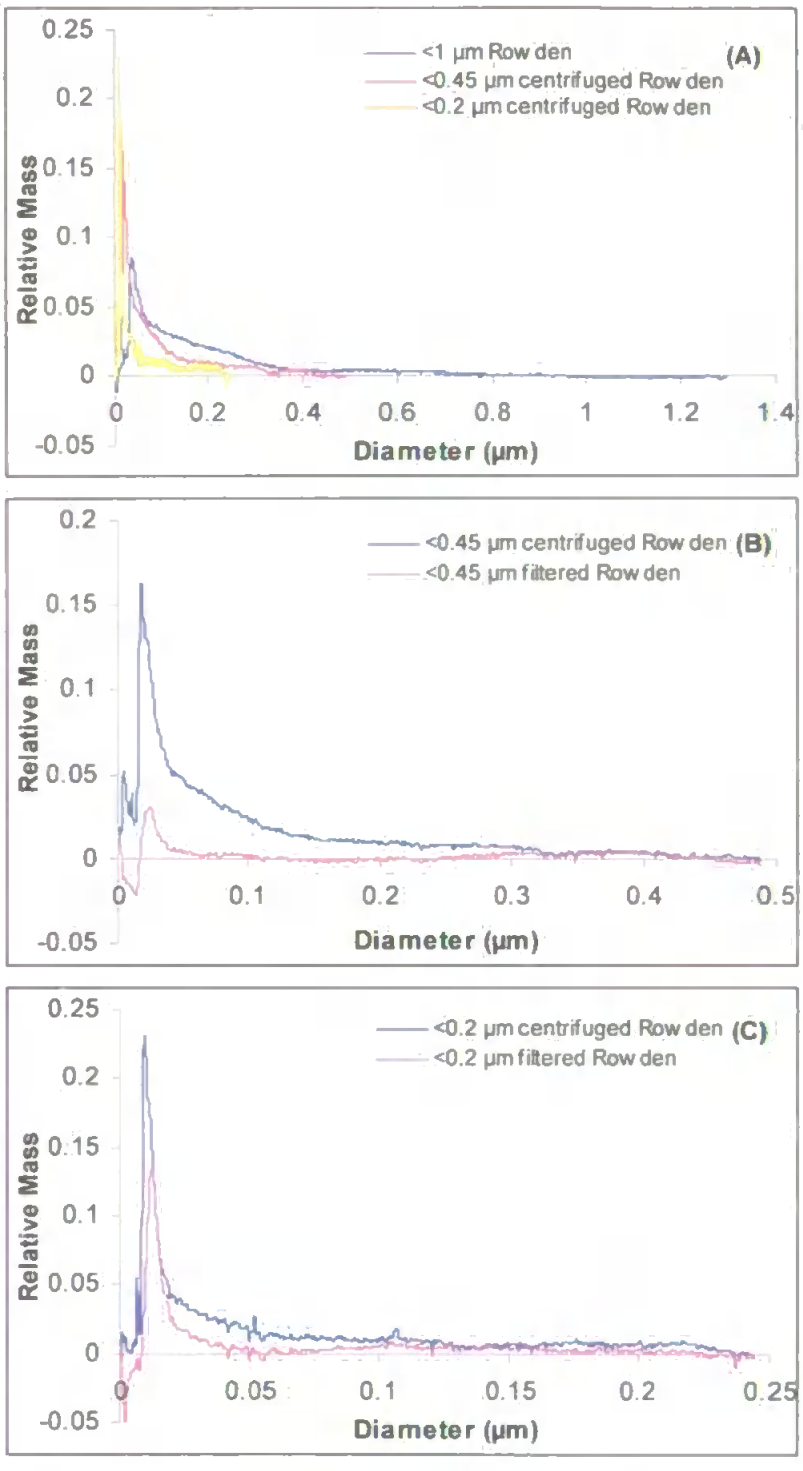

Figure 4.15. FlFFF particle size distributions for Rowden soil suspensions (0.25 % m/v): (A) PSDs for <0.2 and <0.45 µm centrifuged fractions and <1 µm starting material with data averaged for three runs; (B) PSDs for <0.45 µm filtered and centrifuged fractions with data averaged for three runs; (C) PSDs for <0.2 µm filtered and centrifuged fractions with data averaged for three runs.

Table 4.1. Comparison of peak area and % loss between the filtered and centrifuged fractions for each of the 1, 0.5 and 0.25 % m/v Rowden soil suspensions.

Sample concentration (% m/v)	Peak area for each fraction as calculated in ORIGIN				% loss of filtered fraction from centrifuged fraction	
	<0.2 µm centrifuged	<0.2 µm filtered	<0.45 µm centrifuged	<0.45 µm filtered	<0.2 µm	<0.45 µm
1	0.457	0.049	1.348	0.096	89	93
0.5	0.475	0.070	0.873	0.049	85	94
0.25	0.223	0.082	0.461	0.037	63	92

Throughout these experiments there is no evidence that the channel is being overloaded at higher concentrations (1 % m/v). This is because the retention time at peak maximum for the <1 µm samples does not shift left at higher concentrations, which would occur if the channel was being overloaded with particulate samples [51]. Therefore it is reasonable to use soil suspensions of 1 % m/v concentration that have been settled for 1 h to determine the entire colloidal range of soil samples.

4.3.5 Real soil runoff samples

The storm discharge hydrograph is shown in Fig. 4.16 for the period sampled, where the maximum flow rate of 0.56 L s^{-1} occurred at 13:00 on 6th May 2004. The fractograms (Fig. 4.17A) show good response for all the five runoff samples which shows that FlFFF is capable of analysing real samples during storm events. This is a promising result as size information on colloidal material in real soil runoff samples can be used to determine how pollutants associated with colloidal material are transported during rain events from land to water. The PSDs (Fig. 4.17B) show little difference between the samples collected at different times considering that the flow rate or discharge changed during the sampling period (Fig. 4.16) which could have affected the amount of colloidal material in the runoff samples. However this may not be an entirely accurate result as the samples were unavoidably stored overnight in the dark at 4 °C and collected the next day. Ideally the samples should be collected and analysed immediately or at least within 12 h of collection.

Therefore future work will involve sampling at higher temporal resolution to monitor colloidal transport during a rain event.

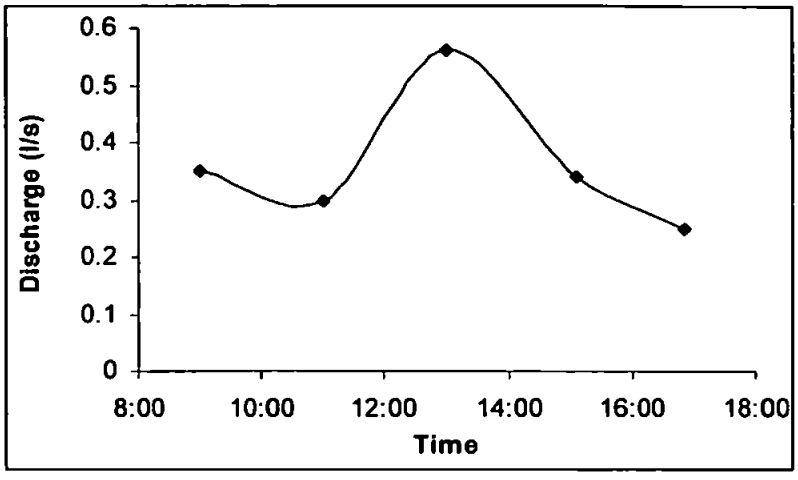

Figure 4.16. Storm discharge hydrograph for sampling period during storm event on 6th May 2004 at the Rowden plot, IGER.

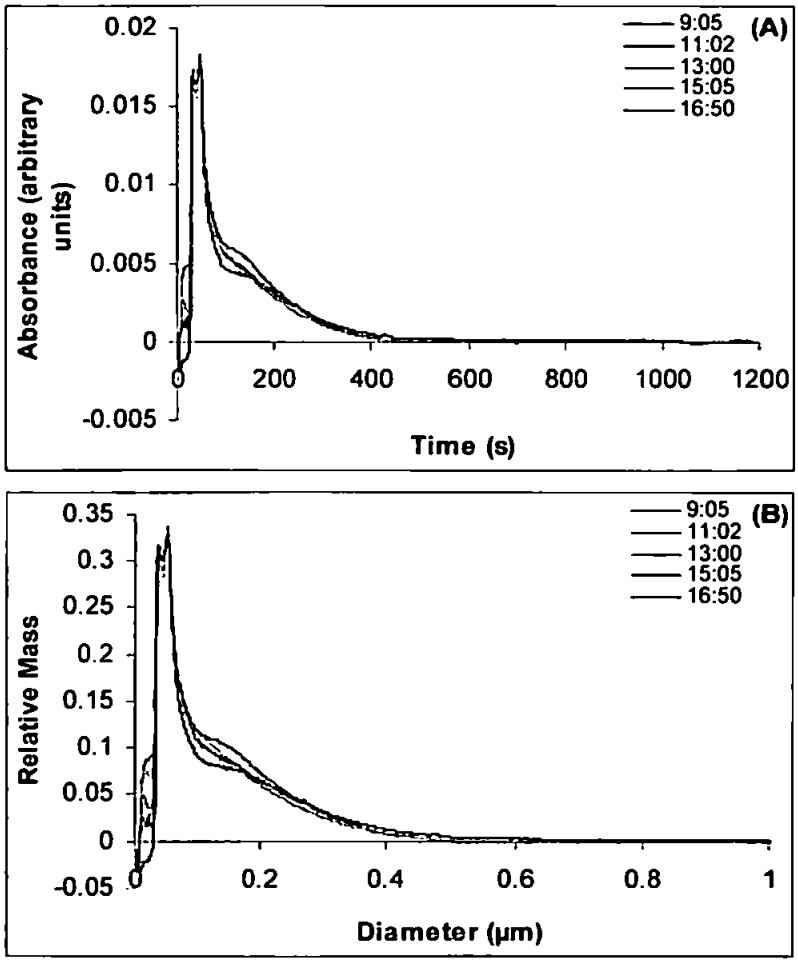

Figure 4.17. Real runoff samples collected during a storm event: (A) Fractograms for Rowden runoff samples after 1 h settling; (B) PSDs for Rowden runoff samples after 1 h settling.

4.4 Conclusions

FlFFF has been used to determine the appropriate settling and preparation protocol for soil suspension samples. From the settling experiments, it is recommended that soil suspension samples are settled gravitationally at a constant temperature (20 °C) as soon as possible after sampling to obtain the <1 μm fraction. The settling time should not exceed 1 h to ensure that the sample has not aggregated over longer settling times.

Centrifugation was shown to remove a small amount of material when the <1 μm fraction was used to prepare the smaller size fractions (<0.2 and <0.45 μm), however filtration was shown to remove much larger amounts of material than centrifugation for the same fractions. This was also observed when lower concentrations of 0.5 and 0.25 % m/v soil suspensions were analysed. Therefore centrifugation has again been shown to be more appropriate than filtration when working with soil suspensions, which was the same finding as with the previous SdFFF work in Chapter 3. However, as even centrifugation removes a small amount of material, FlFFF can be used to analyse the entire colloidal range without needing to centrifuge or filter the samples as long as particles greater than 1 μm have been removed before analysis. Preliminary experiments have analysed real runoff samples in the whole colloidal range using the optimised FlFFF system without the need for centrifugation or filtration.

4.5. References

[1] Vaillancourt, R. D.; Balch, W. M. Size distribution of marine submicron particles determined by flow field-flow fractionation. *Limnology and Oceanography* **2000**, *45*, 485-492.

[2] Beckett, R.; Wood, F. J.; Dixon, D. R. Size and chemical characterization of pulp and paper mill effluents by flow field-flow fractionation and resin adsorption techniques. *Environmental Technology* **1992**, *13*, 1129-1140

[3] Dixon, D. R.; Wood, F. J.; Beckett, R. Characterization of organics in pulp and paper mill effluents before and after physicochemical treatment. *Environmental Technology* **1992**, *13*, 1117-1127.

[4] Williams, S. K. R.; Keil, R. G. Monitoring the biological and physical reactivity of dextran carbohydrates in seawater incubations using flow field-flow fractionation. *Journal of Liquid Chromatography & Related Technologies* **1997**, *20*, 2815-2833.

[5] Zanardi-Lamardo, E.; Clark, C. D.; Zika, R. G. Frit-inlet/frit outlet flow field-flow fractionation: methodology for colored dissolved organic material in natural waters. *Analytica Chimica Acta* **2001**, *443*, 171-181.

[6] Beckett, R.; Bigelow, J. C.; Jue, Z.; Giddings, J. C. Analysis of humic substances using flow field-flow fractionation in *Influence of Aquatic Humic Substances on Fate and Treatment of Pollutants*, MacCarthy, P.; Suffet, I. H., Eds., Acs Advances in Chemistry Series No. 219, American Chemical Society, Washington D. C., 1989, pp.65-80.

[7] Beckett, R.; Jue, Z.; Giddings, J. C. Determination of molecular weight distributions of fulvic and humic acids using flow field-flow fractionation. *Environmental Science & Technology* **1987**, *21*, 289-295.

[8] Dycus, P. J. M.; Healy, K. D.; Stearman, G. K., Wells, M. J. M. Diffusion coefficients and molecular weight distributions of humic and fulvic acids determined by flow field-flow fractionation. *Separation Science and Technology* **1995**, *30*, 1435-1453.

[9] Kammer, F. v. d.; Förstner, U. Natural colloid characterization using flow-field-flow-fractionation followed by multi-detector analysis. *Water Science and Technology* **1998**, *37*, 173-180.

[10] Lead, J. R.; Wilkinson, K. J.; Balnois, E.; Cutak, B. J.; Larive, C. K.; Assemi, S.; Beckett, R. Diffusion coefficients and polydispersities of the suwannee river fulvic acid: Comparison of fluorescence correlation spectroscopy, pulsed-field gradient nuclear magnetic resonance, and flow field-flow fractionation. *Environmental Science & Technology* **2000**, *34*, 3508-3513.

[11] Pelekani, C.; Newcombe, G.; Snoeyink, V. L.; Hepplewhite, C.; Assemi, S.; Beckett, R. Characterization of natural organic matter using high performance size exclusion chromatography. *Environmental Science & Technology* **1999**, *33*, 2807-2813.

[12] Petteys, M. P.; Schimpf, M. E. Characterization of hematite and its interaction with humic material using flow field-flow fractionation. *Journal of Chromatography A* **1998**, *816*, 145-158.

[13] Schimpf, M. E.; Petteys, M. P. Characterization of humic materials by flow field-flow fractionation. *Colloids and Surfaces A: Physicochemical and Engineering Aspects* **1997**, *120*, 87-100.

[14] Thang, N. M.; Geckeis, H.; Kim, J. I.; Beck, H. P. Application of the flow field flow fractionation (FFFF) to the characterization of aquatic humic colloids: evaluation and optimization of the method. *Colloids and Surfaces A: Physicochemical and Engineering Aspects* **2001**, *181*, 289-301.

[15] van den Hoop, M. A. G. T.; van Leeuwen, H. P. Influence of molar mass distribution on the complexation of heavy metals by humic material. *Colloids and Surfaces A: Physicochemical and Engineering Aspects* **1997**, *120*, 235-242.

[16] Andersson, K.; Hassellöv, M.; Lyvén, B. Colloidal trace element size distributions in freshwaters determined by flow field-flow fractionation coupled to ICPMS – a comparison of 12 Scandinavian rivers in: Hassellöv, M. Thesis, Göteberg University, Sweden, 1999.

[17] Hassellöv, M.; Lyvén, B.; Haraldsson, C.; Sirinawin, W. Determination of continuous size and trace element distribution of colloidal material in natural water by on-line coupling of flow field-flow fractionation with ICPMS. *Analytical Chemistry* **1999**, *71*, 3497-3502.

[18] Amarasiriwardena, D.; Siripinyanond, A.; Barnes, R. M. Trace elemental distribution in soil and compost-derived humic acid molecular fractions and colloidal organic matter in municipal wastewater by flow field-flow fractionation-inductively coupled plasma mass spectrometry (flow FFF-ICP-MS). *Journal of Analytical Atomic Spectrometry* **2001**, *16*, 978-986.

[19] Lyvén, B.; Hassellöv, M.; Haraldsson, C.; Turner, D. R. Optimisation of on-channel preconcentration in flow field-flow fractionation for the determination of size distributions of low molecular weight colloidal material in natural waters. *Analytica Chimica Acta* **1997**, *357*, 187-196.

[20] Beckett, R.; Hart, B. T., Use of Field-Flow Fractionation Techniques to Characterize Aquatic Particles, Colloids, and Macromolecules, in Buffle, J. and van Leeuwen, H. P. (Eds.), *Environmental Particles*, Volume 2, Lewis Publishers Boca Raton, Florida, 1993, pp. 165-205.

[21] Buffle, J.; Leppard, G. G. Characterization of aquatic colloids and macromolecules. 1. Structure and behavior of colloidal material. *Environmental Science & Technology* **1995**, *29*, 2169-2175.

[22] Haygarth, P. M.; Jarvis, S. C., Eds.; *Agriculture, Hydrology and Water Quality*, CABI Publishing, Oxford, New York, 2002, pp. 1-502.

[23] Haygarth, P. M.; Hepworth, L.; Jarvis, S. C. Forms of phosphorus transfer in hydrological pathways from soil under grazed grassland. *European Journal of Soil Science* **1998**, *49*, 65-72.

[24] Haygarth, P. M.; Jarvis, S. C. Transfer of phosphorus from agricultural soils. *Advances in Agronomy*, **1999**, *66*, 195-249.

[25] Abuashour, J.; Joy, D, M.; Lee, H.; Whiteley, H. R.; Zelin, S. Transport of microorganisms through soil. *Water, Air, and Soil Pollution*, **1994**, *75*, 141-158.

[26] Jones, D. L.; Campbell, G.; Kaspar, C. W. Human enteric pathogens. In *Agriculture, Hydrology and Water Quality*; Haygarth, P. M.; Jarvis, S.C., Eds.; CAB International, Wallingford, 2002.

[27] Oliver, D. M.; Clegg, C. D.; Haygarth, P. M.; Heathwaite, A. L. Assessing the potential for pathogen transfer from grassland soils to surface waters. *Advances in Agronomy*, (in press).

[28] Gevao, B.; Jones, K. C. Pesticides and persistent organic pollutants. In *Agriculture, Hydrology and Water Quality*; Haygarth, P. M.; Jarvis, S.C. Eds.; CAB International, Wallingford, 2002.

[29] Goulding, K. Nitrate leaching from arable and horticultural land. *Soil Use and Management* **2000**, *16*, 145-151.

[30] Scholefield, D.; Tyson, K. C.; Garwood, E. A.; Armstrong, A. C.; Hawkins, J.; Stone, A. C. Nitrate leaching from grazed grassland lysimeters – effects of fertilizer input, field drainage, age of sward and patterns of weather. *Journal of Soil Science* **1993**, *44*, 601-613.

[31] Giddings, J. C. Retention (steric) inversion in field-flow fractionation: Practical implications in particle size, density and shape analysis. *Analyst* **1993**, *118*, 1487-1494.

[32] Chen, B.; Beckett, R. Development of SdFFF-ETAAS for characterising soil and sediment colloids. *Analyst* **2001**, *126*, 1588-1593.

[33] Chen, B.; Hulston, J.; Beckett, R. The effect of surface coatings on the association of orthophosphate with natural colloids. *The Science of the Total Environment* **2000**, *263*, 23-35.

[34] Chittleborough, D. J.; Hotchin, D. M.; Beckett, R. Sedimentation field-flow fractionation - a new technique for the fractionation of soil colloids. *Soil Science* **1992**, *153*, 341-348.

[35] Ranville, J. F.; Chittleborough, D. J.; Shanks, F.; Morrison, R. J. S.; Harris, T.; Doss, F.; Beckett, R. Development of sedimentation field-flow fractionation-inductively coupled plasma mass-spectrometry for the characterization of environmental colloids. *Analytica Chimica Acta* **1999**, *381*, 315-329.

[36] Taylor, H. E.; Garbarino, J. R.; Murphy, D. M.; Beckett, R. Inductively coupled plasma mass-spectrometry as an element-specific detector for field-flow fractionation particle separation. *Analytical Chemistry* **1992**, *64*, 2036-2041.

[37] van Berkel, J.; Beckett, R. Determination of adsorption characteristics of the nutrient orthophosphate to natural colloids by sedimentation field-flow fractionation. *Journal of Chromatography A* **1996**, *733*, 105-117.

[38] Lee, H.; Williams, S. K. R.; Giddings, J. C. Particle size analysis of dilute environmental colloids by flow field-flow fractionation using an opposed flow sample concentration technique. *Analytical Chemistry* **1998**, *70*, 2495-2503.

[39] Siripinyanond, A.; Barnes, R. M.; Amarasiriwardena, D. Flow field-flow fractionation-inductively coupled plasma mass spectrometry for sediment bound trace metal characterization. *Journal of Analytical Atomic Spectrometry* **2002**, *17*, 1055-1064.

[40] Hassellöv, M.; Lyvén, B.; Beckett, R. Sedimentation field-flow fractionation coupled online to inductively coupled plasma mass spectrometry - New possibilities for studies of trace metal adsorption onto natural colloids. *Environmental Science & Technology* **1999**, *33*, 4528-4531.

[41] Buffle, J.; Leppard, G. G. Characterization of aquatic colloids and macromolecules. 2. Key role of physical structures on analytical results. *Environmental Science & Technology* **1995**, *29*, 2176-2184.

[42] Giddings, J. C.; Williams, P. S.; Benincasa, M. A. Rapid breakthrough measurement of void volume for field-flow fractionation channels. *Journal of Chromatography* **1992**, *627*, 23-35.

[43] Heathwaite, L.; Haygarth, P.; Matthews, R.; Preedy, N.; Butler, P. Evaluating colloidal phosphorus delivery to surface waters from diffuse agricultural sources. *Journal of Environmental Quality* **2005**, *34*, 287-298.

[44] Findlay, D. C.; Colborne, G. J. N.; Cope, D. W.; Harrod, T. R.; Hogan, D. V.; Staines, S. V. *Soils and their use in South West England. Soil Survey of England and Wales. Bull. 14*, Harpenden, UK. Whitstable Litho Ltd., Whitstable, UK, 1984.

[45] Preedy, N.; McTiernan, K.; Matthews, R.; Heathwaite, L.; Haygarth, P. Rapid incidental phosphorus transfers from grassland. *Journal of Environmental Quality* **2001**, *30*, 2105-2112.

[46] Beckett, R.; Nicholson, G.; Hart, B. T.; Hansen, M.; Giddings, J. C. Separation and size characterization of colloidal particles in river water by sedimentation field-flow fractionation. *Water Research* **1988**, *22*, 1535-1545.

[47] Murphy, D. M.; Garbarino, J. R.; Taylor, H. E.; Hart, B. T.; Beckett, R. Determination of size and element composition distributions of complex colloids by sedimentation field-flow fractionation inductively-coupled plasma-mass spectrometry *Journal of Chromatography* **1993**, *642*, 459-467.

[48] Chen, Y.-W.; Buffle, J. Physicochemical and microbial preservation of colloid characteristics of natural water samples. II: Physicochemical and microbial evolution. *Water Research* **1996**, *30*, 2185-2192.

[49] Chen, Y.-W.; Buffle, J. Physicochemical and microbial preservation of colloid characteristics of natural water samples. I: Experimental conditions *Water Research* **1996**, *30*, 2178-2184.

[50] Assemi, S.; Newcombe, G.; Hepplewhite, C.; Beckett, R. Characterization of natural organic matter fractions separated by ultrafiltration using flow field-flow fractionation. *Water Research* **2004**, *38*, 1467-1476.

[51] Schimpf, M.; Caldwell, K. D.; Giddings, J. C. (Eds.), *Field-Flow Fractionation Handbook*, Wiley, New York, 2000.

Chapter 5

A Portable Flow Injection Monitor for the Determination of Phosphorus in Soil Suspensions

5.1 Introduction

Phosphorus (P) in soil leachate and agricultural runoff waters occurs in particulate, dissolved and colloidal forms [1]. The dissolved fraction is operationally defined as the fraction that passes through a 0.2 or 0.45 μm membrane. Other operationally defined phosphorus species are described in Chapter 1. The colloidal fraction spans this 0.2 or 0.45 μm threshold therefore phosphorus associated with colloidal material (0.001-1 μm) will be present in both the dissolved and particulate fractions. Phosphorus losses are increased during storm events due to surface runoff containing phosphorus adsorbed to soil particles, and to runoff from freshly applied fertilisers or manure containing dissolved phosphorus [2-9].

Reactive phosphorus (RP) in the orthophosphate form can be determined by flow injection (FI) combined with spectrophotometric detection using molybdenum blue chemistry [10-12]. RP consists of orthophosphate, labile condensed and organic phosphates, and labile colloidal material. For particulate phosphorus and non-labile colloidal material (part of the total phosphorus (TP) fraction) a digestion method is required to break down P containing bonds before spectrophotometric analysis [13]. There are many different digestion methods used for the determination of TP and these are discussed in section 5.3.4.

The aim of this work was to optimise a portable FI monitor for the determination of RP, using two different optimisation methods. Once optimised the system was used to determine the effect of silicate as it is a potential interferent when analysing soil leachate and runoff waters [12,14,15]. The determination of TP was also investigated by optimising an acidic peroxydisulphate autoclaving method. This was achieved using model P containing compounds representative of those compounds found in soil leachate and agricultural runoff samples.

5.2 Experimental

5.2.1 Laboratory ware

All glassware and bottles were first cleaned overnight in nutrient free detergent (Neutracon®, Decon Laboratories, UK), rinsed three times with ultra-pure water (Elga Maxima®, 18.2 MΩ), soaked in 10 % (v/v) HCl for 24 h, again rinsed three times with ultra-pure water and dried at room temperature.

5.2.2 Reagents and standards

All solutions were prepared with ultra-pure water and all reagents were of AnalaR grade (VWR International, Dorset, UK) or equivalent, unless otherwise stated. A 3 mM PO_4-P stock solution was prepared by dissolving 0.4393 g of potassium dihydrogen orthophosphate (oven dried for 1 h at 105 °C) in 1 L of ultra-pure water. Working standards in the range 0.8 – 8 µM PO_4-P were prepared by dilution of the stock solution. For the determination of the limit of detection and linear range, standards in the range 0.5 – 25 µM PO_4-P were prepared by dilution of the stock solution.

Two reagents were prepared, these were: ammonium molybdate solution (10 g ammonium molybdate and 35 mL sulphuric acid in 1 L of ultra-pure water), and tin(II) chloride solution (0.2 g tin(II) chloride and 2 g hydrazinium sulphate and 28 mL sulphuric acid in 1 L ultra-pure water).

The silicate standards used in the silicate interference study (section 5.2.6) were prepared by dilution of 1000 mg L^{-1} silicate SpectrosoL® solution to give working standards in the range 1 – 60 mg L^{-1}.

The model compounds (Sigma-Aldrich, Dorset, UK) used to optimise the acidic peroxydisulphate digestion method were phytic acid (PTA), penta-sodium triphosphate

(STP), adenosine-5'-triphosphoric acid disodium dihydrogen salt (5'-ATP-Na_2), cocarboxylase (COCA) and methyltriphenylphosphonium bromide (MTP), representative of a refractory C-O-P compound, a P-O-P compound, two C-O-P and P-O-P bond containing compounds, and a C-P compound respectively. The structural formulas for the model compounds are shown in Fig. 5.1. Further discussion about the choice of model compounds is discussed in section 5.3.4. All reagents and standards were ultra-sonicated for 15 min before use to remove any bubbles in the solutions.

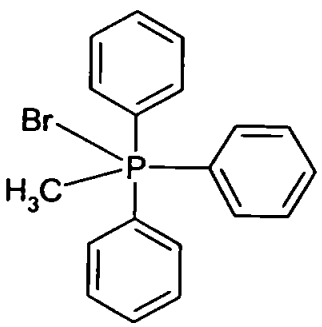

Methyltriphenylphosphonium bromide (MTP)

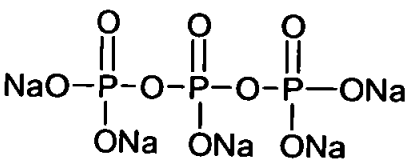

Penta-sodium triphosphate (STP)

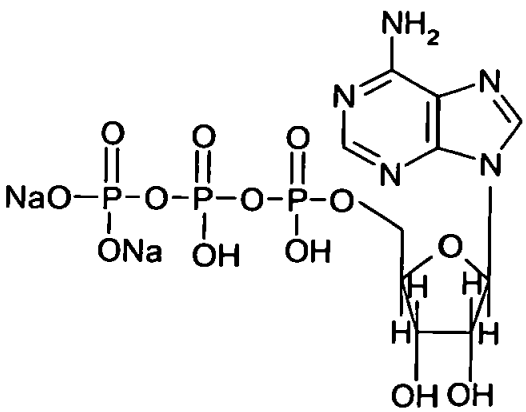

Adenosine-5'-triphosphoric acid disodium dihydrogen salt (5'-ATP-Na_2)

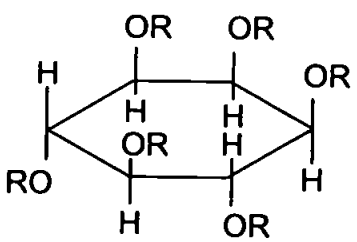

where $R=PO_3H_2$

Phytic acid (PTA)

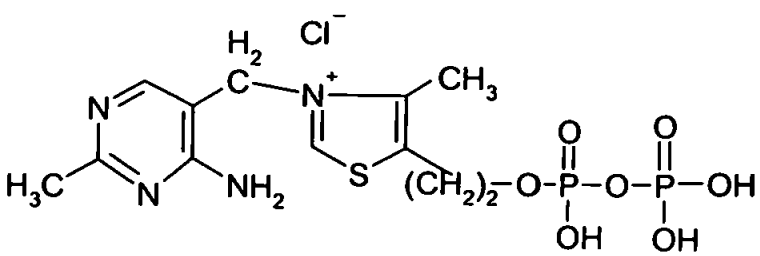

Cocarboxylase (COCA)

Figure 5.1. Structural formulas for the model compounds used in the optimisation of the autoclave digestion.

5.2.3 Flow injection instrumentation

Coles *et al.* developed a prototype flow injection instrument to monitor nitrate in the River Frome, Dorset [16]. This instrument was later modified by Hanrahan *et al.* [11] to monitor phosphate in the River Frome. All FI monitor components including the PSD-1000 Ocean Optics miniature fibre-optic spectrometer (Anglia Instruments Ltd., Cambridge, UK), miniature tungsten halogen lamp (LS-1 Ocean Optics Inc., Orlando, USA) and control box were housed in an impact resistant IP67 rated polycarbonate box (Fibox, Finland) (Fig. 5.2). The FI manifold for the monitor is shown in Fig. 5.3.

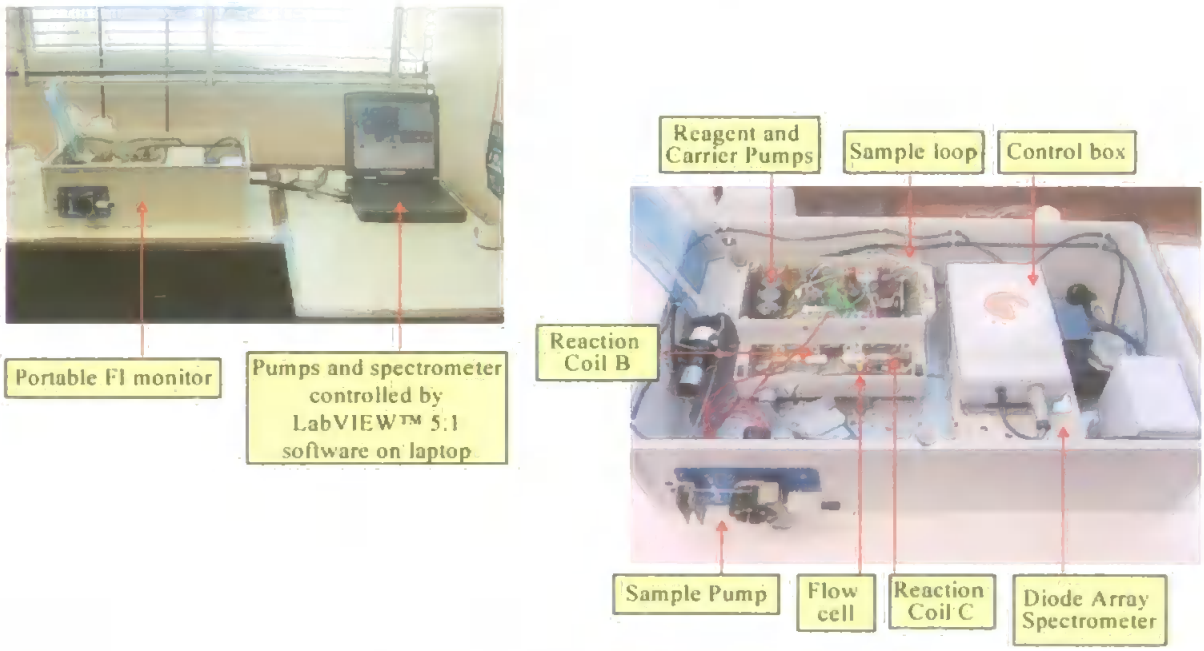

Figure 5.2. Portable FI monitor for the determination of PO_4-P.

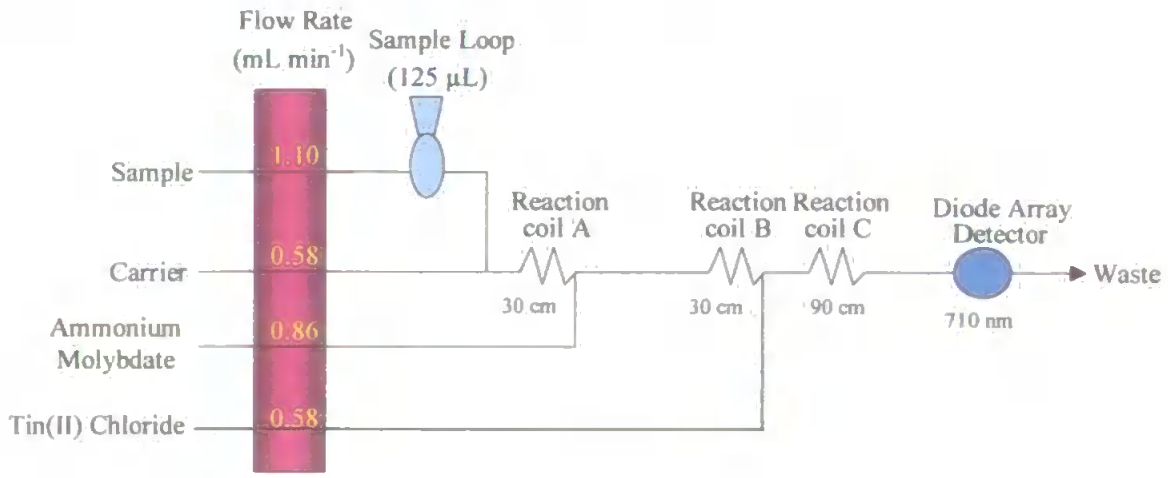

Figure 5.3. FI manifold for the determination of PO_4-P with optimised flow rates and reaction coil lengths.

The monitor was controlled by a notebook PC, a Toshiba Satellite 4030CDS (Toshiba Information Systems Ltd., Surrey, UK). Software written in LabVIEW™ 5.1 (National Instruments Corp., Berks, UK) (Fig. 5.4) controlled the automation of the manifold via a DAQCard™-DIO-24 card, and data acquisition from the spectrometer via a DAQCard™-700. The PO_4-P species were measured at 710 nm and processed by subtracting the absorbance at a non-absorbing wavelength (447 nm). This was done to remove the effect of pulsing caused by the micro-pumps.

The portable FI monitor consisted of three solenoid-operated self-priming micro-pumps (Bio-Chem Valve series 120SP12-25, PD Marketing, Chichester, UK) connected to solenoid switching valves (Bio-Chem Valve series 075T12-32, PD Marketing) with 0.8 mm i.d. PTFE tubing (Fisher Scientific, UK). The solenoid pumps were used for the carrier and two reagents whereas the sample was injected using a peristaltic pump fitted externally to the side of the box. The solenoid switching valves were automated using LabVIEW™ 5.1, and Fig. 5.5 demonstrates the direction of the carrier and reagent flows during sample loading and injection.

5.2.4 Optimisation of FI monitor for reactive phosphorus

Two types of optimisation were carried out. A univariate optimisation where one parameter at a time was changed keeping the other variables constant and a multivariate simplex optimisation where all the variables under investigation were changed together to determine the optimum response. The focus of this optimisation was based on maximising the detector response to enhance sensitivity, as the ultimate aim was to couple the FI monitor with FlFFF, which requires greater sensitivity as the sample is diluted during the FlFFF separation process. However for field deployments other parameters are important such as minimising waste and reagent consumption, and analysis time.

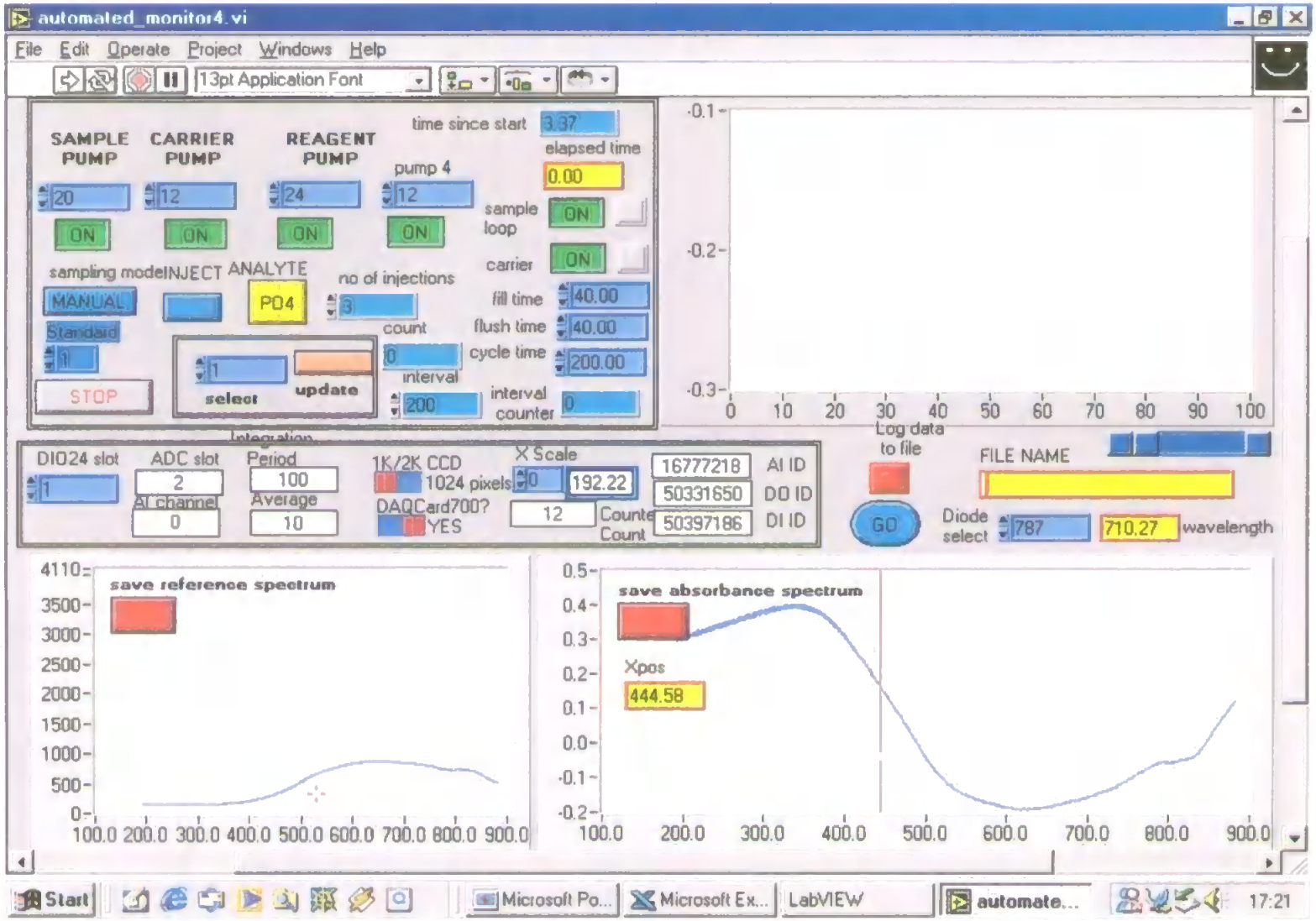

Figure 5.4. LabVIEW™ 5.1 software used to automate the portable FI monitor and acquire data from the spectrometer.

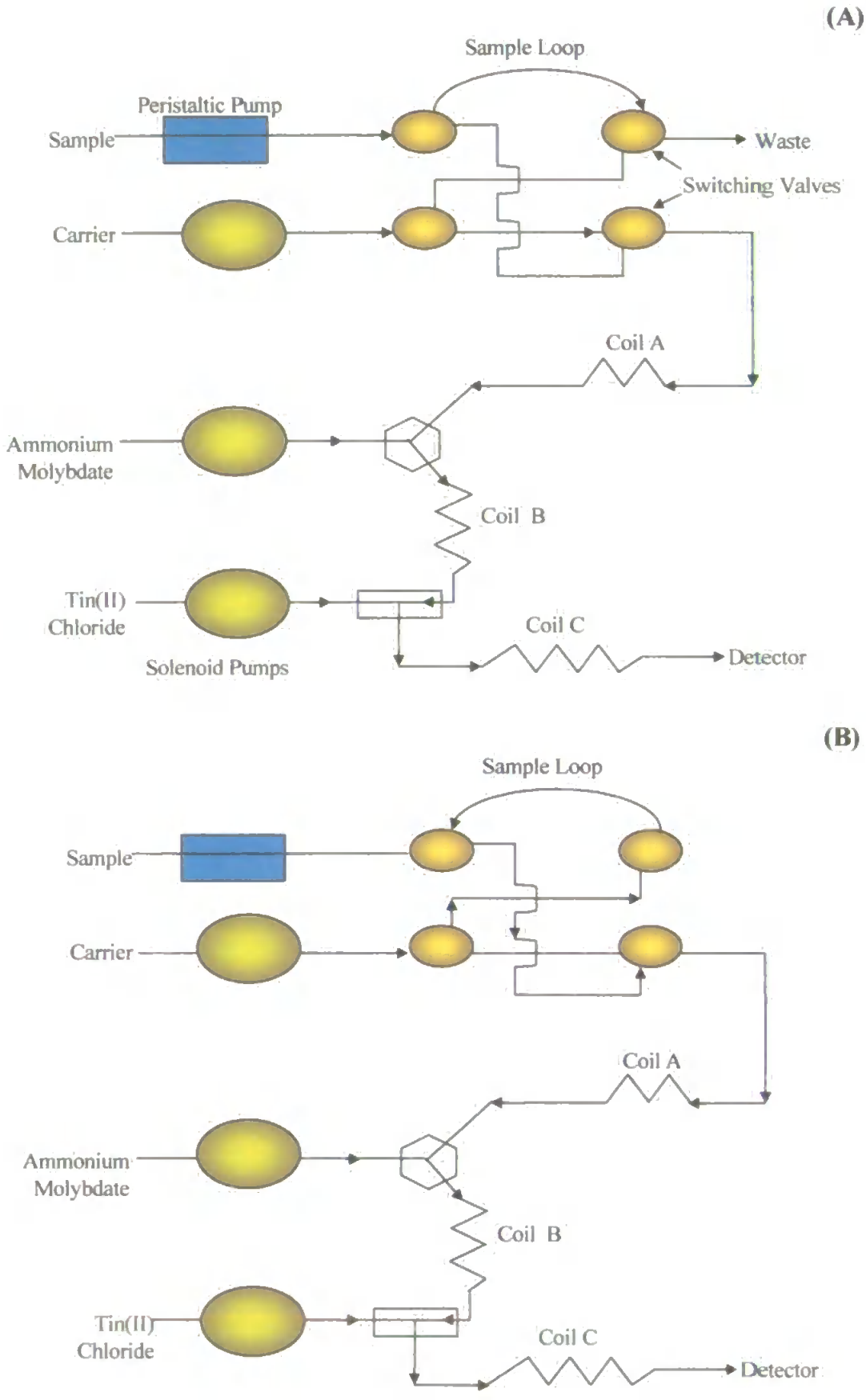

Figure 5.5. Direction of solenoid switching valves during: (A) Sample loading; (B) Injection of sample. Modified from Hanrahan *et al.* [11].

Before the optimisations were carried out, the solenoid pumps were calibrated to convert the digital units used in the LabVIEW™ program (Fig. 5.4) into flow rates (mL min^{-1}). The mass (or volume) of water pumped during 1 min at an initial flow rate of 5 digital units was measured. This was carried out in triplicate and the mean calculated. The flow rate was then increased to 10 digital units and the mass of water again measured. This was repeated at every 5 digital unit intervals to a maximum of 40 digital units. The means of the masses of water were plotted against the flow rate in digital units to give a calibration graph for each pump. From these calibration graphs, the flow rate range of 0-40 digital units corresponded to flow rate ranges of 0-1.74 mL min^{-1}, 0-1.44 mL min^{-1}, and 0-1.79 mL min^{-1} for the carrier, ammonium molybdate and tin(II) chloride pumps respectively.

Univariate optimisation: The variables chosen to be optimised were the flow rates for the carrier, ammonium molybdate and tin(II) chloride reagents. The lengths of the reaction coils B and C were also changed to determine the optimum response. Each of these variables was optimised separately while the other variables were kept constant. The constant values were chosen as those previously used by Hanrahan *et al.* [11] which were flow rates of 0.58 mL min^{-1} (or 12 digital units) for the carrier and tin(II) chloride and 0.86 mL min^{-1} (or 24 digital units) for the ammonium molybdate. The flow rate ranges investigated was 0.25-0.75 mL min^{-1} (or 4-16 digital units), 0.5-1.0 mL min^{-1} (or 13-28 digital units) and 0.25-0.75 mL min^{-1} (or 4-16 digital units) for the carrier, ammonium molybdate and tin(II) chloride pumps respectively. The response from a blank of ultra-pure water and a chosen standard of 4.5 μM PO_4-P was recorded at different flow rates for each pump. The coil length range investigated was 10-120 cm for both reaction coils B and C.

Simplex optimisation: This multivariate optimisation was carried out using a simplex algorithm written in BASIC with the conditions described in Table 5.1. The response from a blank and a 4.5 μM PO_4-P standard were determined for each set of changed variables,

and as many experiments as required were carried out until the response no longer improved. Only the pump flow rates were optimised in this experiment where pumps 1, 2 and 3 were the carrier, ammonium molybdate and tin(II) chloride pumps respectively.

Table 5.1. Experimental conditions for simplex optimisation

FI Variable	Units	Minimum Value	Maximum Value	Precision	Precision of Response	Starting Conditions
Carrier Pump	Digital units	4	28	1	0.001	12
Ammonium Molybdate Pump	Digital units	4	28	1	0.001	24
Tin(II) Chloride Pump	Digital units	4	28	1	0.001	12

5.2.5 Analytical figures of merit

Linear range and limit of detection: These were determined using a range of 0.5 – 25 μM PO_4-P standards. The limit of detection was calculated from the mean of the blank plus three times the standard deviation of the blank.

Reproducibility: The reproducibility of the method was investigated by measuring the response for twelve injections of a 4.5 μM PO_4-P standard.

5.2.6 Silicate interference study

High levels of silicate in soil leachate or agricultural runoff samples can be a possible additive interference and therefore the concentrations of phosphorus as orthophosphate can be overestimated in the presence of silicate, this is discussed further in section 5.3.3. To determine whether silicate interfered with this FI method the response of a range of silicate standards (2-60 mg L^{-1}) was measured. The response was then determined for 1 and 8 μM PO_4-P standards spiked with the same concentrations of silicate as those analysed with no phosphorus present.

5.2.7 Optimisation of an autoclaving method for the determination of total phosphorus

An acid peroxydisulphate digestion method based on the method of Haygarth *et al.* [17] was used for the determination of total phosphorus for the model compounds shown in Fig. 5.1. This autoclave method was then slightly modified (Method 2) to improve recoveries for the model compounds.

Method 1: Working standards were prepared by dilution of the 3 mM PO_4-P stock solution to give a range of 0.8-8 μM PO_4-P. Twenty mL of the working standards was pipetted into 100 mL glass autoclave bottles with black plastic screw caps (Fisher Scientific, Leicestershire, UK). These containers were used because of the ability to withstand the high temperatures within the autoclave.

Stock solutions of 3 mM P were prepared from the model compounds. Standards of 4.5 μM P were prepared by dilution of the stock solutions. Twenty mL of the 4.5 μM P model compounds was pipetted into glass autoclave bottles. All of the model compounds were prepared in duplicate to determine repeatability.

One mL 0.5 M sulphuric acid and 0.15 g potassium peroxydisulphate were added to 20 mL sample, and autoclaved for 45 min at 121 °C. Before placing the bottles in the autoclave the caps of the bottles were loosened by half a turn. After autoclaving the samples were allowed to cool to room temperature.

Method 2: The same protocol was followed as in Method 1 except the concentration of the potassium peroxydisulphate was increased from 0.15 to 0.8 g giving a concentration of 40 g L^{-1} instead of 8 g L^{-1}. This concentration was chosen as McKelvie *et al.* had obtained high recoveries for dissolved organic phosphorus in natural and waste water samples using 40 g L^{-1} peroxydisulphate [18]. The method was optimised by adjusting the concentration

of the peroxydisulphate alone as this was considered to be the most important parameter, rather than digestion time or temperature, for improving recoveries [19].

5.3 Results and Discussion

5.3.1 Optimisation of FI monitor for reactive phosphorus

Two optimisations were carried out; these were univariate and simplex optimisation methods. The univariate method works by changing one variable and keeping the others constant, and repeating for each variable, however when all the optimum values determined for each variable are used the optimum response may not be achieved due to interactive effects between the variables. Therefore a simplex optimisation was used where all variables can be changed at the same time and the optimum response determined from a changing combination of all variables. The univariate method was used to reduce the number of variables used in the simplex optimisation, which simplifies the simplex method, by reducing the number of experiments required to determine the optimum response.

Univariate optimisation: The pump flow rate ranges investigated here (as described in section 5.2.4) were previously used by Hanrahan for the optimisation of the FI monitor [20]. The responses for the blank and 4.5 μM PO_4-P standard are shown for each pump in Fig. 5.6. The response obtained for the blank was subtracted from the response for the standard and the standard-blank response also plotted in Fig. 5.6. This subtracted response was then used to determine the optimum pump flow rate. This was repeated for the reaction coil lengths and these are shown in Fig. 5.7.

The profiles of the univariate optimisations for the reagents ammonium molybdate and tin(II) chloride (Fig. 5.6B and C respectively) did not change greatly over the pump flow rate range investigated and the profile for the carrier (Fig 5.6A) increased up to 13 digital

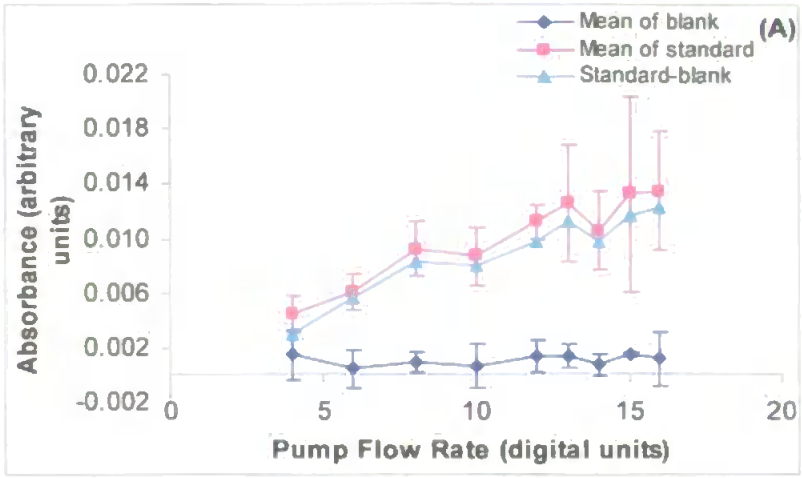

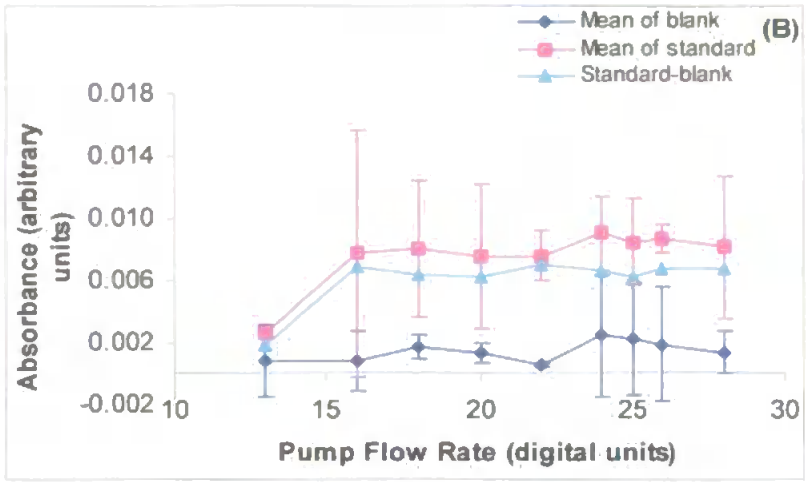

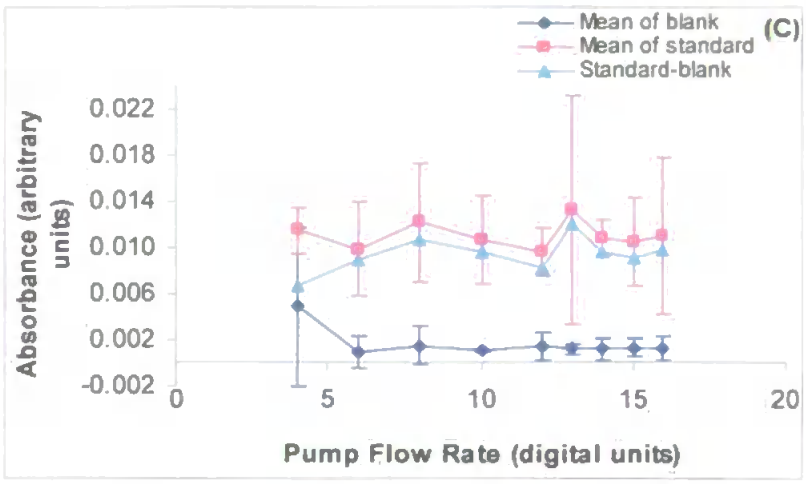

Figure 5.6. Univariate optimisation flow rate results for: (A) Carrier pump; (B) Ammonium molybdate pump; (C) Tin(II) chloride pump. Error bars show ± 3 standard deviations, n = 3.

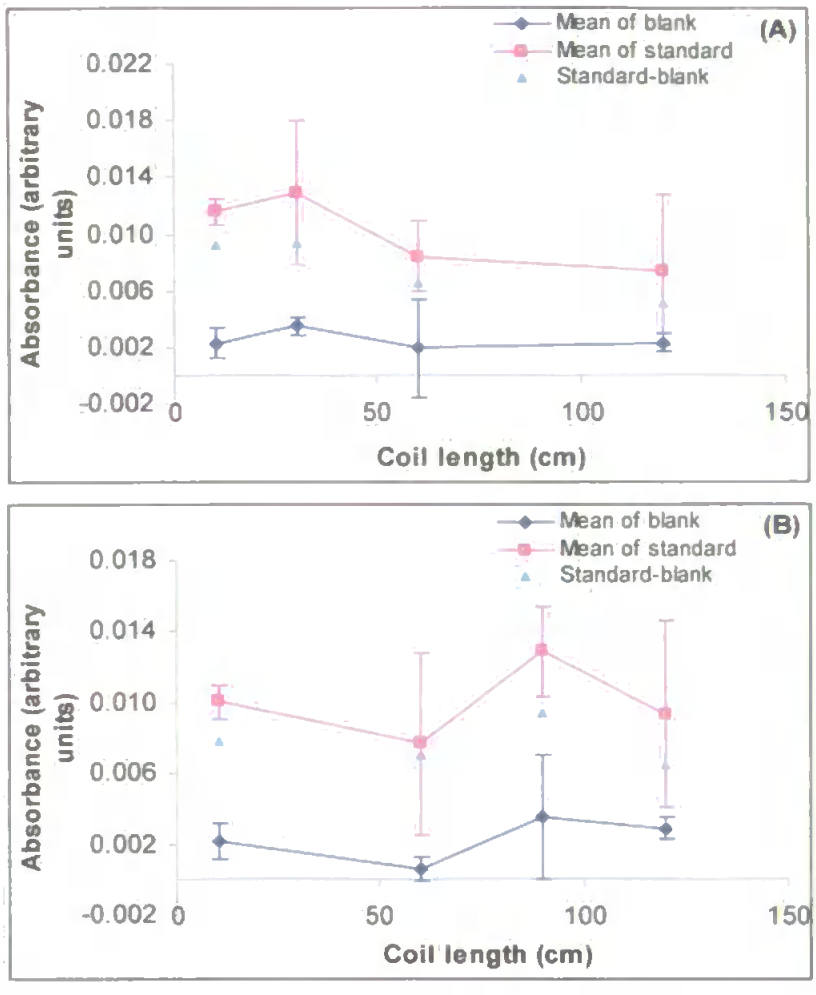

Figure 5.7. Univariate optimisation coil length results for: (A) Reaction coil B; (B) Reaction coil C. Error bars show ± 3 standard deviations, n = 3.

units and then there was no great change above 13 digital units. The carrier pump flow rate could have been extended above 16 digital units to determine whether there is any change in response as it could be expected that there may be a decrease in response due to insufficient time for the molybdenum blue complex to form [21]. The results in Fig. 5.7 show that the response for all coil lengths were similar with a slight improvement in response when 30 and 90 cm were used for coils B and C respectively, and these were not investigated further. Therefore none of the physical parameters have a major impact on the sensitivity of the FI monitor suggesting that the chemistry involved should be the main focus on further optimising the system rather than flow rates or reaction coil lengths if further improvements in sensitivity are required.

Therefore the flow rates were chosen on the basis of what was thought to be a reasonable combination for the three pumps and this was chosen to be 16, 22 and 14 digital units for the carrier, ammonium molybdate and tin(II) chloride respectively. When a calibration was carried out, the regression was $y = 0.0032x + 0.0019$, (x: concentration (μM), y: absorbance (arbitrary units)), $r^2 = 0.9765$. This shows no improvement on the flow rates initially used of 12, 24, 12 digital units as calibrations using these initial values gave regressions of $y = 0.0033x + 1 \times 10^{-4}$, ($x$: concentration (μM), y: absorbance (arbitrary units)), $r^2 = 0.9986$, and the absorbance for the blanks were lower using the initial values.

Simplex optimisation: A simplex is defined as a geometric figure that has $n + 1$ vertexes (corners) with respect to n factors [22]. When a simplex is used for optimisation of experimental systems, each vertex will correspond to a set of experimental conditions. For 2 factors the simplex will be a triangle and this case is used to demonstrate how simplex optimisation works and shown in Fig. 5.8. The initial simplex is defined as points 1, 2 and 3, at each of these points there is a set of different experimental conditions for each variable (2 in this case). The response is determined at each of these points, with the worst response determined at point 3. By reflecting point 3 to give point 4, a better response is obtained, however this response is also now better than the response found at point 1, therefore point 1 is now reflected to give a better response at point 5. This process continues until there are no further improvements in response as points 6 and 8 give worse responses than points 5 and 7. As three pump flow rates were examined for optimisation then the number of vertexes was 4 [23].

The univariate approach eliminated the need to examine the effect of the reaction coils in the simplex optimisation. This simplified the simplex method as it was easier to alter the pump flow rates digitally using the LabVIEW™ program rather than changing the length of the reaction coil lengths every time a simplex experiment was carried out.

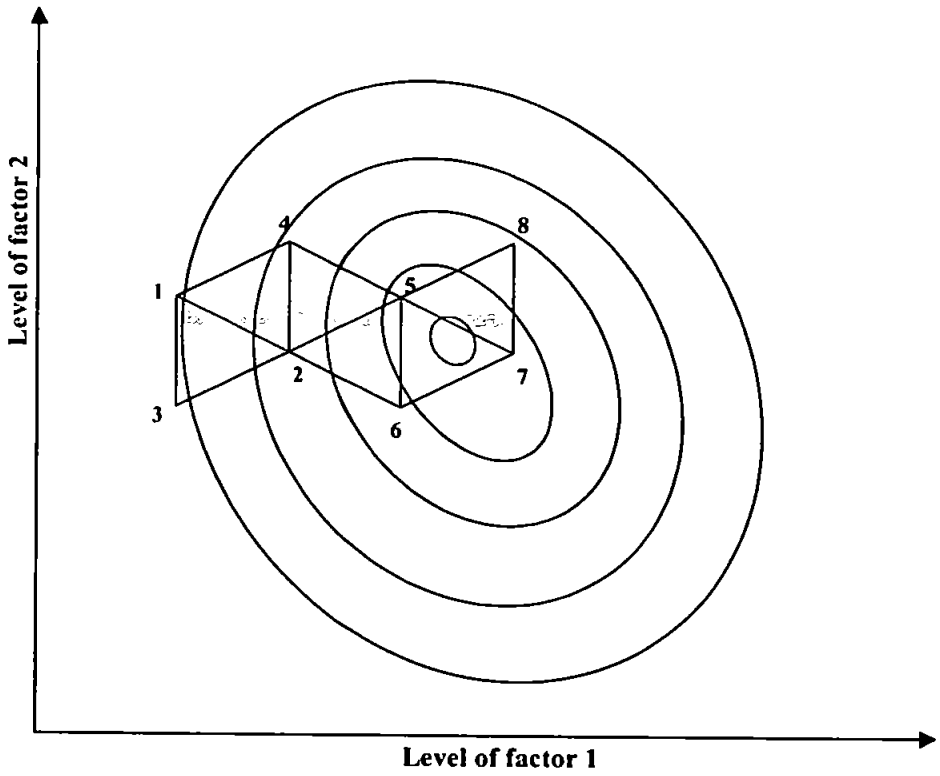

Figure 5.8. Simplex optimisation for two factors/variables [22].

The pump flow rates were optimised using the simplex conditions shown in Table 5.1. There are several terms used in this table:

- The minimum and maximum values are the limits user-defined for each variable that the simplex algorithm can use, unlike the limited range for the pump flow rates studied in the univariate optimisation, the range here was extended to 4-28 digital units for each pump.
- Precision is the minimum increment of a variable that can be measured, here the precision was chosen as 1 because the digital values of the pumps have a minimum change of 1 digital unit.
- Precision of response defines the minimum increment of response that can be measured, therefore a change in 0.001 was chosen to be a considerable change in response for this FI manifold.
- The starting conditions for the pumps were chosen as the original conditions used for this FI manifold by Hanrahan *et al.* i.e. 12, 24, and 12 digital units for the carrier, ammonium molybdate and tin(II) chloride pumps respectively [11].

The simplex optimisation proceeded as shown in Table 5.2 where each of the pump flow rates were changed until fifteen experiments had been completed. Once fifteen experiments had been completed it was decided that there was no further improvement in response. The difference in response between the blanks and standards were calculated and plotted (Fig. 5.9). From these experiments, it can be seen that like the univariate method the response was similar for each set of variables used with the highest responses obtained with runs 6 and 12. A reason why the responses were similar is that the flow rates were all effectively in the steady state region resulting in similar absorbance values. Therefore calibrations were carried out using the variables used in runs 6 and 12 which gave the slightly higher responses giving regressions of $y = 0.0022x + 0.0012$, r^2 of 0.9662, and $y = 0.0024x - 0.0002$, r^2 0.9804, (x: concentration (μM), y: absorbance (arbitrary units)), for runs 6 and 12 respectively, which again were no improvement on calibrations obtained using the original conditions. Therefore 12, 24, 12 digital units was used for the carrier and reagent pump flow rates, this was also preferable to using the conditions used in experiments 6 and 12 as there was slightly less reagent consumption. These conditions were therefore used in all further work.

Table 5.2. Simplex experiments where fifteen runs were carried out using different combinations of flow rates.

Experiment Number	Carrier Pump (digital units)	Ammonium Molybdate Pump (digital units)	Tin(II) Chloride Pump (digital units)
1	12	24	12
2	21	24	12
3	17	33	12
4	17	27	21
5	25	28	19
6	25	20	23
7	28	13	28
8	24	25	28
9	20	19	28
10	24	19	21
11	28	18	28
12	18	23	18
13	21	16	14
14	23	23	24
15	21	26	25

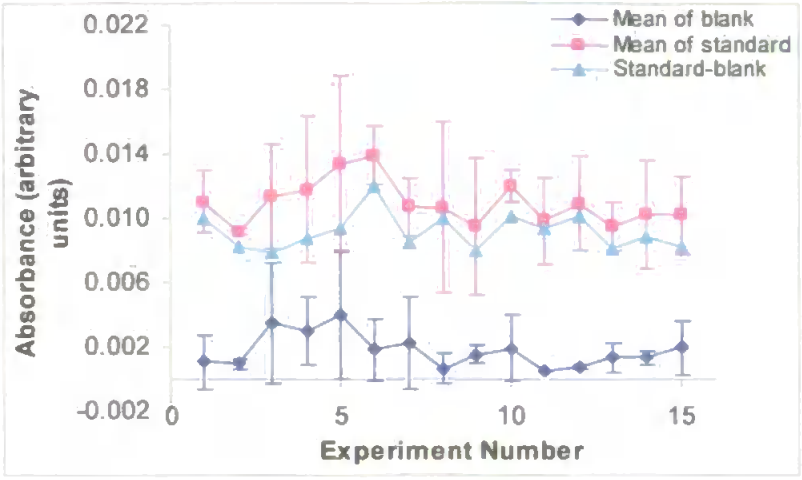

Figure 5.9. Simplex optimisation results using the experimental conditions shown in Table 5.2. Error bars show ± 3 standard deviations, n = 3.

5.3.2 Analytical figures of merit

Linear range and limit of detection: Once the pump flow rates for the carrier, ammonium molybdate and tin(II) chloride and the reaction coil lengths had been optimised, the linear range and limit of detection were determined. The linear range was 0.8-8 μM PO_4-P with a limit of detection of 0.6 μM PO_4-P calculated from the mean of the blank plus three times the standard deviation of the blank. Therefore this is suitable for most runoff samples. A typical calibration is shown in Fig. 5.10 with r^2 of 0.9965. In 1 h, 6 standards or samples can be analysed in triplicate giving a total of 18 injections with a 200 s cycle. In 1 h, reagent consumption is calculated to be 35 mL for the carrier and tin(II) chloride and 52 mL for ammonium molybdate. As the FI monitor is portable, the length of field deployment possible at a sampling frequency of 30 min is about 19 h. This maximum length of time was based on the consumption of the ammonium molybdate reagent. Slight modification e.g. to the volume of reagent bags would allow the monitor to be deployed for 24 h and therefore the diurnal variability of phosphorus could be investigated. Separate experiments showed that the reagents were stable for at least 24 h.

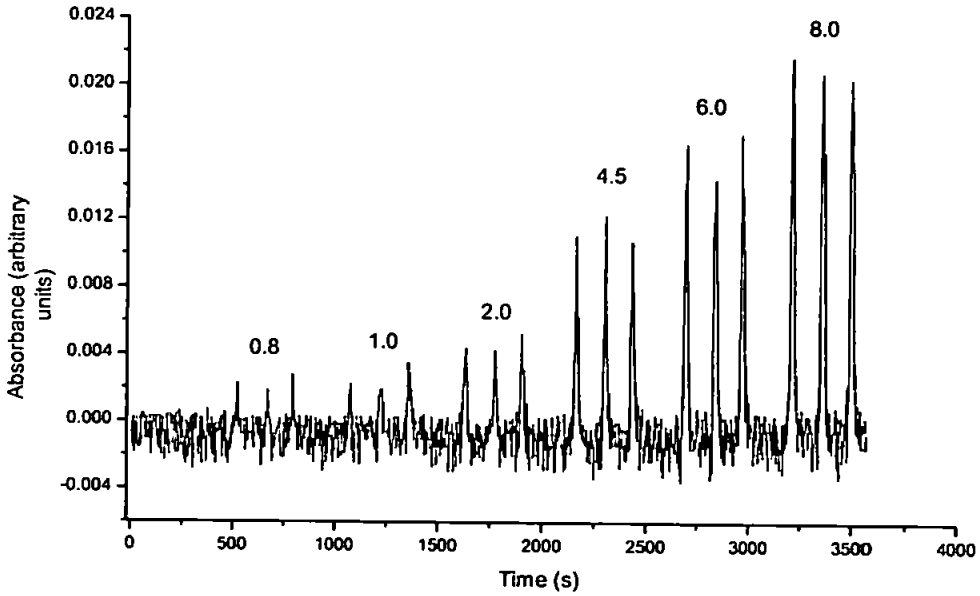

Figure 5.10. A typical calibration using standards in the range 0.8-8.0 μM PO_4-P.

Reproducibility: The reproducibility of the method was investigated by measuring the response for twelve injections of a 4.5 μM PO_4-P standard with a RSD of 5.4 %, and this is shown in Fig. 5.11.

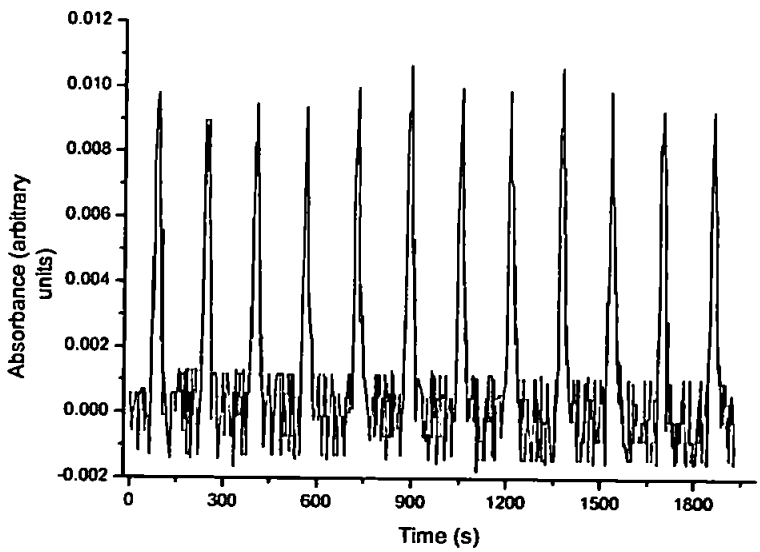

Figure 5.11. Twelve replicate injections for a 4.5 μM PO_4-P standard.

5.3.3 Silicate interference study

Both P and Si react with acidic molybdate to form 12-phosphomolybdic acid and 12-silicomolybdic acid respectively, which are both reduced to form molybdenum blue, potentially resulting in serious mutual interference in their determination [12,14,15]. The phosphomolybdenum blue complex has two absorbance maxima and these occur at 710 and 880 nm [24]. The complex formed when Si(IV) reacts with molybdate has a broad band absorbance (λ_{max} 790 nm) which overlaps the 710 nm used in this work, possibly resulting in an increased peak height and overestimation of phosphorus [12]. When acidity is increased and pH decreased, the kinetics for the rate of formation of the silicon molybdate complex is slower than the rate of formation of the phosphomolybdate complex. This kinetic difference allows for the simultaneous determination of P and Si [14]. Más *et al.* simultaneously determined phosphate and silicate based on this kinetic difference and the analytical signals were recorded at different times by splitting the starting flow into two channels of different length and diameter [14]. There are ways to avoid silicate interference such as ensuring that the pH favours the formation of phosphomolybdenum blue complex by increasing the concentration of sulphuric acid used in the reagent. Masking agents such as tartaric acid have also been used to reduce or eliminate silicate interference in the determination of P [25]. Also Si is more temperature dependent than P as heating at 65 °C will result in the fast formation of both the molybdenum blue complexes hence increasing silicate interference [26].

The silicate standards were analysed and no significant response was seen for the standards of concentration 2, 5, 8 and 10 mg L^{-1} as they were all below the limit of detection and at 60 mg L^{-1} a peak was observed equivalent to 0.95 µM PO_4-P. The results from analysing the spiked 1 and 8 µM PO_4-P standards are shown in Tables 5.3 and 5.4. The equivalent PO_4-P concentration was again determined and there was no interference up to 8 mg L^{-1} Si. At 60 mg L^{-1} Si the equivalent PO_4-P concentration was 3.1 and 9.8 µM for the spiked 1

and 8 μM PO_4-P standards respectively. Therefore it was shown that there was unlikely to be any silicate interference for the samples analysed in this work as the concentration of silicate in soil leachates and runoff waters has been reported by Peat *et al.* as typically no greater than 8 mg L^{-1} [12]. Jarvie *et al.* reported that a typical mean silicate value for rural, agricultural and urban/industrial rivers were 2.8, 8.8 and 8.0 mg L^{-1} SiO_2 respectively [27].

Table 5.3. Silicate interference study results for 1 μM PO_4-P standard spiked with increasing amounts of silicate.

Sample	Absorbance (arbitrary units)				Standard Deviation	RSD (%)	Equivalent PO_4-P (μM)
	1	2	3	Mean			
1 μM PO_4-P	0.0037	0.0041	0.0036	0.0038	0.0003	7.2	1.0
with 2 mgL^{-1} Si	0.0041	0.0046	0.0046	0.0044	0.0003	6.3	1.3
with 5 mgL^{-1} Si	0.0048	0.0046	0.0038	0.0044	0.0005	11.5	1.3
with 8 mgL^{-1} Si	0.0048	0.0041	0.0048	0.0046	0.0004	7.9	1.4
with 10 mgL^{-1} Si	0.0059	0.0057	0.0052	0.0056	0.0004	6.6	1.9
with 60 mgL^{-1} Si	0.0087	0.0073	0.0084	0.0081	0.0007	9.0	3.1

Table 5.4. Silicate interference study results for 8 μM PO_4-P standard spiked with increasing amounts of silicate.

Sample	Absorbance (arbitrary units)				Standard Deviation	RSD (%)	Equivalent PO_4-P (μM)
	1	2	3	Mean			
8 μM PO_4-P	0.0232	0.0223	0.0222	0.0226	0.0005	2.4	8.0
with 2 mgL^{-1} Si	0.0246	0.0234	0.0228	0.0236	0.0009	4.0	8.5
with 5 mgL^{-1} Si	0.0239	0.0240	0.0222	0.0234	0.0010	4.4	8.4
with 8 mgL^{-1} Si	0.0228	0.0244	0.0243	0.0239	0.0009	3.8	8.7
with 10 mgL^{-1} Si	0.0227	0.0227	0.0239	0.0231	0.0007	3.0	8.3
with 60 mgL^{-1} Si	0.0260	0.0267	0.0261	0.0263	0.0003	1.3	9.8

5.3.4 Digestion techniques for the determination of total phosphorus

Digestion techniques for environmental samples are necessary for the determination of total phosphorus (TP) and total dissolved phosphorus (TDP). This is because many of the phosphorus species present contain P-O-P, C-O-P and C-P bonds that need to be broken down to release phosphorus as phosphate, which can then be determined using

molybdenum blue chemistry [28]. The digestion technique must also be able to release phosphorus from biological material e.g. algal cells and plant detritus and adsorbed/occluded P from sediments [13]. Traditional methods of digestion for natural water samples include fusion, dry ashing, perchloric acid, sulphuric acid-nitric acid and boiling on a hot plate, with more recent methods generally using autoclaving, UV photo-oxidation and microwave heating [13]. UV photo-oxidation can be used for organic phosphorus compounds in marine and freshwaters [29-31] but condensed polyphosphates present in the sample will not be broken down by UV photo-oxidation alone [1, 32-34] and therefore require heating to 90-120 °C in the presence of acid [13]. To ensure that all polyphosphates present in the sample are decomposed, either boiling with HCl or potassium peroxydisulphate after UV irradiation is therefore recommended [35]. McKelvie *et al.* used an on-line UV photo-oxidation flow injection (FI) technique with alkaline peroxydisulphate and found that results were comparable with a batch peroxydisulphate method [18].

Autoclaving methods are generally straightforward, give reproducible results and use sealed vessels that are less prone to contamination [13, 27, 36, 37]. The following section is therefore a summary of different autoclaving techniques, combined with peroxydisulphate in either an acidic or alkaline media, for the determination of phosphorus in natural waters, soil solutions and sediments (see Table 5.5). Most methods described in Table 5.5 are based on spectrophotometric detection but ICP-MS and ICP-AES have, in recent years, been used to determine phosphorus in agricultural runoff waters and soils and results were comparable with spectrophotometric methods [78, 79]. In addition, microwave digestion combined with ICP-MS detection has been used to determine phosphorus in marine environmental samples and plant leaves with good recoveries [80-82]. However microwave heating for batch sample digestion and in FI systems with spectrophotometric

detection for on-line TDP and TP digestion [1] is less widely used than UV photo-oxidation or autoclaving.

Alkaline peroxydisulphate. Menzel and Corwin first used autoclaving with peroxydisulphate in 1965 for the digestion of seawater samples [40]. Koroleff developed an alkaline peroxydisulphate alternative in 1969 [54], which was then slightly modified [53] and simplified by introducing a borate buffer [38]. This enabled the simultaneous determination of TP and total nitrogen (TN), as nitrogen bonds are only hydrolysed/oxidised in alkaline media [49]. Using a borate buffer, the pH is alkaline (*ca.* 9.7) at the start of the digestion process and becomes acidic (pH 4-5) as the sodium hydroxide decomposes [33, 42, 49]. Hosomi and Sudo also reported that pH change was important and in their method the pH decreased from 12.8 to 2.0-2.1 to ensure that even condensed polyphosphates were digested [44].

Alkaline digestion of model phosphorus compounds has been found to be efficient for turbid water samples [75-77] although the concentration of suspended particulate material needs to be diluted to <150 mg L^{-1} and difficulties can arise when this material is of soil origin rather than biological origin, e.g. algal cells and plant detritus. The alkaline method has therefore been used to determine TP in turbid lake waters and suspensions of particulate material [77].

Alkaline peroxydisulphate autoclaving, rather than acid peroxydisulphate, is recommended for the digestion of marine waters. This is because in the acid method, peroxydisulphate oxidises the chloride in seawater to free chlorine, thus reducing the oxidising power of the peroxydisulphate [19]. It is also recommended for the simultaneous determination of TP and TN.

Table 5.5. Acidic and alkaline peroxydisulphate autoclave digestion methods.
* with recoveries given in parentheses when reported

Matrix	Digestion Reactant	Digestion time	Digestion temperature	pH	Model Compounds*	Comments	Ref.
Drainage waters	Digestion reagent: 5g $K_2S_2O_8$ and 5 mL 4.5 M H_2SO_4 in 100 mL distilled deionised water. 4 mL reagent added to 50 mL sample	30 min	115°C	Not reported	Not reported	Same method as [38]	[39]
Drainage waters	0.15 g $K_2S_2O_8$ and 1 mL 0.5 M H_2SO_4 added to 20 mL sample	1 h	120°C	Not reported	Not reported	Same method as [37]	[5]
Estuarine Waters	8 mL of 5 % $K_2S_2O_8$ added to 50 mL seawater	1 h	120°C	Final pH 1.5-1.8	Orthophosphate, phenylphosphoric acid, phenylphosphorous acid	Same method as [40], but autoclaving time was increased from 30 min to 1 h. Quantitative recovery for model compounds at the 50 µg P level	[41]
Fresh and seawater	Acidic peroxydisulphate digestion reagent: 5g $K_2S_2O_8$ and 5 mL 4.5 M H_2SO_4 in 100 mL distilled deionised water. 4 mL reagent added to 50 mL sample. Alkaline peroxydisulphate digestion reagent: 5 g $K_2S_2O_8$ and 3 g H_3BO_3 in 100 mL 0.375 M NaOH. 5 mL reagent added to 50 mL sample	30 min	115°C	For alkaline method, initial pH *ca.* 9.7, final pH 4-5	Model compounds added to demineralised water and seawater:2-AEP (108, 77, 108, 88%), PTA (100, 70, 101, 95%), 5'-GMP-Na_2 (99, 93, 100, 94%), PC (98, 37, 99, 96%), FMN (99, 99, 100, 97%), G-6-P-Na (100, 95, 101, 92%), AMP (99, 94, 100, 93%), RP (100, 94, 103, 95%), PEP-3CHA (100, 100, 101, 101%), β-GLY (99, 100, 100, 96%)	Recoveries in parentheses are in the order: acidic demineralised water, acidic seawater, alkaline demineralised water, alkaline seawater. Acidic and alkaline peroxydisulphate methods [38] compared to continuous flow UV irradiation and high temperature combustion. Alkaline peroxydisulphate method recommended for marine waters	[42]
Fresh waters	Digestion reagent: 40 g $K_2S_2O_8$ and 9 g NaOH in 1 L distilled water. 5 mL reagent added to 10 mL sample	1 h	120°C	Initial pH 12.8, final pH 2.0-2.1	National Bureau of Standard Reference Material 1571 orchard leaves (98%), National Institute of Environmental Studies (NIES) Reference Material No.1 pepper bush (96%), NIES Reference Material No.2 pond sediment (100%), NIES Reference Material No.3 chlorella (100%) all of concentration 50 mg L^{-1}. Model compounds:5'-ATP-Na_2 (99-100%), 5'-ADP-Na_2 (98%), TSPP (99-100%), SHMP (94-97%), STP (96-97%), G-6-P-K_2 (99-102%)	Analysed for TN and TP. Obtained higher recoveries for orchard leaves than [43]	[44]
Fresh waters	1 g $K_2S_2O_8$ and sufficient H_2SO_4 to make the sample 0.15 M acid	2 h	120°C	Not reported	Not reported		[45]
Lake waters	'Strong' acid: 25 mL 18 M H_2SO_4 and 1 mL 18M HNO_3 in 1 L deionised water.1 mL 'strong' acid and 2.5 mL aqueous 4% w/v $K_2S_2O_8$ added to 25 mL sample	30 min	Not reported, however in the UV digestion, sample maintained at 85°C in the silica coil	Not reported	Dipotassium hydrogenphosphate (100%), STP (100%), AMP (100%)	Compared UV digestion to autoclaving. Recoveries for lake water samples were 100% for the peroxydisulphate digestion and 97% for the UV digestion	[46]
Lake, river and pond waters, raw sewage	Digestion reagent: 55 mL H_2SO_4 and 60 g $K_2S_2O_8$ in 1 L solution. 2.5 mL reagent added to 35 mL sample	1 h	Not reported	Not reported	G-1-P-K_2 (97.5%), G-6-P-K_2 (105%), DNA (sodium salt) (115%), AMP (95%), 5'-ADP-Na_2 (102.5%), 5'-ATP-Na_2 (107.5%), SOP (100%), β-GLY (107.5%), TSPP (62.5%), STP (110%), SHMP (100%), disodium hydrogen orthophosphate (97.5%)	Autoclave method was compared to the hot-plate $H_2SO_4/K_2S_2O_8$ digestion. Autoclave method gave more precise values for model compounds than the hot plate procedure	[47]
Natural waters	Digestion reagent: 0.15 g $K_2S_2O_8$ and 1 mL 0.5 M H_2SO_4. 1 mL reagent added to 20 mL sample	45 min	121°C	Not reported	G-1-P (101.0%), G-6-P (103.1%), ATP (101.6%), NPP (101.9%), cAMP (101.8%), α-GLY (102.3%), myo-inositol 2-monophosphate (97.4%), PTA (85.6%), 2-AEP (99.2%), TSPP (99.5%), STP (97.7%), trisodium trimetaphosphate (98.8%), KHP (99.1%)	Method modified from [24]	[48]
Natural waters	Acidic peroxydisulphate digestion reagent: 5 g $K_2S_2O_8$ and 5 mL 4.5 M H_2SO_4 in 100 mL distilled deionised water. 0.8 mL digestion reagent added to 10 mL sample. Alkaline peroxydisulphate digestion reagent: 50 g $K_2S_2O_8$, 30 g H_3BO_3 and 350 mL NaOH in 1 L distilled deionised water. 1.3 mL digestion reagent added to 10 mL sample	30 min	120°C	For alkaline method, initial pH *ca.* 9.7, final pH 4-5	NPP, α-GLY, G-6-P, tripolyphosphate, trimetaphosphate, ATP, 5'-GDP, 2-AEP. Recoveries shown on a figure, so precise values cannot be given. In general, recoveries *ca.* >58% for acidic method and *ca.* >26% for alkaline method.	Compared acidic peroxydisulphate [38] and alkaline peroxydisulphate [49] autoclaving methods with magnesium nitrate high-temperature oxidation, magnesium peroxydisulphate high-temperature oxidation, and UV oxidation. Magnesium nitrate high-temperature oxidation was found to be the best method	[33]

Table 5.5. (continued).

Matrix	Digestion Reactant	Digestion time	Digestion temperature	pH	Model Compounds[a]	Comments	Ref.
Orchard leaves and aufwuchs	Digestion reagent: 13.4 g $K_2S_2O_8$ and 6 g NaOH in 1 L to give 200 mg peroxydisulphate per 15 mL aliquot. Other levels of peroxydisulphate also used (300, 400 and 500 mg)	1 h	100-110°C	Initial pH 12.00 for orchard leaf samples, final pH 2.5. Initial pH 12.8 for aufwuchs samples, final pH 3.7	National Bureau of Standards reference material 1571 (orchard leaf) (86.9-88.7 % using 500 mg peroxydisulphate), and aufwuchs (93.6 % using 300 mg peroxydisulphate, and 101.4 % using 400 mg peroxydisulphate)	Analysed for TN and TP. Maximum recovery for orchard leaf when 500 mg peroxydisulphate was used, and 300 or 400 mg peroxydisulphate for aufwuchs	[43]
Pond water	Acidic peroxydisulphate digestion: 0.5 g $K_2S_2O_8$ and 1 mL H_2SO_4 solution (300 mL conc. H_2SO_4 in 1L distilled water) added to 50 mL sample. Alkaline peroxydisulphate digestion: 5 mL 0.075 N NaOH and 0.1 mg $K_2S_2O_8$ added to 10 mL sample. After digestion, 1 mL borate buffer (61.8 g H_3BO_3 and 8 g NaOH in 1 L distilled water) added	30 min	110°C	Not reported	Water samples spiked with 0.2 mg L^{-1} KHP. Recoveries for acidic method were 88-113%, and for the alkaline method 85-112%	Acidic and alkaline peroxydisulphate methods same as [50]	[51]
River water	Digestion reagent: 0.15 g $K_2S_2O_8$ and 1 mL 0.5 M H_2SO_4. 1 mL added to 20 mL sample	45 min	121°C	Not reported	Not reported	Method modified from [24]	[52]
River water	Digestion reagent: 20 g $K_2S_2O_8$ and 3 g NaOH in 1 L distilled deionised water. 5 mL reagent added to 5 mL sample	30 min	120°C	Initial pH 12.57, final pH 2.0	KHP (99.6%), TSPP (97.2%), STP (99.2%), β-GLY (96.5%), SHMP (97.6%), G-1-P (99.5%), AMP (100.8%), ADP (98.9%), ATP (98.1%)	Results from this method were an improvement on the alkaline oxidation method for TN and TP of [53], which was in turn a modified method from [54]	[55]
Seawater	Two concentrations of $K_2S_2O_8$ added (4 mg mL^{-1}, and 40 mg mL^{-1}) to 10 mL sample acidified with sulphuric acid to pH 3	90 min	125°C	pH 3	Not reported	3 methods compared: autoclaving (acidic peroxydisulphate method based on [38]), UV irradiation and sequential use of both. The latter method gave the best recoveries	[19]
Seawater	8 mL of 5 % $K_2S_2O_8$ added to 50 mL seawater	30 min	120°C	Final pH 1.5-1.8	PFA (96.5%), 1-AEP (85.5%), 2-AEP (81.2%)	Compared their nitrate oxidation method with peroxydisulphate oxidation method from [40]	[56]
Seawater	Digestion reagent: 50g $K_2S_2O_8$, 30 g H_3BO_3, 350 mL 1M NaOH in 1 L deionised water. 4 mL reagent added to 30 mL sample	30 min	110-115°C	Initial pH 9.7, final pH 5-6	KHP (0.25-7 μM)	Alkaline peroxydisulphate method for TP and TN based on [38]	[49]
Seawater	8 mL of 5 % $K_2S_2O_8$ added to 50 mL seawater	30 min	120°C	Final pH 1.5-1.8	lecithin (101%), PC (98%), AMP (99%), zooplankton (100%)	Recoveries of model compounds relative to sulphuric acid-hydrogen peroxide digestion [57]	[40]
Sediments and soils	1 mL 5.5 M H_2SO_4, 0.4 g $K_2S_2O_8$ and 1 mL distilled deionised water added to 10-50 mg sample	1 h	130°C	Not reported	Not reported	Acid peroxydisulphate digestion compared to perchloric acid digestion	[58]
Sewage	Digestion reagent: 9 g NaOH and 40 g $K_2S_2O_8$ in 1 L distilled deionised water. 2 mL digestion reagent added to 10 mL sample	90 min	120°C	Not reported, however KCl/acetate buffer pH 4.5	sodium dihydrogen phosphate (93% using 0.15 M KCl/acetate), STP (85% using 0.4 M KCl/acetate), TSPP (96% using 0.4 M KCl/acetate)	Anion exchange chromatography used to separate ortho- and poly-phosphates using either 0.15 or 0.4 M KCl/acetate as the eluting buffer. No polyphosphates detected in raw sewage samples	[59]
Soil extracts	Digestion reagent: 0.39 M $K_2S_2O_8$ and 0.6 M NaOH. 2 mL reagent added to 8 mL sample	1 h	120°C	Not reported	Not reported	Same method (Lachat method 30-115-001-1-B) as [60]	[61]
Soil extracts	Digestion reagent: 13.4 g $K_2S_2O_8$ dissolved in 1 L 0.3 M NaOH. 15 mL reagent added to 10 mL sample. Added 1.5 mL 0.3 M HCl and made up to 50 mL after autoclaving	30 min	110°C	Not reported	KHP, PTA dodeca sodium salt (99% for 0.1 mg L^{-1}, and 106% for 1.0 mg L^{-1})	Analysed for TN and TP. PTA dissolved in different extractants: water, 0.1 M $CaCl_2$, and 0.2 M H_2SO_4, and recoveries were comparable. Alkaline peroxydisulphate method appropriate for soil extracts when concentration of total organic carbon <100 mg L^{-1}	[62]

Table 5.5. (continued).

Matrix	Digestion Reactant	Digestion time	Digestion temperature	pH	Model Compounds*	Comments	Ref.
Soil leachate	0.15 g $K_2S_2O_8$ and 1 mL 0.5 M H_2SO_4 added to 20 mL sample	1 h	120°C	Not reported	Not reported	Same method as [37]	[63-67]
Soil leachate	8 mg $K_2S_2O_8$ and 50 µL 0.5 M H_2SO_4 added to 1 mL sample	1 h	120°C	Not reported	KHP (101%), PTA (76%), TSPP (95%), STP, 1-AEP (86%), G-6-P-Na (84%), 5'-ATP-Na_2 (69%)	Preconcentration and separation method for trace P compounds using a scaled down version of [37]	[68]
Soil solutions	Digestion reagent: 0.05 M H_2SO_4 and 16 g L^{-1} $K_2S_2O_8$. 1 mL reagent added to 1 mL sample	30 min	110°C	Not reported	Not reported		[69]
Soil solutions	Digestion reagent: 50 mg $K_2S_2O_8$ and 0.1 mL 5.5 M H_2SO_4 added to 1 mL sample. After digestion, solutions diluted to 10 mL with deionised water	1 h	120°C	Not reported	KHP, PTA (93.2-95.0% in concentration range 3.23-32.26 µM)	Acid peroxydisulphate digestion compared to sulphuric-perchloric acid, nitric acid, and nitric-perchloric acid digestion. Better recoveries were found for PTA using sulphuric-perchloric acid and acid peroxydisulphate digestion methods	[70]
Soil solutions	Digestion reagent: 13.4 g $K_2S_2O_8$ dissolved in 1 L 0.3 M NaOH. 15 mL reagent added to 10 mL sample. Added 1.5 mL 0.3 M HCl and made up to 50 mL after autoclaving	30 min	110°C	Not reported	Not reported	Same method as [62]	[71]
Soil solutions	0.15 g $K_2S_2O_8$ and 1 mL 0.5 M H_2SO_4 added to 20 mL sample	45 min	121°C	Not reported	Not reported	Method modified from [24]	[17]
Soil solutions	0.15 g $K_2S_2O_8$ and 1 mL 0.5 M H_2SO_4 added to 20 mL sample	1 h	120°C	Not reported	PTA (89%), G-6-P-Na (89%), tetra-potassium pyrophosphate (102%), 5'-ATP-Na_2 (96%), AMP (96%), KHP	Acidic method compared to peroxide-Kjeldahl, and nitric acid-sulphuric acid digestions [72].Acidic peroxydisulphate method found to be the best method	[37]
Surface runoff	0.5 g $K_2S_2O_8$ and 1 mL H_2SO_4 solution (300 mL conc. H_2SO_4 in 1L distilled water) added to 50 mL sample	30 min	110°C	Not reported	Not reported	Same method as peroxydisulphate method in [50]	[73]
Surface runoff	$K_2S_2O_8$ and H_2SO_4	30 min	120°C	Not reported	Not reported		[74]
Turbid lake and river waters	Optimum digestion reagent: 0.27 M $K_2S_2O_8$ and 0.24 M NaOH. 2 mL reagent added to 10 mL sample	1 h	120°C	Final pH 2	NIES No 3 Chlorella (90-96% up to 1000 mg P L^{-1}) and No 2 Pond sediment (75-85% up to 1000 mg P L^{-1}). Model compounds added to distilled and lake water: KHP, G-6-P (113%), PTA (101%), α-GLY (108%), PEP (103%), 2-AEP (104%), PFA (106%), *0*-phosphonyl ethanolamine (109%), SHMP (114%), aluminium phosphate (23%)	Compared alkaline peroxydisulphate autoclaving method to microwave and hot-plate digestion and Kjeldahl digestion for TN and TP. Results showed that all methods used were suitable for turbid lake samples when suspended material is of biological origin	[75]
Turbid lake and river waters	Optimum digestion reagent: 0.27 M $K_2S_2O_8$ and 0.24 M NaOH. 2 mL reagent added to 10 mL sample	1 h	120°C	Final pH 2	NIES No 3 Chlorella (99-101% up to 100 µg P L^{-1}) and No 2 Pond sediment (98-104% up to 60 µg P L^{-1}, and 88% at 100 µg P L^{-1}). Model compounds added to distilled and lake water: KHP (93-99%), PTA (93-106%), 2-AEP (93-101%), α-GLY (94-102%), PFA (93-105%), *0*-phosphonylethanol (91-106%), PEP (93-117%)	Compared alkaline peroxydisulphate autoclave method to microwave digestion, and similar results were found	[76]
Turbid lake waters	Digestion reagent: 9 g NaOH, and 40 g $K_2S_2O_8$ in 1 L water. 2 mL reagent added to 10 mL sample	1 h	120°C	Not reported	NIES No 3 Chlorella (94-107% up to 100 µg P L^{-1}, and 90% at 250 µg P L^{-1}) and No 2 Pond sediment (92-109% up to 100 µg P L^{-1}, and 88% at 250 µg P L^{-1}). Model compounds added to lake water: KHP (99%), STP (96%), AMP (94%), β-GLY (103%)	Compared alkaline peroxydisulphate method to nitric acid-sulphuric acid digestion method [50]. Results showed no significant difference between the two methods	[77]
Water (overland flow)	Digestion reagent: 0.39 M $K_2S_2O_8$ and 0.6 M NaOH. 2 mL reagent added to 8 mL sample	1 h	120°C	Not reported	Not reported		[60]

Acid peroxydisulphate. An acid peroxydisulphate method developed by Gales *et al.* [83] has been adopted by the US Environmental Protection Agency [84]. Eisenreich *et al.* simplified the method [24] and various modifications of this approach are now used to digest different types of samples such as soil solutions, natural waters and river water [17, 48, 52]. The alkaline peroxydisulphate method for soil extracts is only appropriate if the total organic carbon concentration is <100 mg L^{-1} and manganese is <1 mg L^{-1}. Above this manganese concentration, coloured solutions or precipitates are formed, which interfere with the digestion step [62]. This interference is avoided when using acid peroxydisulphate and solutions are colourless after digestion [37].

Pote *et al.* described standard methods for the determination of TP and TDP using sulphuric acid-nitric acid, and peroxydisulphate digestions [85] and recommended the use of sulphuric acid-nitric acid digestion to achieve good recoveries for most samples. However this digestion method can be potentially dangerous if salts precipitate during digestion [41] and is less easy to control than the peroxydisulphate method [37, 72]. Rowland and Haygarth compared a mild peroxydisulphate method to the more rigorous sulphuric acid-nitric acid method [72] for soil solutions and leachates. The latter method gave erratic recoveries and was more prone to contamination due to the open digestion vessels used [37]. Peroxydisulphate autoclaving is also safer than perchloric acid digestion [58, 86]. The acid peroxydisulphate method generally gives good recoveries for model compounds and is simple and easy to use and is therefore recommended for TP and TDP determinations in natural waters and, particularly, soil solutions.

Model compounds. It is advisable to test the efficiency of any digestion method using a range of model phosphorus containing compounds that reflect different chemical bonds and stabilities and are representative of naturally occurring compounds (see Table 5.6). The majority of relevant compounds contain C-O-P and/or P-O-P bonds. Few compounds

reported in the literature contain C-P bonds, which are very resistant to oxidation and hydrolysis [87].

Phosphonates are refractory organic phosphorus compounds and can be released into seawater from biological sources [33, 42, 88], and have been detected in soil leachate [68]. As phosphonates contain a strong C-P bond that is resistant to acid hydrolysis [88], they are useful compounds for recovery studies [33, 42, 48, 75, 76, 88]. Condensed inorganic (e.g. sodium tripolyphosphate) and organic (e.g. adenosine-5'-triphosphate) phosphates and cocarboxylase have also been shown to be resistant to UV irradiation alone [12, 34]. By using acid or alkaline peroxydisulphate autoclaving, however, these compounds have been successfully broken down [48, 55, 75, 76].

Inositol phosphates are an important class of naturally occurring organic phosphorus compounds [89]. Phytic acid, for example, is one of the more resistant compounds to hydrolysis and is also one of the most refractory organic phosphorus compounds found in soils [12, 13, 70]. Other organic phosphorus compounds found in soil leachate and runoff are the sugar phosphorus compounds, e.g. D-glucose-1-phosphate, D-glucose-6-phosphate, which are labile [68]. Organic condensed phosphates e.g. adenosine-5'-triphosphate and adenosine-5'-diphosphate are also important as they originate from all living systems, e.g. algae, bacteria, fungi, insects, plant and animal tissues [68].

It is therefore recommended that model compounds selected for digestion studies should include one with a P-O-P bond (e.g. sodium tripolyphosphate), a refractory C-O-P compound (e.g. phytic acid), a labile C-O-P compound (e.g. D-glucose-1-phosphate or D-glucose-6-phosphate), a refractory C-P compound (e.g. 2-aminoethylphosphonate), and a compound containing C-O-P and P-O-P bonds (e.g. adenosine-5'-triphosphate).

Table 5.6. Model Compounds used in autoclaving digestion methods.

Model Compound	Synonyms	Abbreviation used in text	Chemical Formula	Structural Formula
Adenosine-5'-monophosphate	Adenosine-5'-monophosphoric acid; 5-adenylic acid; adenosine phosphate; tert-adenylic acid; ergadenylic acid	AMP	$C_{10}H_{14}N_5O_7P$	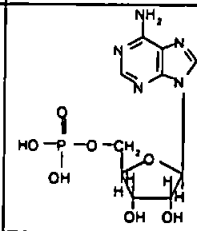
Adenosine-3',5'-cyclic monophosphate	Adenosine-3',5'-cyclophosphoric acid; cyclic AMP; 3',5'-cyclic AMP	CAMP	$C_{10}H_{12}N_5O_6P$	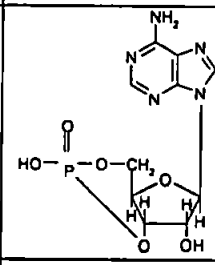
adenosine-diphosphate		ADP	$C_{10}H_{15}N_5O_{10}P_2$	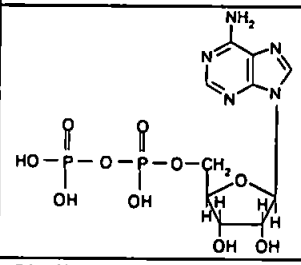
adenosine-5'-diphosphate (sodium salt)		5'-ADP-Na_2	$C_{10}H_{13}N_5O_{10}P_2Na_2$	Similar to ADP
Adenosine-5'-triphosphate		ATP	$C_{10}H_{16}N_5O_{13}P_3$	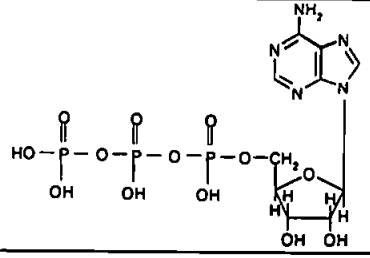

Table 5.6. (continued).

Model Compound	Synonyms	Abbreviation used in text	Chemical Formula	Structural Formula
Adenosine triphosphate disodium	Adenosine 5'-(tetrahydrogen triphosphate) disodium salt; adenosine 5'-triphosphate, disodium salt; adenosine 5'-triphosphate, disodium salt hydrate	5'-ATP-Na_2	$C_{10}H_{14}N_5O_{13}P_3Na_2$	Similar to ATP
1-aminoethylphosphonate	1-aminoethylphosphonic acid	1-AEP	$C_2H_8NO_3P$	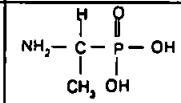
2-aminoethylphosphonate	2-aminoethylphosphonic acid	2-AEP	$C_2H_8NO_3P$	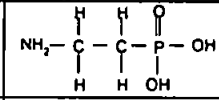
glucose-1-phosphate	Glucose-1-phosphoric acid	G-1-P	$C_6H_{13}O_9P$	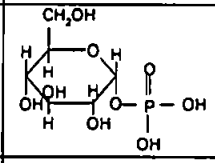
glucose-1-phosphate dipotassium salt	Glucose-1-phosphoric acid (dipotassium salt)	G-1-P-K_2	$C_6H_{11}O_9PK_2$	Similar to G-1-P
glucose-6-phosphate	Glucose-6-phosphoric acid	G-6-P	$C_6H_{13}O_9P$	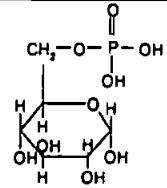
glucose-6-phosphoric acid (dipotassium salt)	α-D-glucose-6-phosphoric acid dipotassium salt	G-6-P-K_2	$C_6H_{11}O_9PK_2$	Similar to G-6-P
glucose-6'-phosphate sodium salt		G-6-P-Na	$C_6H_{12}O_9PNa$	Similar to G-6-P
DL-α-glycerophosphate disodium salt	rac-glycerol 1-phosphate disodium salt; DL-α-glycerophosphate	α-GLY	$C_3H_7O_6PNa_2$	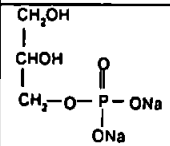

Table 5.6. (continued).

Model Compound	Synonyms	Abbreviation used in text	Chemical Formula	Structural Formula
β –glycerophosphate disodium salt hydrate	Glycerol 2-phosphate disodium salt hydrate; sodium β-glycerophosphate	β-GLY	$C_3H_7O_6PNa_2$	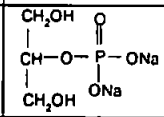
guanosine 5'-diphosphate		5'-GDP	$C_{10}H_{15}N_5O_{11}P_2$	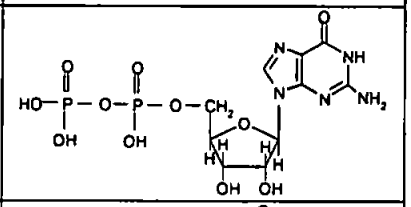
guanosine-5'-monophosphate disodium hydrate		5'-GMP-Na_2	$C_{10}H_{12}N_5O_8PNa_2$	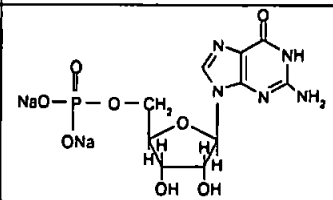
4-nitrophenyl phosphate	p-nitrophenyl phosphate	NPP	$C_6H_4NO_6PNa_2$	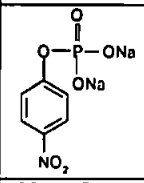
phospho(enol) pyruvate		PEP	$C_3H_5O_6P$	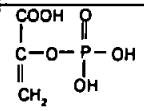
phosphoenolpyruvic acid tri(cyclohexylamine) salt		PEP-3CHA	$C_3H_2O_6P$ $(C_6H_{11}NH_3)_3$	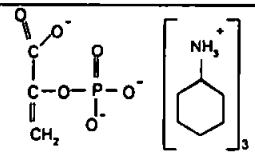
phosphonoformate	Phosphonoformic acid	PFA	CH_3O_5P	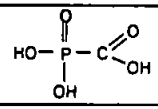

Table 5.6. (continued).

Model Compound	Synonyms	Abbreviation used in text	Chemical Formula	Structural Formula
phosphoryl choline chloride calcium salt tetrahydrate	Phosphocholine chloride calcium salt tetrahydrate; calcium phosphorylcholine chloride	PC	$C_5H_{13}NO_4PCaCl.4H_2O$	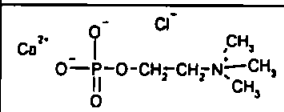
phosphoserine		SOP	$C_3H_8NO_6P$	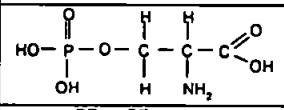
phytic acid	myo-inositol hexakis (dihydrogen phosphate); inositol hexaphosphoric acid	PTA	$C_6H_{18}O_{24}P_6$	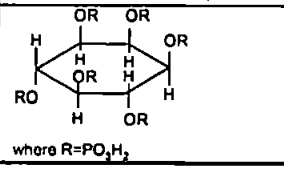
riboflavine-5'-monophosphate sodium salt	Riboflavin 5'-phosphate; FMN-Na	FMN	$C_{17}H_{20}N_4O_9PNa$	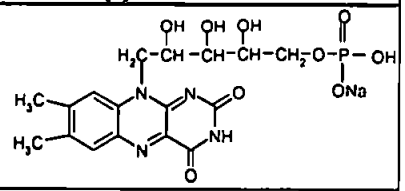
ribose-5-phosphate disodium salt dihydrate	D-ribofuranose 5-phosphate	RP	$C_5H_9O_8PNa_2$	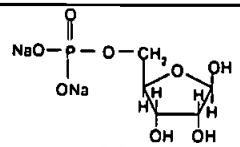
tetrasodium pyrophosphate	Sodium pyrophosphate; pyrophosphoric acid tetrasodium salt; diphosphoric acid, tetrasodium salt	TSPP	$Na_4O_7P_2$	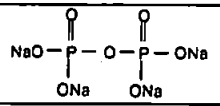
sodium tripolyphosphate	Pentasodium tripolyphosphate dihydrate; sodium triphosphate; sodium polyphosphate; triphosphoric acid pentasodium anhydrous	STP	$Na_5P_3O_{10}$	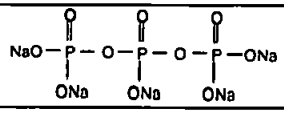
Sodium hexametaphosphate	Sodium metaphosphate; sodiumpolymetaphosphate	SHMP	$(NaPO_3)_n$	

Orthophosphate (e.g. as potassium dihydrogen orthophosphate) should also be used in all recovery studies as a method control [42]. One should also be aware that specific matrices may require additional model compounds. For example acid soils and sediments may well contain phosphorus associated with iron or aluminium phases which are relatively resistant to oxidative dissolution [13].

5.3.5 Optimisation of an autoclaving method for the determination of total phosphorus

Method 1: The model compounds used in this study were representative of compounds found in soil leachate and agricultural runoff as described in section 5.3.4. Peroxydisulphate was used as the oxidant in this autoclave digestion method. When peroxydisulphate decomposes in neutral or alkaline solution, the first stage in the decomposition is as follows and can be initiated by sunlight, dust or impurities in the solution [35, 90]:

$$K_2S_2O_8 + H_2O \rightarrow 2KHSO_4 + \tfrac{1}{2}O_2 \quad (1)$$

and in dilute acid, the first stage is:

$$K_2S_2O_8 + 2H_2O \rightarrow 2KHSO_4 + H_2O_2 \quad (2)$$

therefore in all of these mediums the $KHSO_4$ (present as $SO_4^{-\bullet}$ radicals) will subsequently react with water to form hydroxyl radicals in the second stage of the chain reaction [35]:

$$SO_4^{-\bullet} + H_2O \rightarrow HSO_4^- + OH^\bullet \quad (3)$$

with the next stages of the chain reaction for the decomposition of the peroxydisulphate ion being:

$$S_2O_8^{2-} + OH^\bullet \rightarrow HSO_4^- + SO_4^{-\bullet} + \tfrac{1}{2}O_2 \quad (4)$$

$$SO_4^- + OH^\bullet \rightarrow HSO_4^- + \tfrac{1}{2}O_2 \quad (5)$$

These equations show how the reaction time is limited by the decomposition of the peroxydisulphate, and decomposition is faster as the temperature increases and the pH decreases [13]. Therefore experimental conditions must be such that the bonds of the P-containing compounds in the sample are broken down before the peroxydisulphate has decomposed.

The recoveries for the model compounds are shown in Fig. 5.12A. Recoveries were relatively low: adenosine-5'-triphosphoric acid disodium dihydrogen salt (74 ± 7 %), cocarboxylase (68 ± 17 %), methyltriphenylphosphonium bromide (93 ± 6 %), phytic acid (60 ± 32 %) and penta-sodium triphosphate (95 ± 4 %). From these results it can be seen that the inorganic condensed penta-sodium triphosphate containing P-O-P bonds was easily broken down using this autoclave method, whereas the refractory phytic acid containing C-O-P bonds was the most resistant to hydrolysis. In this method there may not have been sufficient amount of peroxydisulphate to oxidise the compounds before the peroxydisulphate decomposed, therefore the concentration was increased as shown in Method 2.

Method 2: When the concentration of peroxydisulphate was increased from 8 to 40 g L^{-1} the recoveries shown in Fig. 5.12B were greatly improved for adenosine-5'-triphosphoric acid disodium dihydrogen salt (108 ± 11 %), cocarboxylase (88 ± 10 %), methyltriphenylphosphonium bromide (102 ± 6 %), phytic acid (105 ± 10 %), and penta-sodium triphosphate (92 ± 5 %). Therefore there was sufficient peroxydisulphate when 40 g L^{-1} was used to oxidise the model compounds and improve the recoveries than when a lower concentration was used. Hence it is recommended that the digestion of soil suspension samples need 40 g L^{-1} peroxydisulphate in acidic medium added to each sample and autoclaved for 45 min at 121 °C.

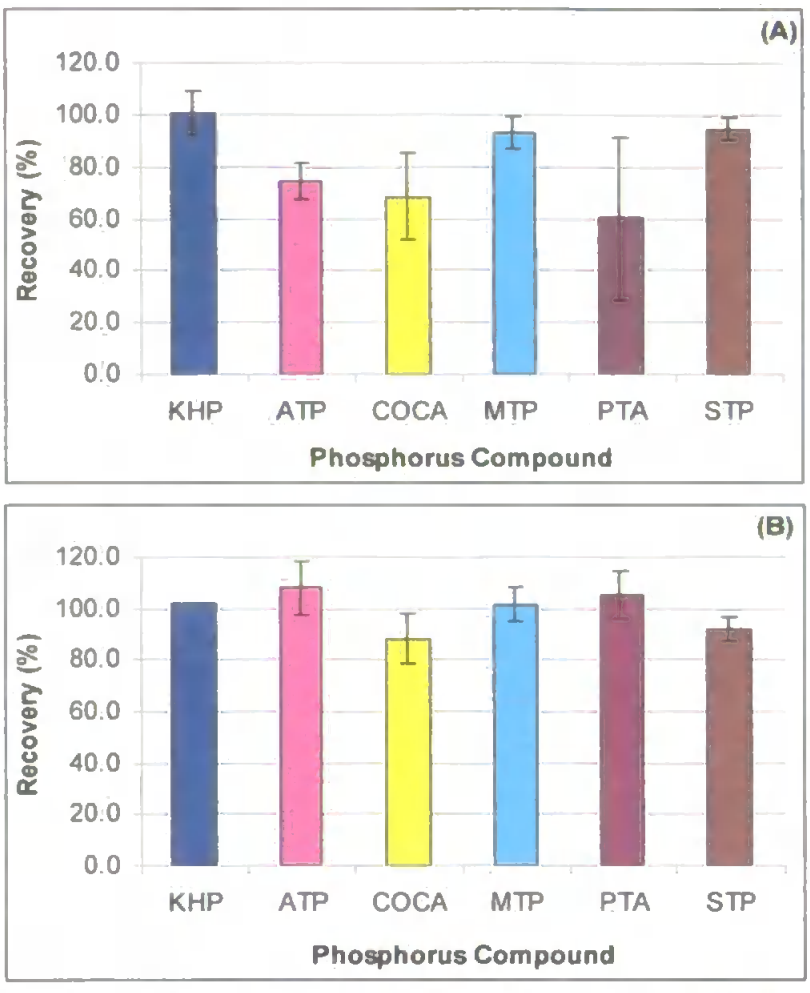

Figure 5.12. Recoveries (%) of autoclaved 4.5 µM P compounds digested using two different methods: (A) Method 1; (B) Method 2. KHP - potassium dihydrogen orthophosphate; 5'-ATP-Na_2 – adenosine-5'-triphosphoric acid disodium dihydrogen salt; COCA – cocarboxylase; MTP – methyltriphenylphosphonium bromide; PTA – phytic acid; STP – penta-sodium triphosphate. Error bars ± 3 standard deviations.

5.4 Conclusions

A portable FI monitor with spectrophotometric detection was optimised using univariate and multivariate methods for the determination of phosphorus in its orthophosphate form. The linear range was determined as 0.8-8 µM PO_4-P with a limit of detection of 0.6 µM PO_4-P. It was shown that there was no silicate interference with the molybdenum blue chemistry at concentrations of silicate up to 8 mg L^{-1} and minimal interference up to 60 mg L^{-1} Si. As levels of silicate in soil leachate and runoff samples are usually no greater than 8 mg L^{-1}, there was unlikely to be any silicate interference with this method.

The acidic peroxydisulphate digestion method used initially was optimised by increasing the amount of peroxydisulphate. Recoveries of a selection of model compounds containing different types of phosphorus bonds were greatly improved using the higher concentrations (40 g L^{-1}) of peroxydisulphate than when the lower concentration (8 g L^{-1}) of peroxydisulphate was used. The recoveries for when 8 g L^{-1} and 40 g L^{-1} peroxydisulphate was used are shown in parentheses respectively for: adenosine-5'-triphosphoric acid disodium dihydrogen salt (74 ± 7 %; 108 ± 11 %), cocarboxylase (68 ± 17 %; 88 ± 10 %), methyltriphenylphosphonium bromide (93 ± 6 %; 102 ± 6 %), phytic acid (60 ± 32 %; 105 ± 10 %), and penta-sodium triphosphate (95 ± 4 %; 92 ± 5 %).

5.5 References

[1] McKelvie, I. D.; Peat, D. M. W.; Worsfold, P. J. Techniques for the quantification and speciation of phosphorus in natural waters. *Analytical Proceedings Including Analytical Communications* **1995**, *32*, 437-445.

[2] Holtan, H.; Kamp-Nielsen, L.; Stuanes, A. O. Phosphorus in soil, water and sediment: An overview. *Hydrobiologia* **1988**, *170*, 19-34.

[3] Carpenter, S. R.; Caraco, N. F.; Correll, D. L.; Howarth, R. W.; Sharpley, A. N.; Smith, V. H. Nonpoint pollution of surface waters with phosphorus and nitrogen. *Ecological Applications* **1998**, *8*, 559-568.

[4] Sharpley, A. N.; McDowell, R. W.; Kleinman, P. J. A. Phosphorus loss from land to water: integrating agricultural and environmental management. *Plant and Soil* **2001**, *237*, 287-307.

[5] Simard, R. R.; Beauchemin, S.; Haygarth, P. M. Potential for preferential pathways of phosphorus transport. *Journal of Environmental Quality* **2000**, *29*, 97-105.

[6] Withers, P. J. A.; Lord, E. I. Agricultural nutrient inputs to rivers and groundwaters in the UK: policy, environmental management and research needs. *The Science of the Total Environment* **2002**, *282-283*, 9-24.

[7] Sharpley, A. N.; Kleinman, P.; McDowell, R. Innovative management of agricultural phosphorus to protect soil and water resources. *Communications in Soil Science and Plant Analysis* **2001**, *32*, 1071-1100.

[8] Mainstone, C. P.; Parr, W. Phosphorus in rivers - ecology and management. *The Science of the Total Environment* **2002**, *282-283*, 25-47.

[9] Withers, P. J. A.; Davidson, I. A.; Foy, R. H. Prospects for controlling nonpoint phosphorus loss to water: A UK perspective. *Journal of Environmental Quality* **2000**, *29*, 167-175.

[10] Benson, R. L.; McKelvie, I. D.; Hart, B. T.; Truong, Y. B.; Hamilton, I. C. Determination of total phosphorus in waters and wastewaters by on-line UV/thermal induced digestion and flow injection analysis. *Analytical Chimica Acta* **1996**, *326*, 29-39.

[11] Hanrahan, G.; Gledhill, M.; Fletcher, P. J.; Worsfold, P. J. High temporal resolution field monitoring of phosphate in the River Frome using flow injection with diode array detection. *Analytica Chimica Acta* **2001**, *440*, 55-62.

[12] Peat, D. M. W.; McKelvie, I. D.; Matthews, G. P.; Haygarth, P. M.; Worsfold, P. J. Rapid determination of dissolved organic phosphorus in soil leachates and runoff waters by flow injection analysis with on-line photo-oxidation. *Talanta* **1997**, *45*, 47-55.

[13] Maher, W.; Woo, L. Procedures for the storage and digestion of natural waters for the determination of filterable reactive phosphorus, total filterable phosphorus and total phosphorus. *Analytica Chimica Acta* **1998**, *375*, 5-47.

[14] Más, F.; Estela, J. M.; Cerdá, V. Simultaneous spectrophotometric determination of silicate and phosphate by flow injection analysis. *International Journal of Environmental Analytical Chemistry* **1991**, *43*, 71-78.

[15] Worsfold, P. J.; Clinch, J. R.; Casey, H. Spectrophotometric field monitor for water quality parameters: The determination of phosphate. *Analytica Chimica Acta* **1987**, *197*, 43-50.

[16] Coles, S.; Nimmo, M.; Worsfold, P. A portable flow-injection instrument incorporating a miniature spectrometer for the real-time monitoring of nitrate in rivers. *Laboratory Robotics and Automation*, **2000**, *12*, 183-193.

[17] Haygarth, P. M.; Warwick, M. S.; House, W. A. Size distribution of colloidal molybdate reactive phosphorus in river waters and soil solution. *Water Research* **1997**, *31*, 439-448.

[18] McKelvie, I. D.; Hart, B. T.; Caldwell, T. J.; Cattrall, R. W. Spectrophotometric determination of dissolved organic phosphorus in natural waters using in-line photo-oxidation and flow injection. *Analyst*, **1989**, *114*, 1459-1463.

[19] Ridal, J. J.; Moore, R. M. A re-examination of the measurement of dissolved organic phosphorus in seawater. *Marine Chemistry* **1990**, *29*, 19-31.

[20] Hanrahan, G. PhD Thesis, University of Plymouth, UK, 2001.

[21] Williams, K. E.; Haswell, S. J.; Barclay, D. A.; Preston, G. Determination of total phosphate in waste waters by on-line microwave digestion incorporating colorimetric detection. *Analyst* **1993**, *118*, 245-248.

[22] Miller, J. C.; Miller, J. N. *Statistics for Analytical Chemistry*, 3rd Edition, Ellis Horwood Limited, England, 1993.

[23] Walters, F. H.; Parker, L. R.; Morgan, S. L.; Deming, S. N. *Sequential Simplex Optimisation*, CRC Press, Boca Raton, Florida, 1991.

[24] Eisenreich, S. J.; Bannerman, R. T.; Armstrong, D. E. A simplified phosphorus analytical technique. *Environmental Letters* **1975**, *9*, 43-53.

[25] Yaqoob, M.; Nabi, A.; Worsfold, P. J. Determination of nanomolar concentrations of phosphate in freshwaters using flow injection with luminol chemiluminescence detection. *Analytica Chimica Acta* **2004**, *510*, 213-218.

[26] Ciavatta, C.; Antisari, L. V.; Sequi, P. Interference of soluble silica in the determination of orthophosphate-phosphorus. *Journal of Environmental Quality* **1990**, *19*, 761-764.

[27] Jarvie, H. P.; Withers, P. J. A.; Neal, C. Review of robust measurement of phosphorus in river water: sampling, storage, fractionation and sensitivity. *Hydrology and Earth System Sciences* **2002**, *6*, 113-132.

[28] Murphy, J.; Riley, J. P. A modified single solution method for the determination of phosphate in natural waters. *Analytica Chimica Acta* **1962**, *27*, 31-36.

[29] Gardolinski, P. C. F. C.; Worsfold, P. J.; McKelvie, I. D. Seawater induced release and transformation of organic and inorganic phosphorus from river sediments. *Water Research* **2004**, *38*, 688-692.

[30] Aminot, A.; Kérouel, R. An automated photo-oxidation method for the determination of dissolved organic phosphorus in marine and fresh water. *Marine Chemistry* **2001**, *76*, 113-126.

[31] Pérez-Ruiz, T.; Martínez-Lozano, C.; Tomás, V.; Martín, J. Flow-injection spectrofluorimetric determination of dissolved inorganic and organic phosporus in waters using on-line photo-oxidation. *Analytica Chimica Acta*, **2001**, *442*, 147-153.

[32] Robards, K.; McKelvie, I. D.; Benson, R. L.; Worsfold, P. J.; Blundell, N. J.; Casey, H. Determination of carbon, phosphorus, nitrogen and silicon species in waters. *Analytica Chimica Acta* **1994**, *287*, 147-190.

[33] Ormaza-González, F. I.; Statham, P. J. A comparison of methods for the determination of dissolved and particulate phosphorus in natural waters. *Water Research* **1996**, *30*, 2739-2747.

[34] Solórzano, L.; Strickland, J. D. H. Polyphosphate in seawater. *Limnology and Oceanography* **1968**, *13*, 515-518.

[35] Golimowski, J.; Golimowska, K. UV-photooxidation as pretreatment step in inorganic analysis of environmental samples. *Analytica Chimica Acta*, **1996**, *325*, 111-133.

[36] O'Connor, P. W.; Syers, J. K. Comparison of methods for the determination of total phosphorus in waters containing particulate material. *Journal of Environmental Quality* **1975**, *4*, 347-350.

[37] Rowland, A. P.; Haygarth, P. M. Determination of total dissolved phosphorus in soil solutions. *Journal of Environmental Quality* **1997**, *26*, 410-415.

[38] Koroleff, F. Determination of total phosphorus. In: Grasshoff, K.; Ehrhardt, M.; Kremling, K. (Eds.), *Methods of Seawater Analysis*, 2nd Edition, Verlag-Chemie, Weinheim, 1983, pp. 167-173.

[39] Nguyen, L.; Sukias, J. Phosphorus fractions and retention in drainage ditch sediments receiving surface runoff and subsurface drainage from agricultural catchments in the North Island, New Zealand. *Agriculture, Ecosystems and Environment* **2002**, *92*, 49-69.

[40] Menzel, D. W.; Corwin, N. The measurement of total phosphorus in seawater based on the liberation of organically bound fractions by persulfate oxidation. *Limnology and Oceanography* **1965**, *10*, 280-282.

[41] Jenkins, D. The differentiation, analysis, and preservation of nitrogen and phosphorus forms in natural waters. *Advances in Chemistry Series*, **1968**, *73*, 265-280.

[42] Kérouel, R.; Aminot, A. Model compounds for the determination of organic and total phosphorus dissolved in natural waters. *Analytica Chimica Acta*, **1996**, *318*, 385-390.

[43] Langner, C. L.; Hendrix, P. F. Evaluation of a persulfate digestion method for particulate nitrogen and phosphorus. *Water Research* **1982**, *16*, 1451-1454.

[44] Hosomi, M.; Sudo, R. Simultaneous determination of total nitrogen and total phosphorus in freshwater samples using persulfate digestion. *International Journal of Environmental Studies*, **1986**, *27*, 267-275.

[45] Golterman, H. L.; Clymo, R. S.; Ohnstad, M. A. M. *Methods for the Physical and Chemical Analysis of Fresh Waters*, IBP Handbook No.8, Blackwell Scientific Publications, Oxford, 1978.

[46] Goulden, P. D.; Brooksbank, P. The determination of total phosphate in natural waters. *Analytica Chimica Acta* **1975**, *80*, 183-187.

[47] Jeffries, D. S.; Dieken, F. P.; Jones, D. E. Performance of the autoclave digestion method for total phosphorus analysis. *Water Research* **1979**, *13*, 275-279.

[48] Denison, F. H.; Haygarth, P. M.; House, W. A.; Bristow, A. W. The measurement of dissolved phosphorus compounds: Evidence for hydrolysis during storage and implications for analytical definitions in environmental analysis. *International Journal of Environmental Analytical Chemistry* **1998**, *69*, 111-123.

[49] Valderrama, J. C. The simultaneous analysis of total nitrogen and total phosphorus in natural waters. *Marine Chemistry* **1981**, *10*, 109-122.

[50] Eaton, A. D.; Clesceri, L. S.; Greenburg, A. E. (Eds.), *Standard Methods for the Examination of Water and Wastewater*, American Public Health Association-American Water Works Association-Water Environment Federation (APHA-AWWA-WEF), 18th Edition, Washington D. C., USA, 1992.

[51] Gross, A.; Boyd, C. E. A digestion procedure for the simultaneous determination of total nitrogen and total phosphorus in pond water. *Journal of the World Aquaculture Society* **1998**, *29*, 300-303.

[52] Hanrahan, G.; Gledhill, M.; House, W. A.; Worsfold, P. J. Phosphorus loading in the Frome catchment, UK: Seasonal refinement of the coefficient modeling approach. *Journal of Environmental Quality* **2001**, *30*, 1738-1746.

[53] D'Elia, C. F.; Steudler, P. A.; Corwin, N. Determination of total nitrogen in aqueous samples using persulfate digestion. *Limnology and Oceanography* **1977**, *22*, 760-764.

[54] Koroleff, F. Determination of total nitrogen in natural waters by means of persulfate oxidation (in Swedish). *International Council for the Exploration of the Sea (ICES) Pap. C. M. 1969/C:8*, revised 1970.

[55] Ebina, J.; Tsutsui, T.; Shirai, T. Simultaneous determination of total nitrogen and total phosphorus in water using peroxodisulfate oxidation. *Water Research* **1983**, *17*, 1721-1726.

[56] Cembella, A. D.; Antia, N. J.; Taylor, F. J. R. The determination of total phosphorus in seawater by nitrate oxidation of the organic component. *Water Research* **1986**, *20*, 1197-1199.

[57] Redfield, A. C.; Smith, H. P.; Ketchum, B. The cycle of organic phosphorus in the Gulf of Maine. *Biological Bulletin* **1937**, *73*, 421-443.

[58] Nelson, N. S. An acid-persulfate digestion procedure for determination of phosphorus in sediments. *Communications in Soil Science and Plant Analysis* **1987**, *18*, 359-369.

[59] Jolley, D.; Maher, W.; Cullen, P. Rapid method for separating and quantifying orthophosphate and polyphosphates: Application to sewage samples. *Water Research* **1998**, *32*, 711-716.

[60] Halliwell, D.; Coventry, J.; Nash, D. Inorganic monophosphate determination in overland flow from irrigated grazing systems. *International Journal of Environmental Analytical Chemistry* **2000**, *76*, 77-87.

[61] Coventry, J. L.; Halliwell, D. J.; Nash, D. M. The orthophosphate content of bicarbonate soil extracts. *Australian Journal of Soil Research* **2001**, *39*, 415-421.

[62] Williams, B. L.; Shand, C. A.; Hill, M.; O'Hara, C.; Smith, S.; Young, M. E. A procedure for the simultaneous oxidation of total soluble nitrogen and phosphorus in extracts of fresh and fumigated soils and litters. *Communications in Soil Science and Plant Analysis* **1995**, *26*, 91-106.

[63] Heathwaite, L.; Haygarth, P.; Matthews, R.; Preedy, N.; Butler, P. Evaluating colloidal phosphorus delivery to surface waters from diffuse agricultural sources. *Journal of Environmental Quality* **2005**, *34*, 287-298.

[64] Preedy, N.; McTiernan, K.; Matthews, R.; Heathwaite, L.; Haygarth, P. Rapid incidental phosphorus transfers from grassland. *Journal of Environmental Quality* **2001**, *30*, 2105-2112.

[65] Turner, B. L.; Haygarth, P. M. Phosphorus forms and concentrations in leachate under four grassland soil types. *Soil Science Society of America Journal* **2000**, *64*, 1090-1099.

[66] Haygarth, P. M.; Hepworth, L.; Jarvis, S. C. Forms of phosphorus transfer in hydrological pathways from soil under grazed grassland. *European Journal of Soil Science* **1998**, *49*, 65-72.

[67] Haygarth, P. M.; Jarvis, S. C. Soil derived phosphorus in surface runoff from grazed grassland lysimeters. *Water Research* **1997**, *31*, 140-148.

[68] Espinosa, M.; Turner, B. L.; Haygarth, P. M. Preconcentration and separation of trace phosphorus compounds in soil leachate. *Journal of Environmental Quality* **1999**, *28*, 1497-1504.

[69] Hens, M.; Merckx, R. The role of colloidal particles in the speciation and analysis of "dissolved" phosphorus. *Water Research* **2002**, *36*, 1483-1492.

[70] Martin, M.; Celi, L.; Barberis, E. Determination of low concentrations of organic phosphorus in soil solution. *Communications in Soil Science and Plant Analysis* **1999**, *30*, 1909-1917.

[71] Chapman, P. J.; Shand, C. A.; Edwards, A. C.; Smith, S. Effects of storage and sieving on the phosphorus composition of soil solution. *Soil Science Society of America Journal* **1997**, *61*, 315-321.

[72] Methods for the Examination of Waters and Associated Materials: Phosphorus in Waters, Effluents and Sewages, HMSO London, England, 1980, pp. 26-28.

[73] Aase, J. K.; Bjorneberg, D. L.; Westermann, D. T. Phosphorus runoff from two water sources on a calcareous soil. *Journal of Environmental Quality* **2001**, *30*, 1315-1323.

[74] Uusitalo, R.; Turtola, E.; Kauppila, T.; Lilja, T. Particulate phosphorus and sediment in surface runoff and drainflow from clayey soils. *Journal of Environmental Quality* **2001**, *30*, 589-595.

[75] Maher, W.; Krikowa, F.; Wruck, D.; Louie, H.; Nguyen, T.; Huang, W. Y. Determination of total phosphorus and nitrogen in turbid waters by oxidation with alkaline potassium peroxodisulfate and low pressure microwave digestion, autoclave heating or the use of closed vessels in a hot water bath: comparison with Kjeldahl digestion. *Analytica Chimica Acta* **2002**, *463*, 283-293.

[76] Woo, L.; Maher, W. Determination of phosphorus in turbid waters using alkaline potassium peroxodisulphate digestion. *Analytica Chimica Acta* **1995**, *315*, 123-135.

[77] Lambert, D.; Maher, W. An evaluation of the efficiency of the alkaline persulphate digestion method for the determination of total phosphorus in turbid waters. *Water Research* **1995**, *29*, 7-9.

[78] Cantarero, A.; López, M. B.; Mahía, J.; Maestro, M. A.; Paz, A. Determination of total and dissolved phosphorus in agricultural runoff samples by inductively coupled plasma mass spectrometry. *Communications in Soil Science and Plant Analysis* **2002**, *33*, 3431-3436.

[79] Dancer, W. S.; Eliason, R.; Lekhakul, S. Microwave assisted soil and waste dissolution for estimation of total phosphorus. *Communications in Soil Science and Plant Analysis* **1998**, *29*, 1997-2006.

[80] Maher, W.; Krikowa, F.; Kirby, J.; Townsend, A. T.; Snitch, P. Measurement of trace elements in marine environmental samples using solution ICPMS. Current and future applications. *Australian Journal of Chemistry* **2003**, *56*, 103-116.

[81] Maher, W.; Forster, S.; Krikowa, F.; Snitch, P. Chapple, G.; Craig, P. Measurement of trace elements and phosphorus in marine animal and plant tissues by low-volume microwave digestion and ICP-MS. *Atomic Spectroscopy* **2001**, *22*, 361-369.

[82] Esslemont, G.; Maher, W.; Ford, P.; Krikowa, F. The determination of phosphorus and other elements in plant leaves by ICP-MS after low-volume microwave digestion with nitric acid. *Atomic Spectroscopy* **2000**, *21*, 42-45.

[83] Gales Jr., M. E.; Julian, E. C.; Kroner, R. C. Method for quantitative determination of total phosphorus in water. *Journal American Water Works Association* 1966, *58*, 1363-1368.

[84] US Environmental Protection Agency, Methods for the Chemical Analysis of Water and Wastes, 1971.

[85] Pote, D. H.; Daniel, T. C. Analysing for Total Phosphorus and Total Dissolved Phosphorus in Water Samples. In: Pierzynski, G. M.(Ed.), *Methods of Phosphorus Analysis for Soils, Sediments, Residuals, and Water*, Southern Co-operative Series Bulletin No.396, A Publication of SERA-IEG-17, North Carolina State University, 2000.

[86] Harwood, J. E.; Van Steenderen, R. A.; Kühn, A. L. A comparison of some methods for total phosphate analyses. *Water Research* **1969**, *3*, 425-432.

[87] Corbridge, D. E. C. *Phosphorus – An Outline of its Chemistry, Biochemistry and Technology*, 3rd Edition, Elsevier, Amsterdam, 1985.

[88] Cembella, A. D.; Antia, N. J. The determination of phosphonates in seawater by fractionation of the total phosphorus. *Marine Chemistry* **1986**, *19*, 205-210.

[89] Turner, B. L.; Papházy, M. J.; Haygarth, P. M.; McKelvie, I. D. Inositol phosphates in the environment. *Philosophical Transactions of the Royal Society of London. B.* **2002**, *357*, 449-469.

[90] House, D. A. Kinetics and mechanism of oxidations by peroxydisulfate, *Chemical Reviews* **1962**, *62*, 185-203.

Chapter 6

Combining FlFFF and FI Techniques for the Determination of Phosphorus in Soil Suspensions

6.1 Introduction

Colloidal material in soil suspension samples can be determined using FFF as shown in Chapters 3 and 4. The colloidal material can potentially transport phosphorus from land to water, and as FIA with spectrophotometric detection can determine reactive phosphorus (RP) and total phosphorus (TP) as shown in Chapter 5, by combining FlFFF and FIA, information on the phosphorus species associated with colloidal material can be determined.

There has only been one report where FFF has been coupled with FIA and this was achieved by Chantiwas *et al.* [1]. They coupled GrFFF with FIA and chemiluminescence detection for the size based iron speciation of particles. Other studies have investigated the effect of colloidal surface coatings on the adsorptive behaviour of orthophosphate [2,3]. River sediment and soil samples were radio-labelled with $^{33}PO_4^{3-}$ and analysed using SdFFF coupled with ICP-MS to determine the surface adsorption density of orthophosphate and the chemical composition of the colloidal samples as a function of particle size. These studies were aimed at reaching a better understanding of the behaviour of pollutants in the environment with regards to pollutant-particle association. However there are currently no reports of FlFFF being coupled with FIA for the determination of phosphorus.

The aim of this work was therefore to combine FlFFF with the portable FI monitor to determine the RP and TP with different size fractions. The different size fractions were chosen to represent the two most common operational fractions isolated by traditional membrane filtration i.e. <0.2 and <0.45 μm fractions. These fractions were prepared using centrifugation alone, as centrifugation was found to recover more material in soil suspension samples than filtration as shown in Chapters 3 and 4. A 1 % m/v soil suspension was prepared and the <1 μm fraction extracted before centrifugation was used

to obtain the <0.2 and <0.45 μm fractions. The centrifuged fractions (<0.2 and <0.45 μm) and the <1 μm fractions were injected into the FlFFF and simultaneously determined for phosphorus with the FI monitor. For this preliminary investigation only the Rowden soil was used to prepare and centrifuge the fractions for subsequent phosphorus determination.

6.2 Experimental

6.2.1 Laboratory ware

All glassware and bottles were first cleaned overnight in nutrient free detergent (Neutracon®, Decon Laboratories, UK), rinsed three times with ultra-pure water (Elga Maxima®, 18.2 MΩ), soaked in 10 % (v/v) HCl for 24 h, again rinsed three times with ultra-pure water and dried at room temperature. All solutions were prepared with ultra-pure water and all reagents were of AnalaR grade (VWR International, UK) or equivalent, unless otherwise stated.

The FlFFF carrier solution consisted of 0.02 % m/v sodium azide (NaN_3; VWR, Poole, England) in ultra-pure water. The carrier was de-gassed before use by filtering through a 0.2 μm polycarbonate membrane under suction. This carrier was used for both the channel flow and crossflow.

For the FIA experiments, a 3 mM PO_4-P stock solution was prepared by dissolving 0.4393 g of potassium dihydrogen orthophosphate (oven dried for 1 h at 105 °C) in 1 L of ultra-pure water. Working standards in the range 0.8 – 8 μM PO_4-P were prepared by dilution of the stock solution. Two reagents were prepared, these were: ammonium molybdate solution (10 g ammonium molybdate and 35 mL sulphuric acid in 1 L of ultra-pure water), and tin(II) chloride solution (0.2 g tin(II) chloride and 2 g hydrazinium sulphate and 28 mL sulphuric acid in 1 L ultra-pure water).

6.2.2 Preparation of Rowden soil suspensions

Rowden soil suspensions of 1 % m/v concentration were prepared by suspending 1 g soil in 100 mL ultra-pure water. Three replicate samples in 250 mL bottles were shaken gently for 16 h and settled in 600 mL beakers for 1 h. The top 20 mL layer containing the <1 μm fraction was pipetted out from each beaker and pooled together. The sample was pooled to give a large enough volume for the RP and TP experiments, and the samples were pooled together with the confidence that there was no significant difference between the samples. This is due to the results obtained from experiments conducted in Chapter 4, section 4.3.2, where good repeatability was demonstrated between replicate samples that had been settled and injected into the FlFFF giving an RSD for peak area of 3.4 %. The pooled sample was then used to prepare the centrifuged fractions (<0.2 and <0.45 μm).

Centrifugation: The 1 % m/v soil suspension was pipetted into 12 polypropylene tubes (1.5 mL volume) and placed into an MSE MicroCentaur microcentrifuge (Sanyo, UK), and centrifuged for 4 min at 3000 rpm (at 25 °C) to obtain the <0.45 μm fraction. The supernatants were decanted from all the centrifuge tubes and pooled together to give a total volume of about 18 mL. This process was repeated to obtain the <0.2 μm fraction by centrifuging the 1 % m/v soil suspension for 3 min at 8000 rpm (at 25 °C).

6.2.3 FlFFF for Rowden soil suspensions

The <1 μm Rowden soil suspension and the centrifuged fractions (<0.2 and <0.45 μm) were injected into a Rheodyne injector valve with 20 μL sample loop overfilling five times with 100 μL sample to ensure complete loop filling, and greater precision. The sample was flushed from the loop with carrier solution into the top of the channel. After an injection delay of 2.7 s, the switching valve was changed automatically to load (stopflow) mode and the carrier bypassed the channel and flowed directly to the detector. At the end of the relaxation time the switching valve then automatically changed back to inject (run) mode,

allowing the channel flow to flow through the channel to the detector and the run commenced.

The channel flow rate was 1.2 mL min^{-1}, and the crossflow rates for <1 μm, <0.45 μm and <0.2 μm particle size ranges were V_c = 0.1, 0.2 and 0.4 mL min^{-1} respectively. The absorbance of the eluent was recorded using a Waters 2487 dual wavelength absorbance detector (Waters, Milford, MA, USA) at 254 nm with a sensitivity of 0.02 AUFS. All samples were injected in triplicate runs and results shown are means of three runs, unless otherwise stated. Blank runs were also carried out at the different crossflow rates by injecting 20 μL of ultra-pure water.

6.2.4 Portable FI monitor for determination of reactive phosphorus and total phosphorus

The portable FI monitor with spectrophotometric detection described in Chapter 5 was used to determine the RP and TP for each of the <1, <0.45 and <0.2 μm fractions. The FIA was carried out at the same time as the FlFFF experiments. The RP was determined by directly injecting the samples in triplicate after the FI monitor was first calibrated with the PO_4-P standards. For the determination of TP in each fraction the optimised autoclave procedure described in Chapter 5 was used. As the soil suspension sample was used for many different analyses i.e. FlFFF, RP and TP with the FI monitor in this chapter, the reagents and sample volumes for the optimised autoclave method were halved to conserve on sample. The autoclave method was therefore as follows:

Twenty mL of the working standards prepared for the RP experiment was pipetted into 100 mL glass autoclave bottles (Fisher Scientific, Leicestershire, UK). One mL 0.5 M sulphuric acid and 0.8 g potassium peroxydisulphate was added to 20 mL of the standards, whereas 0.5 mL 0.5 M sulphuric acid and 0.4 g potassium peroxydisulphate was added to 10 mL sample. These were all autoclaved for 45 min at 121 °C. Before placing the bottles in the

autoclave the caps of the bottles were loosened by half a turn. After autoclaving, the standards and samples were allowed to cool to room temperature, then analysed on the FI monitor.

6.3 Results and Discussion

6.3.1 Fractograms and particle size distributions for Rowden soil suspensions

Fractograms were obtained by plotting detector response against elution time (or volume) of the emerging sample. The dead volume was removed from each of the fractograms to give corrected elution time (or volume), and all runs were blank-subtracted. The results shown are means of triplicate runs. The fractograms were then converted to particle size distributions (PSDs) using an Excel program but were not corrected for light scattering effects [4-6]. The fractograms and particle size distributions for the <1 μm Rowden soil suspensions and the centrifuged fractions (<0.2 and <0.45 μm) are shown in Figs. 6.1A and 6.1B respectively. These show the same particle size distribution as observed for the 1 % m/v Rowden soil suspensions and the centrifuged fractions (<0.2 and <0.45 μm) analysed in Chapter 4, with the particle size threshold for each fraction close to the expected thresholds of 0.2, 0.45 and 1 μm.

6.3.2 Portable FI monitor for determination of reactive phosphorus

The calibration graph obtained for the PO_4-P standards (0.8 – 8.0 μM PO_4-P) had a r^2 of 0.9947 with a linear equation $y = 0.0017x + 0.0014$ for the best-fit line (x: concentration (μM), y: absorbance (arbitrary units)). The <1 μm Rowden soil suspension and the centrifuged <0.2 and <0.45 μm fractions were analysed and the concentrations calculated using the equation of the best-fit line. The <1 μm Rowden soil suspensions required dilution by half to bring it into the measurement range of the FI monitor. The concentrations for the <1, <0.45 and <0.2 μm were determined to be 13.5, 2.0 and 1.1 μM PO_4-P respectively as shown in Fig. 6.2.

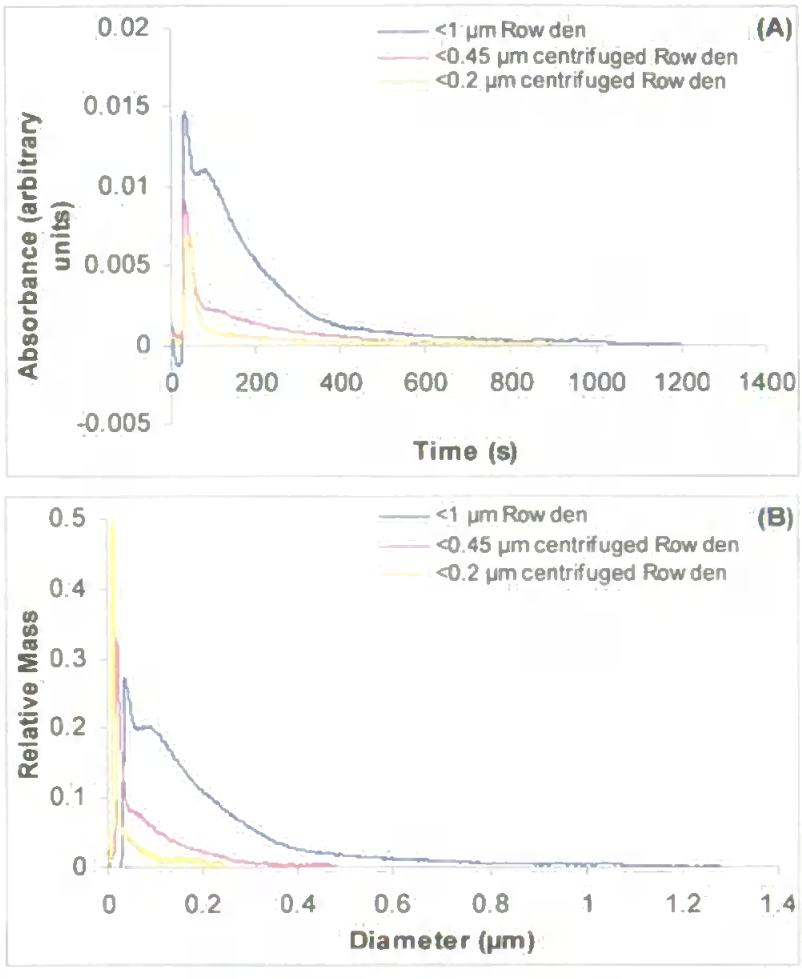

Figure 6.1. FlFFF results for Rowden soil suspensions (1 % m/v): (A) Fractograms for <1, <0.45 and <0.2 µm fractions with data averaged for three runs; (B) PSDs for for <1, <0.45 and <0.2 µm fractions with data averaged for three runs.

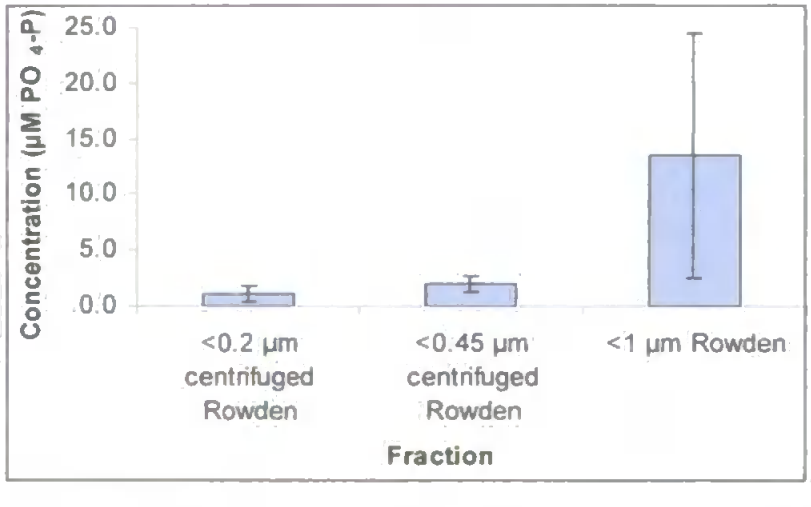

Figure 6.2. FI results for the <1 µm Rowden soil suspension and the centrifuged <0.2 and <0.45 µm fractions analysed for RP with the concentrations calculated using $y = 0.0017x + 0.0014$ line. Error bars ± 3 standard deviations, n = 3.

6.3.3 Portable FI monitor for determination of total phosphorus

It was observed that the autoclaved samples were initially clear on removal from the autoclave but as the temperature of the samples cooled to room temperature they became a cloudy yellow colour. The calibration graph obtained for the autoclaved PO_4-P standards had a r^2 of 0.9957 with a linear equation $y = 0.0021x + 0.0011$ for the best-fit line (x: concentration (μM), y: absorbance (arbitrary units)). The <1 μm Rowden soil suspension and the centrifuged <0.2 and <0.45 μm fractions were analysed and the concentrations calculated using the equation of the best-fit line as shown in Fig. 6.3. All of the samples required diluting to bring them into the measurement range of the FI monitor. The <1 μm sample needed to be diluted five times, the <0.45 μm sample needed to be diluted three times and the <0.2 μm sample was diluted twice. The concentrations for the <1, <0.45 and <0.2 μm were determined to be 49.0, 21.7, and 14.3 μM PO_4-P respectively.

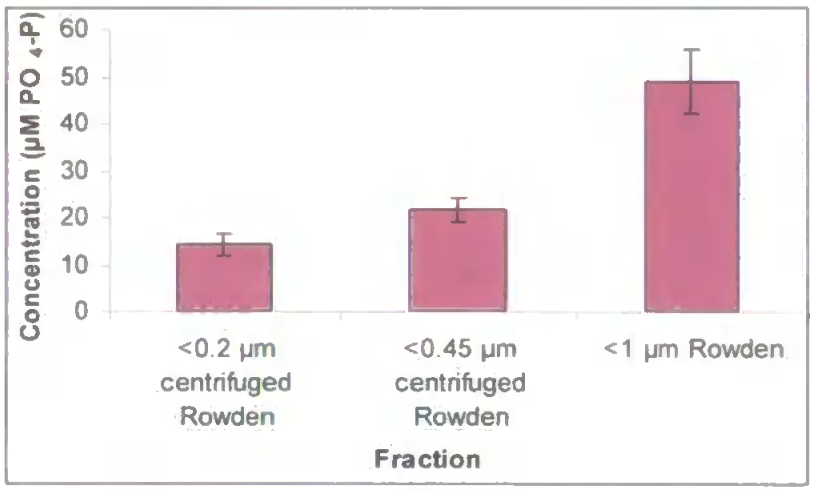

Figure 6.3. FI results for the <1 μm Rowden soil suspension and the centrifuged <0.2 and <0.45 μm fractions analysed for TP with the concentrations calculated using $y = 0.0021x + 0.0011$. Error bars ± 3 standard deviations, n = 3.

A mass balance was carried out to determine the % amount of RP and TP in each of the fractions: 0-0.2, 0.2-0.45, and 0.45-1 μm assuming that the total amount of RP and TP was found in the <1 μm fraction, results shown in Fig. 6.4. From this preliminary experiment it was observed that the majority of RP and TP was found in the 0.45 – 1 μm fraction.

However this may not be an accurate representation of how P is associated with the different size fractions as it can be seen in Fig. 6.1B that centrifugation to <0.2 and <0.45 μm could possibly have removed a large proportion of the colloidal matter in the target size range. Therefore the amount of RP and TP present in the fractions below <0.45 μm may be significantly underestimated. To provide a more accurate representation of how the P is associated with colloids the FlFFF eluent should be collected as different size fractions and injected into the FI monitor without the need to use centrifugation. The amount of RP and TP associated with the different size fractions would then be more accurately determined, however the sensitivity of the FI monitor would need improving in order for the P to be detected, this is discussed in Chapter 7.

Other studies have used filtration to determine how P is associated with colloids. Haygarth *et al.* found that for the fractionation of soil surface runoff water, 71 % of the total RP was associated with particles >0.45 μm, whereas for river water 55 % of the total RP was associated with material <1000 MW [7]. Shand *et al.* reported that in soil solutions 23 % of RP was associated with colloids >0.22 μm and 46 % of the organic P (determined using photo-oxidation) was also associated with colloids >0.22 μm [8]. As these studies have used filtration, these values may not be accurate representations of how the P is distributed, as it has been shown throughout this work that separation techniques such as filtration and centrifugation can underestimate the colloidal material and hence the P species associated with the colloids. Therefore this work emphasises the need for suitable techniques able to examine how phosphorus is associated with colloids.

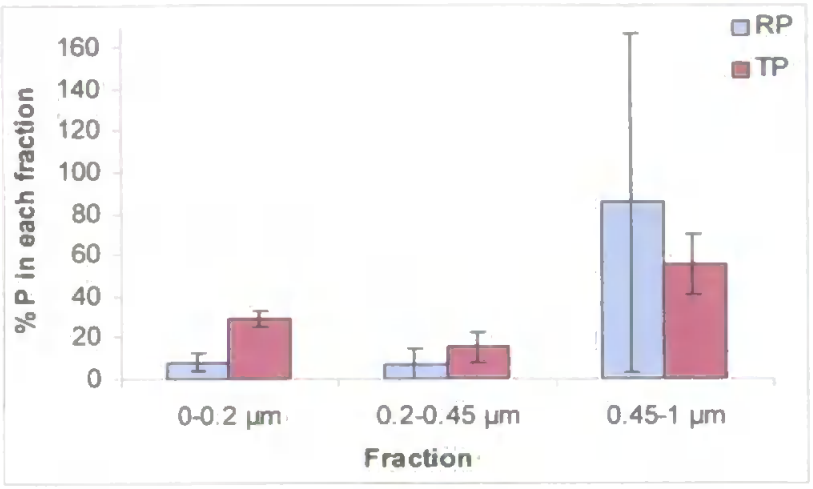

Figure 6.4. Comparison of RP and TP (as %) in the size fractions: 0-0.2, 0.2-0.45, and 0.45-1 µm. These values may not be a true representative of how P is distributed as centrifugation has removed some material in the <0.2 and <0.45 µm fractions therefore there may be some underestimation of P in these fractions. Error bars ± 3 standard deviations.

6.4 Conclusions

The results presented in this chapter are promising as soil suspension samples were fractionated using centrifugation and the different size fractions then analysed for phosphorus. However the broader environmental interpretation of these results should be treated with caution because the experiment was only carried out once with one type of soil. Also the work in this chapter was carried out predominantly to test the hypothesis that FlFFF and FIA could be combined together. Further work is required as ideally the eluent from the FlFFF after UV detection would be collected using the same size fractions of 0-0.2, 0.2-0.45, and 0.45-1 µm. The phosphorus in each of these fractions would then be determined using the FI monitor. This would then remove the centrifugation step, which was shown to remove some of the material prior to FlFFF analysis, as FlFFF is able to separate samples over the whole colloidal range. In order to analyse the FlFFF eluent, the detection limit of the FI monitor could be improved (discussed in Chapter 7, section 2.2),

or the sample loading could be modified to involve a pre-concentration step prior to FlFFF analysis.

6.5 References

[1] Chantiwas, R.; Beckett, R.; Jakmunee, J.; McKelvie, I. D.; Grudpan, K. Gravitational field-flow fractionation in combination with flow injection analysis or electrothermal AAS for size based iron speciation of particles. *Talanta* **2002**, *58*, 1375-1383.

[2] Chen, B.; Hulston, J.; Beckett, R. The effect of surface coatings on the association of orthophosphate with natural colloids. *The Science of the Total Environment* **2000**, *263*, 23-35.

[3] van Berkel, J.; Beckett, R. Determination of adsorption characteristics of the nutrient orthophosphate to natural colloids by sedimentation field-flow fractionation. *Journal of Chromatography A* **1996**, *733*, 105-117.

[4] Taylor, H. E.; Garbarino, J. R.; Murphy, D. M.; Beckett, R. Inductively coupled plasma mass-spectrometry as an element-specific detector for field-flow fractionation particle separation. *Analytical Chemistry* **1992**, *64*, 2036-2041.

[5] Murphy, D. M.; Garbarino, J. R.; Taylor, H. E.; Hart, B. T.; Beckett, R. Determination of size and element composition distributions of complex colloids by sedimentation field-flow fractionation inductively-coupled plasma-mass spectrometry *Journal of Chromatography* **1993**, *642*, 459-467.

[6] Beckett, R.; Nicholson, G.; Hart, B. T.; Hansen, M.; Giddings, J. C. Separation and size characterization of colloidal particles in river water by sedimentation field-flow fractionation. *Water Research* **1988**, *22*, 1535-1545.

[7] Haygarth, P. M.; Warwick, M. S.; House, W. A. Size distribution of colloidal molybdate reactive phosphorus in river waters and soil solution. *Water Research* **1997**, *31*, 439-448.

[8] Shand, C. A.; Smith, S.; Edwards, A. C.; Fraser, A. R. Distribution of phosphorus in particulate, colloidal and molecular-sized fractions of soil solution. *Water Research* **2000**, *34*, 1278-1284.

Chapter 7

Conclusions and Future Work

7.1 Conclusions

There are some general conclusions and recommended guidelines with respect to the use of FFF and FIA for the determination of phosphorus in agricultural runoff, soil leachate and soil suspension samples that have arisen from this project:

7.1.1 Experimental practicalities of using SdFFF and FlFFF

It is essential that a FFF system is set-up correctly using appropriate experimental conditions to ensure good resolution and retention times that do not differ from the predicted theoretical times. FlFFF and SdFFF have some differences in their relative performance:

1. SdFFF is used to determine particle size distributions (PSDs), whereas FlFFF is more versatile as it can be used to determine PSDs and also molecular weight distributions (MWDs). This is because FlFFF extends the size range that can be separated below 50 nm. An added advantage of determining MWDs is that diffusion coefficient information can also be determined.
2. FlFFF separates on the basis of the size of the molecules or particles alone, and the process is independent of density whereas SdFFF separates on the basis of buoyant mass i.e. size density. The equations used for SdFFF are slightly more complicated because of the exponential decay program that is used to elute the larger particles within a reasonable analysis time which also makes the interpretation of the results more difficult.
3. Two flows are used in FlFFF, the channel flow and crossflow, and therefore the flow rates need to be balanced in both the load and inject mode, whereas in SdFFF there is only the channel flow, as a centrifuge instead of a liquid crossflow provides the field.
4. In FlFFF, the channel and crossflow rates were balanced by adjusting the flow rates with a needle valve on the end of the crossflow line and measuring the flow rates

with a balance. Pressure gauges were used to monitor the pressure in the channel to ensure that the pressures were below 100 psi.

5. The flow rates in FlFFF need to be chosen so that the crossflow is not too strong to avoid sample components being forced against the membrane, thereby causing irreversible retention and, ultimately, clogging of the membrane. The crossflow rates used in this work were therefore modified for different sized samples i.e. crossflow rates of 0.4, 0.2 and 0.1 mL min^{-1} were used for samples with upper particle size thresholds of 0.2, 0.45 and 1 μm respectively.

6. In FlFFF, the membrane determines the lower molecular weight cut-off (MWCO). The membrane can be subject to clogging, this means that the membrane needs replacing at regular intervals and a protocol for the replacement of the membrane and subsequent calculations of channel void volume and thickness have been given in Chapter 2, section 2.5.

7. In SdFFF, the use of a centrifuge to separate the sample requires regular maintenance as an off-track belt or worn bearings in either the system or the motor results in excessive scraping or grinding noises. When a septum injector is used, a small piece of the septum may break and travel into the channel, causing in the most extreme situation, a complete stoppage of the flow.

7.1.2 Soil sampling, treatment and preservation

A recommended method for the preparation of soil suspension samples was presented in Chapter 4 where the soil suspension samples were settled gravitationally at a constant temperature (20 °C) as soon as possible after sampling to obtain the <1 μm fraction. The settling time should not exceed 1 h to ensure that the sample has not aggregated over longer settling times. The samples were found to be stable for at least 12 h when stored at ambient temperature. The samples were kept at this temperature to be compatible with the temperature of the carrier in FlFFF. Two soils with contrasting characteristics were chosen

and analysed using the recommended preparation guidelines to obtain the <1 μm fraction. FlFFF was able to analyse both of these soil types and was therefore an appropriate technique for the determination of PSDs for soil suspension samples.

7.1.3 Centrifugation and filtration for the further fractionation of <1 μm samples

A comparison of centrifugation and filtration techniques for the separation of soil suspension samples into <0.2 and <0.45 μm fractions was carried out with SdFFF analysis in Chapter 3 and FlFFF analysis in Chapter 4. In both chapters it was demonstrated that there are uncertainties of using conventional membrane filtration and centrifugation for soil suspension samples, with filtration removing larger amounts of material than centrifugation when the <1 μm fraction was used to prepare the smaller size fractions (<0.2 and <0.45 μm). It was therefore recommended that centrifugation was preferable to filtration for the fractionation of soil suspension samples.

7.1.4 FFF as a tool for analysing real colloidal samples

This project has emphasised the need for a separation technique capable of analysing samples in the whole colloidal range without the need for centrifugation or filtration preparation methods that have been shown to remove significant amounts of material. SdFFF and FlFFF have been used to determine the PSDs of colloidal samples as long as particles greater than 1 μm have been removed before analysis to avoid steric interference. Therefore FFF has great potential as a robust but mild technology for the physical investigation of the colloidal fraction in aquatic environmental matrices. Also preliminary experiments with real soil runoff samples showed the presence of material over the whole colloidal range using the optimised FlFFF system.

7.1.5 Determination of phosphorus species with a portable FI monitor

A portable FI monitor with spectrophotometric detection was optimised for the determination of RP. A silicate interference study showed that there was no silicate interference with the molybdenum blue chemistry at concentrations of silicate up to 8 mg L^{-1}. An autoclave digestion method was optimised for the determination of TP and TDP. Autoclaving with 40 g L^{-1} of peroxydisulphate gave recoveries for adenosine-5'-triphosphoric acid disodium dihydrogen salt, cocarboxylase, methyltriphenylphosphonium bromide, phytic acid and penta-sodium triphosphate >88 %.

7.1.6 Determination of phosphorus associated with colloidal material

FFF has another advantage as the colloidal material can be combined with FIA to determine phosphorus associated with colloidal material of different sizes. This was demonstrated in Chapter 6 where FlFFF was coupled offline with FIA and spectrophotometric detection. The concentrations of RP in the different size fractions 0-0.2, 0.2-0.45 and 0.45-1 μm was determined as 1.1, 0.9, and 11.5 μM PO_4-P respectively, and the concentrations of TP in the 0-0.2, 0.2-0.45 and 0.45-1 μm fractions was determined as 14.3, 7.4 and 27.3 μM PO_4-P respectively. However these values may not give an accurate representation of how P is distributed over the colloidal range, because centrifugation may have removed some material in the <0.2 and <0.45 μm centrifuged fractions.

7.2 Future Work

From these conclusions there are several further pathways of investigation that could be followed and these are considered below. This future work would mainly involve the use of the FlFFF and the portable FI monitor.

7.2.1 Different soil types and real samples

Only two different soil types were analysed using FlFFF in Chapter 4, therefore future work would involve the preparation of other soil types with different characteristics e.g. sandy loam, clay loam, silty clay, silt loam soils in order to predict phosphorus transfer in different soil types. The PSDs of these samples would then be determined in the colloidal range i.e. <1 μm, in order for comparison with other soils. Soil suspensions have been used as models for soil runoff or leachate samples, therefore during storm events, real runoff samples could be collected and analysed using FlFFF as soon as possible after collection and preferably within the first 12 h where soil suspension samples have been observed to be stable.

7.2.2 Effect of soil temperature

Soil suspension samples have been stored at ambient temperature so as to be compatible with FlFFF experimental conditions, however soils in situ experience different temperatures. Therefore the effect of temperature on soil suspension samples could be investigated to determine whether the temperature by affecting the biology has any effect on the PSDs obtained for the colloidal material and the sample stability. Hence FlFFF could be used as a tool to study how temperature affects the turnover of the microbial population in live soils.

7.2.3 Improving the detection limit of the portable FI monitor

For a FlFFF analysis, only 20 μL of sample is usually injected therefore this needs to be representative of the larger volume of soil agricultural runoff that has been sampled in the field. This will then ensure that a true representation of what is happening in the environment is gained. Also as only 20 μL of sample is injected this sample becomes greatly diluted during a run. Therefore by collecting the eluent after UV detection as different sized fractions and injecting them into the portable FI monitor no response is seen as the concentration is below the detection limit of the system. Therefore for direct coupling between the FlFFF and FI monitor the sensitivity of the FI monitor needs to be increased to enable the P in the eluent to be detected. Initial experiments to combine the two techniques have involved injecting the centrifuged fractions simultaneously into the FlFFF and portable FI monitor. However as it has been shown that fractionation using centrifugation can remove material this preparation technique is preferably avoided.

A possible suggestion to enhance sensitivity is to replace the flow cell with a long path (2 m) liquid core waveguide (LCWG). Other detectors could also be investigated e.g. ICP-MS has been coupled to FlFFF, however, although this technique has been successful for the determination of trace metals it is not sensitive enough for the P determinations that would be required in this work. Pre-concentration methods could also be investigated, as there have been methods of on-line sample pre-concentration in FlFFF, called the opposed flow sample concentration. In this method a third pump was used to focus dilute river water samples near the top of the FlFFF channel before analysis took place.

7.2.4 Improving the FI monitor instrumentation

In section 7.2.3 the sensitivity of the detector used in the FI monitor was discussed, additional improvements could be carried out on the FI monitor including reducing the flow rates as it was observed that the system was relatively independent of flow rates

within the flow rate ranges studied in Chapter 5, section 5.3.1. By reducing flow rates, the reagent consumption will also be reduced. The light source used in the FI monitor was a tungsten halogen light which consumes more power than other light sources such as LEDs, therefore by replacing with LEDs power consumption would be reduced.

7.2.5 Coupling FlFFF off-line and on-line to the portable FI monitor

Once the sensitivity of the FI monitor had been improved, then different size fractions could be collected from the eluent of the FlFFF after UV detection and subsequently injected directly into the FI monitor for RP determination. The TP or TDP could also be determined by autoclaving the different size fractions using the optimised autoclave digestion procedure. If the coupling of the two techniques off-line was successful then the next step would be to couple the FlFFF and the FIA system on-line in a similar manner to FFF-ICP-MS to enable direct determination with less sample handling and contamination. FlFFF combined with sensitive FI-LCWG would generate physical, chemical and spatial/temporal profiles and help in the characterisation and understanding of the dynamics of phosphorus movement through a eutrophic waterbody.

Environ. Sci. Technol. 2005, 39, 1731−1735

Comparison of Centrifugation and Filtration Techniques for the Size Fractionation of Colloidal Material in Soil Suspensions Using Sedimentation Field-Flow Fractionation

LAURA J. GIMBERT,[†,‡] PHILIP M. HAYGARTH,[‡] RONALD BECKETT,[§] AND PAUL J. WORSFOLD*,[†]

School of Earth, Ocean and Environmental Sciences, Plymouth Environmental Research Centre, University of Plymouth, Plymouth PL4 8AA, U.K., Soil Science and Environmental Quality Team, Institute of Grassland and Environmental Research, North Wyke Research Station, Okehampton, Devon EX20 2SB, U.K., and Water Studies Centre, School of Chemistry, Monash University, Clayton, Victoria 3800, Australia

Sedimentation field-flow fractionation (SdFFF) with UV detection is used to systematically investigate the effect of traditional membrane filtration and centrifugation procedures on the isolation of specific size fractions from soil suspensions. Both procedures were used to isolate the nominal <0.45 and <0.2 μm fractions from a clay soil suspension. Results showed that the membrane filtration approach seriously underestimated the total mass of particulate matter present as compared to the centrifugation approach. This has serious implications for the interpretation of results for "colloidal" and "soluble" fractions from soil suspensions and other environmental matrices obtained using the standard membrane approach. The results also show that sedimentation FFF has great potential as a robust and relatively mild technology for studying size distributions in the "colloidal" range for soil suspensions and other aquatic matrices.

Introduction

Colloidal material (0.001−1 μm) in soil leachate and drainage waters is an important vehicle for the transport of contaminants (*1*, *2*) such as phosphorus species (*3*, *4*), pathogens (*5*−*7*), persistent organic pollutants (*8*), and nitrogen species (*9*, *10*). Therefore, accurate and sensitive methods for the separation of particulate and colloidal material from soil suspension samples are essential (*11*−*13*).

Conventional filtration methods have traditionally been used for the separation of dissolved and particulate fractions in environmental samples, using an operationally defined filter pore size of 0.2 or 0.45 μm as the "threshold" (*14*). The colloidal fraction, which spans a wider range than these nominal pore sizes, has therefore been difficult to study. Haygarth et al. and Heathwaite et al. used membrane and ultrafiltration methods to separate different colloidal size ranges in river water and soil leachates, but found that colloids aggregated at the membrane surface (*15*, *16*). Colloids also interact directly with the membrane, resulting in material being retained (*17*), and there can also be memory effects, contamination from the filter, and variable pressure across the membrane.

Many studies have used centrifugation and filtration methods sequentially to prepare soil samples (*18*−*21*). Del Castilho et al. (*22*) studied the difference between centrifuged and membrane-filtered soil suspensions to remove suspended material at a threshold of <0.45 μm and then analyzed the resulting fractions for a range of elements. They found that colloid-associated properties differed between membrane filtration and centrifugation, with membrane filtration producing higher values, and therefore suggested that membrane filtration, being the simpler method, was the preferred technique for the removal of colloidal material. Douglas et al. (*23*) sequentially used three separation techniques: sieving, continuous flow centrifugation, and tangential flow filtration (TFF) to fractionate suspended material in river waters over the particulate and colloidal ranges. The above studies focused on how the elemental content of environmental samples differed using different separation techniques, but did not quantitatively investigate the colloidal size distribution.

To overcome the uncertainties encountered with membrane filtration, and also to be able to characterize the colloidal material, Buffle and Leppard suggested the use of "a promising new technique", field-flow fractionation (FFF), for colloidal fractionation (*17*). This emerging separation technique can be used to obtain information on particle size or relative molecular mass (RMM) distributions in complex environmental matrices over the entire colloidal size range. There are many subtechniques of FFF of which sedimentation (Sd) and flow (Fl) are the most commonly used. FlFFF separates molecules or particles using a cross-flow field, and the process is independent of density, whereas SdFFF separates on the basis of buoyant mass (i.e., size and density) using a centrifugal field. SdFFF has been used successfully to determine the size distribution of colloids in environmental samples such as soil and sediment solutions (*24*, *25*). Results have been verified by collecting different size fractions and analyzing them using electron microscopy (*25*−*27*). Previous studies of soil, sediment, and river water samples have usually used SdFFF coupled with detectors such as ICP-MS to determine elemental composition with respect to different size fractions (*24*, *25*, *27*−*32*). Most of these studies pretreated the samples using gravity sedimentation (*27*) or centrifugation (*24*, *25*, *28*, *31*, *32*) to obtain a <1 μm cutoff to avoid steric interferences (*29*).

The aim of this work was to use SdFFF with UV detection to systematically investigate the effect of traditional membrane filtration and centrifugation procedures on the isolation of specific size fractions from soil suspensions. Particle size thresholds of <0.2 and <0.45 μm were selected to represent the two most common operational fractions isolated by traditional membrane filtration (*17*).

Experimental Section

Sample Preparation. All glassware and plastic bottles were prewashed overnight in 5% nutrient P-free detergent (Extran), rinsed with Milli-Q water three times, and then left overnight in 5% Extran and again rinsed with Milli-Q water three times.

* Corresponding author phone: +44 1752 233006; fax: +44 1752 233009; e-mail: pworsfold@plymouth.ac.uk.
† University of Plymouth.
‡ Institute of Grassland and Environmental Research.
§ Monash University.

10.1021/es049230u CCC: $30.25
Published on Web 01/22/2005

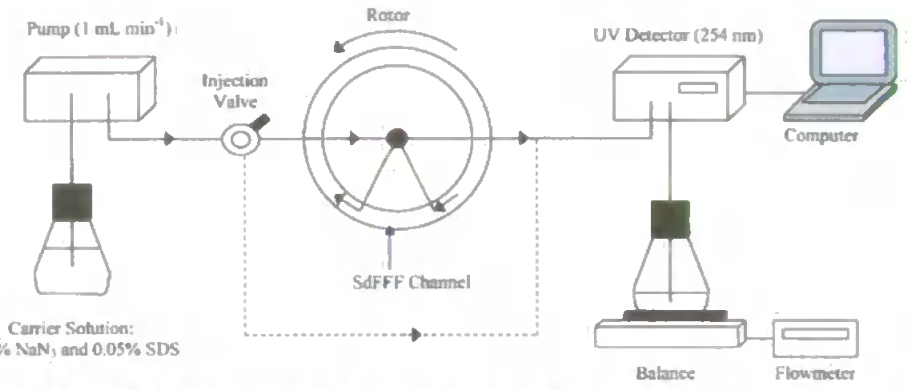

FIGURE 1. Schematic diagram of the SdFFF instrumentation. Bold lines indicate direction of carrier in run/inject mode; dotted lines indicate direction of carrier in stopflow/load mode.

A clay soil sample was previously collected from the B-horizon at Lilydale in Melbourne, Australia (*28*). This is a reddish brown (5YR4/3), light clay Krasnozem soil with a moderate polyhedral structure, 10−20 mm peds, rough fabric, and a firm consistence. The content was 55% clay (<2 μm), 22% silt (2−20 μm), 22% fine sand (20−200 μm), and 1% course sand (200 μm−2 mm) with a pH of 5.2 (in water) and 4.4 (in calcium chloride). The sample was suspended in ultrapure Milli-Q water (Millipore) and screened through a 25 μm mesh nylon sieve. The <1 μm diameter fraction was isolated by repeated centrifugation and stored at 4 °C. The concentration of the <1 μm fraction was determined by drying 10 mL of sample in an oven overnight at 100 °C. The weight of the dried soil sample was 5 g, giving a concentration of 50% (m/v) in the suspension. This is a highly dispersible soil sample, and from experience the particles in this concentrated suspension stay dispersed in water. This suspension was further characterized and found to contain 14 600 mg kg^{-1} aqua regia extractable iron, 19 mg kg^{-1} aqua regia extractable manganese, and 2.5 g kg^{-1} organic matter.

Fractionation of Soil Sample. The 50% (m/v) soil sample was diluted in Milli-Q water to give a 1% (m/v) suspension which was used to prepare the filtered and centrifuged <0.2 and <0.45 μm soil fractions as outlined below. Sedimentation does not occur in diluted (1% m/v) samples (*28*), and hence samples were diluted with Milli-Q water alone rather than adding a surfactant such as sodium dodecyl sulfate (SDS).

Filtration: Two different size fractions (<0.2 and <0.45 μm) were obtained by sequential filtration. The 1% (m/v) soil suspension (25 mL) was sequentially filtered under suction through a 0.45 μm Activon cellulose nitrate membrane filter (47 mm dia) and a 0.2 μm Whatman cellulose nitrate membrane filter (47 mm dia) using a conventional glass filtration unit.

Centrifugation: The 1% (m/v) soil suspension was pipetted into polypropylene tubes (1.7 mL volume) and placed into an Avanti 30 High-Performance benchtop centrifuge with the F2402 fixed-angle rotor. The settling time for each fraction (<0.2 and <0.45 μm) was determined using the following equations:

$$\omega = \left(\frac{2\pi}{60}\cdot \text{rpm}\right) \quad (1)$$

$$t = \frac{18\eta \ln\left(\frac{R}{S}\right)}{\omega^2 d^2 \Delta\rho} \quad (2)$$

where ω is the angular velocity of the centrifuge (rad s^{-1}), d is the particle diameter (cm), $\Delta\rho$ is the density difference between the particles and the suspension medium (g cm^{-3}), η is the viscosity of the suspension medium (g cm^{-1} s^{-1}) where the viscosity of water at 20 °C is 0.010 g cm^{-1} s^{-1}, t is the settling time (s), R is the distance (cm) from the axis of rotation to the level from where the supernatant is decanted from the tube), and S is the distance from the axis of rotation to the surface of the suspension in the tube (cm).

From the above equations, it was determined that the 1% m/v soil suspension (containing <1 μm particles) required a centrifugation time of 10 min at 2000 rpm (357*g*) at 20 °C to obtain the <0.45 μm fraction. The supernatant was decanted, and the pellet was resuspended in Milli-Q water and recentrifuged to ensure that any remaining <0.45 μm particles retained in the pellet were recovered. This was repeated a third time, and the decanted supernatants from the three centrifuge runs were pooled. This process was repeated to obtain the <0.2 μm fraction by centrifuging the 1% m/v soil suspension at 4500 rpm (1810*g*) for 10 min (at 20 °C).

Soil Particle Density. There is broad agreement on reported values for the density of soil mineral particles. Sainz Rozas et al. (*33*) assumed that the density was 2.65 g cm^{-3}, Adriano and Weber (*34, 35*) reported that the typical density range for agricultural soils was 2.6−2.75 g cm^{-3}, and arable surface soils with a high mineral content had a particle density of 2.65 g cm^{-3}, and Wienhold and Tanaka reported the same value (*36*). Other literature sources have assumed a particle density of 2.5 g cm^{-3} for mineral-rich sediments (*29*−*32*). A density of 2.6 g cm^{-3} (hence a density difference of 1.6 g cm^{-3}) represents a typical literature value for agricultural soils of the type used in this study and was therefore used in this work for all centrifugation and SdFFF calculations (*37*).

Sedimentation Field-Flow Fractionation. Details of the SdFFF instrumentation used in this work have been reported elsewhere (*31*). The channel dimensions were radius 15.1 cm, length 86.1 cm, breadth 2.0 cm, and width 0.0144 cm. The carrier was pumped through the channel by a Consta-Metric3000 solvent delivery system (LDC Analytical, USA) at a flow rate of 1 mL min^{-1}. The flow rate was monitored using an Ohaus Precision Plus balance and a flowmeter. A schematic diagram of the SdFFF instrumental setup is shown in Figure 1. The SdFFF carrier solution consisted of 0.05% (m/v) sodium dodecyl sulfate (SDS; VWR, Poole, England) and 0.02% (m/v) sodium azide (NaN_3; VWR, Poole, England) in Milli-Q water. We are confident that the low concentration of SDS used would have no effect on the particle size distribution. The carrier was degassed before use by evacuation for at least 30 min. All runs were carried out at 25 °C.

A power program was used in which, after the relaxation or stopflow time, the initial field was held for time t_1 and then decayed to a holding field where the time constant t_a determined how rapidly the field decayed (*38*). The constants

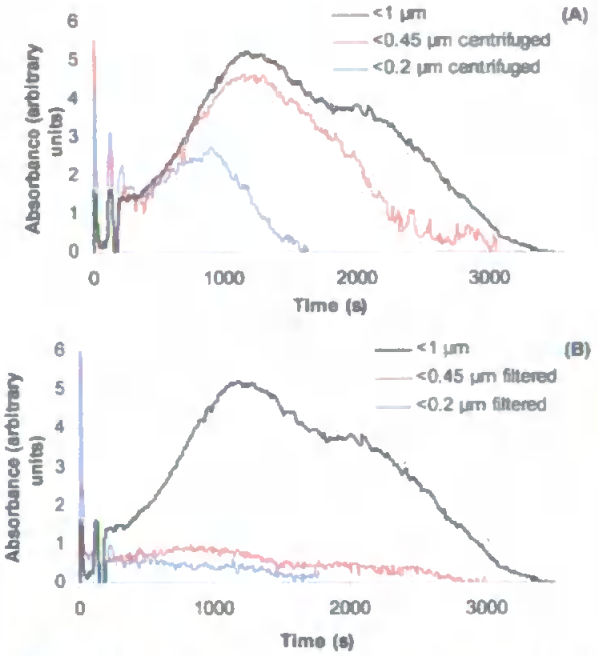

FIGURE 2. SdFFF fractograms for the soil samples comparing filtered and centrifuged fractions with <1 μm starting material: (A) fractogram for <0.2 and <0.45 μm centrifuged fractions with data averaged for the two runs; (B) fractogram for <0.2 and <0.45 μm filtered fractions with data averaged for the two runs.

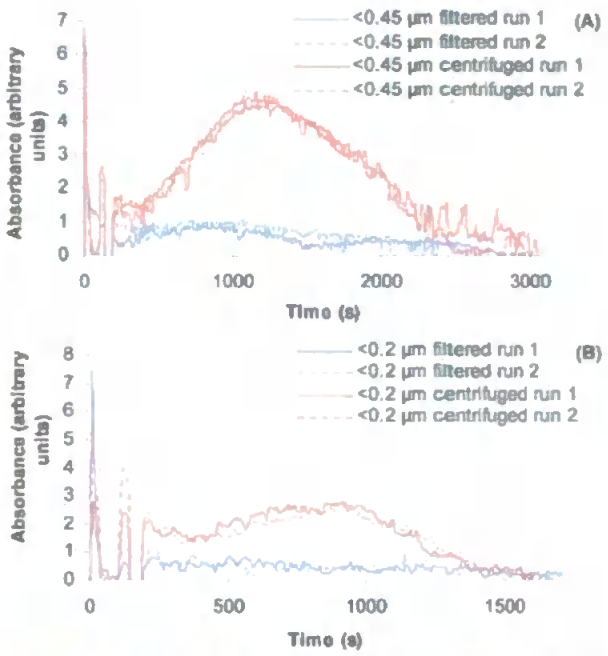

FIGURE 3. SdFFF fractograms for the soil samples showing the good reproducibility observed between two runs: (A) fractograms for <0.45 μm filtered and centrifuged runs; (B) fractograms for <0.2 μm filtered and centrifuged runs.

t_1 and t_a were determined using a computer program written by P. S. Williams (University of Utah, Salt Lake City, UT).

The filtered and centrifuged samples (80 μL), and the 1% (m/v) soil suspension (80 μL), were injected through a rubber septum into the channel. After a few seconds, the carrier solution was switched to bypass the channel and flowed directly through the detector (relaxation/stopflow). After a 10 min relaxation time at a rotation of 1000 rpm (169*g*), the channel flow was restored and the run commenced. The initial field of 1000 rpm was held for a time lag, t_1, of 5.3 min. The decay parameter t_a of − 42.0 min then reduced the field to a holding rotation of 20 rpm (0.067*g*). A DC motor and speed controller (Bodine Electric Co.) powered the rotor.

The absorbance of the eluent was recorded using a Spectra 100 variable wavelength detector (Spectra-Physics, USA) at 254 nm with a sensitivity of 0.02 AUFS. Two runs were carried out for each fraction (<0.2 and <0.45 μm filtered samples; and <0.2 and <0.45 μm centrifuged samples) and the starting material (containing <1 μm particles).

Data Analysis. Fractograms were obtained by plotting detector response against elution volume (or time) of the emerging sample. The fractograms were converted to particle size distributions using an analysis program (Field-Flow Fractionation Research Centre Software, University of Utah, 1990). The fractograms were not corrected for light scattering (*30*, *32*, *39*). The negative peak at 2.7 min after the start of each fractogram, resulting from the sample matrix being different from the carrier solution, has been removed from the figures for clarity.

Results and Discussion

Fractograms of Soil Suspensions. The differences in fractograms for the centrifuged and filtered fractions with the <1 μm starting material are shown in Figure 2A and B, respectively. All data are the means of duplicate injections. The UV response for the filtered fractions for both size cutoffs was significantly lower than that for the corresponding centrifuged fractions. Typical reproducibility for duplicate injections of the centrifuged and filtered fractions is shown in Figure 3A,B for the <0.45 and <0.2 μm runs, respectively.

Particle Size Distributions. The SdFFF instrument was calibrated using polystyrene bead standards of known diameters. The fractograms were converted into particle size distributions (PSDs) and the data for duplicate injections of the starting material, and the <0.45 and the <0.2 μm centrifuged fractions were averaged. These data (Figure 4A) showed that the <1 μm soil sample had a log-normal distribution of particle sizes with a maximum at 0.13 μm and an upper threshold at 0.6 μm. Chen et al. also reported a 0.6 μm threshold value for the same Lilydale sample (*28*). This size threshold was lower than the expected 1 μm based on the sample preparation method used, but similar findings have been reported for other environmental samples (*24*, *25*, *27*, *31*, *32*, *39*). Chittleborough et al. (*27*) reported a threshold value of 0.4 μm for loamy sand samples, and van Berkel et al. (*25*) reported a threshold of 0.6 μm for both soil and suspended river colloids.

The PSDs for the centrifuged <0.45 and <0.2 μm fractions had upper size thresholds of about 0.40 and 0.18 μm, which are close to the expected cutoffs (Figure 4B and C). However, some material less than these cutoff diameters was also removed by centrifugation. This may be due to the heterogeneity of the particle shapes and the assumption made about soil particle density in the calculations applied to the raw fractograms.

For the filtration experiments, the initial concentration of the soil suspension (1% m/v) was high but not extreme. Twenty-five milliliters of suspension was filtered, corresponding to a 0.25 g loading of soil particles, which would be equivalent to filtering 1 L of a 250 mg L^{-1} suspension. This is a realistic experimental design. The fact that the soil suspension could be filtered by suction filtration without complete blockage suggests that filter loading was not excessive. Furthermore, the filtration was sequential, and hence the loading on the 0.2 μm filter was much less than 0.25 g.

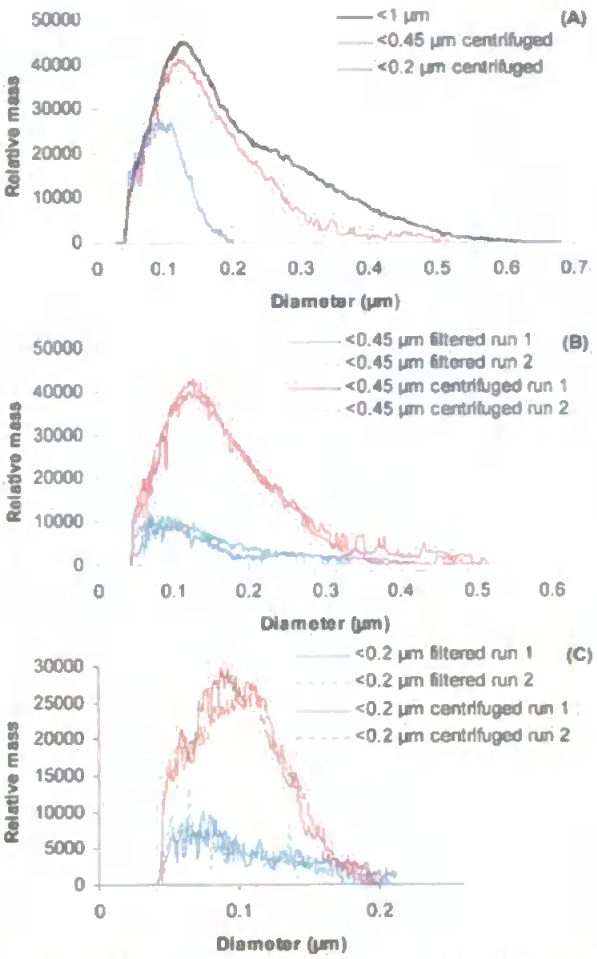

FIGURE 4. SdFFF particle size distributions for the soil samples: (A) particle size distribution for <0.2 and <0.45 μm centrifuged fractions and <1 μm starting material with data averaged for two runs; (B) particle size distribution for two runs of <0.45 μm filtered and centrifuged fractions; (C) particle size distribution for two runs of <0.2 μm filtered and centrifuged fractions.

The particle size distributions for the filtered <0.45 and <0.2 μm fractions show the same particle size thresholds, of about 0.40 and 0.18 μm, respectively, as the centrifuged fractions (Figure 4B and C). Most important, however, is the observation that the relative mass of the filtered fractions is much lower than the centrifuged fractions. The filtration process would have been more affected by particle shape than the centrifugation process because "platey" particles of smaller equivalent spherical diameter (ESD) would be more effectively removed than spherical or cubic particles for any given nominal filter pore size. However, the effect observed in these results is unlikely to be explained by shape. As an example, if all of the particles in the soil suspension were plates (unlikely) with an aspect ratio of 10:1, then the volume would be 10 times lower than for a cube with the same edge length as the plate dimension. This would result in a decrease in the ESD by a factor of about 2.1, and our results show removal by filtration much lower than this ESD for a given filter. Furthermore, SdFFF gives the ESD irrespective of the shape of the particles. The results therefore suggest that conventional <0.45 and <0.2 μm membrane filtration techniques for the separation of soil suspensions, and by implication other aquatic matrices, remove much more of the particulate material than the corresponding centrifugation procedure. An added advantage of centrifugation is that it is a less aggressive approach than membrane filtration for the size fractionation of colloids from environmental matrices.

Practical Applications. For the separation of particles from solution, international water industry "standard" procedures have relied on membrane filtration techniques to operationally define the boundary between "particulate" and "soluble" fractions, with a 0.45 μm nominal pore size membrane being the most commonly used (e.g., ref *40*). This is because it is relatively fast and filters out the majority of the biotic and abiotic particles but will, however, not retain some bacteria and colloidal material smaller than 0.45 μm (*41*). This is an area of much controversy and has been discussed in detail by Haygarth and Sharpley (*14*). The 0.2 μm nominal pore size membrane is slower but much more efficient at removing the microbial phase (bacteria of 0.2−1 μm), as well as algae (>1 μm) (*42*), but smaller unicellular bacteria will still not be retained.

Many of the key studies that have helped to define these boundaries have relied on membrane and ultrafiltration for separation (*15, 16*), but there are uncertainties that surround these techniques. Colloidal material can interact with the membrane, and the increased concentrations of the retained particles at the membrane surface appear to result in the aggregation of smaller colloids (*17*). Del Castilho et al. (*22*) suggested that membrane filtration was preferable to centrifugation as it was the easiest method to use. However, in the present study, the centrifugation method was found to be quick and efficient and yielded fractions with upper size cutoffs much closer to the required values than membrane filtration. Additional experiments, although preliminary in nature, suggest that the observations reported in this paper are also found with contrasting soil types, with more dilute soil suspensions (0.5 and 0.25% m/v) and with flow FFF. This finding has serious implications for the many size-based contaminant speciation studies that have relied on filtration for accurate size fractionation of the particles, for example, the operationally defined filterable reactive phosphorus fraction.

Acknowledgments

L.J.G. would like to thank EPSRC and the Royal Society of Chemistry for the award of a studentship. IGER is supported by the Biotechnology and Biological Sciences Research Council (BBSRC). We also thank Dr. David Nash (Statewide Leader for Soil Chemistry, Primary Industries Research Victoria (PIRVic), Ellinbank 3821, Victoria, Australia) for help with the soil characterization.

Literature Cited

(1) Buffle, J.; Leppard, G. G. Characterization of aquatic colloids and macromolecules. 1. Structure and behavior of colloidal material. *Environ. Sci. Technol.* **1995**, *29*, 2169−2175.
(2) Haygarth, P. M., Jarvis, S. C., Eds. *Agriculture, Hydrology and Water Quality*; CABI Publishing: Oxford, New York, 2002; pp 1−502.
(3) Haygarth, P. M.; Hepworth, L.; Jarvis, S. C. Forms of phosphorus transfer in hydrological pathways from soil under grazed grassland. *Eur. J. Soil Sci.* **1998**, *49*, 65−72.
(4) Haygarth, P. M.; Jarvis, S. C. Transfer of phosphorus from agricultural soils. *Adv. Agron.* **1999**, *66*, 195−249.
(5) Abuashour, J.; Joy, D. M.; Lee, H.; Whiteley, H. R.; Zelin, S. Transport of microorganisms through soil. *Water, Air, Soil Pollut.* **1994**, *75*, 141−158.
(6) Jones, D. In *Agriculture, Hydrology and Water Quality*; Haygarth, P. M., Jarvis, S. C., Eds.; CAB International: Wallingford, 2002.
(7) Oliver, D. M.; Clegg, C. D.; Haygarth, P. M.; Heathwaite, A. L. Assessing the potential for pathogen transfer from grassland soils to surface waters. *Adv. Agron.* (in press).
(8) Gaveo, B.; Jones, K. C. In *Agriculture, Hydrology and Water Quality*; Haygarth, P. M., Jarvis, S. C., Eds.; CAB International: Wallingford, 2002.
(9) Goulding, K. Nitrate leaching from arable and horticultural land. *Soil Use Manage.* **2000**, *16*, 145−151.

(10) Scholefield, D.; Tyson, K. C.; Garwood, E. A.; Armstrong, A. C.; Hawkins, J.; Stone, A. C. Nitrate leaching from grazed grassland lysimeters – effects of fertilizer input, field drainage, age of sward and patterns of weather. *J. Soil Sci.* **1993**, *44*, 601–614.
(11) Buffle, J.; Deladoey, P.; Haerdi, W. The use of ultrafiltration for the separation and fractionation of organic ligands in fresh waters. *Anal. Chim. Acta* **1978**, *101*, 339–357.
(12) Kretzschmar, R.; Borkovec, M.; Grolimund, D.; Elimelech, M. Mobile subsurface colloids and their role in contaminant transport. *Adv. Agron.* **1999**, *66*, 121–193.
(13) Rowland, A. P.; Haygarth, P. M. Determination of total dissolved phosphorus in soil solutions. *J. Environ. Qual.* **1997**, *26*, 410–415.
(14) Haygarth, P. M.; Sharpley, A. N. Terminology for phosphorus transfer. *J. Environ. Qual.* **2000**, *29*, 10–15.
(15) Haygarth, P. M.; Warwick, M. S.; House, W. A. Size distribution of colloidal molybdate reactive phosphorus in river waters and soil solution. *Water Res.* **1997**, *31*, 439–448.
(16) Heathwaite, A. L.; Matthews, R.; Preedy, N.; Haygarth, P. *J. Environ. Qual.* **2004**, in press.
(17) Buffle, J.; Leppard, G. G. Characterization of aquatic colloids and macromolecules. 2. Key role of physical structures on analytical results. *Environ. Sci. Technol.* **1995**, *29*, 2176–2184.
(18) Martínez, C. E.; Jacobson, A. R.; McBride, M. B. Aging and temperature effects on DOC and elemental release from a metal contaminated soil. *Environ. Pollut.* **2003**, *122*, 135–143.
(19) Hilger, S.; Sigg, L.; Barbieri, A. Size fractionation of phosphorus (dissolved, colloidal and particulate) in two tributaries to Lake Lugano. *Aquat. Sci.* **1999**, *61*, 337–353.
(20) McDowell, R. W.; Sharpley, A. N. Soil phosphorus fractions in solution: influence of fertiliser and manure, filtration and method of determination. *Chemosphere* **2001**, *45*, 737–748.
(21) Tyler, G. Effects of sample pretreatment and sequential fractionation by centrifuge drainage on concentrations of minerals in a calcareous soil solution. *Geoderma* **2000**, *94*, 59–70.
(22) del Castilho, P.; van Faassen, R.; Moerman, R. Differences between super-centrifuged and membrane-filtrated soil solutions obtained from bulked and non-bulked topsoils by soil centrifugation. *Fresenius' J. Anal. Chem.* **1996**, *354*, 756–759.
(23) Douglas, G. B.; Beckett, R.; Hart, B. T. Fractionation and concentration of suspended particulate matter in natural-waters. *Hydrol. Process* **1993**, *7*, 177–191.
(24) Chen, B.; Beckett, R. Development of SdFFF-ETAAS for characterising soil and sediment colloids. *Analyst* **2001**, *126*, 1588–1593.
(25) van Berkel, J.; Beckett, R. Determination of adsorption characteristics of the nutrient orthophosphate to natural colloids by sedimentation field-flow fractionation. *J. Chromatogr., A* **1996**, *733*, 105–117.
(26) Beckett, R.; Murphy, D.; Tadjiki, S.; Chittleborough, D. J.; Giddings, J. C. Determination of thickness, aspect ratio and size distributions for platey particles using sedimentation field-flow fractionation and electron microscopy. *Colloids Surf., A* **1997**, *120*, 17–26.
(27) Chittleborough, D. J.; Hotchin, D. M.; Beckett, R. Sedimentation field-flow fractionation—a new technique for the fractionation of soil colloids. *Soil Sci.* **1992**, *153*, 341–348.
(28) Chen, B.; Hulston, J.; Beckett, R. The effect of surface coatings on the association of orthophosphate with natural colloids. *Sci. Total Environ.* **2000**, *263*, 23–35.
(29) Hassellöv, M.; Lyvén, B.; Beckett, R. Sedimentation field-flow fractionation coupled online to inductively coupled plasma mass spectrometry – New possibilities for studies of trace metal adsorption onto natural colloids. *Environ. Sci. Technol.* **1999**, *33*, 4528–4531.
(30) Murphy, D. M.; Garbarino, J. R.; Taylor, H. E.; Hart, B. T.; Beckett, R. Determination of size and element composition distributions of complex colloids by sedimentation field-flow fractionation inductively coupled plasma-mass spectrometry *J. Chromatogr.* **1993**, *642*, 459–467.
(31) Ranville, J. F.; Chittleborough, D. J.; Shanks, F.; Morrison, R. J. S.; Harris, T.; Doss, F.; Beckett, R. Development of sedimentation field-flow fractionation-inductively coupled plasma mass-spectrometry for the characterization of environmental colloids. *Anal. Chim. Acta* **1999**, *381*, 315–329.
(32) Taylor, H. E.; Garbarino, J. R.; Murphy, D. M.; Beckett, R. Inductively coupled plasma mass-spectrometry as an element-specific detector for field-flow fractionation particle separation. *Anal. Chem.* **1992**, *64*, 2036–2041.
(33) Sainz Rozas, H. R.; Echeverría, H. E.; Picone, L. I. Denitrification in maize under no-tillage: Effect of nitrogen rate and application time. *Soil Sci. Soc. Am. J.* **2001**, *65*, 1314–1323.
(34) Adriano, D. C.; Weber, J. T. Influence of fly ash on soil physical properties and turfgrass establishment. *J. Environ. Qual.* **2001**, *30*, 596–601.
(35) Brady, N. C. *The Nature and Properties of Soils*; MacMillan: New York, 1984.
(36) Wienhold, B. J.; Tanaka, D. L. Soil property changes during conversion from perennial vegetation to annual cropping. *Soil Sci. Soc. Am. J.* **2001**, *65*, 1795–1803.
(37) Rowell, D. L. *Soil Science: Methods and Applications*; Longman Scientific & Technical: Essex, England, 1994.
(38) Williams, P. S.; Giddings, J. C. Power programmed field-flow fractionation—a new program form for improved uniformity of fractionating power. *Anal. Chem.* **1987**, *59*, 2038–2044.
(39) Beckett, R.; Nicholson, G.; Hart, B. T.; Hansen, M.; Giddings, J. C. Separation and size characterization of colloidal particles in river water by sedimentation field-flow fractionation. *Water Res.* **1988**, *22*, 1535–1545.
(40) Haygarth, P. M.; Edwards, A. C. Sample collection, handling, preparation and storage. In *Methods of Phosphorus Analysis for Soils, Sediments, Residuals and Water*; Pierzynski, G. M., Ed.; Southern Co-Operative Series Bulletin No. 396, A publication of SERA-IEG-17: North Carolina State University, 2000.
(41) Gardolinski, P. C. F. C.; Hanrahan, G.; Achterberg, E. P.; Gledhill, M.; Tappin, A. D.; House, W. A.; Worsfold, P. J. Comparison of sample storage protocols for the determination of nutrients in natural waters. *Water Res.* **2001**, *35*, 3670–3678.
(42) Cotner, J. B.; Wetzel, R. G. Uptake of dissolved inorganic and organic phosphorus compounds by phytoplankton and bacterioplankton. *Limnol. Oceanogr.* **1992**, *37*, 232–243.

Received for review May 25, 2004. Revised manuscript received November 1, 2004. Accepted November 16, 2004.

ES049230U

DTD 5
ARTICLE IN PRESS

Available online at www.sciencedirect.com
SCIENCE DIRECT®

Talanta xxx (2004) xxx–xxx

Talanta

www.elsevier.com/locate/talanta

Sampling, sample treatment and quality assurance issues for the determination of phosphorus species in natural waters and soils

Paul J. Worsfold[a,*], Laura J. Gimbert[a], Utra Mankasingh[a], Omaka Ndukaku Omaka[a], Grady Hanrahan[b], Paulo C.F.C. Gardolinski[c], Philip M. Haygarth[d], Benjamin L. Turner[e], Miranda J. Keith-Roach[a], Ian D. McKelvie[f]

[a] *School of Earth, Ocean and Environmental Sciences, University of Plymouth, Drake Circus, Plymouth, PL48AA, UK*
[b] *Department of Chemistry and Biochemistry, 5151 State University Drive, California State University, Los Angeles, CA 90032, USA*
[c] *Rua Joao Alencar Guimaraes, 54 Curitiba-PR, 80310-420, Brazil*
[d] *Institute of Grassland and Environmental Research, North Wyke, Okehampton, Devon, EX202SP, UK*
[e] *Soil and Water Science Department, University of Florida, Gainesville, FL 32611, USA*
[f] *Water Studies Centre, School of Chemistry, PO Box 23, Monash University, Victoria 3000, Australia*

Received 1 July 2004; received in revised form 15 September 2004; accepted 16 September 2004

Abstract

Phosphorus is an important macronutrient and the accurate determination of phosphorus species in environmental matrices such as natural waters and soils is essential for understanding the biogeochemical cycling of the element, studying its role in ecosystem health and monitoring compliance with legislation. This paper provides a critical review of sample collection, storage and treatment procedures for the determination of phosphorus species in environmental matrices. Issues such as phosphorus speciation, the molybdenum blue method, digestion procedures for organic phosphorus species, choice of model compounds for analytical studies, quality assurance and the availability of environmental CRMs for phosphate are also discussed in detail.

Keywords: Phosphorus; Natural waters; Soils; Sampling; Sample treatment; Sample digestion; Quality assurance

1. Introduction

The determination of phosphorus species in environmental matrices provides essential data for assessing the health of ecosystems, investigating biogeochemical processes and monitoring compliance with legislation. At the catchment scale, for example, phosphorus export from both point and diffuse sources can result in increased primary production and eutrophication, with the potential for seasonal development of toxic algal blooms, which can have a major impact on global water quality [1]. For accurate measurements, knowledge of phosphorus speciation is required as environmental behaviour is often critically dependent on its physico-chemical form. In aquatic systems, for example, phosphorus species are found in "dissolved", "colloidal" and "particulate" fractions, as inorganic and organic compounds and in biotic and abiotic particles [2]. The common operationally defined aquatic forms of phosphorus and the various terms used to describe them are shown schematically in Fig. 1. The reliability and comparability of data for any of these fractions will depend on the operational protocols used and the accuracy of the method.

Most manual and automated methods of phosphorus determination are based on the reaction of phosphate with an acidified molybdate reagent to yield phosphomolybdate heteropolyacid, which is then reduced to an intensely coloured blue compound and determined spectrophoto-

* Corresponding author. Tel.: +44 1752233006; fax: +44 1752233009.
E-mail address: pworsfold@plymouth.ac.uk (P.J. Worsfold).

0039-9140/$ – see front matter © 2004 Published by Elsevier B.V.
doi:10.1016/j.talanta.2004.09.006

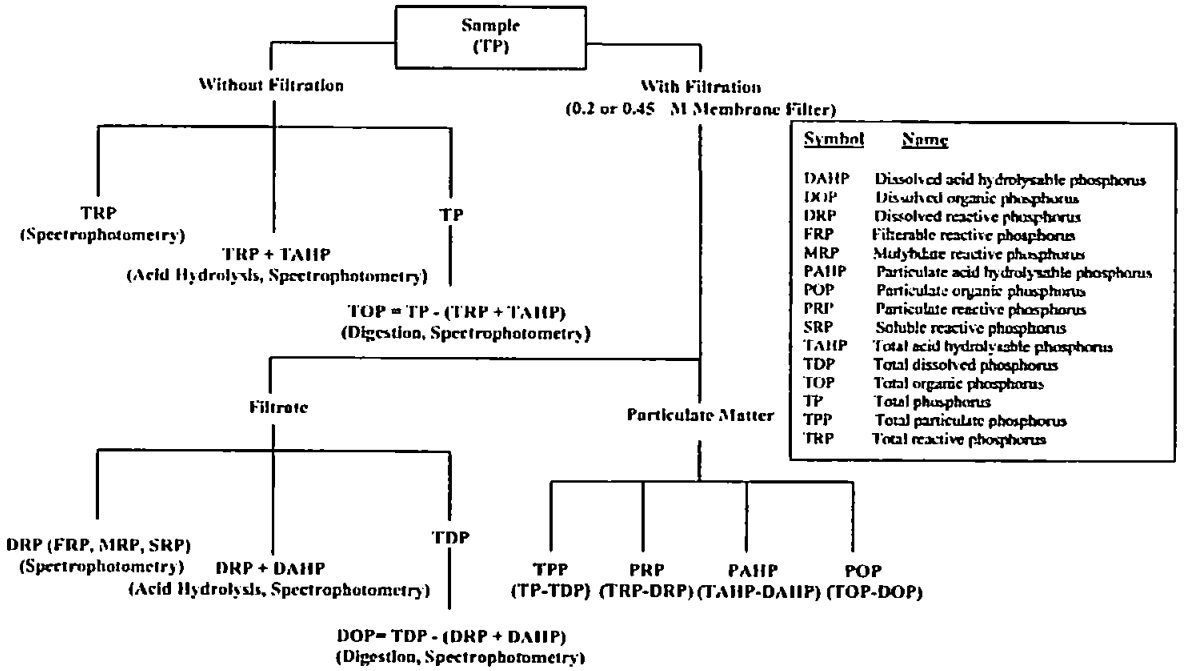

Fig. 1. Operationally defined aquatic P fractions (adapted from [2]).

metrically [3].

$$PO_4^{3-} + 12MoO_4^{2-} + 27H^+ \rightarrow H_3PO_4(MoO_3)_{12} + 12H_2O$$

$$H_3PO_4(MoO_3)_{12} + \text{reducing agent} \rightarrow \text{phosphomolybdenum blue [Mo(VI) } \rightarrow \text{ Mo(V)]}$$

There are many modifications of the original Murphy and Riley method [4], particularly the use of different reductants (e.g. ascorbic acid, tin(II) chloride) and acid strengths. As shown in the above reaction scheme, the phosphomolybdenum blue complex is formed in an acidic environment and its absorbance spectrum is dependent on the acidity, type of reductant and phosphate concentration. Under low acidity conditions, for example, non-linear colour development [5] and non-phosphate sensitized reduction (self-reduction of the molybdate) can occur. A variety of $[H^+]/[MoO_4^{2-}]$ ratios have been reported in the literature, with a ratio of 70 and a pH range of 0.57–0.88 suggested for optimum sensitivity (maximum rate of colour formation) [6].

Ascorbic acid and tin(II) chloride are the most commonly used reductants when determining phosphate concentrations in natural waters. Ascorbic acid acts as a 2-electron reductant [7] with the major advantages being that it is less salt sensitive and colour development is fairly independent of temperature [6]. Ascorbic acid on its own however has the major disadvantage of slow colour development [8], but the addition of antimony as a catalyst increases the rate of reduction of the complex [4]. Using tin(II) chloride generates a product with a wavelength maximum at 690–700 nm as compared with 882 nm for ascorbic acid [2]. This allows greater sensitivity when a solid state detector (using a red light emitting diode light source) is used [9]. However, disadvantages include unstable colour development, a considerable salt error, temperature dependence and unsatisfactory performance at high phosphorus concentrations [10].

Interferences in the formation of the phosphomolybdenum blue complex include arsenate, silicate, chromium, copper, nitrite, nitrate and sulphide [11]. However, arsenate interferences can be eliminated by reducing As(V) to As(III) prior to measurement [6], e.g. by the addition of sodium thiosulphate [12]. The acid/molybdate ratio can be altered to enhance the selectivity for phosphate relative to silicate [4]. In addition, use of an appropriate extraction solvent, e.g. *n*-butanol, is an efficient way of eliminating interference from silicate [13].

The phosphorus determined in the filtered fraction using the above reaction is defined as "molybdate reactive" phosphorus (MRP) or dissolved reactive phosphorus (DRP). It has also been called soluble reactive phosphorus (SRP) and filterable reactive phosphorus (FRP). However, this method also determines acid labile phosphorus containing compounds (organic and condensed phosphorus species) which can lead to overestimation of free phosphate [3,6]. Similar problems have been reported in the determination of total reactive (unfiltered) phosphorus (TRP) [3]. Methods have been developed to minimise this overestimation including a critical timing technique ('the 6 second method') in which the acid strength is adjusted prior to the formation of the complex [14] and complexing excess molybdate with a citrate–arsenate reagent [15]. Phosphorus containing organic compounds and con-

densed phosphates can also be determined using the molybdate reaction following chemical, photochemical, thermal or microwave digestion (see Section 3).

2. Natural waters

Phosphorus concentrations in natural waters fluctuate with changes in physico-chemical conditions and biological activity. In chalk-based catchments, for example, phosphorus is influenced by seasonal fluctuations in pH, dissolved carbon dioxide and total dissolved calcium concentrations [16]. Hydrological conditions also play an important role in aquatic phosphorus concentrations. The majority of phosphorus transport to catchments, from both diffuse and point sources occurs during short periods of increased discharge (e.g. storm events) [17,18], which demonstrates the importance of high temporal resolution monitoring during such events. Submersible or field-based instrumentation is desirable for monitoring dissolved phosphorus because it eliminates the need for sample collection and storage and, although such instrumentation is available [19,20], it is not used on a routine basis. Therefore, a comprehensive and effective sampling, sample treatment and analysis protocol must be adopted in order to minimise the physical, chemical and biological processes that can alter the physico-chemical forms of phosphorus during storage.

2.1. Sampling protocol

It is essential that the scientific objectives (e.g. determining bioavailable phosphorus, measuring seasonal phosphorus loads), safety issues and budgetary constraints are clearly identified prior to undertaking any sampling programme. Having established the scope of the exercise, an essential requirement of any sampling protocol is for the sample to be representative of the body of water from which it originates. It is therefore essential to adopt a well-organized protocol, which retains, as closely as possible, the original composition of the water body of interest. The protocol should be kept as simple as possible while minimizing the possibility of contamination or interferences. In rivers and streams, for example, samples should be collected from the water column at a series of depths and cross-sectional locations as individual grab samples or through the use of automated samplers for time series acquisition. Monitoring stations can be constructed to provide high quality supporting data (e.g. pH, dissolved oxygen, temperature, turbidity) in a judicious fashion via data acquisition/telemetry technology. It is also vital to avoid boundary areas, e.g. at the confluence of streams or rivers and below sewage treatment works, unless their impact on the system is being investigated. Point source phosphorus contributions from sewage treatment works, for example, can have a major affect on the overall water quality of freshwater systems [21]. Globally, phosphorus loading into receiving waters still occurs even though tertiary treatment measures (e.g. based on the reduction of phosphate by precipitation with iron chloride) are being implemented in some countries [22]. Other water bodies pose additional complications and these must be considered when designing a sampling protocol. In lakes and reservoirs, representative sampling is often difficult due to environmental heterogeneity, both spatial and temporal (e.g. seasonal thermal stratification). In order to study biogeochemical cycling in stratified water bodies appropriate depth profiling is required. For a complete study high spatial resolution sampling at the sediment–water interface is also essential but is not discussed further in this paper.

Location and frequency must also be considered when designing a sampling protocol. Site selection will ultimately depend on the problem to be addressed and safety and accessibility are of paramount importance. The frequency of sampling, from continuous to seasonal, will depend on the scientific objectives but will often be constrained by cost. For example, the highest phosphorus loadings in rivers and streams are generally correlated with intense, short-term discharges during autumn and winter months, while the lowest loadings occur in the summer months when discharge is low and biological activity is high [23,24]. In-water processes that affect phosphorus concentrations that must also be considered include plant, algal and bacterial turnover, anthropogenic inputs (e.g. sewage effluent), matrix considerations (e.g. water hardness) and resuspension of bottom sediments from increasing river discharge [21,25].

Prior to any sampling campaign it is essential to adopt an efficient cleaning protocol for all sampling equipment and storage bottles and continue this throughout the study. The walls of sample containers, for example, are excellent substrates for bacterial growth and therefore rigorous cleaning of all laboratory ware is necessary. For phosphate determination, it is recommended that containers be cleaned overnight with a nutrient free detergent, rinsed with ultrapure water, soaked in 10% HCl overnight, and then rinsed again with ultrapure water [26]. Containers should be rinsed at least twice with the water of interest prior to sample collection. In addition, sampling blanks should be taken to monitor and control the sampling process.

2.2. Sample preservation and storage

The overall effectiveness of any sample preservation and storage protocol depends on various factors including the nature of the sample matrix, cleaning procedures for sample containers, container material and size, temperature, chemical treatment (e.g. addition of chloroform) and physical treatment (e.g. filtration, irradiation of sample and pasteurization) [27–29].

Preliminary treatment often involves filtration which differentiates between the dissolved phase (operationally defined as that fraction which passes through a 0.45 or 0.2 μm filter) and suspended matter (that fraction collected on the filter) [30]. It is essential that filtration is carried out im-

mediately after the sample is collected to prevent short-term changes in phosphorus speciation. Polycarbonate or cellulose acetate membrane filters are recommended for dissolved constituents in natural waters [31]. Filtration with a 0.2 μm filter is preferred as it removes the majority of bacteria and plankton that would otherwise alter dissolved phosphorus concentrations during storage [30]. It should be stressed however that some bacteria, as well as viruses, will pass through a 0.2 μm filter. As with sample containers, the filtration apparatus (including individual filters) must be cleaned prior to use with a similar acid wash/ultrapure water rinse procedure. The filtration procedure can be conducted under positive pressure or vacuum. However, excessive pressure gradients should be avoided as rupture of algal cells and the subsequent release of intracellular contents into the sample could occur. In samples of high turbidity it is important to minimise the sample loading to prevent clogging of filter pores.

Table 1 shows a summary of reported storage/preservation methods for phosphorus determination. Physical (i.e. refrigeration, freezing and deep-freezing) and chemical (i.e. addition of chloroform, mercuric chloride and acidification) preservation techniques have been used to help maintain the original phosphorus concentration during storage. It should be noted however that the use of chloroform is now discouraged in some countries because of toxicological risks. In addition, a variety of sample containers have been used including quartz, borosilicate glass, polyethylene, polypropylene, high-density polyethylene (HDPE) and polytetrafluoroethylene (PTFE).

For phosphorus determinations, however, it is difficult to select a generic treatment protocol due to the different effects of specific matrix characteristics (e.g., phosphorus concentration, hardness, salinity, dissolved organic matter and bacterial nutrient uptake) of the sampling location. In chalk catchments, for example, studies have shown that freezing samples is not the best treatment due to the possibility of phosphate being coprecipitated with calcite when thawing the samples [26,46]. Fig. 2a demonstrates this effect, showing an immediate (after 1 day) and continuing (up to 250 days) decrease in DRP concentration in samples analysed for phosphate after storage at −20 °C [26]. Storage at 4 °C is therefore recommended, together with the addition of chloroform to prevent biological growth. However, chloroform should not be used in samples with high organic matter content, as the release of cellular enzymes into the samples is possible [26]. Other studies have recommended immediate analysis after sampling [47] or analysis after a short storage period at 4 °C in the dark (maximum 48 h) [48–51].

In contrast to the extensive studies on phosphate stability during storage, the stability of dissolved organic phosphorus (DOP), as operationally defined, has not been widely studied. Fig. 2b–d show the stability of DOP (strictly this includes all acid hydrolysable phosphorus because acidic digestion conditions were used) from natural water samples (salinities 0, 14 and 32, respectively) over 32 days of storage. The DRP concentration on day 0 (1.17, 1.31 and 0.54 μM for salinities 0, 14 and 32, respectively) was subtracted from all results, which were based on sampling, autoclaving of sub-samples and storage of autoclaved and non-autoclaved sub-samples for subsequent analysis. They showed that there were no significant differences in DOP concentration if the samples were stored at −20 °C, autoclaved and analysed on the same day or if they were autoclaved immediately after collection and stored until analysed. The same trend (not shown) was also observed with phytic acid spiked (1.11, 1.50 and 0.45 μM for salinities 0, 14 and 32, respectively) standards and samples. These results suggest that storage at −20 °C is suitable for DOP determination but the final result is dependent on a reliable determination of the original DRP concentration. Freezing as a method for storage of unfiltered and filtered

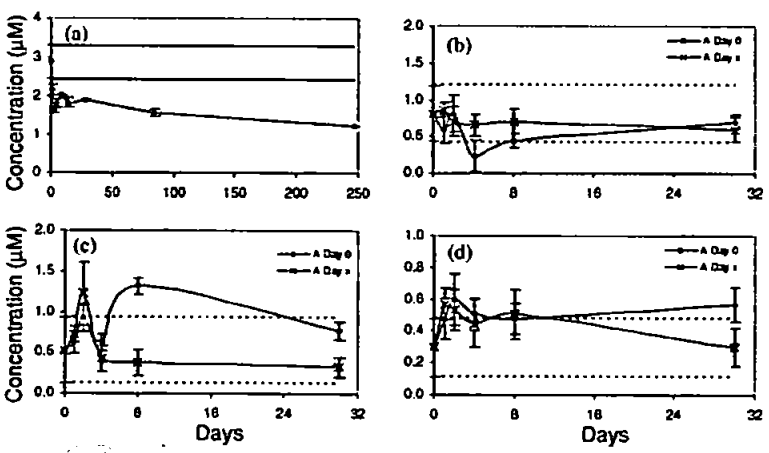

Fig. 2. Changes in the concentration of phosphorus species in natural water samples stored over time. (a) An immediate sharp decrease in DRP concentration in samples stored at −20 °C, followed by a gradual decrease over 250 days of storage. (b–d) The stability of DOP in natural water samples (salinities 0, 14 and 32, respectively) over 32 days of storage at −20 °C. A day 0 are samples autoclaved on day 0 then stored until analysis, and a day *x* are samples stored without treatment then autoclaved and analysed on day *x*. The dotted lines in each figure represent ±3 s of the measured DRP/DOP concentrations on day 0 (i.e. immediately after collection).

Table 1
Storage protocols for the determination of phosphorus species in environmental matrices (updated from [26] which was adapted from a table by Maher and Woo [75])

Phosphorus species	Matrix	Storage method	Maximum storage time	Comments	Ref.
FRP	Distilled, tap and lake water	Refrigerator (4 °C)	1 day	Polypropylene and polycarbonate containers suitable for storage. Glass containers sorbed phosphorus within 1–6 h	[32]
FRP	Standards added to rain water	Room temperature with $HgCl_2$ (0–50 mg L^{-1})	3 days	$HgCl_2$ interfered with method when ascorbic acid was used as a reducing agent	[33]
FRP	River water	−10, 4, 20 °C with/without thymol (0.01%), KF (0.01%), TBT (0.001%), H_2SO_4 (0.05 M) or $CHCl_3$ (5 mL L^{-1})	14 days	Samples showed no decrease in FRP if chloroform added and samples stored at 4 °C	[34]
FRP, TP	Open ocean water	Frozen (quick and slow), cooled (2 °C) with/without $HgCl_2$ (120 mg L^{-1}), phenol (4 mg L^{-1}) and acid (pH 5)	60 days	No significant change in TP concentration when samples frozen with/without acid	[35]
FRP	Coastal and estuarine waters	−10 °C, slow and quick freezing	365 days	Small change in FRP when samples were frozen. Quick freezing reduced losses	[36]
FRP, TP	Tap, lake and river waters	Room temperature, 4 °C, with the addition of $HgCl_2$ (40 mg L^{-1}), H_2SO_4 (0.05 M), and chloroform	16 days	Chloroform at 4 °C was suitable for only 8 days. No significant decreases in concentration (up to day 16) were shown in samples with $HgCl_2$ stored at 4 °C	[37]
FRP	Sea water	Frozen at −40 °C initially, then stored at −20 °C	147–210 days	FRP concentration decreased in samples stored longer than 4 months	[38]
TP, TDP, FRP and TRP	Lake water	Refrigerator (4 °C)	180 days	No change in TP in samples for up to 6 months	[39]
FRP	Stream water	Frozen at −16 °C	4–8 years	No significant change in FRP concentration	[40]
FRP	Soil leachates	Room temperature (5–19 °C), refrigeration (4 °C) frozen (−20 °C) with/without $HgCl_2$ (40–400 mg L^{-1}) and H_2SO_4	1–2 days	Changes occurred within 2 days for all samples with smallest changes in samples stored at room temperature or 4 °C	[41]
FRP	Sea water	Pasteurization and stored at room temperature	18 months	FRP remained constant for 1 year. NH_4 losses after 3 days	[42]
FRP, TP	Stream water	Refrigerator (4 °C), H_2SO_4 (0.05 M), freezing with dry ice and subsequent analysis	8 days	Minimal change observed in highly concentrated (FRP > 1 mg L^{-1}) samples (1–3% loss after 8 days). 47% loss in FRP in lower concentrated samples	[43]
FRP	River water (chalk-based catchment), estuarine water (salinities of 0.5, 10 and 35)	Refrigerator (4 °C) with/without 0.1% (v/v) chloroform, −20 °C with/without 0.1% (v/v) chloroform, −80 °C without chloroform	247 days	For chalk-based samples, 4 °C with 0.1% (v/v) chloroform was the best treatment. Freezing is not recommended due to coprecipitation of inorganic phosphate with calcite	[26]
TP	River and canal water	Room temperature, refrigerator (4 °C) treatment to a pH of < 2 with H_2SO_4	28 days	No significant losses in TP concentration over the 28 day period for treated samples at 4 °C. No losses up to 7 days for room temperature (acidified) samples	[44]
FRP	Water extracts of poultry litter	Room temperature, freezing (−16 to −15 °C)	8 days	No significant losses in FRP concentration in samples stored at room temperature (up to 8 days). Freezing samples lowered concentration (up to 46%) for the 8 day period	[45]

samples for the determination of total and dissolved organic phosphorus has also been recommended by other workers [39,52–53].

3. Soils

Soil pre-treatment and storage can induce marked changes in the solubility of chemicals and therefore presents a critical control on subsequent analysis. This section focuses on phosphorus but it also has wider relevance for other elements. For example, water-extractable phosphorus is markedly influenced by even mild drying of soil. It has been known for some time that soil drying can render considerable concentrations of organic carbon soluble in water [54] and a similar effect was recently reported for phosphorus in a wide range of pasture soils from England and Wales [55]. In the latter study, 7 days air drying from approximate field moisture capacity at 30 °C increased concentrations of water-extractable organic phosphorus by up to 1900%. Organic phosphorus accounted for up to 100% of the solubilized phosphorus. This was at least partly derived from microbial cells, because a strong correlation existed between solubilized organic phosphorus and microbial phosphorus (Fig. 3). It has been reported that rapid rehydration can kill between 17 and 58% of soil microbes through osmotic shock and cell rupture [56] and the contribution of microbial lysis has been subsequently confirmed by direct bacterial cell counting in rewetted Australian pasture soils [57].

In addition to microbial lysis, the physical stresses induced by soil drying also disrupt organic matter coatings on clay and mineral surfaces [58], which may contribute to the solubilisation of both inorganic and organic phosphorus. Indeed, functional classification of water-extractable organic phosphorus from dry Australian pasture soils revealed similar proportions of microbially derived phosphate diesters and phytic acid from the non-biomass soil organic matter [59]. A similar mechanism probably occurs following freezing and thawing [60]. Such processes probably explain the increases in phosphorus extractable in bicarbonate following soil drying [61] because the high ionic strength of bicarbonate solution may reduce the degree of osmotic stress and associated lysis of viable cells compared to extraction with water [62]. The hypothesis that non-biomass organic phosphorus dominates in bicarbonate extracts is supported by the speciation of phosphorus in such extracts, which is dominated by phosphate monoesters and is, therefore, similar to the whole-soil organic phosphorus extracted in strong alkaline solution [63,64].

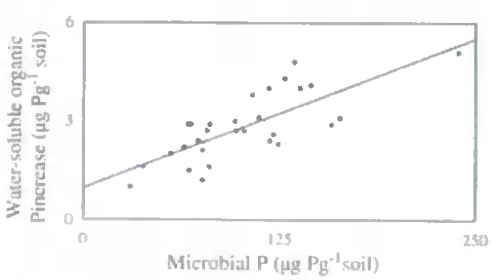

Fig. 3. The increase in water-soluble organic phosphorus after soil drying as a function of soil microbial phosphorus in a wide range of permanent pasture soils from England and Wales. Water-soluble phosphorus was determined by extracting soils at field moisture capacity with water in a 4:1 water:soil ratio for 1 h. Sub-samples were air-dried for 7 days at 30 °C and extracted in an identical manner. Adapted from [57].

The mechanisms by which soil drying could affect the solubility of non-biomass inorganic and organic phosphorus are poorly understood, but probably include both physical and chemical changes. Rapid rehydration of dry soils commonly causes aggregate breakdown [65], which increases the surface area for desorption by exposing surfaces and associated phosphorus protected within aggregates [66]. Such a process has been linked to increases in resin-extractable inorganic phosphorus following soil drying [67]. A more likely process is disruption of organic matter coatings on clay and mineral surfaces by the physical stresses induced during soil drying. This increases organic matter solubility and exposes formerly protected mineral surfaces, and has been attributed to increases in oxalate-extractable silica of up to 200% following drying of Swedish spodic B horizons [68]. Soil drying also increases the crystallinity of pure iron and aluminium oxides, which reduces the specific surface area and phosphorus sorption capacity of these minerals [69]. However, this is inconsistent with reports of increased sorption capacity of dried soils for phosphate and sulphate [70,71].

The effect of drying on phosphorus solubility does not appear to be consistent for all soils. In particular, phosphorus solubility in high organic matter soils may decrease following drying. For example, Schlichting and Leinweber [72] reported that phosphorus recovery from a German peat (pH 5.6) by a sequential fractionation procedure was markedly reduced by pre-treatment, including air-drying, freezing and lyophilization. The greatest reduction in phosphorus recovery followed lyophilization (phosphorus recovery was 75% when extracted fresh, compared with <50% from lyophilized samples) and even after storage at 4 °C for 3 weeks detectable changes were still observed.

The importance of specific artefacts that result from particular pre-treatments will vary depending on the study objectives. For example, assessment of plant-available phosphorus for fertilizer requirements is based on analysis of air-dried soils for practical reasons although field-fresh soils are needed to obtain meaningful data. This is impractical for most purposes, although refrigeration may be an acceptable alternative [58]. In this respect, there is a clear requirement for a detailed study of changes in phosphorus solubility during cold storage for several different soil types. Environmental soil phosphorus tests that involve water extraction routinely use air-dried soils and only measure inorganic phosphorus (e.g. [73,74]). The results of these tests will clearly vary depending on the moisture status of the soil prior to extraction and on the inclusion (or not) of organic phosphorus. If organic phosphorus is included in such tests, the standardization of

soil moisture prior to extraction will be necessary. For details of extraction procedures for soil organic phosphorus see Turner et al. (this issue).

4. Digestion techniques

Digestion techniques for environmental samples are necessary for the determination of total phosphorus (TP) and total dissolved phosphorus (TDP). This is because many of the phosphorus species present contain P–O–P, C–O–P and C–P bonds that need to be broken down to release phosphorus as phosphate, which can then be determined using molybdenum blue chemistry [4]. The digestion technique must also be able to release phosphorus from biological material, e.g. algal cells and plant detritus and adsorbed/occluded P from sediments [75]. Traditional methods of digestion for natural water samples include fusion, dry ashing, perchloric acid, sulphuric acid–nitric acid and boiling on a hot plate, with more recent methods generally using autoclaving, UV photo-oxidation and microwave heating [75]. UV photo-oxidation can be used for organic phosphorus compounds in marine and freshwaters [47,76,77] but condensed polyphosphates present in the sample will not be broken down by UV photo-oxidation alone [2,3,78,79] and also need to be heated to 90–120 °C in the presence of acid [75]. To ensure that all polyphosphates present in the sample are decomposed, either boiling with HCl or potassium peroxydisulfate after UV irradiation is therefore recommended [80]. McKelvie et al. used an on-line UV photo-oxidation flow injection (FI) technique and found that results were comparable with a batch peroxydisulfate method [81].

Autoclaving methods are generally straightforward, give reproducible results and use sealed vessels that are less prone to contamination [75,82–84]. The following section is therefore a summary of different autoclaving techniques, combined with peroxydisulfate in either an acidic or alkaline media, for the determination of phosphorus in natural waters, soil solutions and sediments (see Table 2). Most methods described in Table 2 are based on spectrophotometric detection but ICP-MS and ICP-AES have, in recent years, been used to determine phosphorus in agricultural runoff waters and soils and results were comparable with spectrophotometric methods [128,129]. In addition, microwave digestion combined with ICP-MS detection has been used to determine phosphorus in marine environmental samples and plant leaves with good recoveries [130–132]. However microwave heating for batch sample digestion and in FI systems with spectrophotometric detection for on-line TDP and TP digestion [3] is less widely used than UV photo-oxidation or autoclaving.

4.1. Autoclaving

4.1.1. Alkaline peroxydisulfate

Menzel and Corwin first used autoclaving with peroxydisulfate in 1965 for the digestion of seawater samples [88]. Koroleff developed an alkaline peroxydisulfate alternative in 1969 [102], which was then slightly modified [101] and simplified by introducing a borate buffer [85]. This enabled the simultaneous determination of TP and total nitrogen (TN), as nitrogen bonds are only hydrolysed/oxidised in alkaline media [98]. Using a borate buffer, the pH is alkaline (ca. 9.7) at the start of the digestion process and becomes acidic (pH 4–5) as the sodium hydroxide decomposes [78,90,98]. Hosomi and Sudo also reported that pH change was important and in their method the pH decreased from 12.8 to 2.0–2.1 to ensure that even condensed polyphosphates were digested [92].

The alkaline method has also been used for particulate material but with relatively poor recoveries [133]. For example orchard leaves gave recoveries of 80–90% for TP and TN [91]. Higher recoveries can be obtained by decreasing the ratio of sample to peroxydisulfate [92]. Alkaline digestion of model phosphorus compounds has been found to be efficient for turbid water samples [125–127] although the concentration of suspended particulate material needs to be diluted to $<150\ mg\ L^{-1}$ and difficulties can arise when this material is of soil origin rather than biological origin, e.g. algal cells and plant detritus. The alkaline method has therefore been used to determine TP in turbid lake waters and suspensions of particulate material [127].

Alkaline peroxydisulfate autoclaving, rather than acid peroxydisulfate, is recommended for the digestion of marine waters. This is because in the acid method, peroxydisulfate oxidises the chloride in seawater to free chlorine, thus reducing the oxidising power of the peroxydisulfate [104]. It is also recommended for the simultaneous determination of TP and TN.

4.1.2. Acid peroxydisulfate

An acid peroxydisulfate method developed by Gales et al. [134] has been adopted by the US Environmental Protection Agency [135]. Eisenreich et al. simplified the method [96] and various modifications of this approach are now used to digest different types of samples such as soil solutions, natural waters and river water [18,97,121]. The alkaline peroxydisulfate method for soil extracts is only appropriate if the total organic carbon concentration is $<100\ mg\ L^{-1}$ and manganese is $<1\ mg\ L^{-1}$. Above this manganese concentration, coloured solutions or precipitates are formed, which interfere with the digestion step [111]. This interference is avoided when using acid peroxydisulfate and solutions are colourless after digestion [84].

Pote et al. described standard methods for the determination of TP and TDP using sulphuric acid–nitric acid and peroxydisulfate digestions [136] and recommended the use of sulphuric acid–nitric acid digestion to achieve good recoveries for most samples. However this digestion method can be potentially dangerous if salts precipitate during digestion [89] and is less easy to control than the peroxydisulfate method [84,122]. Rowland and Haygarth compared a mild peroxydisulfate method to the more rigorous sulphuric acid–nitric

Table 2
Acidic and alkaline peroxydisulfate autoclave digestion methods

Matrix	Digestion reactant	Digestion time	Digestion temperature (°C)	pH	Model compounds[a]	Comments	Ref.
Drainage waters	Digestion reagent: 5 g $K_2S_2O_8$ and 5 mL 4.5 M H_2SO_4 in 100 mL distilled deionised water. 4 mL reagent added to 50 mL sample	30 min	115	Not reported	Not reported	Same method as [85]	[86]
Drainage waters	0.15 g $K_2S_2O_8$ and 1 mL 0.5 M H_2SO_4 added to 20 mL sample	1 h	120	Not reported	Not reported	Same method as [84]	[87]
Estuarine waters	8 mL of 5% $K_2S_2O_8$ added to 50 mL seawater	1 h	120	Final pH 1.5–1.8	Orthophosphate, phenylphosphoric acid, phenylphosphorous acid	Same method as [88], but autoclaving time was increased from 30 min to 1 h. Quantitative recovery for model compounds at the 50 μg P level	[89]
Fresh and seawater	Acidic peroxydisulfate digestion reagent: 5 g $K_2S_2O_8$ and 5 mL 4.5 M H_2SO_4 in 100 mL distilled deionised water. 4 mL reagent added to 50 mL sample. Alkaline peroxydisulfate digestion reagent: 5 g $K_2S_2O_8$ and 3 g H_3BO_3 in 100 mL 0.375 M NaOH. 5 mL reagent added to 50 mL sample	30 min	115	For alkaline method, initial pH ca. 9.7, final pH 4–5	Model compounds added to demineralised water and seawater:2-AEP (108, 77, 108, 88%), PTA (100, 70, 101, 95%), 5′-GMP-Na_2 (99, 93, 100, 94%), PC (98, 37, 99, 96%), FMN (99, 99, 100, 97%), G-6-P-Na (100, 95, 101, 92%), AMP (99, 94, 100, 93%), RP (100, 94, 103, 95%), PEP-3CHA (100, 100, 101, 101%), β-GLY (99, 100, 100, 96%)	Recoveries in parentheses are in the order: acidic demineralised water, acidic seawater, alkaline demineralised water, alkaline seawater. Acidic and alkaline peroxydisulfate methods [85] compared to continuous flow UV irradiation and high temperature combustion. Alkaline peroxydisulfate method recommended for marine waters	[90]
Fresh waters	Digestion reagent: 40 g $K_2S_2O_8$ and 9 g NaOH in 1 L distilled water. 5 mL reagent added to 10 mL sample	1 h	120	Initial pH 12.8, final pH 2.0–2.1	National Bureau of Standard Reference Material 1571 orchard leaves (98%), National Institute of Environmental Studies (NIES) Reference Material No. 1 pepper bush (96%), NIES Reference Material No. 2 pond sediment (100%), NIES Reference Material No. 3 chlorella (100%) all of concentration 50 mg L^{-1}. Model compounds:5′-ATP-Na_2 (99–100%), 5′-ADP-Na_2 (98%), TSPP (99–100%), SHMP (94–97%), STP (96–97%), G-6-P-K_2 (99–102%)	Analysed for TN and TP. Obtained higher recoveries for orchard leaves than [91]	[92]
Fresh waters	1 g $K_2S_2O_8$ and sufficient H_2SO_4 to make the sample 0.15 M acid	2 h	120	Not reported	Not reported		[93]
Lake waters	'Strong' acid: 25 mL 18 M H_2SO_4 and 1 mL 18 M HNO_3 in 1 L deionised water. 1 mL 'strong' acid and 2.5 mL aqueous 4% (w/v) $K_2S_2O_8$ added to 25 mL sample	30 min	Not reported, however in the UV digestion, sample maintained at 85 °C in the silica coil	Not reported	Dipotassium hydrogenphosphate (100%), STP (100%), AMP (100%)	Compared UV digestion to autoclaving. Recoveries for lake water samples were 100% for the peroxydisulfate digestion and 97% for the UV digestion	[94]

Table 2 (*Continued*)

Matrix	Digestion reactant	Digestion time	Digestion temperature (°C)	pH	Model compounds[a]	Comments	Ref.
Lake, river and pond waters, raw sewage	Digestion reagent: 55 mL H_2SO_4 and 60 g $K_2S_2O_8$ in 1 L solution. 2.5 mL reagent added to 35 mL sample	1 h	Not reported	Not reported	G-1-P-K_2 (97.5%), G-6-P-K_2 (105%), DNA (sodium salt) (115%), AMP (95%), 5′-ADP-Na_2 (102.5%), SOP (100%), β-GLY (107.5%), TSPP (62.5%), STP (110%), SHMP (100%), disodium hydrogen orthophosphate (97.5%)	Autoclave method was compared to the hot-plate $H_2SO_4/K_2S_2O_8$ digestion. Autoclave method gave more precise values for model compounds than the hot plate procedure	[95]
Natural waters	Digestion reagent: 0.15 g $K_2S_2O_8$ and 1 mL 0.5 M H_2SO_4. 1 mL reagent added to 20 mL sample	45 min	121 °C	Not reported	G-1-P (101.0%), G-6-P (103.1%), ATP (101.6%), NPP (101.9%), cAMP (101.8%), α-GLY (102.3%), myo-inositol 2-monophosphate (97.4%), PTA (85.6%), 2-AEP (99.2%), TSPP (99.5%), STP (97.7%), trisodium trimetaphosphate (98.8%), KHP (99.1%)	Method modified from [96]	[97]
Natural waters	Acidic peroxydisulfate digestion reagent: 5 g $K_2S_2O_8$ and 5 mL 4.5 M H_2SO_4 in 100 mL distilled deionised water. 0.8 mL digestion reagent added to 10 mL sample. Alkaline peroxydisulfate digestion reagent: 50 g $K_2S_2O_8$, 30 g H_3BO_3 and 350 mL NaOH in 1 L distilled deionised water. 1.3 mL digestion reagent added to 10 mL sample	30 min	120 °C	For alkaline method, initial pH ca. 9.7, final pH 4-5	NPP, α-GLY, G-6-P, tripolyphosphate, trimetaphosphate, ATP, 5′-GDP, 2-AEP. Recoveries shown in a figure, so precise values cannot be given. In general, recoveries ca. >58% for acidic method and ca. >26% for alkaline method	Compared acidic peroxydisulfate [85] and alkaline peroxydisulfate [98] autoclaving methods with magnesium nitrate high-temperature oxidation, magnesium peroxydisulfate high-temperature oxidation, and UV oxidation. Magnesium nitrate high-temperature oxidation was found to be the best method	[78]
Orchard leaves and aufwuchs	Digestion reagent: 13.4 g $K_2S_2O_8$ and 6 g NaOH in 1 L to give 200 mg peroxydisulfate per 15 mL aliquot. Other levels of peroxydisulfate also used (300, 400 and 500 mg)	1 h	100–110	Initial pH 12.00 for orchard leaf samples, final pH 2.5. Initial pH 12.8 for auchwuchs samples, final pH 3.7	National Bureau of Standards reference material 1571 (orchard leaf) (86.9–88.7% using 500 mg peroxydisulfate), and aufwuchs (93.6% using 300 mg peroxydisulfate, and 101.4% using 400 mg peroxydisulfate)	Analysed for TN and TP. Maximum recovery for orchard leaf when 500 mg peroxydisulfate was used, and 300 or 400 mg peroxydisulfate for aufwuchs	[91]
Pond water	Acidic peroxydisulfate digestion: 0.5 g $K_2S_2O_8$ and 1 mL H_2SO_4 solution (300 mL conc. H_2SO_4 in 1 L distilled water) added to 50 mL sample. Alkaline peroxydisulfate digestion: 5 mL 0.075 N NaOH and 0.1 mg $K_2S_2O_8$ added to 10 mL sample. After digestion, 1 mL borate buffer (61.8 g H_3BO_3 and 8 g NaOH in 1 L distilled water) added	30 min	110	Not reported	Water samples spiked with 0.2 mg L^{-1} KHP. Recoveries for acidic method were 88–113%, and for the alkaline method 85–112%	Acidic and alkaline peroxydisulfate methods same as [99]	[100]

Table 2 (*Continued*)

Matrix	Digestion reactant	Digestion time	Digestion temperature (°C)	pH	Model compounds[a]	Comments	Ref.
River water	Digestion reagent: 0.15 g $K_2S_2O_8$ and 1 mL 0.5 M H_2SO_4. 1 mL added to 20 mL sample	45 min	121 °C	Not reported	Not reported	Method modified from [96]	[18]
River water	Digestion reagent: 20 g $K_2S_2O_8$ and 3 g NaOH in 1 L distilled deionised water. 5 mL reagent added to 5 mL sample	30 min	120°C	Initial pH 12.57, final pH 2.0	KHP (99.6%), TSPP (97.2%), STP (99.2%), β-GLY (96.5%), SHMP (97.6%), G-1-P (99.5%), AMP (100.8%), ADP (98.9%), ATP (98.1%)	Results from this method were an improvement on the alkaline oxidation method for TN and TP of [101], which was in turn a modified method from [102]	[103]
Seawater	Two concentrations of $K_2S_2O_8$ added (4 and 40 mg mL^{-1}) to 10 mL sample acidified with sulphuric acid to pH 3	90 min	125	pH 3	Not reported	Three methods compared: autoclaving (acidic peroxydisulfate method based on [85]), UV irradiation and sequential use of both. The latter method gave the best recoveries	[104]
Seawater	8 mL of 5% $K_2S_2O_8$ added to 50 mL seawater	30 min	120	Final pH 1.5–1.8	PFA (96.5%), 1-AEP (85.5%), 2-AEP (81.2%)	Compared their nitrate oxidation method with peroxydisulfate oxidation method from [88]	[105]
Seawater	Digestion reagent: 50g $K_2S_2O_8$, 30 g H_3BO_3, 350 mL 1 M NaOH in 1 L deionised water. 4 mL reagent added to 30 mL sample	30 min	110–115	Initial pH 9.7, final pH 5–6	KHP (0.25–7 μM)	Alkaline peroxydisulfate method for TP and TN based on [85]	[98]
Seawater	8 mL of 5% $K_2S_2O_8$ added to 50 mL seawater	30 min	120	Final pH 1.5–1.8	lecithin (101%), PC (98%), AMP (99%), zooplankton (100%)	Recoveries of model compounds relative to sulphuric acid-hydrogen peroxide digestion [106]	[88]
Sediments and soils	1 mL 5.5 M H_2SO_4, 0.4 g $K_2S_2O_8$ and 1 mL distilled deionised water added to 10–50 mg sample	1 h	130	Not reported	Not reported	Acid peroxydisulfate digestion compared to perchloric acid digestion	[107]
Sewage	Digestion reagent: 9 g NaOH and 40 g $K_2S_2O_8$ in 1 L distilled deionised water. 2 mL digestion reagent added to 10 mL sample	90 min	120	Not reported, however KCl/acetate buffer pH 4.5	Sodium dihydrogen phosphate (93% using 0.15 M KCl/acetate), STP (85% using 0.4 M KCl/acetate), TSPP (96% using 0.4 M KCl/acetate)	Anion exchange chromatography used to separate ortho- and poly-phosphates using either 0.15 or 0.4 M KCl/acetate as the eluting buffer. No polyphosphates detected in raw sewage samples	[108]
Soil extracts	Digestion reagent: 0.39 M $K_2S_2O_8$ and 0.6 M NaOH. 2 mL reagent added to 8 mL sample	1 h	120	Not reported	Not reported	Same method (La Chat method 30-115-001-1-B) as [109]	[110]
Soil extracts	Digestion reagent: 13.4 g $K_2S_2O_8$ dissolved in 1 L 0.3 M NaOH. 15 mL reagent added to 10 mL sample. Added 1.5 mL 0.3 M HCl and made up to 50 mL after autoclaving	30 min	110	pH 2	KHP, PTA dodeca sodium salt (99% for 0.1 mg L^{-1}, and 106% for 1.0 mg L^{-1})	Analysed for TN and TP. PTA dissolved in different extractants: water, 0.1 M $CaCl_2$, and 0.2 M H_2SO_4, and recoveries were comparable. Alkaline peroxydisulfate method appropriate for soil extracts when concentration of total organic carbon <100 mg L^{-1}	[111]

Table 2 (*Continued*)

Matrix	Digestion reactant	Digestion time	Digestion temperature (°C)	pH	Model compounds[a]	Comments	Ref.
Soil leachate	0.15 g $K_2S_2O_8$ and 1 mL 0.5 M H_2SO_4 added to 20 mL sample	1 h	120	Not reported	Not reported	Same method as [84]	[112–116]
Soil leachate	8 mg $K_2S_2O_8$ and 50 μL 0.5 M H_2SO_4 added to 1 mL sample	1 h	120	Not reported	KHP (101%), PTA (76%), TSPP (95%), STP, 1-AEP (86%), G-6-P-Na (84%), 5′-ATP-Na_2 (69%)	Preconcentration and separation method for trace P compounds using a scaled down version of [84]	[117]
Soil solutions	Digestion reagent: 0.05 M H_2SO_4 and 16 g L^{-1} $K_2S_2O_8$. 1 mL reagent added to 1 mL sample	30 min	110	Not reported	Not reported		[118]
Soil solutions	Digestion reagent: 50 mg $K_2S_2O_8$ and 0.1 mL 5.5 M H_2SO_4 added to 1 mL sample. After digestion, solutions diluted to 10 mL with deionised water	1 h	120	Not reported	KHP, PTA (93.2–95.0% in concentration range 3.23–32.26 μM)	Acid peroxydisulfate digestion compared to sulphuric–perchloric acid, nitric acid, and nitric–perchloric acid digestion. Better recoveries were found for PTA using sulphuric-perchloric acid and acid peroxydisulfate digestion methods	[119]
Soil solutions	Digestion reagent: 13.4 g $K_2S_2O_8$ dissolved in 1 L 0.3 M NaOH. 15 mL reagent added to 10 mL sample. Added 1.5 mL 0.3 M HCl and made up to 50 mL after autoclaving	30 min	110	pH 2	Not reported	Same method as [111]	[120]
Soil solutions	0.15 g $K_2S_2O_8$ and 1 mL 0.5 M H_2SO_4 added to 20 mL sample	45 min	121	Not reported	Not reported	Method modified from [96]	[121]
Soil solutions	0.15 g $K_2S_2O_8$ and 1 mL 0.5 M H_2SO_4 added to 20 mL sample	1 h	120	Not reported	PTA (89%), G-6-P-Na (89%), tetra-potassium pyrophosphate (102%), 5′-ATP-Na_2 (96%), AMP (96%), KHP	Acidic method compared to peroxide-Kjeldahl, and nitric acid-sulphuric acid digestions [122]. Acidic peroxydisulfate method found to be the best method	[84]
Surface runoff	0.5 g $K_2S_2O_8$ and 1 mL H_2SO_4 solution (300 mL conc. H_2SO_4 in 1 L distilled water) added to 50 mL sample	30 min	110	Not reported	Not reported	Same method as peroxydisulfate method in [99]	[123]
Surface runoff	$K_2S_2O_8$ and H_2SO_4	30 min	120	Not reported	Not reported		[124]
Turbid lake and river waters	Optimum digestion reagent: 0.27 M $K_2S_2O_8$ and 0.24 M NaOH. 2 mL reagent added to 10 mL sample	1 h	120	Final pH 2	NIES No 3 Chlorella (99–101% up to 100 μg P L^{-1}) and No 2 Pond sediment (98–104% up to 60 μg P L^{-1}, and 88% at 100 μg P L^{-1}). Model compounds added to distilled and lake water: KHP, G-6-P (113%), PTA (101%), α-GLY (108%), PEP (103%), 2-AEP (104%), PFA (106%), *o*-phosphonyl ethanolamine (109%), SHMP (114%), aluminium phosphate (23%)	Compared alkaline peroxydisulfate autoclaving method to microwave and hot-plate digestion and Kjeldahl digestion for TN and TP. Results showed that all methods used were suitable for turbid lake samples when suspended material is of biological origin	[125]

Table 2 (*Continued*)

Matrix	Digestion reactant	Digestion time	Digestion temperature (°C)	pH	Model compounds[a]	Comments	Ref.
Turbid lake and river waters	Optimum digestion reagent: 0.27 M $K_2S_2O_8$ and 0.24 M NaOH. 2 mL reagent added to 10 mL sample	1 h	120 °C	Final pH 2	NIES No 3 Chlorella (99–101% up to 100 μg P L^{-1}) and No 2 Pond sediment (98–104% up to 60 μg P L^{-1}, and 88% at 100 μg P L^{-1}). Model compounds added to distilled and lake water: KHP (93–99%), PTA (93–106%), 2-AEP (93–101%), α-GLY (94–102%), PFA (93–105%), *O*-phosphonylethanol (91–106%), PEP (93–117%)	Compared alkaline peroxydisulfate autoclave method to microwave digestion, and similar results were found	[126]
Turbid lake waters	Digestion reagent: 9 g NaOH, and 40 g $K_2S_2O_8$ in 1 L water. 2 mL reagent added to 10 mL sample	1 h	120 °C	Not reported	NIES No. 3 Chlorella (94–107% up to 100 μg P L^{-1}, and 90% at 250 μg P L^{-1}) and No 2 Pond sediment (92–109% up to 100 μg P L^{-1}, and 88% at 250 μg P L^{-1}). Model compounds added to lake water: KHP (99%), STP (96%), AMP (94%), β-GLY (103%)	Compared alkaline peroxydisulfate method to nitric acid–sulphuric acid digestion method [99]. Results showed no significant difference between the two methods	[127]
Water (overland flow)	Digestion reagent: 0.39 M $K_2S_2O_8$ and 0.6 M NaOH. 2 mL reagent added to 8 mL sample	1 h	120 °C	Not reported	Not reported		[109]

[a] With recoveries given in parentheses when reported.

acid method [122] for soil solutions and leachates. The latter method gave erratic recoveries and was more prone to contamination due to the open digestion vessels used [84]. Peroxydisulfate autoclaving is also safer than perchloric acid digestion [107,137]. The acid peroxydisulfate method generally gives good recoveries for model compounds and is simple and easy to use and is therefore recommended for TP and TDP determinations in natural waters and, particularly, soil solutions.

4.2. Model compounds

It is advisable to test the efficiency of any digestion method using a range of model phosphorus containing compounds that reflect different chemical bonds and stabilities and are representative of naturally occurring compounds (see Table 3). The majority of relevant compounds contain C–O–P and/or P–O–P bonds. Few compounds reported in the literature contain C–P bonds, which are very resistant to oxidation and hydrolysis [138].

Phosphonates are refractory organic phosphorus compounds and can be released into seawater from biological sources [78,90,139], and have been detected in soils [140] and soil leachate [117]. As phosphonates contain a strong C–P bond that is resistant to acid hydrolysis [139], they are useful compounds for recovery studies [78,90,97,125,126,139]. Condensed inorganic (e.g. sodium tripolyphosphate) and organic (e.g. adenosine-5′-triphosphate) phosphates and cocarboxylase [141] have also been shown to be resistant to UV irradiation alone [79]. With acid or alkaline peroxydisulfate autoclaving, however, these compounds have been successfully broken down [97,103,125,126].

Inositol phosphates are an important class of naturally occurring organic phosphorus compounds [142]. Phytic acid, for example, is one of the more resistant compounds to hydrolysis and is also one of the most refractory organic phosphorus compounds found in soils [75,119,141]. Other organic phosphorus compounds found in soil leachate and runoff are the sugar phosphorus compounds, e.g. D-glucose-1-phosphate and D-glucose-6-phosphate, which are labile [117]. Organic condensed phosphates, e.g. adenosine-5′-triphosphate and adenosine-5′-diphosphate are also important as they originate from all living systems, e.g. algae, bacteria, fungi, insects, plant and animal tissues [117].

It is therefore recommended that model compounds selected for digestion studies should include one with a P–O–P bond (e.g. sodium tripolyphosphate), a refractory C–O–P compound (e.g. phytic acid), a labile C–O–P compound (e.g. D-glucose-1-phosphate or D-glucose-6-phosphate), a refractory C–P compound (e.g. 2-aminoethylphosphonate), and a compound containing C–O–P and P–O–P bonds (e.g. adenosine-5′-triphosphate). Orthophosphate (e.g. as potassium dihydrogen orthophosphate) should also be used in all recovery studies as a method control [90]. One should also be aware that specific matrices may require additional model compounds. For example, acid soils and sediments may well contain phosphorus associated with iron or alu-

Table 3
Model compounds used in autoclave based digestion methods

Model compound	Synonyms	Abbreviation used in text	Chemical formula	Structural formula
Adenosine-5′-monophosphate	Adenosine-5′-monophosphoric acid; 5-adenylic acid; adenosine phosphate; tert-adenylic acid; ergadenylic acid	AMP	$C_{10}H_{14}N_5O_7P$	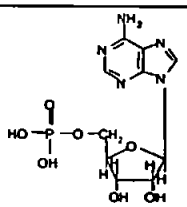
Adenosine-3′,5′-cyclic monophosphate	Adenosine-3′,5′-cyclophosphoric acid; cyclic AMP; 3′,5′-cyclic AMP	cAMP	$C_{10}H_{12}N_5O_6P$	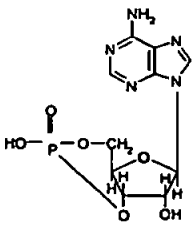
Adenosine-diphosphate		ADP	$C_{10}H_{15}N_5O_{10}P_2$	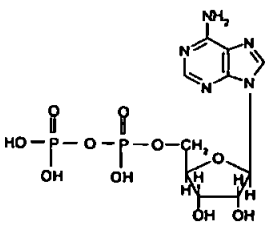
adenosine-5′-diphosphate (sodium salt)		5′-ADP-Na_2	$C_{10}H_{13}N_5O_{10}P_2Na_2$	Similar to ADP
Adenosine-5′-triphosphate		ATP	$C_{10}H_{16}N_5O_{13}P_3$	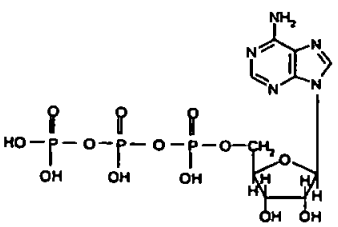
Adenosine triphosphate disodium	Adenosine 5′-(tetrahydrogen triphosphate) disodium salt; adenosine 5′-triphosphate, disodium salt; adenosine 5′-triphosphate, disodium salt hydrate	5′-ATP-Na_2	$C_{10}H_{14}N_5O_{13}P_3Na_2$	Similar to ATP
1-Aminoethylphosphonate	1-Aminoethylphosphonic acid	1-AEP	$C_2H_8NO_3P$	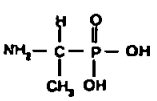
2-Aminoethylphosphonate	2-Aminoethylphosphonic acid	2-AEP	$C_2H_8NO_3P$	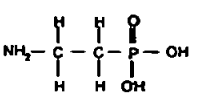
Glucose-1-phosphate	Glucose-1-phosphoric acid	G-1-P	$C_6H_{13}O_9P$	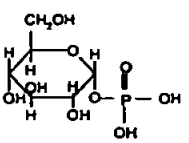

Table 3 (*Continued*)

Model compound	Synonyms	Abbreviation used in text	Chemical formula	Structural formula
Glucose-1-phosphate dipotassium salt	Glucose-1-phosphoric acid (dipotassium salt)	G-1-P-K_2	$C_6H_{11}O_9PK_2$	Similar to G-1-P
Glucose-6-phosphate	Glucose-6-phosphoric acid	G-6-P	$C_6H_{13}O_9P$	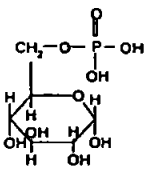
Glucose-6-phosphoric acid (dipotassium salt)	α-D-Glucose-6-phosphoric acid dipotassium salt	G-6-P-K_2	$C_6H_{11}O_9PK_2$	Similar to G-6-P
Glucose-6'-phosphate sodium salt		G-6-P-Na	$C_6H_{12}O_9PNa$	Similar to G-6-P
DL-α-Glycerophosphate disodium salt	rac-Glycerol 1-phosphate disodium salt; DL-α-glycerophosphate	α-GLY	$C_3H_7O_6PNa_2$	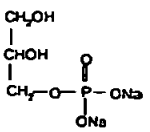
β-Glycerophosphate disodium salt hydrate	Glycerol 2-phosphate disodium salt hydrate; sodium β-glycerophosphate	β-GLY	$C_3H_7O_6PNa_2$	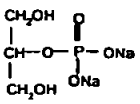
Guanosine 5'-diphosphate		5'-GDP	$C_{10}H_{15}N_5O_{11}P_2$	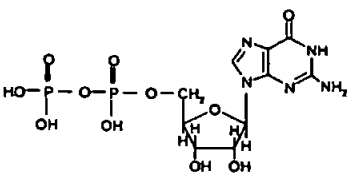
Guanosine-5'-monophosphate disodium hydrate		5'-GMP-Na_2	$C_{10}H_{12}N_5O_8PNa_2$	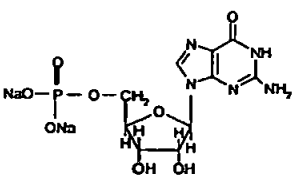
4-Nitrophenyl phosphate	*p*-Nitrophenyl phosphate	NPP	$C_6H_4NO_6PNa_2$	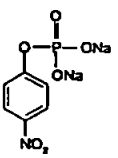
Phospho(enol) pyruvate		PEP	$C_3H_5O_6P$	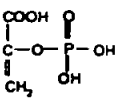
phosphoenolpyruvic acid tri(cyclohexylamine) salt		PEP-3CHA	$C_3H_2O_6P(C_6H_{11}NH_3)_3$	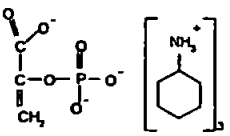
Phosphonoformate	Phosphonoformic acid	PFA	CH_3O_5P	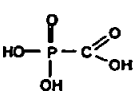

Table 3 (*Continued*)

Model compound	Synonyms	Abbreviation used in text	Chemical formula	Structural formula
Phosphoryl choline chloride calcium salt tetrahydrate	Phosphocholine chloride calcium salt tetrahydrate; calcium phosphorylcholine chloride	PC	$C_5H_{13}NO_4PCaCl{\cdot}4H_2O$	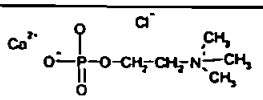
Phosphoserine		SOP	$C_3H_8NO_6P$	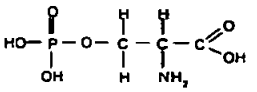
Phytic acid	Myo-inositol hexakis (dihydrogen phosphate); inositol hexaphosphoric acid	PTA	$C_6H_{18}O_{24}P_6$	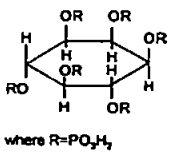 where R=PO_3H_2
Riboflavine-5′-monophosphate sodium salt	Riboflavin 5′-phosphate; FMN-Na	FMN	$C_{17}H_{20}N_4O_9PNa$	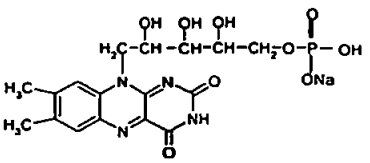
Ribose-5-phosphate disodium salt dihydrate	D-Ribofuranose 5-phosphate	RP	$C_5H_9O_8PNa_2$	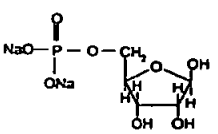
Tetrasodium pyrophosphate	Sodium pyrophosphate; pyrophosphoric acid tetrasodium salt; diphosphoric acid, tetrasodium salt; pyrophosphoric acid, tetrasodium salt	TSPP	$Na_4O_7P_2$	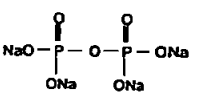
Sodium tripolyphosphate	Pentasodium tripolyphosphate dihydrate; sodium triphosphate; sodium polyphosphate; triphosphoric acid pentasodium anhydrous	STP	$Na_5P_3O_{10}$	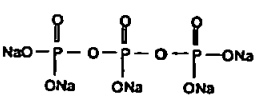
Sodium hexametaphosphate	Sodium metaphosphate; metaphosphoric acid, hexasodium salt; sodium polymetaphosphate	SHMP	$(NaPO_3)_n$	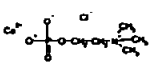

minium phases, which are relatively resistant to oxidative dissolution [75].

4.3. Recovery studies using alkaline and acidic peroxydisulfate autoclaving

Typical phosphorus recoveries for a range of model compounds, digested using alkaline and acid peroxydisulfate autoclaving, are shown in Fig. 4. The alkaline peroxydisulfate digestion method can be used for the simultaneous determination of TP and TN [85]. This was chosen because the borate buffer ensures that the pH is initially alkaline, to break down nitrogen containing bonds, and becomes acidic during the digestion process to break down phosphorus containing bonds. An amount of 5 mL of digestion reagent (5 g potassium peroxydisulfate and 3 g boric acid dissolved in 100 mL 0.0375 M sodium hydroxide) was added to 50 mL sample. The samples were then autoclaved for 30 min a 121 °C. Model compounds chosen were phytic acid, sodium tripolyphosphate and adenosine-5′-triphosphate, and were therefore representative of a refractory C–O–P compound, a P–O–P compound and a C–O–P and P–O–P bond containing com-

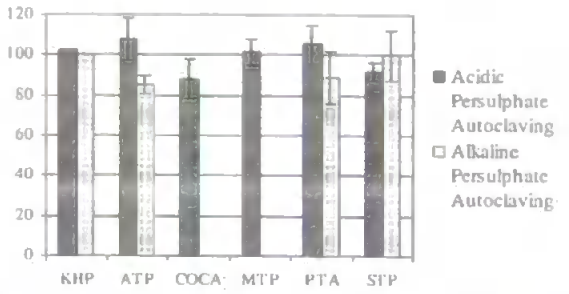

Fig. 4. Comparison of recoveries for a selection of model compounds using acidic and alkaline peroxydisulfate (40 g L^{-1}) autoclave digestions. KHP: potassium dihydrogen orthophosphate; ATP: adenosine-5′-triphosphate; COCA: cocarboxylase; MTP: methyltriphenylphosphonium bromide; PTA: phytic acid; STP: sodium tripolyphosphate. Error bars show ±3 standard deviations.

pound, respectively. Recoveries were 89 ± 13% for phytic acid, 100 ± 13% for sodium tripolyphosphate and 85 ± 4% for adenosine-5′-triphosphate.

The acid peroxydisulfate digestion method used was based on the method of Haygarth et al. [121]. A 1 mL 0.5 M sulphuric acid and 0.15 g potassium peroxydisulfate was added to 20 mL sample, and autoclaved for 45 min at 121 °C. The same compounds were used, plus two additional compounds that were not used in any of the autoclave methods listed in Table 2, but have been used in UV digestion studies, namely cocarboxylase containing C–O–P and P–O–P bonds [141] and methyltriphenylphosphonium bromide containing C–P bonds [143]. Recoveries were relatively low: adenosine-5′-triphosphate (74 ± 7%), cocarboxylase (68 ± 17%), methyltriphenylphosphonium bromide (93 ± 6%), phytic acid (60 ± 32%) and sodium tripolyphosphate (95 ± 4%). When the concentration of peroxydisulfate was increased from 8 to 40 g L^{-1} [81] however recoveries were greatly improved for adenosine-5′-triphosphate (108 ± 11%), cocarboxylase (88 ± 10%), methyltriphenylphosphonium bromide (102 ± 6%), phytic acid (105 ± 10%), and sodium tripolyphosphate (92 ± 5%). Peroxydisulfate concentration is the most important parameter, rather than digestion time or temperature, for improving recoveries, particularly for seawater samples [104].

4.4. Enzymatic degradation

Fig. 1 shows that DOP and total organic phosphorus (TOP) can be determined by difference following complete digestion, e.g. by autoclaving the sample (see Section 4.1). It is however desirable to be able to quantify specific organic compounds. To do this a more selective approach to digestion is required, such as the use of phosphate cleaving enzymes. This section therefore considers the use of acid and alkaline phosphatases and the particular sub-class of phytases.

Phosphatases belong to the class of enzymes called hydrolases [144] and their subclasses are alkaline phosphatase (EC.3.1.3.1) and acid phosphatase (EC.3.1.3.2). They hydrolyse phosphate monoesters to produce an alcohol and orthophosphate. Phosphatases play a key role in metabolic reactions such as the synthesis of organic phosphate compounds (transphosphorylation) and transport across cell membranes [145] and they have been isolated from a variety of sources. Alkaline phosphatase is the most studied phosphomonoesterase and has been isolated from, e.g. *Escherichia coli* [146,147]. Acid phosphatases show broad selectivity towards phosphomonoesters and have also been isolated from *E. coli* [146].

Strickland and Parsons established a classical method using phosphatase for the determination of phosphate [148] but this method was susceptible to product inhibition by reactive phosphate already present in the sample. McKelvie and coworkers immobilised *E. coli* onto CNBr-activated sepharose 4B beads in a FI system with an optimum pH of 8. The recovery of alkaline phosphatase hydrolysable phosphorus was low in natural waters but good in sediments [146]. They also applied alkaline phosphatase to soils [59]. Acid and alkaline phosphatase and phytase have been used in combination to investigate organic phosphorus speciation in soils [149].

Inositol hexaphosphate forms the bulk of extractable soil organic phosphorus [146,149,50]. Phytases (EC 3.1.3.8) are members of the family of histidine acid phosphatases [150,151] that are found in plants and micro-organisms, which catalyse the hydrolysis of phytate (myo-inositol hexakis-phosphate 1, 2, 3, 4, 5, 6) to less phosphorylated myo-inositol phosphates and free orthophosphates. Phytase from plant sources, e.g. wheat, first acts on the C_6 atom while that from microbial sources acts on the C_3 atom. McKelvie et al. [59,152] used a FI system with immobilised phytase for the determination of phytic acid in soils. Adenosine-5′-triphosphate was also hydrolysed but in low yields compared with phytic acid. Phytase has also been applied to the determination of phytic acid in the marine environment, but with low recoveries [152].

Enzymatic methods are important for assessing the potential biological availability of organic phosphorus but other methods are also needed for complete identification and this remains a challenging area of analysis.

5. Quality assurance and quality control

Phosphorus is a key determinand in most environmental monitoring and research programmes [153] and only accurate analytical data permits valid conclusions to be drawn about the phosphorus status of water bodies and soils. In addition to DRP it is also important to obtain accurate total phosphorus (TP) data because this parameter is used for load calculations, e.g. to determine discharges from sewage treatment works [154]. This has important implications regarding decisions on the installation (or not) of costly phosphorus removal technology. Programmes involving multi-national participation and international databanks [76] require adequate quality assurance/quality control (QA/QC) schemes to ensure

the data integrity necessary for the comparison of data from various sources. Adherence to QA guidelines, participation in interlaboratory studies, use of reference materials (RMs) and certified reference materials (CRMs) are all means of achieving good data quality for phosphorus determinations [155].

5.1. Certified reference materials

A CRM is a reference material for which component values have been certified by a technically valid procedure and is accompanied by or traceable to a certificate or other documentation issued by a certifying body [156,157]. The use of CRMs is the most efficient way to measure and control accuracy [158] and can help produce reliable calibration and validation of measurement procedures [159]. CRMs can be either calibration CRMs, which are high purity substances or synthetically prepared mixtures, or matrix-matched CRMs, which can be natural samples or artificial samples simulating the composition of natural samples [158]. Few CRMs are commercially available for the determination of phosphorus species in environmental matrices (see Table 4), despite the need for such materials [155]. CRMs are not currently available for all environmental matrices routinely analysed for phosphorus species, such as estuarine waters, nor do they adequately span the range of phosphorus concentrations characteristic of environmental matrices. The National Research Council of Canada (NRCC) recognized the urgent need for CRMs for nutrients, including orthophosphate, for use in the marine sciences. MOOS-1, a natural seawater CRM available for the determination of nutrients in seawater, was developed in direct response to this need [159]. Analysis of MOOS-1 was carried out in 2002 by 25 expert laboratories participating in the 'NOAA/NRC 2nd intercomparison study for nutrients in seawater' [160]. Laboratories were predominantly selected on the basis of their previous satisfactory performance in a NOAA 2000 intercomparison study [159]. Flow and manual methods were used all based on the spectrophotometric procedures of Strickland and Parsons [148]. Eighteen of the 25 laboratories achieved satisfactory z-scores (see Section 5.2) for the determination of phosphate in seawater as shown in Fig. 5.

5.2. Intercomparison exercises

Inter-laboratory comparison studies are an essential feature of method development and validation [150] and play an important role in the certification of reference materials, such as described for MOOS-1 [159]. Performance in intercomparison studies undertaken by NOAA/NRC in 2000 and 2002 [159,160] was used to assess the capabilities of international laboratories to quantify nutrients in MOOS-1, including orthophosphate. Z-scores [162] have been widely used for the statistical assessment of data in intercomparison exercises to give a comparative indication of performance with $|Z| < 2$ indicating satisfactory performance [160,163–166].

The main objectives of interlaboratory comparison studies are to determine inter-laboratory precision and accuracy and provide an impartial view of in-house quality control procedures. Participation can also identify best practise with respect to method, sample preparation, sample storage and training needs. The QUASIMEME project (Quality Assurance of Information for Marine Environmental Monitoring in Europe), now known as QUASIMEME Laboratory Performance Studies, was established to assist EU labs in developing their QA/QC procedures to satisfy the data quality requirements of monitoring programmes in which they participated such as the International Marine Monitoring Programmes of the Oslo and Paris Commissions (OSPARCOM), the Helsinki Commission (HELCOM) and the MEDPOL programme [163,167]. Initially funded by the EU (1992–1996), the programme still continues by subscription of participating institutes. All institutes, worldwide, involved in chemical measurements in seawater are eligible to participate. The laboratory programmes for proficiency testing of most determinands are conducted twice per year and routinely include

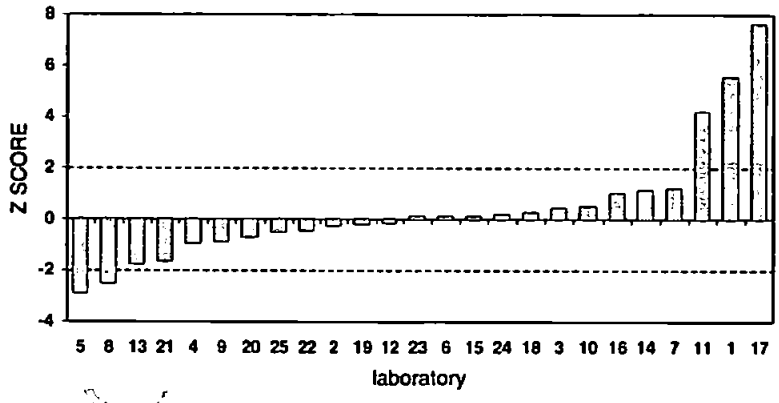

Fig. 5. Plot of z-scores obtained by laboratories participating in the NOAA 2002 intercomparison study for the analysis of orthophosphate in MOOS-1. z-Scores calculated from the mean orthophosphate concentration, with the assigned value set at 1.6 ± 0.21 μM. $|z| \leq 2$ represent the satisfactory z score value for MOOS-1 [159,160].

Table 4
Commercially available CRMs for the determination of phosphorus species in environmental matrices

CRM	Matrix	Phosphorus species	Concentration	Comments	Supplier	Ref.
MOOS-1	Seawater	Orthophosphate	$1.56 \pm 0.07\ \mu mol\ L^{-1}$	Natural seawater sample, of Cape Breton Island, NS, Canada at a depth of 200 m	NRC	[159,160]
QC RW1	Freshwater	Orthophosphate	$100\ \mu g\ L^{-1}$	Artificial sample, distributed as an ampoule to be 100 times with pure water	VKI	[161]
QC RW2	Freshwater	Total phosphorus	$200\ \mu g\ L^{-1}$	Artificial sample, distributed as an ampoule to be 100 times with pure water	VKI	[161]
Australian natural water CRM	Natural water/freshwater	Orthophosphate	$27 \pm 0.8\ \mu g\ L^{-1}$	Natural water sample obtained from Christmas Creek in the Lamington National Park, Qld., Australia	Queensland Health Scientific Services	
		Total dissolved phosphorus	$37 \pm 1.2\ \mu g\ L^{-1}$			
BCR-616	Groundwater (high carbonate content)	Orthophosphate	$3.36 \pm 0.13\ mg\ kg^{-1}$	Artificial groundwater sample, prepared from ultrapure water, to which required salts were added; stabilized by autoclaving	BCR	www.irmm.jrc.be
SRM®-2702	Marine sediment	Total phosphorus	$0.1552 \pm 0.0.0066\%$	Material for SRM® was collected from Chesapeake Bay, USA, freeze-dried, seived at 70 μm (100% passing) and cone blended, then radiation sterilized and bottled	NIST	www.nist.gov
SRM®-1646a	Estuarine sediment	Total phosphorus	$0.027 \pm 0.0.001\%$	Material for SRM® was dredged from Chesapeake Bay, USA, freeze-dried, lightly deagglomerated and < 1 mm fraction ball milled and the < 75 μm blended and bottled	NIST	www.nist.gov
BCR-684	River sediment	NaOH-extractable P	$500 \pm 21\ mg\ kg^{-1}$	Material for the CRM was collected from the lower reaches of the River Po, Italy, then sieved and the <2 mm fraction was dried, lightly deagglomerated, crushed and hammer-milled and < 90 μm blended and bottled	BCR	www.irmm.jrc.be
		HCl-extractable	$536 \pm 28\ mg\ kg^{-1}$			
		Inorganic P	$1113 \pm 24\ mg\ kg^{-1}$			
		Organic P	$209 \pm 9\ mg\ kg^{-1}$			
		Conc. HCL-extract P	$1373 \pm 35\ mg\ kg^{-1}$			

aqueous test materials containing orthophosphate and TP at concentrations similar to those found in estuarine, coastal and open water environments [168]. Regular testing is necessary to assure the quality of environmental data submitted since the performance of many laboratories does not remain constant [163,169]. The assessment of the quality of data must be made at the time that the environmental samples are analysed. Such exercises provide vital information for improving the quality and performance of laboratories and a structure for developing robust analytical techniques. To this end, the QUASIMEME Laboratory Performance Study was designed to follow the IUPAC/ISO/AOAC international protocol for international testing [162,170]. All laboratories that submit data to the UK National Marine Monitoring Programme (NMMP) routinely participate in QUASIMEME as a means of external QA/QC of the data collected, including orthophosphate [171]. There have been several other national and international intercomparison exercises including the se-

ries of International Council for the Exploration of the Seas (ICES) exercises [164] and the Australian National Low level Nutrient (ANLLN) exercise.

5.3. Databases

Environmental monitoring and research programmes generate large amounts of information and can provide valuable databases of analytical information if appropriate QA/QC measures are used to preserve data quality. For example, databases have been generated from of the NMMP and the 'Winter Monitoring of the Western Irish Sea' programme [165] and both incorporated QA/QC schemes to ensure data integrity. Legislation such as the EU Water Framework Directive outlines an approach for managing water quality in the member states of the European Union which will require monitoring and environmental quality data (including P data) to be collected by member states and presented at the EU level. There is therefore the potential to add to the repository of data already held by the European Environmental Agency, and adherence to QA/QC practices such as intercomparison studies in conjunction with routine in-house use of RMs and CRMs is essential if such data are to be of practical use. Phosphorus data are also incorporated within larger assessment exercises dealing with broader issues such as water quality and eutrophication, e.g. the National Estuarine Eutrophication assessment in the United States [172].

6. Conclusions

Accurate determination of P species in environmental matrices is an important pre-requisite for understanding the biogeochemical cycling of the element. This in turn is essential for investigating the impact of phosphorus on ecosystem health. Key aspects of the analytical process for obtaining high quality phosphorus data are robust sampling and sample treatment protocols (see also Maher and Woo [75]). These cannot be universal due to the variability in behaviour of different matrices but nonetheless guidelines can be provided for aspects such as filtration, chemical treatment and storage conditions. For soils, wetting and drying have a considerable affect on phosphorus solubility.

In addition, for the determination of different phosphorus fractions and individual phosphorus containing compounds, particular attention needs to be given to the digestion process. Autoclaving (typically with peroxydisulfate in acid or alkaline media) is a widely used method that gives good recoveries but it is important to quantify this using a range of environmentally relevant model phosphorus containing compounds. Selective enzymatic degradation (typically using phosphatases) is a useful additional approach for the quantification of individual phosphorus containing compounds (or classes of compounds).

A critical aspect of the overall analytical process for any laboratory is participation in intercomparison exercises. This is particularly important for phosphorus determination due to the lability of the element in biologically active environmental matrices. To supplement such exercises the availability of more environmental certified reference materials is an important requirement. Finally, co-operation between analytical scientists and environmental scientists is fundamental to the generation of high quality, publicly available databases on the spatial and temporal variability of phosphorus species in aquatic and terrestrial ecosystems.

References

[1] B.A. Moss, Chem. Ind. 11 (1996) 407.
[2] K. Robards, I.D. McKelvie, R.L. Benson, P.J. Worsfold, N.J. Blundell, H. Casey, Anal. Chim. Acta 287 (1994) 147.
[3] I.D. McKelvie, D.M.W. Peat, P.J. Worsfold, Anal. Proc. Anal. Comm. 32 (1995) 437.
[4] J. Murphy, J.P. Riley, Anal. Chim. Acta 27 (1962) 31.
[5] P.G.W. Jones, C.P. Spencer, J. Mar. Biol. Ass. UK 43 (1963) 251.
[6] L. Drummond, W. Maher, Anal. Chim. Acta 302 (1995) 69.
[7] S.R. Crouch, H.V. Malmstadt, Anal. Chem. 39 (1967) 1084.
[8] J. Riley, J.P. Murphy, J. Mar. Biol. Ass. UK 37 (1958) 235.
[9] P.J. Worsfold, J.R. Clinch, H. Casey, Anal. Chim. Acta 197 (1987) 43.
[10] J.E. Harwood, W.H.J. Hattingh, Environmental Phosphorus Handbook, Wiley, New York, 1973.
[11] C. Neal, M. Neal, H. Wickham, Sci. Tot. Environ. 251/252 (2000) 511.
[12] O. Broberg, K. Pettersson, Hydrobiologia 170 (1988) 45.
[13] K. Sugawara, S. Kanamori, Bull. Chem. Soc. Jpn. 34 (1961) 258.
[14] W. Chamberlain, J. Shapiro, J. Limnol. Oceanogr. 14 (1969) 921.
[15] W.A. Dick, M.A. Tabatabai, J. Envrion. Qual. 6 (1983) 105.
[16] G. Hanrahan, M. Gledhill, W.A. House, P.J. Worsfold, Water Res. 37 (2003) 3579.
[17] J. Hilton, P. Buckland, G.P. Irons, Hydrobiologia 472 (2002) 77.
[18] G. Hanrahan, M. Gledhill, W.A. House, P.J. Worsfold, J. Environ. Qual. 30 (2001) 1738.
[19] A.R.J. David, T. McCormack, A.W. Morris, P.J. Worsfold, Anal. Chim. Acta 361 (1998) 63.
[20] G.H. Hanrahan, M. Gledhill, P.J. Fletcher, P.J. Worsfold, Anal. Chim. Acta 440 (2001) 55.
[21] L. May, W.A. House, M. Bowes, J. McEvoy, Sci. Total Environ. 269 (2001) 117.
[22] Commission on the European Communities, Council Directive 91/15/EC, COM 98 (1998) 775.
[23] O.D. Ansa-Asare, I.L. Marr, M.S. Cresser, Water Res. 34 (2000) 1079.
[24] C. Neal, M. Harrow, R.J. Williams, Sci. Total Environ. 210/211 (1998) 205.
[25] J.M. Dorioz, E.A. Cassell, A. Orand, K.G. Eisenman, Hydrol. Proc. 12 (1989) 285.
[26] P.C.F.C. Gardolinski, G. Hanrahan, E.P. Achterberg, M. Gledhill, A.D. Tappin, W.A. House, P.J. Worsfold, Water Res. 35 (2001) 3670.
[27] E.D. Klingaman, D.W. Nelson, J. Environ. Qual. 5 (1976) 42.
[28] D.S. Kirkwood, Mar. Chem. 38 (1992) 151.
[29] J. Zhang, P.B. Ortner, Water Res. 32 (1998) 2553.
[30] A.J. Horowitz, K.A. Elrick, M.R. Colberg, Water Res. 26 (1992) 753.
[31] G.E.M. Hall, G.F. Bonham-Carter, A.J. Horowitz, K. Lum, C. Lemieux, B. Quemarais, J.R. Garbarino, Appl. Geochem. 11 (1996) 243.
[32] J.C. Ryden, J.K. Syers, R.F. Harris, Analyst 97 (1972) 903.

[33] J.O. Skjemstad, R. Reeves, J. Environ. Qual. 7 (1978) 137.
[34] P. Pichete, K. Jamati, P.D. Golden, Water Res. 13 (1979) 1187.
[35] J.W. Morse, M. Hunt, J. Zulling, A. Mucci, T. Mendez, Ocean Sci. Eng. 7 (1982) 75.
[36] R.W. MacDonald, F.A. McLauglin, Water Resour. Res. 29 (1982) 95.
[37] M.J. Fishman, L.J. Schroder, M.W. Shockey, Int. J. Environ. Stud. 26 (1986) 231.
[38] L.A. Clementson, S.E. Wayte, Water Res. 26 (1992) 1171.
[39] D. Lambert, W. Maher, I. Hogg, Water Res. 26 (1992) 645.
[40] R.J. Avanzino, V.C. Kennedy, Water Resour. Res. 16 (1993) 3357.
[41] P.M. Haygarth, C.D. Ashby, S.C. Jarvis, J. Environ. Qual. 24 (1995) 1133.
[42] A. Aminot, R. Kerouel, Anal. Acta Chim. 351 (1997) 299.
[43] A.R. Kotlash, B.C. Chessman, Water Res. 32 (1998) 3731.
[44] P.M. Burke, S. Hill, N. Iricanin, C. Douglas, P. Essex, D. Tharin, Environ. Monit. Assess. 80 (2002) 149.
[45] A.S. Tasistro, P.F. Vendrell, M.L. Cabrera, D.E. Kissel, W.C. Johnson, Comm. Soil Sci. Plant Anal. 35 (2004) 719.
[46] W.A. House, H. Casey, S. Smith, Water Res. 20 (1986) 923.
[47] P.C.F.C. Gardolinski, P.J. Worsfold, I.D. McKelvie, Water Res. 38 (2004) 688.
[48] J.B. Cotner, R.G. Wetzel, Limnol. Oceanogr. 37 (1992) 232.
[49] M.D. Ron Vaz, A.C. Edwards, C.A. Shand, M. Cresser, Talanta 39 (1992) 1479.
[50] I.D. McKelvie, B.T. Hart, T.J. Cardwell, R.W. Cattrall, Talanta 40 (1993) 1981.
[51] W.A. House, F.H. Denison, Water Res. 32 (1998) 1819.
[52] R.G. Perkins, G.J.C. Underwood, Water Res. 35 (2001) 1399.
[53] I.T. Webster, P.W. Ford, G. Hancock, Mar. Freshwater Res. 52 (2001) 127.
[54] H.F. Birch, Plant Soil 12 (1960) 81.
[55] B.L. Turner, P.M. Haygarth, Nature 411 (2001) 258.
[56] T.L. Kieft, E. Soroker, M.K. Firestone, Soil Biol. Biochem. 19 (1987) 119.
[57] B.L. Turner, J.P. Driessen, P.M. Haygarth, I.D. McKelvie, Soil Biol. Biochem. 35 (2003) 187.
[58] R. Bartlett, B. James, Soil Sci. Soc. Am. J. 44 (1980) 721.
[59] B.L. Turner, I.D. McKelvie, P.M. Haygarth, Soil Biol. Biochem. 34 (2002) 27.
[60] M.D. Ron Vaz, A.C. Edwards, C.A. Shand, M.S. Cresser, Eur. J. Soil Sci. 45 (1994) 353.
[61] B.L. Turner, P.M. Haygarth, Soil Sci. Soc. Am. J. 67 (2003) 344.
[62] G.P. Sparling, K.N. Whale, A.J. Ramsay, Aust. J. Soil Res. 23 (1985) 613.
[63] T.Q. Zhang, A.F. Mackenzie, F. Sauriol, Soil Sci. 164 (1999) 662.
[64] B.L. Turner, B.J. Cade-Menun, D.T. Westermann, Soil Sci. Soc. Am. J. 67 (2003) 1168.
[65] E. Amézketa, J. Sustain. Agr. 14 (1999) 83.
[66] Z. Nevo, J. Hagin, Soil Sci. 102 (1966) 157.
[67] R.G. Olsen, M.N. Court, J. Soil Sci. 33 (1982) 709.
[68] M. Simonsson, D. Berggren, J.P. Gustafsson, Soil Sci. Soc. Am. J. 63 (1999) 1116.
[69] J.R. McLaughlin, J.C. Ryden, J.K. Syers, J. Soil Sci. 32 (1981) 365.
[70] R.J. Haynes, R.S. Swift, Geoderma 35 (1985) 145.
[71] S.D. Comfort, R.P. Dick, J. Baham, Soil Sci. Soc. Am. J. 55 (1991) 968.
[72] A. Schlichting, P. Leinweber, Commun. Soil Sci. Plant Anal. 33 (2002) 1617.
[73] D.H. Pote, T.C. Daniel, A.N. Sharpley, P.A. Moore, D.R. Edwards, D.J. Nichols, Soil Sci. Soc. Am. J. 60 (1996) 855.
[74] R.W. McDowell, A.N. Sharpley, J. Environ. Qual. 30 (2001) 508.
[75] W. Maher, L. Woo, Anal. Chim. Acta 375 (1998) 5.
[76] A. Aminot, R. Kérouel, Mar. Chem. 76 (2001) 113.
[77] T. Pérez-Ruiz, C. Martínez-Lozano, V. Tomás, J. Martín, Anal. Chim. Acta 442 (2001) 147.
[78] F.I. Ormaza-González, P.J. Statham, Water Res. 30 (1996) 2739.
[79] L. Solórzano, J.D.H. Strickland, Limnol. Oceanogr. 13 (1968) 515.
[80] J. Golimowski, K. Golimowska, Anal. Chim. Acta 325 (1996) 111.
[81] I.D. McKelvie, B.T. Hart, T.J. Caldwell, R.W. Cattrall, Analyst 114 (1989) 1459.
[82] H.P. Jarvie, P.J.A. Withers, C. Neal, Hydrol. Earth Syst. Sci. 6 (2002) 113.
[83] P.W. O'Connor, J.K. Syers, J. Environ. Qual. 4 (1975) 347.
[84] A.P. Rowland, P.M. Haygarth, J. Environ. Qual. 26 (1997) 410.
[85] F. Koroleff, Determination of total phosphorus, in: K. Grasshoff, M. Ehrhardt, K. Kremling (Eds.), Methods of Seawater Analysis, 2nd ed., Verlag-Chemie, Weinheim, 1983, pp. 167–173.
[86] L. Nguyen, J. Sukias, Agric. Ecosyst. Environ. 92 (2002) 49.
[87] R.R. Simard, S. Beauchemin, P.M. Haygarth, J. Environ. Qual. 29 (2000) 97.
[88] D.W. Menzel, N. Corwin, Limnol. Oceanogr. 10 (1965) 280.
[89] D. Jenkins, Adv. Chem. Ser. 73 (1968) 265.
[90] R. Kérouel, A. Aminot, Anal. Chim. Acta 318 (1996) 385.
[91] C.L. Langner, P.F. Hendrix, Water Res. 16 (1982) 1451.
[92] M. Hosomi, R. Sudo, Int. J. Environ. Stud. 27 (1986) 267.
[93] H.L. Golterman, R.S. Clymo, M.A.M. Ohnstad, Methods for the Physical and Chemical Analysis of Fresh Waters, IBP Handbook No. 8, Blackwell Scientific Publications, Oxford, 1978.
[94] P.D. Goulden, P. Brooksbank, Anal. Chim. Acta 80 (1975) 183.
[95] D.S. Jeffries, F.P. Dieken, D.E. Jones, Water Res. 13 (1979) 275.
[96] S.J. Eisenreich, R.T. Bannerman, D.E. Armstrong, Environ. Lett. 9 (1975) 43.
[97] F.H. Denison, P.M. Haygarth, W.A. House, A.W. Bristow, Int. J. Environ. Anal. Chem. 69 (1998) 111.
[98] J.C. Valderrama, Mar. Chem. 10 (1981) 109.
[99] A.D. Eaton, L.S. Clesceri, A.E. Greenburg (Eds.), Standard Methods for the Examination of Water and Wastewater, American Public Health Association–American Water Works Association–Water Environment Federation (APHA–AWWA–WEF), Washington, DC, USA, 1992.
[100] A. Gross, C.E. Boyd, J. World Aquacult. Soc. 29 (1998) 300.
[101] C.F. D'Elia, P.A. Steudler, N. Corwin, Limnol. Oceanogr. 22 (1977) 760.
[102] F. Koroleff, Int. Counc. Explor. Sea (ICES) Pap. C. M. 1969/C:8, revised 1970.
[103] J. Ebina, T. Tsutsui, T. Shirai, Water Res. 17 (1983) 1721.
[104] J.J. Ridal, R.M. Moore, Mar. Chem. 29 (1990) 19.
[105] A.D. Cembella, N.J. Antia, F.J.R. Taylor, Water Res. 20 (1986) 1197.
[106] A.C. Redfield, H.P. Smith, B.H. Ketchum, Biol. Bull. 73 (1937) 421.
[107] N.S. Nelson, Commun. Soil Sci. Plant Anal. 18 (1987) 359.
[108] D. Jolley, W. Maher, P. Cullen, Water Res. 32 (1998) 711.
[109] D. Halliwell, J. Coventry, D. Nash, Int. J. Environ. Anal. Chem. 76 (2000) 77.
[110] J.L. Coventry, D.J. Halliwell, D.M. Nash, Aust. J. Soil Res. 39 (2001) 415.
[111] B.L. Williams, C.A. Shand, M. Hill, C. O'Hara, S. Smith, M.E. Young, Commun. Soil Sci. Plant Anal. 26 (1995) 91.
[112] A.L. Heathwaite, R. Matthews, N. Preedy, P. Haygarth, J. Environ. Qual., in press.
[113] N. Preedy, K. McTiernan, R. Matthews, L. Heathwaite, P. Haygarth, J. Environ. Qual. 30 (2001) 2105.
[114] B.L. Turner, P.M. Haygarth, Soil Sci. Soc. Am. J. 64 (2000) 1090.
[115] P.M. Haygarth, L. Hepworth, S.C. Jarvis, Eur. J. Soil Sci. 49 (1998) 65.
[116] P.M. Haygarth, S.C. Jarvis, Water Res. 31 (1997) 140.
[117] M. Espinosa, B.L. Turner, P.M. Haygarth, J. Environ. Qual. 28 (1999) 1497.
[118] M. Hens, R. Merckx, Water Res. 36 (2002) 1483.
[119] M. Martin, L. Celi, E. Barberis, Commun. Soil Sci. Plant Anal. 30 (1999) 1909.

[120] P.J. Chapman, C.A. Shand, A.C. Edwards, S. Smith, Soil Sci. Soc. Am. J. 61 (1997) 315.
[121] P.M. Haygarth, M.S. Warwick, W.A. House, Water Res. 31 (1997) 439.
[122] Methods for the Examination of Waters and Associated Materials: Phosphorus in Waters, Effluents and Sewages, HMSO London, England, 1980, pp. 26–28.
[123] J.K. Aase, D.L. Bjorneberg, D.T. Westermann, J. Environ. Qual. 30 (2001) 1315.
[124] R. Uusitalo, E. Turtola, T. Kauppila, T. Lilja, J. Environ. Qual. 30 (2001) 589.
[125] W. Maher, F. Krikowa, D. Wruck, H. Louie, T. Nguyen, W.Y. Huang, Anal. Chim. Acta 463 (2002) 283.
[126] L. Woo, W. Maher, Anal. Chim. Acta 315 (1995) 123.
[127] D. Lambert, W. Maher, Water Res. 29 (1995) 7.
[128] A. Canturero, M.B. López, J. Mahía, A. Paz, Comm. Soil Sci. Plant Anal. 33 (2002) 3431.
[129] W.S. Dancer, R. Eliason, S. Lekhakul, Commun. Soil Sci. Plant Anal. 29 (1998) 1997.
[130] W. Maher, F. Krikowa, J. Kirby, A.T. Townsend, P. Snitch, Aust. J. Chem. 56 (2003) 103.
[131] W. Maher, S. Forster, F. Krikowa, P. Snitch, G. Chapple, P. Craig, At. Spect. 22 (2001) 361.
[132] G. Esslemont, W. Maher, P. Ford, F. Krikowa, J. Anal. At. Spect. 14 (1999) 1193.
[133] M.M. Smart, F.A. Reid, A.R. Jones, Water Res. 15 (1981) 919.
[134] M.E. Gales Jr., E.C. Julian, R.C. Kroner, J. Am. Wat. Wks. Ass. 58 (1966) 1363.
[135] US Environmental Protection Agency, Methods for the Chemical Analysis of Water and Wastes, 1971.
[136] D.H. Pote, T.C. Daniel, Analysing for total phosphorus and total dissolved phosphorus in water samples. In: G.M. Pierzynski (Ed.), Methods of Phosphorus Analysis for Soils, Sediments, Residuals, and Water, Southern Co-operative Series Bulletin No. 396, A Publication of SERA-IEG-17, North Carolina State University, 2000.
[137] J.E. Harwood, R.A. Van Steenderen, A.L. Kühn, Water Res. 3 (1969) 425.
[138] D.E.C. Corbridge, Phosphorus – An Outline of its Chemistry, Biochemistry and Technology, 3rd ed., Elsevier, Amsterdam, 1985.
[139] A.D. Cembella, N.J. Antia, Mar. Chem. 19 (1986) 205.
[140] R.H. Newman, K.R. Tate, Comm. Soil Sci. Plant Anal. 11 (1980) 835.
[141] D.M.W. Peat, I.D. McKelvie, G.P. Matthews, P.M. Haygarth, P.J. Worsfold, Talanta 45 (1997) 47.
[142] B.L. Turner, M. Paphazy, P.M. Haygarth, I.D. McKelvie, Philos. Trans. R. Soc. Lond., Ser. B 357 (2002) 449.
[143] J.T.H. Goossen, J.G. Kloosterboer, Anal. Chem. 50 (1978) 707.
[144] Nomenclature Committee of the International Union of Biochemistry, Enzyme Nomenclature, Academic Press, Orlando, Florida, 1984, p. 280.
[145] U. Padmanabhan, S. Dasgupta, B.B. Biswas, D. Dasgupta, J. Biol. Chem. 276 (2001) 23.
[146] Y. Shan, I.D. McKelvie, B.T. Hart, Limnol. Oceanogr. 39 (1994) 1993.
[147] J. Feder, et al., in: E.J. Griffith (Ed.), Environmental Phosphorus Handbook, Wiley, New York, 1973, p. 475.
[148] J.D. Strickland, T.R. Parsons, A Practical Handbook of Seawater Analysis, Bull. Fish. Res. Bd. Can., 1968, p. 167.
[149] H.K. Pant, A.C. Edwards, D. Vaughan, Biol. Fertil. Soils 17 (1994) 196.
[150] J.M.T. Carneiro, E.A.G. Zagatto, J.L.M. Santhos, J.L.F.C. Lima, Anal. Chim. Acta 474 (2002) 161.
[151] W. Markus, L. Pasamontes, R. Remy, J. Kohler, E. Kuszner, M. Gadient, F. Muller, A.G.M. Van Loon, Appl. Environ. Microbiol. 64 (1998) 4446.
[152] I.D. McKelvie, B.T. Hart, T.J. Cardwell, R.W. Cattrall, Anal. Chim. Acta 316 (1995) 277.
[153] Ph. Quevauviller, Anal. Chim. Acta 123 (1998) 991.
[154] G. Hanrahan, P. Gardolinski, M. Gledhill, P. Worsfold, Environmental monitoring of nutrients, in: F. Burden, A. Guenther, U. Forstner, I. McKelvie (Eds.), Environmental Monitoring, McGraw Hill, New York, 2002, p. 1100.
[155] Ph. Quevauviller, Anal. Chim. Acta 123 (1998) 997.
[156] ISO, Terms and Definitions Used in Connection with Reference Materials, ISO Guide 30-1981, International Standards Organization, 1981, Geneva.
[157] J.K. Taylor, Quality Assurance of Chemical Methods, Lewis Publishers, Michigan, 1990.
[158] M.J. Benoliel, Ph. Quevauviller, Analyst 123 (1998) 977.
[159] S. Willie, V. Clancy, Anal. Bioanal. Chem. 378 (2004) 1239.
[160] S. Willie, V. P. Clancy, Second Intercomparison for Nutrients in Seawater. NOAA Technical Memo 158. Available from the website of the National Oceanic and Atmospheric Administration, Center for Coastal Monitoring and Assessment. http://ccmaserver.nos.noaa.gov/. Cited 4 May 2004.
[161] J. Merry, Fresenius J. Anal. Chem. 352 (1995) 148.
[162] M. Thompson, R. Wood, J. AOAC Int. 76 (1993) 926.
[163] D.E. Wells, Mar. Poll. Bull. 29 (1994) 143.
[164] A. Aminot, D.S. Kirkwood, Mar. Poll. Bull. 29 (1994) 159.
[165] E. McGovern, E. Monaghan, M. Bloxham, A. Rowe, C. Duffy, A. Quinn, B. McHugh, T. McMahon, M. Smyth, M. Naughton, M. McManus, E. Nixon, Marine Environment and Health Series, No. 4., Marine Institute, Ireland, 2002, p. 73.
[166] D.S. Kirkwood, A. Aminot, S.R. Carlberg, Mar. Poll. Bull. 32 (1996) 640.
[167] A. Aminot, D. Kirkwood, S. Carlberg, Mar. Poll. Bull. 35 (1997) 28.
[168] QUASIMEME Laboratory Performance Studies, QUASIMEME Laboratory Performance Studies, Year 8, June 2003 to 2004. Issue 1 – 2003. QUASIMEME Laboratory Performance Studies, Scotland, 2003, p. 27. Available from the website of QUASIMEME, FRS Marine Laboratory. http://www.quasimeme.marlab.ac.uk. Cited 3 May 2004.
[169] D.E. Wells, W. Cofino, Mar. Poll. Bull. 35 (1997) 146.
[170] ISO/IEC, proficiency testing by interlaboratory comparisons, Guide 43-1, International Standards Organization, 1996, Geneva.
[171] B. Miller, J.E. Dobson, Report On The National Marine Chemical Analytical Quality Control Scheme 2002. National Marine Monitoring Programme, Scotland, 2003, p. 42. Available from the website of Fisheries Research Services, Scottish Executive Environment and Rural Affairs Department. http://www.marlab.ac.uk. Cited 3 May 2004.
[172] S.B. Bricker, C.G. Clement, D.E. Pirhalla, S.P. Orlando, D.R.G. Farrow, National Estuarine Eutrophication Assessment: Effects of Nutrient Enrichment in the Nation's Estuaries. NOAA, National Ocean Service, Special Projects Office and the National Centers for Coastal Ocean Science. Silver Spring, MD, 1999, p. 71.

Environmental applications of flow field-flow fractionation (FlFFF)

Laura J. Gimbert, Kevin N. Andrew, Philip M. Haygarth, Paul J. Worsfold

Field-flow fractionation (FFF) is an emerging family of techniques used to obtain information on particle size or relative molecular mass (RMM) distributions in complex matrices, such as environmental and biological samples. Flow FFF (FlFFF) is the most widely used version of the technique and is applicable to macromolecules, particles and colloids ranging from 0.001 μm (approximately 1000 molecular mass) up to at least 50 μm in diameter. This article describes the various components of FlFFF instrumentation, the nature of the separation process and the theory that relates retention time to RMM. Summary tables of the application of FlFFF to environmental and biological matrices and the detection of polymers and inorganic colloids are also presented.

Abbreviations: DRI, Differential refractive index; ElFFF, Electrical field-flow fractionation; ESMS, Electrospray mass spectrometry; FlFFF, Flow field-flow fractionation; GrFFF, Gravitational field-flow fractionation; ICP-MS, Inductively coupled plasma-mass spectrometry; LIBS, Laser-induced breakdown spectroscopy; LLS, Laser light scattering; MALLS, Multi-angle laser light scattering; MWCO, Molecular mass cut off; RI, Refractive index; RMM, Relative molecular mass; SdFFF, Sedimentation field-flow fractionation; SF, SPLITT fractionation; ThFFF, Thermal field-flow fractionation; UV, Ultraviolet detector

Laura J. Gimbert, Kevin N. Andrew, Philip M. Haygarth[1], Paul J. Worsfold*
School of Environmental Sciences, Plymouth Environmental Research Centre, University of Plymouth, Plymouth, Devon PL4 8AA, UK

[1]Soil Science and Environmental Quality Group, Institute of Grassland and Environmental Research, North Wyke Research Station, Okehampton, Devon EX20 2SB, UK

*Corresponding author.
Tel.: +44 (0)1752 233006;
Fax: +44 (0)1752 233009;
E-mail: pworsfold@plymouth.ac.uk

1. Introduction

Giddings first proposed the theory of FFF in the 1960s [1]. It is a separation technique similar to liquid chromatography but, unlike chromatography, the separation channel does not require a stationary phase and contains no packing material [2]. In FFF, molecular degradation of samples is minimised [3] and there are fewer problems with adsorption or size exclusion [4]. Particle-size distributions, diffusion-coefficient characterisation and RMM information can all be obtained using this relatively mild separation technique [5]. There are many sub-techniques of FFF, which include sedimentation (Sd), flow (Fl), thermal (Th), electrical (El) and gravitational (Gr) FFF, and the earliest commercial SdFFF, ThFFF and FlFFF instruments were available in the late 1980s and early 1990s from Du Pont and FFFractionation in the USA [2].

Of the different sub-techniques, FlFFF is the most versatile and widely used, because displacement of the sample components by a crossflow acting as the field is universal [2]. FlFFF is applicable to macromolecules, particles and colloids ranging from 0.001 μm (approximately 1000 molecular mass) up to at least 50 μm in diameter [6]. FlFFF has great flexibility in terms of sample type, carrier liquid (solvent), pH and ionic strength [7]. It provides high selectivity and speed, simple coupling to detectors and ready collection of fractions [8]. A possible limitation of FlFFF can be molecular mass cut-off of the membrane that determines the lowest molecular size that can be retained in the channel. Loss of sample through the membrane, or more likely by adsorptive interactions with the membrane, can also occur [3].

Variations of FlFFF incorporate the use of different channels [8], such as asymmetrical [9–11] and hollow-fibre channels [12,13]. However, this article focuses on the symmetrical FlFFF sub-technique, where the crossflow is achieved by pumping the carrier liquid directly across the channel through porous frits [14].

Split-flow thin-cell (SPLITT) fractionation (SF) is a technique similar to FFF except that it has the ability to separate relatively large quantities of sample (mg or g) in a reasonable amount of time. The channel is similar to a FFF channel (described in Section 2) and has at least one flow splitter at the outlet and sometimes at the inlet of the channel. It differs

0165-9936/$ - see front matter © 2003 Published by Elsevier B.V. doi:10.1016/S0165-9936(03)01103-8

Nomenclature

d	hydrodynamic diameter	$\langle v \rangle$	cross-sectional average velocity of carrier liquid
D	diffusion coefficient	v_r	sample migration velocity
f	friction coefficient	$\dot{V}$	volumetric channel flow rate
F	driving force	V_c	volumetric crossflow rate
H	plate height	V^0	void volume
k	Boltzmann's constant (1.38×10^{-16} g cm^2/s^2 K)	Vr	retention volume
ℓ	mean layer thickness	w	channel thickness
M	relative molecular mass	Z	mean displacement
R	retention ratio	η	viscosity of carrier liquid (η=0.01 g/cm s at 20°C)
T	absolute temperature	λ	retention parameter
t^0	void time	σ^2	variance
t_r	retention time		
U	field-induced transport velocity		

from FFF as it can only resolve the sample into two sharply defined fractions that are collected and analysed [2,15].

2. Instrumentation

Separation in FlFFF takes place in a thin, ribbon-like channel that has a rectangular cross-section and triangular end pieces. A schematic diagram of a FlFFF channel is shown in Fig. 1. The typical dimensions of a channel are 25–50 cm long, about 2–3 cm wide, and 50–250 μm thick [16]. The channel comprises two machined blocks with inset porous frits that clamp together a Mylar or Teflon spacer and a membrane. Plexiglas (polymethylmethacrylate) blocks have been used when working with aqueous solutions [17–21], because the presence of any air pockets or bubbles can easily be observed through these blocks. Any bubbles will form regions of non-uniform crossflow, and will show up as broadened peaks, perhaps with spikes or a noisy baseline on the fractogram.

Ceramic frits with a pore size of 2–5 μm are used in commercial instruments [2]. The membrane acts as the accumulation wall and is stretched across the bottom frit. Selection of an appropriate membrane depends on the macromolecules or particles being separated and the pore size should be small enough to retain the analytes but large enough to allow the carrier solution to pass through it. There are many different types of membranes available with varying molecular mass cut-off points. However, it is essential that the membrane is flat and smooth because any flaws will affect the separation process.

Two pumps usually control the channel flow and crossflow in a FlFFF system; the most commonly used are high-performance liquid chromatography (HPLC) pumps because they supply accurately controlled flow rates in a convenient manner [2]. It is possible to use one pump and split the flow and, occasionally, an additional pump that pulls the liquid from the channel or crossflow outlet has been used [22–24]. This pump is used to achieve rapid flow equilibration and reduce or eliminate the need for flow measurement and regulation. In general, flow rates in normal mode FlFFF are in the range 0.2–5 mL/min. In steric mode, faster flow rates lead to the formation of hyperlayers, which allow extremely fast, efficient separation of μm-sized particles [2].

Errors occur when the two incoming flow rates are not equal to the corresponding outgoing flow rates. When variations occur, retention times will be different from those predicted and may vary between runs, so the flow rates in FlFFF need to be accurately measured and regulated. This is achieved by either using a crossflow loop incorporating a HPLC or syringe pump (recirculating mode), or measuring the flow rates of the channel and crossflow outlets and placing a pressure restrictor on at least one outlet (non-recirculating mode). In recirculating mode, the rate of the crossflow entering the channel should be equal to the flow being drawn from the channel by the HPLC or syringe pump. In non-recirculating mode, flow rates can be measured using a stopwatch and a burette or, preferably, an electronic balance.

In the crossflow loop, the crossflow outlet is connected to the inlet of the pump, and the outlet is connected to the crossflow inlet. To avoid cavitation of the carrier liquid within the pump, the channel should be pressurised by placing a back-pressure regulator at the axial outlet of the channel. In FlFFF, the pore size of the membrane determines the pressure required to obtain

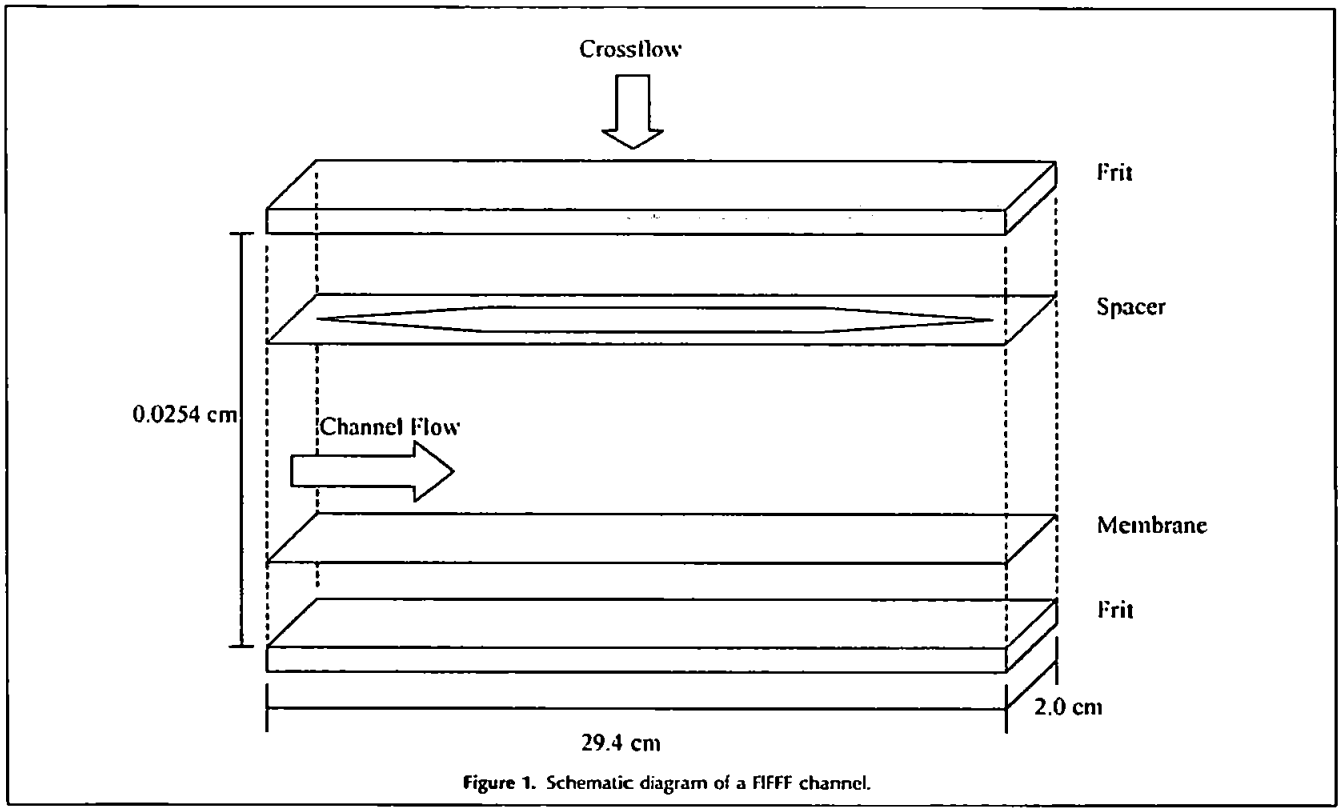

Figure 1. Schematic diagram of a FlFFF channel.

the desired crossflow rate, but generally the pressures in the system are low, usually less than 100 psi.

3. Frit inlet and outlet

There are other variations of symmetrical FlFFF with channels that have a frit or split-flow inlet. This configuration utilises either a frit element embedded in the wall opposite the accumulation wall of the channel near the inlet or a thin flow splitter that divides the inlet region into two flow spaces. Hydrodynamic relaxation achieved using this configuration is an alternative to field-driven relaxation, is rapid and does not require a stop-flow procedure. The sample components are driven to the vicinity of their equilibrium positions by the channel flow, which does not need to be stopped or bypassed, thus avoiding disruption in the channel [25].

A frit-outlet configuration has been used for concentration enhancement to increase the detection sensitivity. The sample-free carrier liquid that flows above the sample layers is skimmed out so that only the concentrated sample flows through the detector [26]; this is especially useful when analysing environmental samples with low analyte concentrations [27]. Another method of on-line sample pre-concentration, called the opposed flow sample concentration (OFSC), has been used effectively to determine colloids in river water [20].

4. Carrier liquid

The carrier liquid used in FlFFF needs to be chosen carefully so that there is no appreciable swelling of the membrane, as this can lead to non-uniform flows in the channel. The carrier liquid should also be of low viscosity because the crossflow field required to produce a given crossflow is directly proportional to the viscosity of the medium. In FlFFF, aqueous solutions are usually used as carrier liquids, although non-aqueous solvents have been used [22,28]. The aqueous carrier liquids are usually filtered through a 0.2-μm filter and sometimes degassed by heating or by bubbling helium gas through the carrier. Doubly distilled and deionised water is recommended for the preparation of aqueous carrier liquids and a surfactant or buffer is usually added. Several anionic and non-ionic surfactants have been used [2] and these are shown in Table 1. In choosing an appropriate surfactant, any interference with the detector response, potential interactions with channel materials, the resulting ionic strength, and the effective dispersion of the particles need to be considered. The use of buffers in aqueous carrier liquids is particularly useful when analysing biological materials

Table 1. Surfactants used in FlFFF

Surfactant type	Name
Anionic	FL-70 (oleic acid, sodium carbonate, tergitol, tetrasodium EDTA, polyethylene glycol, and triethanolamine); SDS
Non-ionic	Brij-35 (polyoxyethylene ether: 23 lauryl ether); Pluronic F68; Triton X-100 (octylphenoxy polyethoxy ethanol); Tween 20 (polyoxyethylene sorbitan); Tween 60 (polyoxyethylene sorbitan)
Cationic	CTAB (cetyl trimethylammonium bromide)

[7,26,29–31]. A bactericide, such as sodium azide at a concentration of 0.01–0.02% (m/v), is frequently added to prevent bacterial growth.

5. Detectors

Many detectors have been used in FlFFF, but the most common is a UV/visible spectrophotometer. Photodiode arrays have been used to obtain the entire UV/visible spectra of eluting samples instead of monitoring a single wavelength [32,33]. By coupling detectors on-line, more detailed information can be obtained about the sample being analysed and UV/visible spectrophotometry has been coupled with, e.g., multi-angle laser light scattering (MALLS), differential refractive index (DRI), fluorescence and, more recently, inductively coupled plasma-mass spectrometry (ICP-MS) [5,23,34–36]. Other detectors that have been occasionally used are electrospray mass spectrometry (ESMS) [37] and laser induced breakdown spectroscopy (LIBS) [38,39].

6. The separation process

In FlFFF, there are two liquid flows acting on the sample components. One is the channel flow that runs through the channel, and the other is a crossflow that flows perpendicular to the channel and passes through the inlet frit into the channel and exits through the membrane and outlet frit. The channel flow is laminar with a parabolic flow profile [2] and hence the velocity is zero at the walls of the channel, because of frictional drag, and increases to a maximum in the centre of the channel.

A common procedure for injecting a sample is called 'stop-flow relaxation', in which a small volume sample (typically 3–10 μL) is injected into the channel flow. After a short delay period that allows the sample to move into the channel from the injector, the channel flow is stopped for a certain amount of time (relaxation time or stop-flow time), allowing only the crossflow to act on the sample [2]. A typical FlFFF manifold in both the load (stop-flow) and inject (run) configurations is shown in Figs. 2a and 2b, respectively. Stop-flow time is determined to be sufficient by calculating the time for two channel volumes of crossflow to pass across the channel [40]. During this relaxation time, the channel flow is diverted around the channel and flows directly to the detector to avoid a large baseline disturbance. The crossflow carrier liquid passes through the membrane during the relaxation time and the sample accumulates near the membrane surface.

A steady state distribution is reached when the crossflow driving force is balanced by the diffusion (Brownian motion) of macromolecules or particles back into the channel [32]. Exponential concentration distributions of different mean layer thicknesses are formed at the membrane for each different component [17]. The position of the macromolecules is determined by their diffusion coefficients; the smallest macromolecules, with the highest diffusion coefficients and largest mean layer thicknesses, will spread out farthest from the membrane. When the channel flow is reintroduced, the run commences and the smaller macromolecules that encounter the higher velocity of the laminar flow profile will be eluted from the channel first [41]. As a result, molecules of different sizes have different retention times and their diffusion coefficients can be calculated directly from theoretical equations, whereas their RMMs are determined from a calibration graph. A separate calibration graph is needed for each type of polymer because of differences in molecular conformation. The theoretical aspects of this process are described in Section 8.

7. Operating modes in FlFFF

There are two operating modes in FlFFF. Normal or Brownian mode, as described above, is applicable to macromolecules and colloids less than about 1–2 μm in size. The alternative steric/hyperlayer mode can cover the range 0.5–100 μm [6].

A schematic diagram depicting how a sample is separated in normal mode is shown in Fig. 3. The normal operating mode was so called because this was the only operating mode used in FFF until the steric mode was introduced in the late 1970s [18].

In the steric/hyperlayer operating mode, shown schematically in Fig. 4, the larger particles elute first and this inversion in elution order is referred to as steric inversion [42]. It generally occurs around diameters of 1 μm, when the Brownian motion of the molecules becomes too weak to oppose the field and all particles

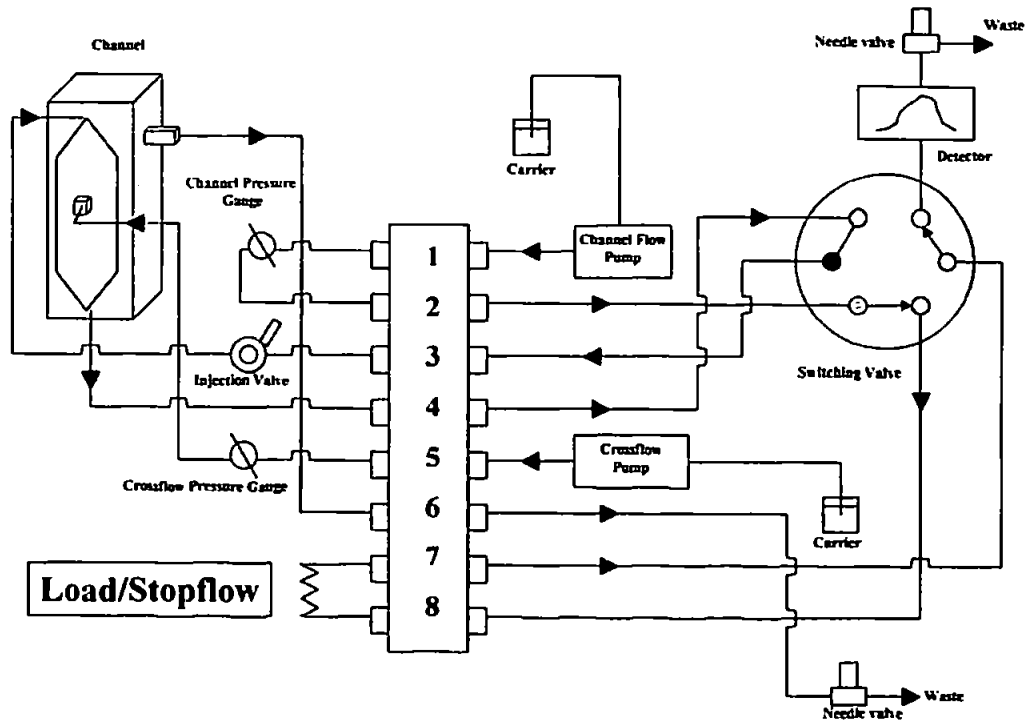

Figure 2a. A typical FlFFF manifold in load (stop-flow) position.

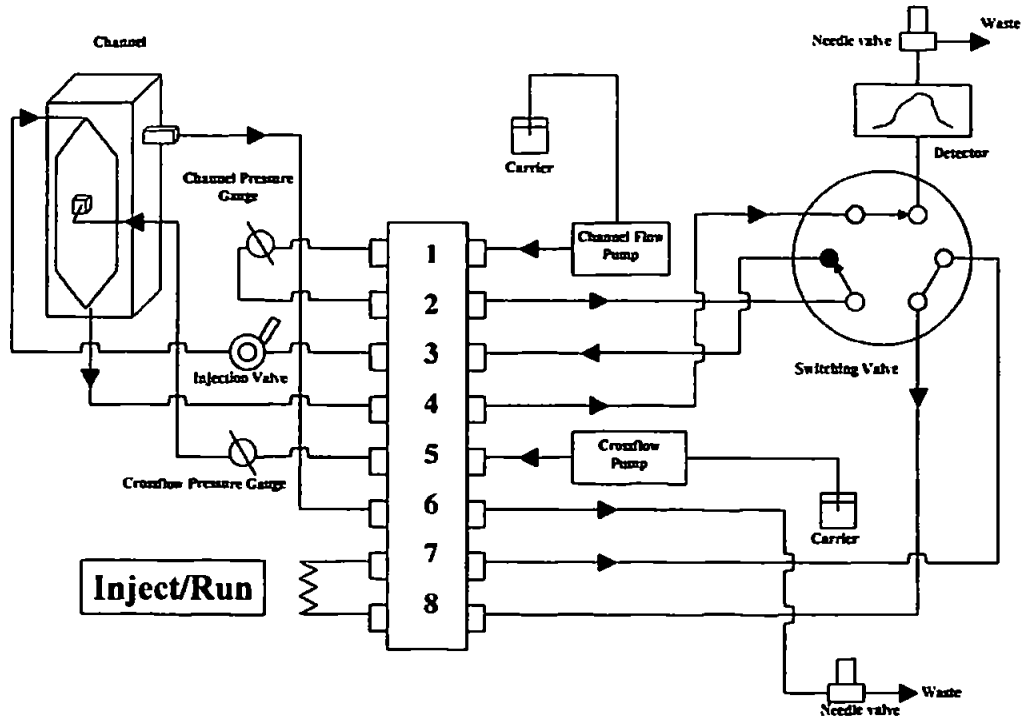

Figure 2b. A typical FlFFF manifold in inject (run) position.

are initially forced onto the accumulation wall. The particles are also subjected to a lifting force from the channel flow along the membrane and reach an equilibrium position in the channel at which the lift forces balance the crossflow force. Larger particles experience greater lift and are therefore further away from the membrane and consequently elute before smaller particles [6].

Programmed FlFFF, in which the field strength or flow velocity is varied during the run in order to speed up the elution of slowly migrating components whilst maintaining the resolution of early eluting components, has also been used [2,18]. In flow programming, the incoming and outgoing flow rates need to be equalised at all times during the run. Again, this can be achieved using a crossflow loop, with a flowmeter incorporated in the loop, as the outlet flow rate is forced to equal the incoming flow rate at all times. In this set-up, the channel needs to be pressurised by placing a back-pressure regulator at the axial outlet of the channel and this pressure should be higher than that needed to establish the desired crossflow rate. This method has been used successfully to analyse environmental [43] and biological [7] samples.

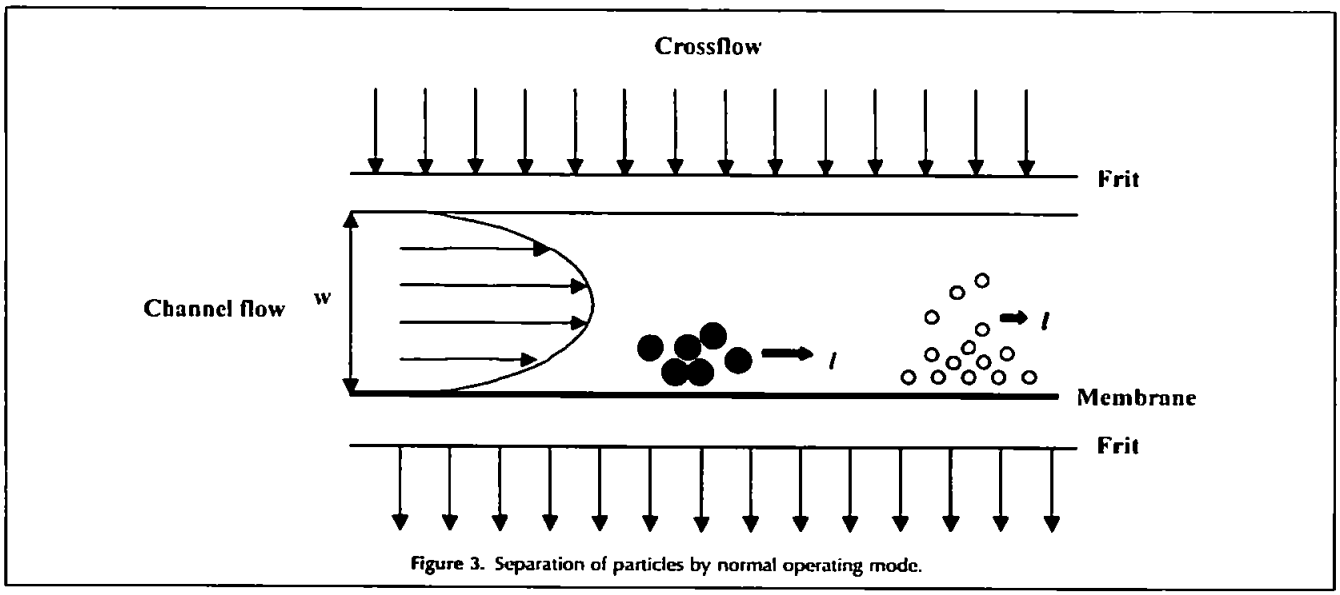

Figure 3. Separation of particles by normal operating mode.

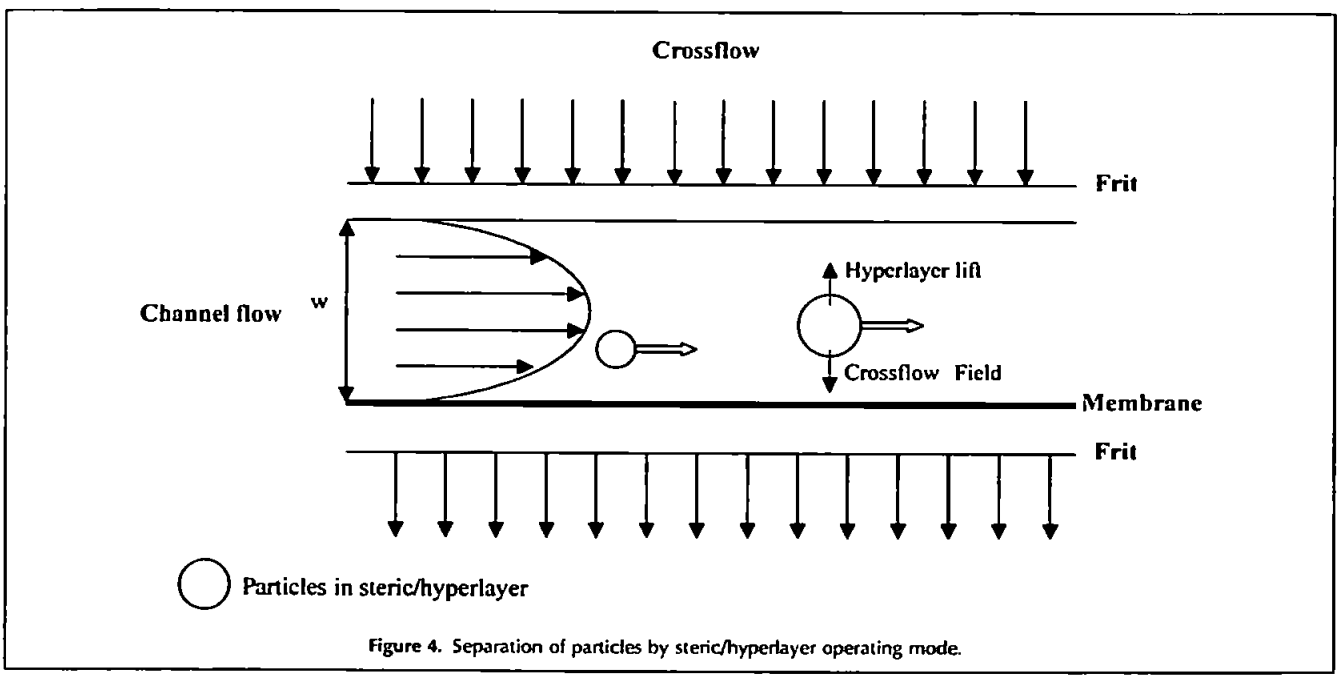

Figure 4. Separation of particles by steric/hyperlayer operating mode.

8. Theoretical aspects

The following is a summary of the important relationships between key instrumental parameters. They provide a sound basis for the experimental optimisation of the system and all terms are defined in the lists of abbreviations and nomenclature (under the abstract at the start of the article and on page 2, respectively). A fractogram is obtained by plotting the detector response against the elution volume or time of the emerging sample.

The relative elution behaviour of each sample component can be determined by calculating the retention ratio, R, which is the ratio of the average velocities of the sample components and the carrier liquid [6]. From chromatographic theory, R is defined as:

$$R = \frac{v_r}{\langle v \rangle} = \frac{t^0}{t_r} = \frac{V^0}{V_r} \quad (1)$$

and, from FFF theory, as:

$$R = 6\lambda\left[\coth\left(\frac{1}{2\lambda}\right) - 2\lambda\right] \quad (2)$$

λ (the retention parameter) can be expressed as follows:

$$\lambda = \frac{\ell}{w} = \frac{D}{Uw} = \frac{kT}{Fw} \quad (3)$$

where ℓ is the mean layer thickness of each sample component and w is the channel width. ℓ can also be expressed in terms of the diffusion coefficient of the particle (D) and its field-induced transport velocity (U) or the ratio of the thermal energy (kT) to the driving force (F) exerted on the particle. The retention parameter can also be expressed using the Nernst-Einstein equation ($f = kT/D$) as:

$$\lambda = \frac{D}{wU} = \frac{V^0 D}{w^2 V_c} \quad (4)$$

and alternatively using the Stokes equation ($f = 3\pi\eta d$) as:

$$\lambda = \frac{kTV^0}{3\pi\eta w^2 V_c d} \quad (5)$$

The retention time in FlFFF is expressed as:

$$t_r = \frac{\pi\eta w^2 d V_c}{2kT\dot{V}} \quad (6)$$

These relationships were first derived by Giddings and further details can be found elsewhere [2]. The diffusion coefficient can therefore be calculated and related to the RMM (M) (where A' and b are constants for a given polymer-solvent system) by:

$$D = A'M^{-b} \quad (7)$$

Using calibration standards, a calibration graph can be obtained by plotting log D against log M and the molar mass of sample components can be determined from Equations (1), (2), (4) and (7).

The resolution is generally very high in FFF compared with other chromatographic methods in spite of the significant peak broadening, which results in low plate heights, so, although the peaks are broad, the resolution is good. The plate height (H) is defined as the variance (σ^2) of the elution profile divided by the mean displacement (Z) of the profile [2,40]:

$$H = \frac{\sigma^2}{Z} \quad (8)$$

9. Applications

Tables 2–5 summarise the application of FlFFF to environmental (Table 2) and biological (Table 3) matrices and to the detection of polymers (Table 4) and inorganic colloids (Table 5). Each table is ordered alphabetically in terms of analytes and states the crossflow system, the membrane, the carrier liquid and the detector used in each application. There are also specific technical comments, where appropriate. The focus of this article is environmental applications and the references cited in Table 2 are discussed in more detail below.

Environmental applications include assessments of colloids in freshwater and seawater, characterisation of dissolved organic material, including fulvic and humic acids, and colloidally associated trace elements in natural and effluent waters. From this limited range of available published information, it is clear that the technology is currently under-utilised in environmental research, reflecting, in part, its relative infancy combined with the challenges and complexities of environmental matrices [33]. Notwithstanding these difficulties, FlFFF offers potential benefits to the environmental science community in all fluid-based systems where contaminants are closely associated with colloids. Of particular importance are particle movements through fluids. Colloids, being organic or inorganic in nature, could themselves be the contaminant or the vehicle for the transfer of associated chemical contaminants, and there have been some modest attempts with sedimentation FFF to separate soil particles in this context [e.g. 86–88].

Table 2. Environmental applications

Analyte	Crossflow	Membrane*	Carrier liquid	Detector	Comments	Ref.
Colloids (in coastal seawater)	Recirculating	Regenerated cellulose, 10,000 Da nominal MWCO	Seawater with addition of biological non-ionic surfactant (Pluronic F68) to final concentration of 0.1% (v/v)	UV (254 nm)	Used polystyrene latex beads (standards). Channel with frit outlet	[44]
Dissolved organic material (coloured, in river and coastal waters)	Recirculating	Regenerated cellulose, 3000 Da nominal MWCO for globular compounds (FFFractionation)	0.005% FL-70, 0.05 M Trisma and 0.029 M HCl prepared in organic-free distilled water, to give pH 8 and ionic strength 0.08 M	UV (330 nm) and fluorescence	Frit inlet/frit outlet FIFFF (FIFO-FIFFF). Also used polystyrene sulphonate, sodium salt standards	[27]
Diesel soot particles	Not stated	Regenerated cellulose (YM-10, Amicon), 10,000 MWCO	Doubly distilled and deionised water containing 0.01% (w/v) Triton X-100, 0.02% (w/v) NaN_3	UV (254 nm)	Also used polystyrene latex standards	[45]
Dissolved organic carbon (in fresh and marine waters)	Non-recirculating	Modified polyether sulphone (Omega), 1000 MWCO-optimum membrane	(i) 25 mM Tris, 20 mM sodium chloride (ii) 10 mM borate, 20 mM sodium chloride – optimal carriers	UV (270 nm)	Various ultrafilter membranes and carrier solutions investigated. FIFFF system modified to allow on-channel pre-concentration. Also used polystyrene sulphonate standards	[41]
Dissolved organic matter (pulp and paper mill effluents)	Non-recirculating	Cellulose acetate, (manufactured in laboratory), 20–50 μm thick	Distilled deionised water with 0.05 M tris buffer adjusted to pH 8.0±0.1 by addition of HCl, ionic strength about 0.03 M	UV (254 nm)	Used sodium polystyrene sulphonate standards and polystyrene latex beads. Membrane manufactured to overcome sample interaction problems in refs. [33,49]	[46,47]
Dissolved organic matter (in seawater)	Recirculating	Regenerated cellulose (YM-10, Amicon), 10,000 Da nominal MWCO	UV-oxidised seawater	UV and fluorescence	Flow-rate programmable FFF system. Dextrans used as model dissolved organic matter compounds. Also used polystyrene latex beads (standards) in same carrier with addition of 0.1% (v/v) FL-70	[43]
Fulvic acids	Not stated	Cellulose acetate membrane	Deionised water, with pH and ionic strength adjusted to that of samples with NaOH, HCl and NaCl	UV (254 nm)		[48]

(continued on next page)

Table 2 (*continued*)

Analyte	Crossflow	Membrane*	Carrier liquid	Detector	Comments	Ref.
Fulvic and humic acids	Not stated	Cellulose acetate membrane (Osmonics), 1000 g/mol nominal MWCO (determined with proteins)	Several carrier liquids studied (Tris and phosphate buffer), but DI water adjusted to pH 8.5 with NaOH – optimal carrier	UV (254 nm)	Two channel designs used: symmetric and asymmetric. Used polystyrene sulphonate standards	[14]
Fulvic and humic acids	Non-recirculating	Polypropylene-backed polysulphone, (PM10F, Amicon), 10,000 MWCO	Two carrier liquids used: (i) 0.05 M TRISMA, 0.0268 M HNO_3, 0.00308 M NaN_3 (ii) 0.05% FL-70 and 0.03% NaN_3, pH 7- optimal carrier	UV (254 and 270 nm) with a reference at 450 nm	Also used polystyrene sulphonate standards	[32]
Fulvic and humic acids	Non-recirculating	Polysulphone (PTGC, Millipore), 10,000 nominal MWCO for globular proteins	0.05 M TRISMA, 0.0268 M HNO_3, 0.00308 M NaN_3, pH 7.9	UV (254 nm) or variable wavelength detector	Some sample-wall interaction. Also used polystyrene sulphonate standards and some biological test samples	[49]
Fulvic and humic acids (adsorption with hematite)	Recirculating	(A) Cellulose acetate, 1000 g/mol nominal MWCO (B) Regenerated cellulose, 10,000 g/mol nominal MWCO	Two carrier solutions used: (i) DI water used for adsorption products and hematite (ii) DI water containing 0.05 vol% FL-70, 0.02 wt% NaN_3 used for hematite	(A) UV (260 nm for hematite in FL-70, and 280 nm for adsorption products); (B) coupled with MALLS	Two instruments used: (A) and (B). Also used polystyrene latex particle standards	[50]
Humic substances	Recirculating	Different membranes: regenerated cellulose, 1 kDa (Wyatt Technology), 5 and 10kDa cut-off (Schleicher and Schuell); polyethersulphone, 2 and 4 kDa (Wyatt Technology). Regenerated cellulose with 5 kDa cut-off was optimum membrane	Different carriers: 0.01% Tween 20, 0.02 w/V% NaN_3; 10^{-4} M NaOH; 0.05 or 0.005 M Tris buffer. Ionic strength and pH adjusted by NaOH and $NaClO_4$ respectively. All solutions prepared in ultrapure water. Optimal carrier: 0.005 M Tris-buffer, pH 9.1	UV. Humic and fulvic acids (254 nm), polystyrene sulphonate reference colloids (225 nm)	Also used protein and polystyrene sulphonate reference colloids	[51]
Humic substances	Non-recirculating	Cellulose acetate	0.05 M TRISMA, 0.0268 M HNO_3, 0.00308 M NaN_3, pH 7.8	UV (254 nm)	Used polystyrene sulphonate standards	[52]
Humic substances	Non-recirculating	(i) Polysulphone (PTGC, Millipore), 10,000 MWCO for globular proteins (ii) Cellulose (YC05, Amicon), with specified 500-Da pore size	0.05 M TRISMA, 0.0268 M HNO_3, 0.00308 M NaN_3, pH 7.9	UV (254 nm), several fractograms recorded with photodiode array detector	Same method as [49]. Some sample interaction with membrane still occurs. Also used polystyrene sulphonate standards and some biological test samples	[33]
Humic substances	Recirculating	Not stated, but carrier solution in membrane filtrated (10,000 MWCO) water	0.05% SDS, 0.02% NaN_3 in ultrapurified, membrane-filtered water	UV, fluorescence and MALLS	Also used polystyrene latex beads. Crossflow field programming used	[53]

(continued on next page)

Table 2 (*continued*)

Analyte	Crossflow	Membrane*	Carrier liquid	Detector	Comments	Ref.
Humic substances (in drinking water sources)	Not stated	Cellulose acetate membrane, 100 MWCO	0.05M TRISMA, 0.0268 M HNO_3, 0.00308 M NaN_3, pH 7.9	UV (254 nm)	Used polystyrene sulphonate standards	[3]
Phytoliths (biosilicate plant microfossils)	Recirculating	Polypropylene membrane (Celgard, Hoechst-Celanese) having size cut-off of 50 nm	0.15% (v/v) FL-70, 0.02% (w/v) NaN_3 in deionised and degassed water	UV (260 nm)	Also used polystyrene latex standards. Flow field programming used	[16]
River sediment and water	Non-recirculating	0.03 µm Polycarbonate with hydrophilic poly(vinylpyrrolidone) (PVP) coating (Poretics) – optimal membrane	0.1% SDS, 0.1% NaN_3 in doubly distilled deionised water – optimal carrier	UV (254 nm)	Opposed flow sample concentration (OFSC) technique. Various ultrafiltration and microfiltration membranes and carrier solutions investigated. Also used proteins and polystyrene latex beads standards	[20]
Trace elements complexed to humic acids and colloidal organic material (in municipal wastewater)	Non-recirculating	Polyregenerated cellulose ultrafiltration membrane, 3000 Da MWCO	30 mM TRIS-HNO_3, pH 7.3 or doubly distilled water	UV (254 nm) and ICP-MS	Also used polystyrene sulphonate and protein standards (protein standards not suitable for calibrating humic acids)	[5]
Trace elements in colloidal material (in freshwaters)	Non-recirculating	1000 MWCO ultrafilter membrane (Omega)	Borate buffer solution in Milli-Q water – 5 mM borate, 10 mM sodium chloride, pH 8.1	UV (270 nm) and ICP-MS	Modified to allow injection of large sample volumes [23,41]	[36]
Trace elements in colloidal material (in natural waters)	Non-recirculating	1000 MWCO ultrafilter membrane (Omega)	pH 8.1 buffer containing 5 mM borate, 10 mM sodium chloride in Milli-Q water	UV (270 nm) and ICP-MS	Modified to allow injection of large sample volumes [41] (Pre-concentration method). Also used polystyrene sulphonate standards	[23]

*Membrane type and manufacturer as written in the literature

Table 3. Biological applications

Analyte	Crossflow	Membrane*	Carrier liquid	Detector	Comments	Ref.
DNA	Not stated	Regenerated cellulose (YM-30, Amicon)	Tris-HNO_3 at ionic strength of 0.1 M and pH 7.8	UV (260 nm)		[29]
DNA (cationic lipid complexes)	Non-recirculating	(i) Regenerated cellulose (Millipore), 30,000 MWCO (ii) 0.03 μm pore size polycarbonate (Osmonics) (iii) Polypropylene having 0.05×0.125 μm pore dimensions (Celgard 3402, Hoechst-Celanese)	(i) Distilled and deionised water containing 0.02% (w/v) NaN_3 (ii) 0.089 M Tris-borate buffer, pH 8.59	UV (260 nm), MALLS and RI	Two FIFFF channels used. Channel I with frit outlet. Three membranes and two carrier liquids investigated	[21]
DNA (linear and circular)	Non-recirculating	Diaflo ultrafiltration YM-30, Amicon	Tris-HNO_3 buffer of ionic strength 0.1 M and pH 8.0 with 1.0 mM EDTA. Used doubly distilled water	UV (260 nm)		[54]
Lipoproteins (in plasma)	Recirculating	Many ultrafiltration membranes studied. Most appropriate are YM-30 (30 kDa MWCO), YM-100 (100 kDa MWCO) and XM-300 (300 kDa MWCO), Amicon	Phosphate-buffered saline (PBS) (138 mM sodium chloride, 2.7 mM potassium chloride, 10 mM phosphate buffer salts) at pH 7.4. Doubly distilled deionised water used	UV (280 nm)	Frit-inlet hydrodynamic relaxation FIFFF system. Used isocratic and programmed-field procedures. Also used proteins	[7]
Lipoproteins (in plasma)	Not stated	Regenerated cellulose (YM-30, Amicon)	Phosphate buffer at pH 7.4	UV (280 nm)	Frit-inlet channel used, no stop-flow procedure necessary	[29]
Lipoproteins and proteins	Recirculating	YM-1 or YM-10 ultrafiltration membranes, Amicon	Phosphate-buffered saline (PBS) (138 mM sodium chloride, 2.7 mM potassium chloride, 10 mM phosphate-buffered salts) at pH 7.4. Doubly distilled deionised water used	UV (280 nm)	Frit-inlet and frit-outlet FIFFF system	[26]
Liposomes	Not stated	Regenerated cellulose (YM-10, Amicon)	(i) TRIS-HCl buffer solution, pH 7.8 (ii) PBS buffer (iii) Lactose solution with NaCl (iv) 3.08 mM NaN_3	UV (254 nm)	Different carrier solutions used. Liposome samples (prepared in four different electrolyte solutions) are run using the corresponding solution as carrier. Also used polystyrene latex standards [carrier- 0.05% SDS and 0.02% NaN_3, in ultrapure water (purified by reverse osmosis and deionised)]	[55]
Mucin (biological surfactant)	Not stated	YM10, Amicon, 10,000 Da MWCO	PBS containing 0.1% FL-70	UV (254 nm)	Analysed bovine submaxillary gland mucin coating on polystyrene latex particles	[31]

(continued on next page)

Table 3 (*continued*)

Analyte	Crossflow	Membrane*	Carrier liquid	Detector	Comments	Ref.
Pollen grains	Not stated	Ultrafiltration membrane YM30, Amicon	Isoton II solution using doubly distilled deionised water	UV (254 nm)	Used frit inlet FIFFF channel	[56]
Protein conjugates	Not stated	Polypropylene (Celgard 2400, Hoechst-Celanese)	Water	UV (200 nm)		[29]
Proteins	Not stated	Regenerated cellulose, (YM-10, Amicon)	Tris-HNO_3 at ionic strength of 0.1 M and pH 7.8	UV (280 nm)		[29]
Proteins	Not stated	Polypropylene (Celgard 2400, Hoechst-Celanese)	Phosphate buffer at pH 7.5	UV (280 nm)		[29]
Proteins	Non-recirculating	Channel I: YM-10, Amicon, 10,000 MWCO Channel II: YC-5, Amicon, 5,000 MWCO Channel III: Cellulose, (YM5, Amicon), 5,000 MWCO	Channel I and III: Tris-HNO_3 (ionic strength 0.1 M) and 1mM EDTA (pH 7.9). Channel II: PBS (containing 120 mM sodium chloride, 2.7 mM potassium chloride, 10 mM phosphate buffer salts) at pH 7.4. Used doubly distilled water in all carriers	UV (280 nm)	Two frit-inlet channels (hydrodynamic relaxation) and one conventional channel used for stop-flow experiments	[30]
Proteins	Non-recirculating	Regenerated cellulose ultrafiltration membrane (FFFractionation), 3000 Da MWCO	0.1 M TRIS-HNO_3, pH 8	UV (280 nm) and ICP-MS		[57]
Proteins	Non-recirculating	Regenerated cellulose (YM10, Amicon), 10,000 MWCO	For PS: 0.1% FL-70 and 0.02% NaN_3; For protein standards: Tris buffer solution at various pH and ionic strengths; For real samples: potassium phosphate buffer	UV	Also used polystyrene latex standards	[58]
Proteins (wheat)	Recirculating to give optimum resolution	Cellulose (YM-10, Amicon), 10,000 Da MWCO	0.05 M acetic acid in deionised distilled water containing 0.002% FL-70, pH 3.1	UV (210 nm)	Different operating conditions using automated FIFO FIFFF. Optimum conditions was for frit-inlet flow and crossflow to be recirculating. Also used protein standards	[59]
Proteins (wheat)	Not stated	Cellulose, (YM-10, Amicon)	0.05 M acetic acid with 0.002% FL-70	UV (210 nm)	Also used proteins	[60]
Proteins (wheat)	Not stated	YM-10 membrane	0.05 M acetic acid with different concentrations of surfactants: Brij 35, CTAB, FL-70, SDS, Tween 20, Tween 80, Triton X-100. Best choice was FL-70	UV (210 nm)	Also used proteins	[61]

* Membrane type and manufacturer as written in the literature

Table 4. Application to Polymers

Analyte	Crossflow	Membrane*	Carrier liquid	Detector	Comments	Ref.
Acrylate latex, polystyrene latex standards	Not stated	Regenerated cellulose (YM-30, Amicon)	Doubly distilled water with 0.05% (w/v) SDS, 0.02% (w/v) NaN_3	UV (254 nm)		[62]
Amphiphilic pullulan	Not stated	Not stated	0.1 M $LiNO_3$ for carboxymethylpullulan; 10 mM Tris-HCl, pH 7.4 in Milli-Q water for other amphiphilic pullulans	MALLS and DRI		[63]
Amphiphilic water-soluble copolymers	Recirculating	Ultrafiltration membrane of regenerated cellulose, 10,000 MWCO	0.1 M $LiNO_3$ and 0.02% NaN_3 in Milli-Q water	MALLS and RI		[64]
Gelatin/sodium polystyrene sulphonate, gelatin/sodium poly(2-acrylamido-2-methylpropanesulphonate) (NaPAMS)	Not stated	Not stated	10 mM sodium acetate buffered at pH 5.6 containing 0.1% Tween-20	UV (254 nm)	Also used polystyrene standards	[65]
Poly(ethylene oxide)	Non-recirculating	PLGC-regenerated cellulose ultrafiltration membrane (Millipore)	(i) Doubly distilled deionised water, (ii) 0.025 M sodium sulphate (iii) 0.025 M potassium sulphate	Interferometry		[19]
Poly(l-lactide) microspheres	Not stated	Regenerated cellulose (YM-30, Amicon)	Ultrapure water (reverse osmosis and deionised) containing 0.05% SDS and 0.02% NaN_3	UV (254 nm)	Also used polystyrene latex beads	[66]
Polyacrylamide standards, commercial flocculants	Recirculating	Regenerated cellulose, 10^4 nominal MWCO (FFFractionation)	Dilute nitric acid in Milli-Q water at pH 3.8±0.1, vacuum filtered to 0.22 µm	MALLS and DRI	Channel with frit outlet. Crossflow field decay runs	[67]
Polyacrylamide, polystyrene-divinylbenzene latex standards	Recirculating	Regenerated cellulose, 10^4 nominal MWCO (FFFractionation)	Dilute nitric acid in Milli-Q water at pH 3.8±0.1, bulk filtered to 0.2 µm – optimal carrier	UV (230 nm), MALLS and DRI	Also used commercial polyacrylamide. Channel with frit outlet. Crossflow field decay runs	[68]
Polysaccharide (gum arabic)	Not stated	Regenerated cellulose, 10,000 g/mol MWCO	0.1 M $LiNO_3$, using Milli-Q water	MALLS and DRI		[69]
Polysaccharide (pullulan)	Recirculating	Regenerated cellulose (YM-10)	Deionised and distilled water with 0.1M $NaNO_3$, 0.02% (w/w) NaN_3	MALLS and DRI		[70]
Polystyrene	Non-recirculating	Cellulose nitrate membrane (EI 41, Schleicher and Schuell)	Organic solvent ethylbenzene used	RI		[22]
Polystyrene core-shell latex particles	Not stated	Regenerated cellulose ultrafiltration membrane (YM30, Amicon)	Phosphate buffers at different pHs	UV (254 nm)	Also used polystyrene latex standards	[71]
Polystyrene latex and dextran	Recirculating	Not stated	0.1 M $NaNO_3$ containing 0.02% w/w NaN_3	MALLS and DRI	Also analysed cationic polyelectrolyte and a pectin solution. Also analysed bovine serum albumin (globular protein) and tobacco mosaic virus using SDS with NaN_3 as carrier	[4]

(continued on next page)

Table 4 *(continued)*

Analyte	Crossflow	Membrane*	Carrier liquid	Detector	Comments	Ref.
Polystyrene latex beads (standards)	Non-recirculating	Diaflo YM10 membrane, Amicon	Doubly distilled water with 0.1% FL-70, 0.02% NaN_3	UV (254 nm)	Two FIFFF systems: split inlet and frit inlet (hydrodynamic relaxation)	[25]
Polystyrene latex beads (standards)	Not stated	Celgard 2400 microfiltration membrane (Hoechst-Celanese) and YM30 ultrafiltration membrane (Amicon)	Doubly distilled deionised water containing 0.1% (w/v) FL-70 and 0.02% (w/v) NaN_3	UV (254 nm)	Also analysed latex beads (standards) and seeds using ultrafiltration YM10 membrane (Amicon)	[56]
Polystyrene latex microbeads, polyvinylchloride latex (standards)	Non-recirculating	YM10 membrane, Amicon	Doubly distilled water containing 0.1% (v/v) FL-70, 0.02% (w/w) NaN_3	UV (254 nm)	Thin FIFFF	[17]
Polystyrene latex spheres	Recirculating	Cellulose (YM10)	Deionised and double-distilled water containing 0.005% (w/w) SDS, 0.02% (w/w) NaN_3	MALLS and DRI	Used constant and programmable crossflow	[72]
Polystyrene latex standards	Non-recirculating	YM30, Amicon, 30,000 MWCO	Distilled deionised water containing 0.1% (w/w) FL-70, 0.02% (w/w) NaN_3	UV (254 nm)	Used isocratic (non-programmed) and programmed conditions	[73]
Polystyrene latex standards	Recirculating	YM30, Amicon, 30,000 MWCO	Distilled deionised water with 0.1% (w/w) FL-70, 0.02% (w/w) NaN_3	UV (254 nm)	Dual field and flow-programmed lift hyperlayer FFF	[18]
Polystyrene latex standards	Not stated	Regenerated cellulose (YM-30, Amicon), 30,000 MWCO	Surfactants were (i) SDS (ii) FL-70 (iii) Triton X-100. All with 0.02% NaN_3 and in reverse osmotically purified and deionised water	UV (254 nm)	Three surfactants and seven ionic strengths investigated	[74]
Polystyrene latex standards, polysaccharide dextran	Not stated	Not stated	For polystyrene: doubly distilled water containing 0.02% NaN_3, 0.05% (w/w) SDS; for dextran: 0.1M $NaNO_3$ solution, 0.02% (w/w) NaN_3	MALLS and RI	Results compared to FFFF-UV set-up show good agreement	[75]
Polystyrene lattices	Recirculating	Cellulose (YM10)	0.02% (w/w) SDS and 0.02% (w/w) NaN_3	MALLS and DRI		[76]
Polystyrene particles (aqueous mode), polystyrene polymers (non-aqueous mode)	Not stated	PA 30 PET 100 ultrafiltration membrane (Hoechst Celanese), 30,000 MWCO	Variety of non-aqueous and aqueous carriers used: cyclohexane, heptane, isooctane, THF, toluene, water and xylene	UV	Development of a FIFFF instrument capable of operating at ambient and elevated temperatures	[28]
Polystyrene standards	Recirculating	Regenerated cellulose (Schleicher and Schuell), 5 kD MWCO	0.01% Tween 20 in ultrapure water at ionic strength of 10^{-3} M ($NaClO_4$)	LLS and LIBS	Sensitivity better in LIBS than LLS	[38]
Polystyrene sulphonate standards	Not stated	Polyether sulphone, 8K (Nadir, Hoechst-Celanese)	Sodium sulphate with ionic strength of 0.0195 M	UV (200 nm)		[29]
Polystyrene sulphonate standards	Non-recirculating	10,000 MWCO (Pellicon PTGC, Millipore)	Channel I used 67 mM sodium-potassium phosphate buffer solution at pH 7.4 with ionic strength of 0.17 M. Channel II used Tris-HNO_3 buffer at pH 7.3 with an ionic strength of 0.1 M	UV (254 nm)	Two FIFFF systems used. Channel II constructed with a split outlet and employed in high flow rate studies. Channel I used in field-programming experiments	[77]

(continued on next page)

Table 4 (*continued*)

Analyte	Crossflow	Membrane*	Carrier liquid	Detector	Comments	Ref.
Polystyrene sulphonate standards	Recirculating	Cellulose (YM10, FFFractionation)	Deionised and double- distilled water containing 0.1 M $NaNO_3$ and 0.02% (w/w) NaN_3	MALLS and DRI	Used constant and programmable crossflow	[78]
Polystyrene sulphonate standards, polysulphonated polysaccharide	Non-recirculating	Cellulose acetate	0.05 M Tris and 3.08 mM NaN_3. HNO_3 used to adjust pH to 8	UV (254 nm)		[24]
Polystyrene sulphonate, poly(2-vinylpyridine)	Non-recirculating	Isotactic polypropylene (Celgard 2400, Hoechst-Celanese), 50 nm nominal pore width but effective pore size 20 nm	For polystyrene sulphonate: 0.05 M TRIS-HNO_3 buffer at pH 8.6 containing 0.02% (w/w) NaN_3, ionic strength 0.0079 M; so 0.0065 M Na_2SO_4 with ionic strength 0.0195 M then used. For poly (2-vinylpyridine): 0.01 M HNO_3 at pH 2 containing 0.02% (w/w) NaN_3, ionic strength 0.013 M. Carrier solution prepared with distilled and deionised water	UV (254 nm)	Molecules smaller than membrane pores retained in channel	[79]
Polystyrene sulphonate standards, polyethylene glycol standards	Not stated	Modified polyethersulphone ultrafilter membrane (Omega), 1000 Da nominal MWCO	Various buffers of different pH (between 4.7 and 9.3) and ionic strength tested	ESMS	Polystyrene sulphonate standards and UV detector (254 nm) used for separation optimisation. Also analysed malto-oligosaccharides	[37]
Poly (styrenedivinylbenzene) latex beads	Non-recirculating	Diaflo ultrafiltration cellulose membrane type YM5 (Amicon), 5000 MWCO	Distilled water containing 0.1% FL-70, 0.02% NaN_3	UV (254 nm)	Flow/steric FFF	[80]
Polyvinyl pyrrolidone	Not stated	Regenerated cellulose and polysulphone membranes used, both with 10,000 MWCO	Distilled deionised water	MALLS and RI	Two channels used (i) frit inlet or frit outlet operating (ii) frit inlet and frit outlet (FIFO) operating	[81]
(i) Polyvinylpyridine standards (ii) Polystyrene sulphonate standards (iii) Polyacrylamide standards	Non-recirculating	For (i) and (ii): 25 µm thin isotactic polypropylene ultrafiltration membrane (Celgard 2400, Hoechst-Celanese). For (iii) and some (ii): polyethersulphone ultrafiltration membrane (Hoechst-Celanese), 8000 MWCO	For: (i) Aqueous solution of HNO_3; (ii) Tris-HNO_3 buffer; (iii) and some (ii) Aqueous solution of Na_2SO_4. All prepared in distilled and deionised water, and at different ionic strengths and pH	Variable wavelength UV, 254 nm for (i) and for some (ii); 200 nm for (iii) and low-load runs of (ii)		[82]
Poly (2-vinylpyridine) standards	Not stated	Polypropylene (Celgard 2400, Hoechst-Celanese)	0.015 M HNO_3, pH 1.8	UV (254 nm)		[29]
Starch polysaccharides	Not stated	Regenerated cellulose, 10,000 g/mol MWCO	Millipore water containing 0.02% NaN_3	MALLS and DRI	Channel with frit outlet	[83]

* Membrane type and manufacturer as written in the literature

Table 5. Application to inorganic colloids

Analyte	Crossflow	Membrane*	Carrier liquid	Detector	Comments	Ref.
Bentonite colloids	Recirculating	Regenerated cellulose (Schleicher and Schuell), 5 kDa MWCO	0.01% Tween 20, at an ionic strength of 10^{-4} M ($NaClO_4$) buffered to pH ~9 using 5 mM Tris buffer solution	DAWN-DSP-F light scattering photometer and ICP-MS	Also used polystyrene standards	[39]
Silica (chromatographic)	Not stated	YM30 ultrafiltration membrane, Amicon	Doubly distilled deionised water containing 0.1% (w/v) FL-70 and 0.02% (w/v) NaN_3	UV (254 nm)		[56]
Silica (chromatographic)	Not stated	(i) Regenerated cellulose (YM10, Amicon) (ii) Regenerated cellulose (YM30, Amicon) (iii) Polypropylene (Celgard 2400, Hoechst-Celanese)	(i) 10^{-3} M NH_4OH used with Celgard 2400 membrane (ii) Doubly distilled water containing 0.1% FL-70, 0.02% NaN_3 used with YM10 and YM30 membranes	UV (254 nm)	Flow/hyperlayer FFF. Also used polystyrene latex standards	[84]
Silica (fumed)	Not stated	Celgard 2400 microfiltration membrane (Hoechst-Celanese)	Doubly distilled deionised water containing 0.001 M NH_4OH	UV (254 nm)		[56]
Silica spheres, polystyrene microsphere samples	Recirculating	Two channels used, one with membrane (regenerated cellulose, FFFractionation, 10,000 MWCO) and other without	For membrane and membraneless operation (i) 0.01% v/v Triton X-100, 0.02% w/v NaN_3 (ii) 0.01% w/v SDS in Milli-Q water respectively. 5 mM Tris added when effect of pH tested (pH set at 9.5)	UV (330 nm)	Hyperlayer/flow FFF. Comparison of membrane *versus* no membrane	[85]

* Membrane type and manufacturer as written in the literature

There are broadly four topical areas of opportunity:

1. Particle and colloid movements from soil to water, e.g. siltation of salmon-spawning beds and general sedimentation of river basins [89].
2. Colloid and phosphorus movements in relation to eutrophication [90,91].
3. Colloid-associated movement of persistent organic pollutants [92].
4. Colloid and particle movements in relation to transfer of pathogenic organisms [93,94].

The advantage that can be gained from FlFFF is that it potentially allows for on-line separation of contaminants (with appropriate detection technologies) without the problems associated with membrane separations. In particular, it theoretically enables the environmental analytical chemist to characterise the fractogram for a given set of conditions (in relation to sample source) for (a) solids *per se*, in relation to (b) the fractogram distribution of the particular contaminant. This could give rise to 'three-dimensional' physicochemical speciation and help in characterising and understanding, for example, fluid movements through soil columns or the dynamics of phosphorus movement through a eutrophic waterbody. Examples of attempted 'three-dimensional' classifications (i.e. physical, chemical and spatial/temporal) are available as templates for potential applications [95,96], but these used membrane separation followed by batch detection.

In interpreting FlFFF element or pollutant distributions obtained in this way, it should be realised that dissolved forms will escape through the membrane and will not be recorded. In addition, the sample is washed continuously during elution, so easily released components will also be lost.

The application of FFF to environmental matrices has to date used SdFFF as well as FlFFF, particularly in conjunction with atomic spectrometric detection. In terms of the relative performance of FlFFF and SdFFF, the following general statements can be made:

1. FlFFF extends the size range that can be separated below 50 nm, enabling the detection of dissolved macromolecules.
2. FlFFF separates on the basis of the size of the molecules or particles alone, and the process is independent of density, whereas SdFFF separates on the basis of buoyant mass, i.e. size and density. As a result, it is more difficult to interpret the results from SdFFF.

10. Future trends in environmental applications

The above section suggests four generic areas in which FlFFF could potentially provide useful environmental information. A number of developments are required for the technique to be more widely applied in this area. The technique needs to establish a broader user base with appropriate practical support. This will be aided by the increased availability of calibration materials and membranes with low RMM cut-offs and the publication of 'standard' analytical methods for particular applications. Coupling of FlFFF with other detectors, such as flow injection-spectrophotometry incorporating selective derivatisation reactions, will generate novel multidimensional information [97]. This would allow the topical areas of opportunity listed above to be addressed, e.g. on-line molybdate reactive phosphorus detection for studying the dynamic interactions between colloids and phosphorus in relation to eutrophication.

Acknowledgements

LG would like to thank Engineering and Physical Sciences Research Council, UK, and the Royal Society of Chemistry, UK, for the award of a PhD studentship. The authors would like to thank Ron Beckett (Water Studies Centre, Monash University, Australia) for his helpful comments on the manuscript.

References

[1] J.C. Giddings, Sep. Sci. 1 (1966) 123.
[2] M. Schimpf, K.D. Caldwell, J.C. Giddings (Eds.), Field-Flow Fractionation Handbook, Wiley, New York, USA, 2000.
[3] C. Pelekani, G. Newcombe, V.L. Snoeyink, C. Hepplewhite, S. Assemi, R. Beckett, Environ. Sci. Technol. 33 (1999) 2807.
[4] H. Thielking, W.M. Kulicke, J. Microcolumn Sep. 10 (1998) 51.
[5] D. Amarasiriwardena, A. Siripinyanond, R.M. Barnes, J. Anal. At. Spectrom. 16 (2001) 978.
[6] R. Beckett, B.T. Hart, Use of Field-Flow Fractionation Techniques to Characterize Aquatic Particles, Colloids, and Macromolecules, in: J. Buffle, H.P. van Leeuwen (Editors), Environmental Particles, Volume 2, Lewis Publishers, Boca Raton, Florida, USA, 1993, pp. 165-205.
[7] P. Li, M. Hansen, J.C. Giddings, J. Liq. Chrom. Rel. Technol. 20 (1997) 2777.
[8] J.C. Giddings, Science (Washington, DC) 260 (1993) 1456.
[9] J.J. Kirkland, C.H. Dilks, Jr., S.W. Rementer, Anal. Chem. 64 (1992) 1295.
[10] M. van Bruijnsvoort, K.G. Wahlund, G. Nilsson, W.Th. Kok, J. Chromatogr. A 925 (2001) 171.
[11] B. Wittgren, K.G. Wahlund, J. Chromatogr. A 760 (1997) 205.
[12] J.Å. Jönsson, A. Carlshaf, Anal. Chem. 61 (1989) 11.
[13] J.E.G.J. Wijnhoven, J.P. Koorn, H. Poppe, W.Th. Kok, J. Chromatogr. A 699 (1995) 119.
[14] M.E. Schimpf, M.P. Petteys, Colloids Surf. A 120 (1997) 87.
[15] C.B. Fuh, M.N. Myers, J.C. Giddings, Anal. Chem. 64 (1992) 3125.
[16] B.T. Hansen, M.G. Plew, M. Schimpf, J. Archaeol. Sci. 25 (1998) 349.
[17] K.D. Jensen, S.K.R. Williams, J.C. Giddings, J. Chromatogr. A 746 (1996) 137.

[18] S.K. Ratanathanawongs, J.C. Giddings, Anal. Chem. 64 (1992) 6.
[19] M.A. Benincasa, K.D. Caldwell, J. Chromatogr. A 925 (2001) 159.
[20] H. Lee, S.K.R. Williams, J.C. Giddings, Anal. Chem. 70 (1998) 2495.
[21] H. Lee, S.K.R. Williams, S.D. Allison, T.J. Anchordoquy, Anal. Chem. 73 (2001) 837.
[22] S.L. Brimhall, M.N. Myers, K.D. Caldwell, J.C. Giddings, J. Polym. Sci. Part C: Polym. Lett 22 (1984) 339.
[23] M. Hassellöv, B. Lyvén, C. Haraldsson, W. Sirinawin, Anal. Chem. 71 (1999) 3497.
[24] M. Nguyen, R. Beckett, Sep. Sci. Technol. 31 (1996) 453.
[25] M.K. Liu, P.S. Williams, M.N. Myers, J.C. Giddings, Anal. Chem. 63 (1991) 2115.
[26] P. Li, M. Hansen, J.C. Giddings, J. Microcolumn Sep. 10 (1998) 7.
[27] E. Zanardi-Lamardo, C.D. Clark, R.G. Zika, Anal. Chim. Acta 443 (2001) 171.
[28] M.E. Miller, J.C. Giddings, J. Microcolumn Sep. 10 (1998) 75.
[29] J.C. Giddings, M.A. Benincasa, M.K. Liu, P. Li, J. Liq. Chromatogr. 15 (1992) 1729.
[30] M.K. Liu, P. Li, J.C. Giddings, Protein Sci. 2 (1993) 1520.
[31] L. Shi, K.D. Caldwell, J. Colloid Interface Sci. 224 (2000) 372.
[32] P.J.M. Dycus, K.D. Healy, G.K. Stearman, M.J.M. Wells, Sep. Sci. Technol. 30 (1995) 1435.
[33] R. Beckett, J.C. Bigelow, Z. Jue, J.C. Giddings, in: P. MacCarthy, I.H. Suffet (Editors) Influence of Aquatic Humic Substances on Fate and Treatment of Pollutants, ACS Adv. Chem. Ser., No. 219, American Chemical Society, Washington DC, USA (1989) pp. 65–80.
[34] H.E. Taylor, J.R. Garbarino, D.M. Murphy, R. Beckett, Anal. Chem. 64 (1992) 2036.
[35] D.M. Murphy, J.R. Garbarino, H.E. Taylor, B.T. Hart, R. Beckett, J. Chromatogr. 642 (1993) 459.
[36] K. Andersson, M. Hassellöv, B. Lyvén, in: M. Hassellöv, Thesis, Göteborg University, Sweden, 1999.
[37] M. Hassellöv, G. Hulthe, B. Lyvén, G. Stenhagen, J. Liq. Chromatogr. Rel. Technol 20 (1997) 2843.
[38] N.M. Thang, R. Knopp, H. Geckeis, J.I. Kim, H.P. Beck, Anal. Chem. 72 (2000) 1.
[39] M. Plaschke, T. Schäfer, T. Bundschuh, T.N. Manh, R. Knopp, H. Geckeis, J.I. Kim, Anal. Chem. 73 (2001) 4338.
[40] F-1000 Manual, FFFractionation, LLC, Salt Lake City, Utah, USA.
[41] B. Lyvén, M. Hassellöv, C. Haraldsson, D.R. Turner, Anal. Chim. Acta 357 (1997) 187.
[42] J.C. Giddings, Analyst (Cambridge, U.K.) 118 (1993) 1487.
[43] S.K.R. Williams, R.G. Keil, J. Liq. Chromatogr. Rel. Technol. 20 (1997) 2815.
[44] R.D. Vaillancourt, W.M. Balch, Limnol. Oceanogr. 45 (2000) 485.
[45] W.S. Kim, Y.H. Park, J.Y. Shin, D.W. Lee, S. Lee, Anal. Chem. 71 (1999) 3265.
[46] R. Beckett, F.J. Wood, D.R. Dixon, Environ. Technol. 13 (1992) 1129.
[47] D.R. Dixon, F.J. Wood, R. Beckett, Environ. Technol. 13 (1992) 1117.
[48] J.R. Lead, K.J. Wilkinson, E. Balnois, B.J. Cutak, C.K. Larive, S. Assemi, R. Beckett, Environ. Sci. Technol. 34 (2000) 3508.
[49] R. Beckett, Z. Jue, J.C. Giddings, Environ. Sci. Technol. 21 (1987) 289.
[50] M.P. Petteys, M.E. Schimpf, J. Chromatogr. A 816 (1998) 145.
[51] N.M. Thang, H. Geckeis, J.I. Kim, H.P. Beck, Colloids Surf. A 181 (2001) 289.
[52] M.A.G.T. van den Hoop, H.P. van Leeuwen, Colloids Surf. A 120 (1997) 235.
[53] F.v.d. Kammer, U. Förstner, Water Sci. Tech. 37 (1998) 173.
[54] M.K. Liu, J.C. Giddings, Macromolecules 26 (1993) 3576.
[55] M.H. Moon, I. Park, Y. Kim, J. Chromatogr. A 813 (1998) 91.
[56] S.K. Ratanathanawongs, J.C. Giddings, ACS Symp. Ser. 521 (1993) 13.
[57] A. Siripinyanond, R.M. Barnes, J. Anal. At. Spectrom. 14 (1999) 1527.
[58] J.H. Song, W.S. Kim, Y.H. Park, E.K. Yu, D.W. Lee, Bull. Korean Chem. Soc. 20 (1999) 1159.
[59] S.G. Stevenson, T. Ueno, K.R. Preston, Anal. Chem. 71 (1999) 8.
[60] S.G. Stevenson, K.R. Preston, J. Cereal Sci. 23 (1996) 121.
[61] S.G. Stevenson, K.R. Preston, J. Liq. Chromatogr. Rel. Technol. 20 (1997) 2835.
[62] S. Lee, S.P. Rao, M.H. Moon, J.C. Giddings, Anal. Chem. 68 (1996) 1545.
[63] C. Duval, D. Le Cerf, L. Picton, G. Muller, J. Chromatogr. B 753 (2001) 115.
[64] K. Glinel, C. Vaugelade, G. Muller, C. Bunel, Int. J. Polym. Anal. Charact. 6 (2000) 89.
[65] J.S. Tan, C.A. Harrison, J.T. Li, K.D. Caldwell, J. Polym. Sci. Part B 36 (1998) 537.
[66] M.H. Moon, K. Kim, Y. Byun, D. Pyo, J. Liq. Chromatogr. Rel. Technol. 22 (1999) 2729.
[67] R. Hecker, P.D. Fawell, A. Jefferson, J.B. Farrow, Sep. Sci. Technol. 35 (2000) 593.
[68] R. Hecker, P.D. Fawell, A. Jefferson, J.B. Farrow, J. Chromatogr. A 837 (1999) 139.
[69] L. Picton, I. Bataille, G. Muller, Carbohydr. Polym. 42 (2000) 23.
[70] U. Adolphi, W.M. Kulicke, Polymer 38 (1997) 1513.
[71] S.K. Ratanathanawongs, P.M. Shiundu, J.C. Giddings, Colloids Surf. A 105 (1995) 243.
[72] H. Thielking, D. Roessner, W.M. Kulicke, Anal. Chem. 67 (1995) 3229.
[73] A.M. Botana, S.K. Ratanathanawongs, J.C. Giddings, J. Microcolumn Sep. 7 (1995) 395.
[74] M.H. Moon, Bull. Korean Chem. Soc. 16 (1995) 613.
[75] D. Roessner, W.M. Kulicke, J. Chromtogr. A 687 (1994) 249.
[76] S. Bartsch, W.M. Kulicke, I. Fresen, H.U. Moritz, Acta Polym. 50 (1999) 373.
[77] K.G. Wahlund, H.S. Winegarner, K.D. Caldwell, J.C. Giddings, Anal. Chem. 58 (1986) 573.
[78] H. Thielking, W.M. Kulicke, Anal. Chem. 68 (1996) 1169.
[79] M.A. Benincasa, J.C. Giddings, Anal. Chem. 64 (1992) 790.
[80] J.C. Giddings, X. Chen, K.G. Wahlund, M.N. Myers, Anal. Chem. 59 (1987) 1957.
[81] Y. Jiang, M.E. Miller, P. Li, M.E. Hansen, Am. Lab. (Shelton, Conn., USA) 32 (2000) 98.
[82] M.A. Benincasa, J.C. Giddings, J. Microcolumn Sep. 9 (1997) 479.
[83] P. Roger, B. Baud, P. Colonna, J. Chromatogr. A 917 (2001) 179.
[84] S.K. Ratanathanawongs, J.C. Giddings, Chromatographia 38 (1994) 545.
[85] P. Reschiglian, D. Melucci, A. Zattoni, L. Malló, M. Hansen, A. Kummerow, M. Miller, Anal. Chem. 72 (2000) 5945.
[86] D.J. Chittleborough, D.M. Hotchin, R. Beckett, Soil Sci. 153 (1992) 341.
[87] R. Beckett, D. Murphy, S. Tadjiki, D.J. Chittleborough, J.C. Giddings, Colloids Surfaces A 120 (1997) 17.
[88] B. Chen, R. Beckett, Analyst (Cambridge, U.K.) 126 (2001) 1588.
[89] A. Sundborg, Nature Resour. 19 (1983) 10.
[90] P. Haygarth, R. Dils, S. Leaf, Phosphorus in Diffuse Pollution Impacts, in: B.J. D'Arcy, J.B. Ellis, R.C. Ferrier, A. Jenkins, R. Dils (Editors), Terence Dalton Publishers, The Lavenham Press, Lavenham, Suffolk, UK, 2000, pp. 73–84.

[91] P.M. Haygarth, S.C. Jarvis, Adv. Agronomy 66 (1999) 195.
[92] J.H. Koeman, Review of environmental problems caused by the use of fertilisers and pesticides, in: F.P.W. Winteringham (Editor), Environment and Chemicals in Agriculture, Elsevier Applied Science, Dublin, Ireland, 1984
[93] J. Abu-Ashor, D.M. Joy, R.H. Whiteley, S. Zelin, Water, Air, Soil Pollut. 75 (1994) 141.
[94] J. Abu-Ashour, H. Lee, Environ. Toxicol. 15 (2000) 149.
[95] P.M. Haygarth, M.S. Warwick, W.A. House, Water Res. 31 (1997) 439.
[96] R.A. Matthews, N. Preedy, A.L. Heathwaite, P.M. Haygarth, Transfer of colloidal forms of phosphorus from grassland soils, in: SEPA (Editors), 3rd Int. Conf. Diffuse Pollut., IAWQ, Edinburgh, UK, 1998, pp. 11–16
[97] R. Chantiwas, R. Beckett, J. Jakmunee, I.D. McKelvie, K. Grudpan, Talanta 58 (2002) 1375.